Factors Influencing Catenary Behavior in Ductile Steel-Framed Structures

by

George Christopher Kantrales

A thesis submitted to the Graduate Faculty of
Auburn University
in partial fulfillment of the
requirements for the Degree of
Master of Science

Auburn, Alabama
August 4, 2012

Keywords: progressive collapse, catenary force development,
catenary action, cable action, steel-framed structures

Approved by

Hassan H. Abbas, Chair, Assistant Professor of Civil Engineering
James S. Davidson, Associate Professor of Civil Engineering
Justin D. Marshall, Assistant Professor of Civil Engineering

Abstract

Historical precedent has established progressive collapse as a phenomenon characterized by the potential for extreme structural damage and loss of life. In an attempt to mitigate such behavior in conventional structures, several different approaches for analysis and design have been suggested. These methods include both threat-dependent and threat-independent procedures. Under the latter, a common approach is to subject the structure to a notional column-removal scenario and then check the ability of the structure to bridge over the removed member. The structure's response under such circumstances can involve the utilization of catenary, or cable-like, behavior to resist the imposed loads once the flexural capacity of the resisting members has been exhausted and sufficient levels of deflection have been attained.

In this thesis, an analytical investigation of various factors influencing the response of steel structures during progressive collapse is presented. The investigation consisted of two components: a baseline study and a parametric study. The baseline study considered the collapse-response of a specifically designed, eight-story, six-bay, steel-framed structure during four distinct, first-story column-removal scenarios. The general response of the structure during each scenario, its catenary action demands, and connection ductility demands were recorded, discussed, and compared. Following the baseline study, a parametric study was conducted, which considered the effects of changing selected design parameters on the response of the system during collapse. The

investigated parameters included the building location, the number of stories, the number of bays in the lateral load-resisting system, and the building aspect ratio. The *Open System for Earthquake Engineering Simulation* (OpenSees), an open-source finite-element (FE) software package, was utilized for the FE simulations.

The results of the investigation show that each factor can have a significant impact on overall system behavior, and the development of catenary forces in particular.

Acknowledgements

I would first like to acknowledge Dr. Hassan H. Abbas, who provided me with continual advice and support throughout this project. I would also like to thank my other committee members, Dr. James S. Davidson and Dr. Justin D. Marshall, for their time and efforts. Special recognition goes to Mr. Haitham Eletrabi, whose assistance was invaluable to this research, particularly with the development of the structural systems analyzed. Finally, I would like to thank the rest of the structures faculty and my fellow graduate students for being part of two of the most rewarding years of my life. I will remember Auburn University fondly.

Table of Contents

List of Tables

List of Figures

Chapter 1 – Introduction

1.1 Overview

For multi-story structures, unanticipated extreme-loading events can result in extensive structural damage and significant loss of life. Such was the case for the Alfred P. Murrah Building (Oklahoma City, OK) in 1995 when a bomb detonated near a main column resulted in progressive collapse of close to half of the structure (Figure 1-1). The death toll was nearly 170 people, with another 800 injured (Agarwal et al. 2012).

Figure 1-1 Alfred P. Murrah Collapse (accessed from: DefenseImagery.mil)

As a response to an extreme event, progressive collapse is identified by:

> "…a situation where local failure of a primary structural component leads to the collapse of adjoining members which, in turn, leads to additional collapse. Hence, the total collapse is disproportionate to the original cause" (GSA 2003).

As shown by the bombing of the Alfred P. Murrah Building, the consequences of a structure incurring progressive collapse are substantial and, in the event of occurrence, pose a serious threat to the safety of the occupants. As a consequence, it has been the focus of many recent research investigations.

Progressive collapse research has been performed using a variety of analytical techniques. One of the most prominent methods of analysis, commonly referred to as "notional column removal", or a "missing column" scenario, is identified by the construction of a structural model and then a subsequent deletion of one of the column elements. The structure's ability to bridge over this removed element and distribute load to the other primary load-resisting members is then investigated. Often concurrent with this method is the consideration of the beams' development of "catenary", or "cable-like" behavior (Khandelwal and El-Tawil 2007).

Catenary behavior, or "catenary action", is most typically exhibited by beams in what is denoted as the "double-span condition", which ostensibly refers to the doubling of the span of the beams directly above the removed column(s). This mode of response is concordant with the development of large tensile forces in the beams once they are no longer able to sustain loads using flexural behavior alone. This transition is shown below in Figure 1-2.

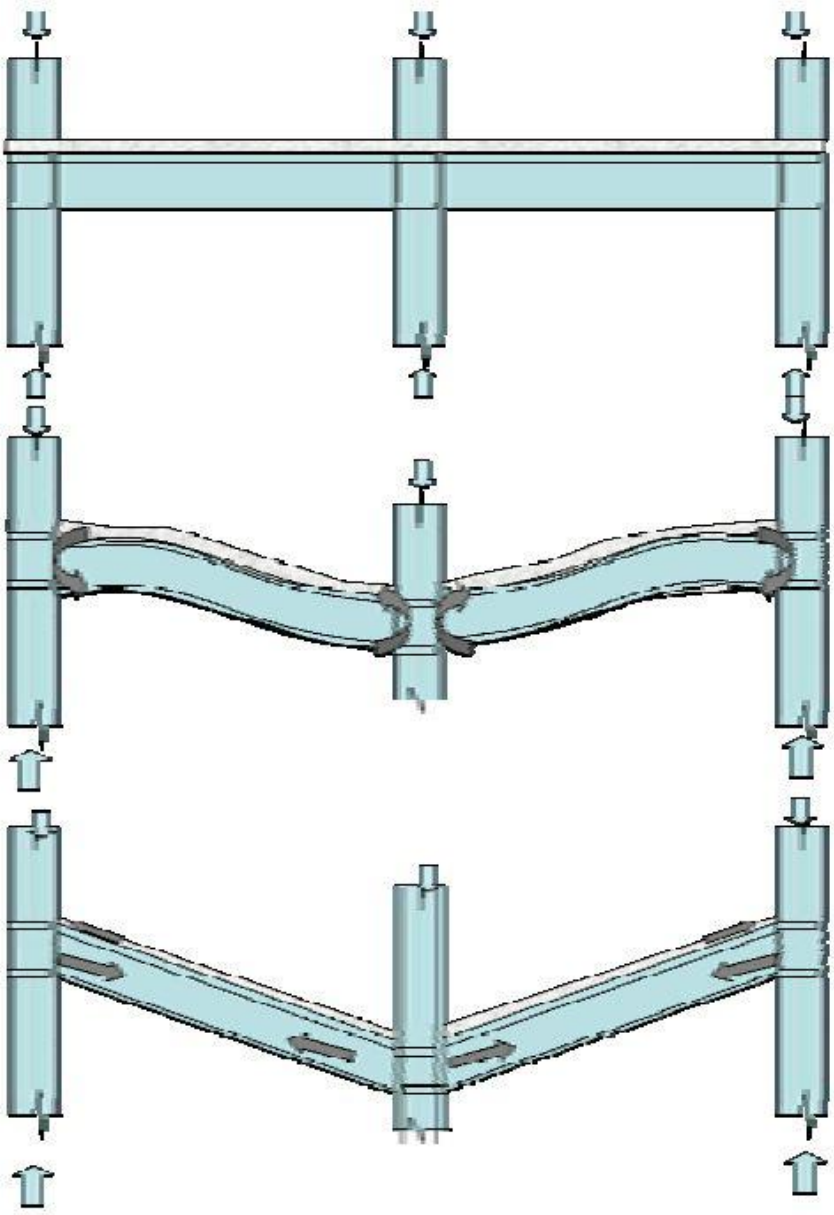

Figure 1-2 Transition to Catenary Behavior (Hamburger and Whittaker 2004)

Since the vertical component of this tensile force is what is used to sustain loads, large deflections are necessary in order to make this an effective method of load-resistance (Khandelwal and El-Tawil 2007).

1.2 Motivation

While there have been a variety of investigations into various aspects of progressive collapse, there have been relatively limited efforts to ascertain the factors influencing catenary action demands in conventional multi-story steel structures and their overall effects on the collapse response of those systems.

Consequently, it is the intent of this thesis to help identify such factors and determine their relative impacts on structural behavior during progressive collapse scenarios.

1.3 Research Objectives

The objectives of this study are as follows:

- Evaluate the impacts of column-removal location on catenary force development and overall system response in multi-story, steel-framed structures
- Determine the effects of specific design and layout considerations on the development of catenary forces in, and the general collapse-resistance of, multi-story, steel-framed structures
- Define the consequences of potential connection ductility demands
- Identify potential areas of revision in prominent design codes

1.4 Tasks

In order to achieve the objectives of this study, the following tasks were performed:

- Review current codes and guidelines pertaining to design for progressive collapse

- Review recent research in the area of progressive collapse, with a particular focus on steel structures
- Develop a realistic, multi-story steel structure (baseline system) and conduct a series of nonlinear-static pushdown analyses considering multiple column removal locations
- Develop variants of the baseline system, modifying several design and layout characteristics, and perform a second series of nonlinear-static pushdown analyses considering only the central column-removal scenario
- Analyze the data obtained from the finite-element models, identifying changes in general collapse response, catenary behavior, and potential connection ductility demands
- From the trends identified, draw general conclusions regarding the relative impacts of the factors studied and provide recommendations for future study

1.5 Scope and Approach

In order to form the basis for this investigation, it was first necessary to design a realistic structural system, designated the "baseline" system, which could be altered for the purposes of the parametric study. Subsequently, the baseline system was used to study various column-removal locations. Seven additional systems were designed for use in the parametric study in order to investigate the impact of the following factors: building location, the number of stories, the number of bays in the lateral load-resisting system, and building aspect ratio. The analytical results for these additional systems were compared against the baseline system, and, if applicable, comparisons were made

between the systems themselves. Based upon these comparisons, conclusions were drawn about the relative impacts of the factors studied.

The investigations conducted as a part of this thesis research pertain to the behavior of multi-story steel structures, no other materials were considered. Specific assumptions and limitations for each study are provided in sections 3.2 and 4.2, along with detailed discussions of the specific methodologies employed.

All analyses were performed using the finite-element software package *Open System for Earthquake Engineering Simulation*, or OpenSees (McKenna et al. 2000). In addition, the commercial software package SAP2000 (CSI 2012) was used for the design of all structural systems.

1.6 Organization of Thesis

Chapter 2 provides relevant background information, including the following sections: a review of current design guidelines, a review of recent research, a theoretical background on specific behavioral aspects pertaining to this thesis, and a discussion on the finite element (FE) modeling techniques employed. Chapter 3 presents the results from the baseline study. Chapter 4 presents the results from the parametric study. Finally, Chapter 5 provides a summary of this investigation, along with general conclusions and recommendations for future research endeavors.

Chapter 2 – Background

2.1 Overview

Within this chapter, all relevant background material related to this thesis research is outlined and explained. First, a comprehensive review of codes and guidelines pertaining to progressive collapse analysis and design in the United States (US) is presented. Second, a concise literature review of relevant investigations is provided. Third, the theoretical background utilized as the foundation of this thesis research is detailed. Finally, the modeling concepts used in the finite element (FE) analyses presented in Chapters 3 and 4 are explained.

2.2 Current Design Guidelines

In this section, relevant design codes and guidelines concerned with the response of structures to progressive collapse behavior are explained. Since the ultimate goal of this research program is to provide suggested revisions to design standards in the US, this review is restricted to main codes and guidelines currently applied in the US.

2.2.1 Minimum Design Loads for Buildings and other Structures (ASCE 7-10)

The American Society of Civil Engineers (ASCE) provides qualitative guidance regarding design for disproportionate collapse in their publication *Minimum Design Loads for Buildings and other Structures* (ASCE 2010). This document is referred to as

ASCE 7-10 in this thesis. In Section 1.4 of ASCE 7-10, general structural integrity is discussed. Within this section, basic requirements are given regarding establishing a minimum level of continuity through main structural components and connections. This is necessary in order to establish an effective load path to the lateral load resisting system.

The commentary to Section 1.4 discusses the general structural integrity requirements in slightly more detail. However, ASCE 7-10 notes the following:

> "…accidents, misuse and sabotage are normally unforeseeable events, they cannot be defined precisely. Likewise, general structural integrity is a quality that cannot be stated in simple terms…ASCE does not intend, at this time, for this standard to establish specific events to be considered during design or for this standard to provide specific design criteria to minimize the risk of progressive collapse" (ASCE 2010).

Within the commentary, ASCE 7-10 discusses the differences between scenarios of general structural collapse and limited local collapse, provides a list of factors that could contribute to general collapse, and enumerates a list of general guidelines to observe in order to produce a more robust design. Some of these guidelines include: developing a good plan layout, providing internal ties, and providing ductile detailing of structural components (ASCE 2010).

Finally, the commentary provides a classification of design approaches used to arrest disproportionate collapse. These definitions were originally developed by Ellingwood and Leyendecker (1978). ASCE 7-10 first classifies "Direct Design" methods

as procedures that provide "explicit consideration of resistance to progressive collapse during the design process…" (ASCE 2010). Conversely, "Indirect Design" methods provide "implicit consideration of resistance to progressive collapse during the design process through the provision of minimum levels of strength, continuity, and ductility" (ASCE 2010).

Finally, in section 2.5 of ASCE 7-10, extreme event load combinations are provided that can be utilized with specific analysis and design procedures aimed at arresting collapse. The first of these combinations is used in order to check the capacity of an existing structural member that has been subjected to an extreme load. This expression is as follows:

$$(0.9 \text{ or } 1.2)\mathrm{D} + \mathrm{A_k} + 0.5\mathrm{L} + 0.2\mathrm{S} \qquad [2.1]$$

where

D = Dead load

L = Live load

A_k = Load resulting from extreme event A

S = Snow load

The second load combination provided by ASCE 7-10 is utilized to check the residual capacity of an existing structure that has been subjected to an extreme event. The combination is expressed as follows:

$$(0.9 \text{ or } 1.2)\mathrm{D} + 0.5\mathrm{L} + 0.2(\mathrm{L_r} \text{or S or R}) \quad [2.2]$$

where

D = Dead load

L = Live load

L_r = Roof live load

S = Snow load

R = Rain load

Adaptations of Equation [2.2] are commonly used for application with the alternate path (AP) method within the United States, specifically in UFC 4-023-03 (UFC 2010).

2.2.2 International Building Code (IBC 2009)

In the 2009 version of the International Building Code (IBC), basic structural integrity requirements are specified for this first time in the code's history. Since this investigation focuses on steel framed structures, only these requirements will be discussed. The IBC specifies tie force requirements for both columns and beams. For columns, the IBC provides the following:

"Each column splice shall have the minimum design strength in tension to transfer dead and live loads tributary to the column between the splice and the splice or base immediately below" (ICC 2009).

Note that this requirement is similar to the vertical tie force requirements specified in UFC 4-023-03. For beams, IBC requires the following:

> "End connections of all beams and girders shall have a minimum nominal axial tensile strength equal to the required vertical shear strength for the allowable stress design (ASD) or two-thirds of the required shear strength for load and resistance factor design (LRFD) but not less than 10 kips (45 kN)…the shear force and the axial tensile force need not be considered to act simultaneously" (ICC 2009).

Proposed revisions to these requirements, based on specifications found in the US and the United Kingdom were presented to the Structural Code Development Committee, but were rejected in 2008 (CPNI 2011).

2.2.3 Department of Defense's Unified Facilities Criteria (UFC 4-023-03)

The Department of Defense's Unified Facilities Criteria (UFC) *Design of Buildings to Resist Progressive Collapse* (UFC 4-023-03) is one of the more well-reviewed documents on progressive collapse design in the US. Since its provisions were used extensively in the course of this thesis research, a more thorough review of this document is provided.

UFC 4-023-03 classifies design approaches as "indirect" or "direct" based upon the corresponding classifications defined within ASCE 7. The direct design approaches described in the UFC are the AP method and the Enhanced Local Resistance (ELR)

method. There is one indirect design approach outlined called the Tie Force (TF) method (UFC 2010).

The current version of UFC 4-023-03, revised in 2010, specifies which design process to utilize based upon Occupancy Categories (OCs). These OCs are correlated to classifications specified in UFC 3-301-01 *Structural Engineering*. Table 2-1 shows the corresponding categories from 3-301-01. Table 2-2 describes how these categories relate to the ones outlines in UFC 4-023-03.

Table 2-1 UFC 3-301-01 Occupancy Categories (UFC 2011)

Occupancy Category	Nature of Occupancy
I	**Buildings and other structures that represent a low hazard to human life in the event of failure, including, but not limited to:** • Agricultural facilities • Certain temporary facilities • Minor storage facilities
II	**Buildings and other structures except those listed in Categories I, III, IV and V**
III	**Buildings and other structures that represent a substantial hazard to human life or represent significant economic loss in the event of failure, including, but not limited to:** • Buildings and other structures whose primary occupancy is public assembly with an occupant load greater than 300 people • Buildings and other structures containing elementary school, secondary school, or daycare facilities with an occupant load greater than 250 • Buildings and other structures with an occupant load greater than 500 • Group I-2 occupancies with an occupant load of 50 or more resident patients, but not having surgery or emergency treatment facilities • Group I-3 occupancies • Power-generating stations; water treatment facilities for potable water, waste water treatment facilities, and other public utility facilities that are not included in Categories IV and V • Buildings and other structures not included in Categories IV and V containing sufficient quantities of toxic, flammable, or explosive substances to be dangerous to the public if released • Facilities having high-value equipment, as designated by the authority having jurisdiction

Table 2-1 UFC 3-301-01 Occupancy Categories (UFC 2011)

IV	**Buildings and other structures designed as essential facilities, including, but not limited to:** • Group I-2 occupancies having surgery or emergency treatment facilities • Fire, rescue, and police stations, and emergency vehicle garages • Designated earthquake, hurricane, or other emergency shelters • Designated emergency preparedness, communication, and operation centers, and other facilities required for emergency response • Emergency backup power-generating facilities required for primary power for Category IV • Power-generating stations and other utility facilities required for primary power for Category IV, if emergency backup power generating facilities are not available • Structures containing highly toxic materials as defined by Section 307, where the quantity of material exceeds the maximum allowable quantities of Table 307.7(2) • Aviation control towers and air traffic control centers required for post earthquake operations where lack of system redundancy does not allow for immediate control of airspace and the use of alternate temporary control facilities is not feasible. Contact the authority having jurisdiction for additional guidance. • Emergency aircraft hangars that house aircraft required for post-earthquake emergency response; if no suitable back up facilities exist • Buildings and other structures not included in Category V, having DoD mission-essential command, control, primary communications, data handling, and intelligence functions that are not duplicated at geographically separate locations, as designated by the using agency • Water storage facilities and pump stations required to maintain water pressure for fire suppression
V[b]	**Facilities designed as national strategic military assets, including, but not limited to:** • Key national defense assets (e.g. National Missile Defense facilities), as designated by the authority having jurisdiction. • Facilities involved in operational missile control, launch, tracking, or other critical defense capabilities • Emergency backup power-generating facilities required for primary power for Category V occupancy • Power-generating stations and other utility facilities required for primary power for Category V occupancy, if emergency backup power generating facilities are not available • Facilities involved in storage, handling, or processing of nuclear, chemical, biological, or radiological materials, where structural failure could have widespread catastrophic consequences, as designated by the authority having jurisdiction.

Table 2-2 UFC 4-023-03 Occupancy Categories (UFC 2010)

Nature of Occupancy	Occupancy Category
• Buildings in Occupancy Category I in \1\ Table 2-2 of UFC 3-301-01. /1/ • Low Occupancy Buildings[A]	I
• Buildings in Occupancy Category II in \1\ Table 2-2 of UFC 3-301-01. /1/ • Inhabited buildings with less than 50 personnel, primary gathering buildings, billeting, and high occupancy family housing[A,B]	II
• Buildings in Occupancy Category III in \1\ Table 2-2 of UFC 3-301-01. /1/	III
• Buildings in Occupancy Category IV in \1\ Table 2-2 of UFC 3-301-01. /1/ • Buildings in Occupancy Category V in \1\ Table 2-2 of UFC 3-301-01. /1/	IV

[A] As defined by UFC 4-010-01 *Minimum Antiterrorism Standards for Buildings*
[B] Occupancy Category II is the minimum occupancy category for these buildings, as their population or function may require designation as Occupancy Category III, IV, or V.

As can be seen from the previous tables, determining a structure's OC is directly related to two aspects: The building's level of occupancy, and its intended use. Consequently, structures that have higher levels of occupancy or that serve more critical functions will have a higher OC. Note that substantial economic loss is included as one of the measures for a structure's level of criticality. The inclusion may be related to the fact that UFC 4-023-03 was developed by the Department of Defense (DOD) for use in the design of DOD facilities. This correlation between owner and designer could potentially create a more vested interest in the economic impacts of system failure (CPNI 2011). For each OC specified, UFC 4-023-03 stipulates unique design requirements. These requirements are shown in Table 2-3.

Table 2-3 UFC 4-023-03 Design Requirements by Occupancy Category (UFC 2010)

Occupancy Category	Design Requirement
I	No specific requirements
II	Option 1: Tie Forces for the entire structure and Enhanced Local Resistance for the corner and penultimate columns or walls at the first story. **OR** Option 2: Alternate Path for specified column and wall removal locations.
III	Alternate Path for specified column and wall removal locations; Enhanced Local Resistance for all perimeter first story columns or walls.
IV	Tie Forces; Alternate Path for specified column and wall removal locations; Enhanced Local Resistance for all perimeter first and second story columns or walls.

From Table 2-3, it can be noted that as the OC of a structure increases, the level of sophistication in the required design and analysis methods also increases.

For relatively low-risk structures, UFC 4-023-03 allows for the use of the so-called Tie Force method. This Indirect Method attempts to enhance the general integrity of a structure through the use of internal ties. The Tie Force method does not require any of the detailed analysis inherent in the AP method and is intended to enhance the overall robustness of the system through a general improvement of continuity and ductility throughout the structure. The fundamental concepts behind the Tie Force method were first proposed by the Institution of Structural Engineers in the United Kingdom in 1971 as a reaction to the Ronan Point Building collapse (IStructE, 1971). Adaptations of this

research have been applied to several design codes, including UFC 4-023-03 (CPNI 2011).

Within UFC 4-023-03, several different types of ties are specified. These classifications include: vertical ties, transverse ties, longitudinal ties and peripheral ties. A depiction of these tie locations is shown below in Figure 2-1.

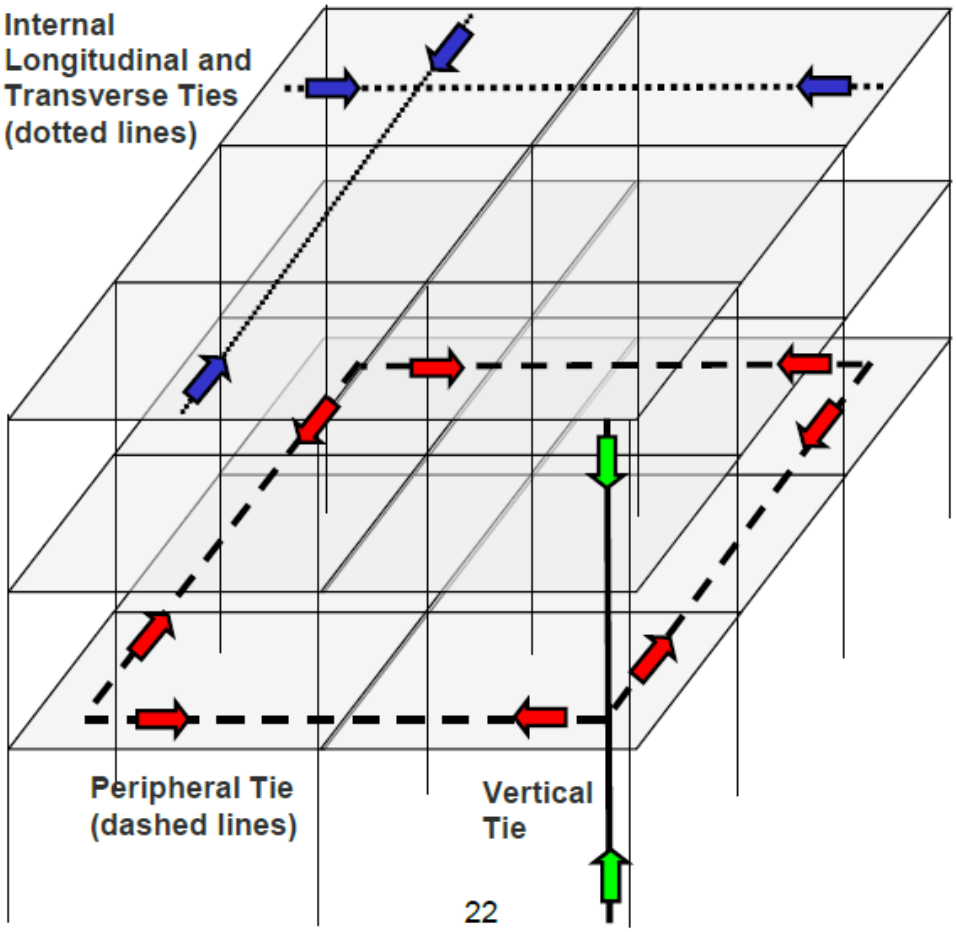

Figure 2-1 Classification of Ties (UFC 2010)

In earlier versions of UFC 4-023-03, tie forces were allowed to be developed through either the structural members themselves or through the floor system that these members support. However, the Tie Force method is intended to take advantage of catenary behavior in order to develop the reserve capacity necessary to arrest collapse. In order to make this transition within structural elements from flexural to catenary behavior, large deflections and rotations are necessary. Due to the lack of established research on the rotational capacity of connections subjected to a combination of axial force and moment under monotonic conditions, there is a lack of confidence in the ability of these connections to undergo the rotations necessary to sustain a large degree of catenary force. Consequently, in the current provisions of UFC 4-023-03, transverse, longitudinal, and peripheral tie forces are primarily intended to be carried within the floor system (Stevens 2008). Utilization of the primary structural members to develop these tie forces is still allowed provided that the designer demonstrates that the members in question, and their associated connections, can carry the required amount of force while undergoing a rotation of 0.2 radians (UFC 2010).

The load combination used by UFC 4-023-03 to determine the required tie forces for a structure is the extreme event load combination from ASCE 7 without consideration for snow and wind load effects (Stevens 2008). Note that the required tie forces resulting from this load combination are not considered additive with those forces obtained from standard design. The combination for a uniform floor load is shown below in Equation [2.3] (UFC 2010).

$$w_F = 1.2D + 0.5L \qquad [2.3]$$

where

w_F = Floor load (lb/ft^2 or kN/m^2)

D = Dead load (lb/ft^2 or kN/m^2)

L = Live load (lb/ft^2 or kN/m^2)

In addition to a uniform floor load, there are also provisions for concentrated loads, variable loads and loads resulting from components and cladding.

For framed structures, the magnitude of the required internal tie force (longitudinal and transverse ties) in the current UFC 4-023-03 is given by Equation [2.4] (UFC 2010).

$$F_i = 3w_F L_1 \qquad [2.4]$$

where

F_i = Required internal tie strength (lb/ft or kN/m)

w_F = Floor load (lb/ft^2 or kN/m^2)

L_1 = Greater of the distances between the centers of the columns, frames or walls supporting any two adjacent floor spaces in the direction under consideration (ft or m)

Equation [2.4] was formulated using membrane theory for uniformly loaded slabs developed by Park and Gamble (2000). A central deflection having a magnitude of 10%

of the short span direction was implicitly assumed. This value was selected based upon the results of various experimental investigations relating to the tensile membrane response of reinforced concrete slabs. This equation also includes an implicit 20% increase to account for inertial effects. This increase was selected based upon the results of the accompanying finite element analyses (Stevens 2008).

UFC 4-023-03 has separate requirements for peripheral tie forces due to the assumptions inherent in the theory. [2.5] shows how the required peripheral tie force may be calculated (UFC 2010).

$$F_P = 6 w_F L_1 L_P \qquad [2.5]$$

where

F_P = Required peripheral tie strength (lb or kN)

w_F = Floor load (lb/ft^2 or kN/m^2)

L_1 = Greater of the distances between the centers of the columns, frames or walls supporting any two adjacent floor spaces in the direction under consideration (ft or m)

L_P = 3 (ft) or 0.91 (m)

The value of L_P chosen for use in Equation [2.5] was selected as the delineating distance between what is considered an "internal" tie and a "peripheral" tie in UFC 4-023-03 and is related to a similar distance used in British standards (Stevens 2008). Note that the constant present in Equation [2.4] has twice the value of the constant present in

Equation [2.5]. The reason for this difference relates to the assumed value of central deflection. When the peripheral tie strength was low, the analytical models showed results with values of deflection exceeding the assumed value (10% of the short span). In order to prevent violation of this assumption, the required peripheral tie force was restricted to twice what would be obtained from using Equation [2.4] with a corresponding width of 3 feet (Stevens 2008).

In addition to internal and peripheral ties, UFC 4-023-03 also outlines requirements for vertical tie forces. These forces are intended to be tensile forces carried by the surrounding columns. Equation [2.6] shows the equation for the required vertical tie force.

$$F_v = w_F A_t \qquad [2.6]$$

where

F_v = Required vertical tie force (lb or kN)

w_F = Floor load (lb/ft^2 or kN/m^2)

A_t = Tributary area of column (ft^2 or m^2)

In addition to specifying tie force magnitudes, UFC 4-023-03 also outlines tie force spacing requirements. Figure 2-2 depicts these limitations for framed structures.

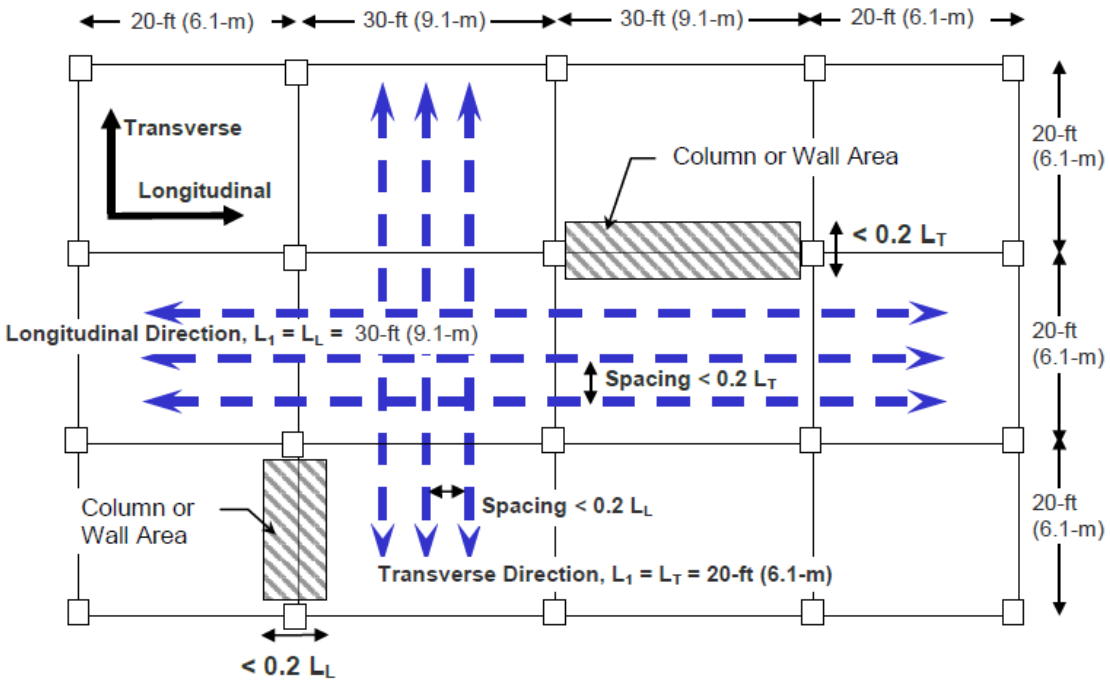

Figure 2-2 Spacing Limitations for Internal and Peripheral Ties (UFC 2010)

Per UFC 4-023-03 requirements, internal ties must be anchored by peripheral ties at each end. The spacing of these internal ties must be less than 20% of the center-to-center spacing of the columns in the direction perpendicular to the ties. Moreover, there are special restrictions in UFC 4-023-03 relating to those structures without internal beams between column locations. For these types of structures, no more than twice the required tie strength may be placed within the column areas indicated in Figure 2-2 (UFC 2010).

In addition to the Tie Force method, UFC 4-023-03 also incorporates two other design methodologies. These two methods, the Specific Local Resistance method and the AP method, are considered Direct Design Methods since they explicitly consider the effects of disproportionate collapse on system behavior (CPNI 2011).

In situations where the provided vertical tie strengths are inadequate, UFC 4-023-03 allows the AP method to be utilized in order show that the structure has adequate strength to resist collapse. The AP method is also required to be implemented in the analysis and design of structures with a higher OC category. There are three different classifications of analysis that may be utilized in the AP method: Linear Static (LSP), Nonlinear Static (NSP), and Nonlinear Dynamic (NSP). These analysis procedures are adaptations of the ones outlined in ASCE 41 and have been modified to account for the differences between seismic applications and progressive collapse scenarios (UFC 2010).

An AP analysis is conducted by removing key vertical structural elements and using one of the three analysis procedures previously mentioned to prove the ability of the structure to provide an "alternate path" with which to redistribute loads around the removed element using other primary structural elements. UFC 4-023-03 defines a "primary" structural element as one that contributes to the collapse resistance of a structure. All other elements that do not contribute to this resistance, such as gravity beams with pinned ends, are classified as secondary. When modeling a structure using the AP method, only the strength and stiffness of the primary structural members are accounted for in the model. For vertical elements with insufficient tie forces, the column itself will be the element removed in the AP analysis. When used as a general design procedure in lieu of the TF method, column removal locations are specified. In this case, corner columns and external columns near the middle of the short and long sides of the structure shall be removed in addition to columns located at abrupt changes in plan geometry or loading. A separate AP analysis shall be conducted for the following plan locations: The first story above grade, the story directly below the roof, the story at mid-

height and the story above the location of a column splice or change in column size (UFC 2010). External column removal locations are depicted below in Figure 2-3.

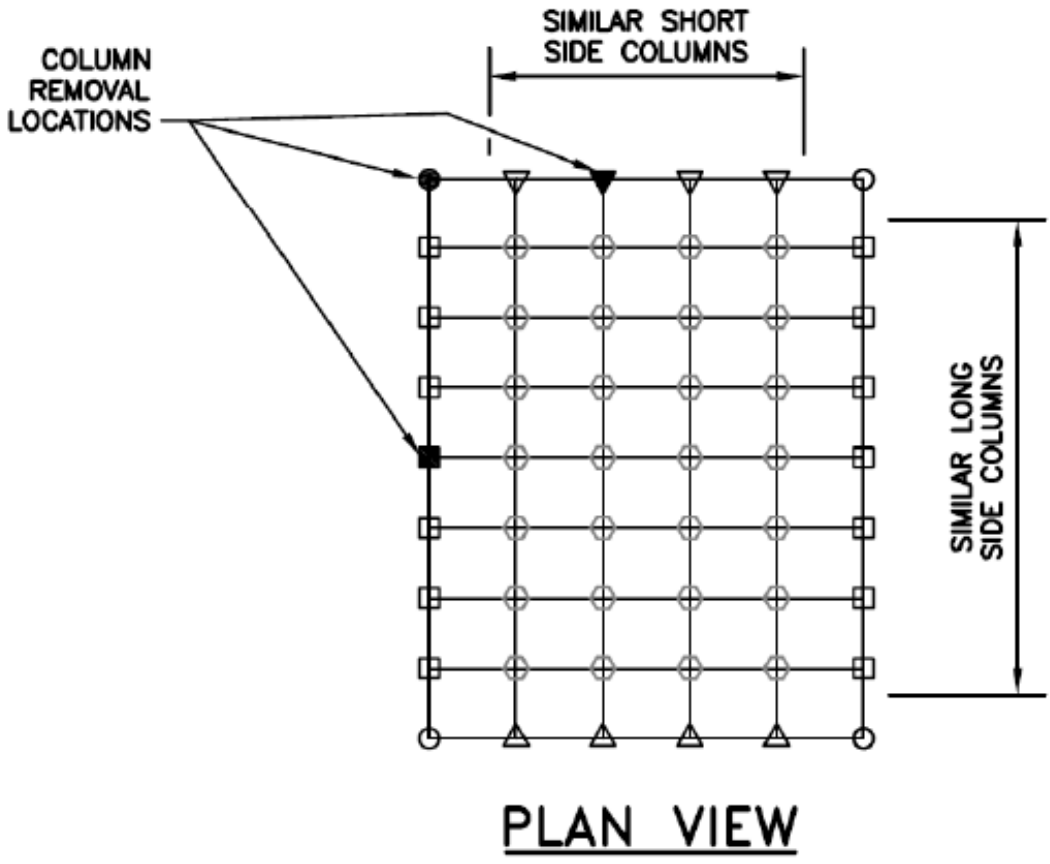

Figure 2-3 External Column Removal Locations (UFC 2010)

Internal columns are also removed for structures with "underground parking or other areas of uncontrolled public access" (UFC 2010). In these cases, columns are removed "near the middle of the short side, near the middle of the long side and at the corner of the uncontrolled space" (UFC 2010). Moreover, internal columns are only removed for stories that contain areas of uncontrolled public access. Figure 2-4 depicts interior column removal locations.

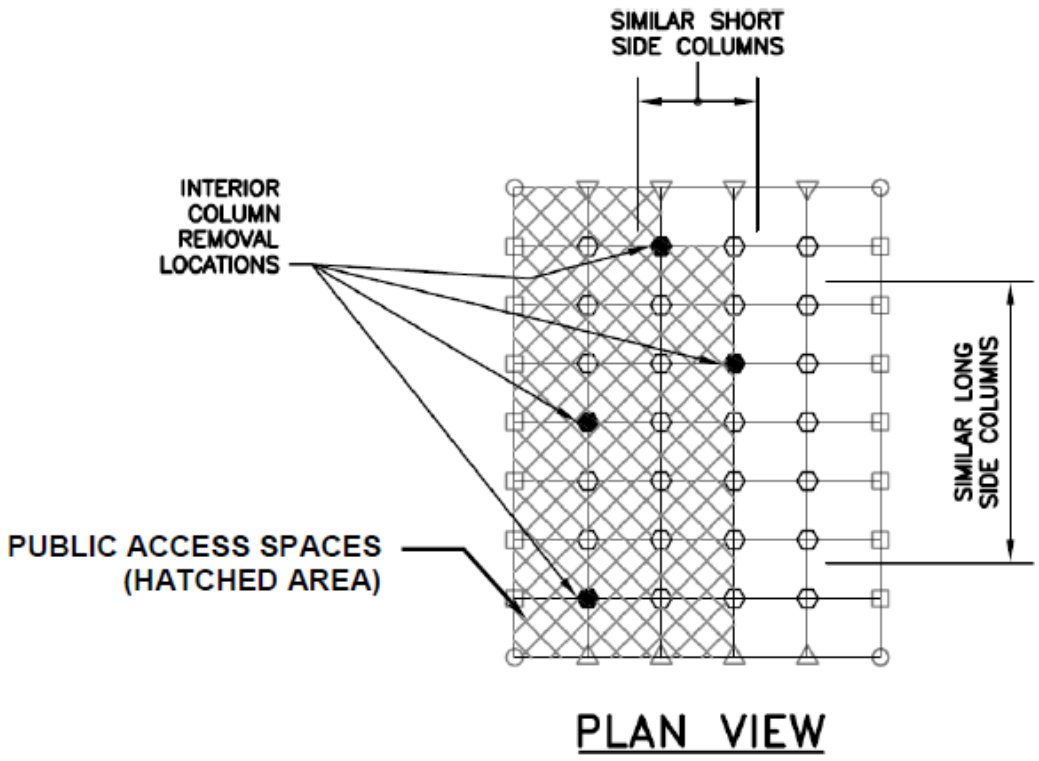

Figure 2-4 Internal Column Removal Locations (UFC 2010)

When columns are notionally removed for an AP analysis, there is no assumed damage to the joint. Consequently, as shown in Figure 2-5, only the clear distance between the story above and below the vertical element will be removed (UFC 2010).

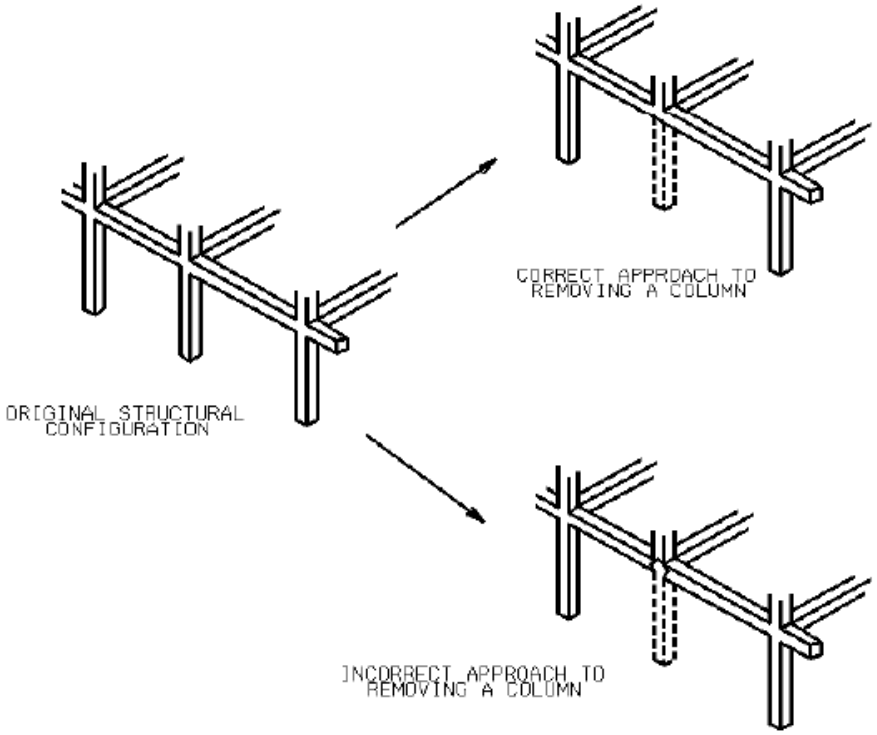

Figure 2-5 Column Removal for AP Method (UFC 2010)

The loading and design criteria for the AP method depend on the type of action being considered. UFC 4-023-03 classifies certain types of behavior as being "force-controlled" or "deformation-controlled". This delineation is based upon criteria set forth in ASCE 41. Stated simply, deformation-controlled actions are those that exhibit considerable deformations prior to failure. Correspondingly, force-controlled behavior is characterized by extremely brittle failure modes (ASCE 2006). Table 2-4 provides examples of these classifications for various types of structural behavior.

Table 2-4 Examples of Deformation-Controlled and Force-Controlled Actions (UFC 2010)

Component	Deformation-Controlled Action	Force- Controlled Action
Moment Frames • Beams • Columns • Joints	 Moment (M) M --	 Shear (V) Axial load (P), V V[1]
Shear Walls	M, V	P
Braced Frames • Braces • Beams • Columns • Shear Link	 P -- -- V	 -- P P P, M
Connections	P, V, M[2]	P, V, M

1. Shear may be a deformation-controlled action in steel moment frame construction.
2. Axial, shear, and moment may be deformation-controlled actions for certain steel and wood connections.

Once behaviors have been classified, the AP method allows for the use of the LSP, the NSP or the NDP in order to determine the sufficiency of the structure to resist collapse for both deformation-controlled and force-controlled actions. As with the TF method, the load combination used with the AP method is the modified version of the extreme event load combination from ASCE 7 that is provided in [2.3]. When applicable, appropriate modification factors are also used to amplify this load in order to account for dynamic and nonlinear effects. Additionally, appropriate LRFD strength reduction factors are intended to be implemented when strength is the limiting criteria for design.

In the AP method, failure is defined differently depending on the type of analysis being conducted and the type of action being considered. For the LSP, capacities modified to include the effects of ductility (where applicable) are compared against member forces for both force and deformation-controlled behavior. As previously mentioned, these capacities are intended to be modified with LRFD strength reduction factors. Force-controlled actions are similarly checked for both nonlinear analysis types. However, unlike the LSP, both nonlinear analysis types use inelastic deformation limits as the limiting criteria for deformation-controlled actions. These limits are provided in ASCE 41 and UFC 4-023-03 (UFC 2010).

Since substantial member ductility and system nonlinearity will influence the accuracy of the LSP, UFC 4-023-03 has implemented a limitation on its usability. In section 3-2.11.1.1 of UFC 4-023-03, structural irregularities are outlined that are perceived to influence the accuracy of the LSP. In the event that the structure in consideration has one of these irregularities, a Demand-Capacity Ratio (DCR) must be determined for all deformation-controlled actions and compared against the UFC specified limit of 2.0. For the contingency when the structure does not satisfy this limitation, one of the nonlinear procedures must be applied in order to explicitly account for the significant nonlinearity (UFC 2010).

The loading arrangement utilized for an analysis using the AP method is shown in Figure 2-6.

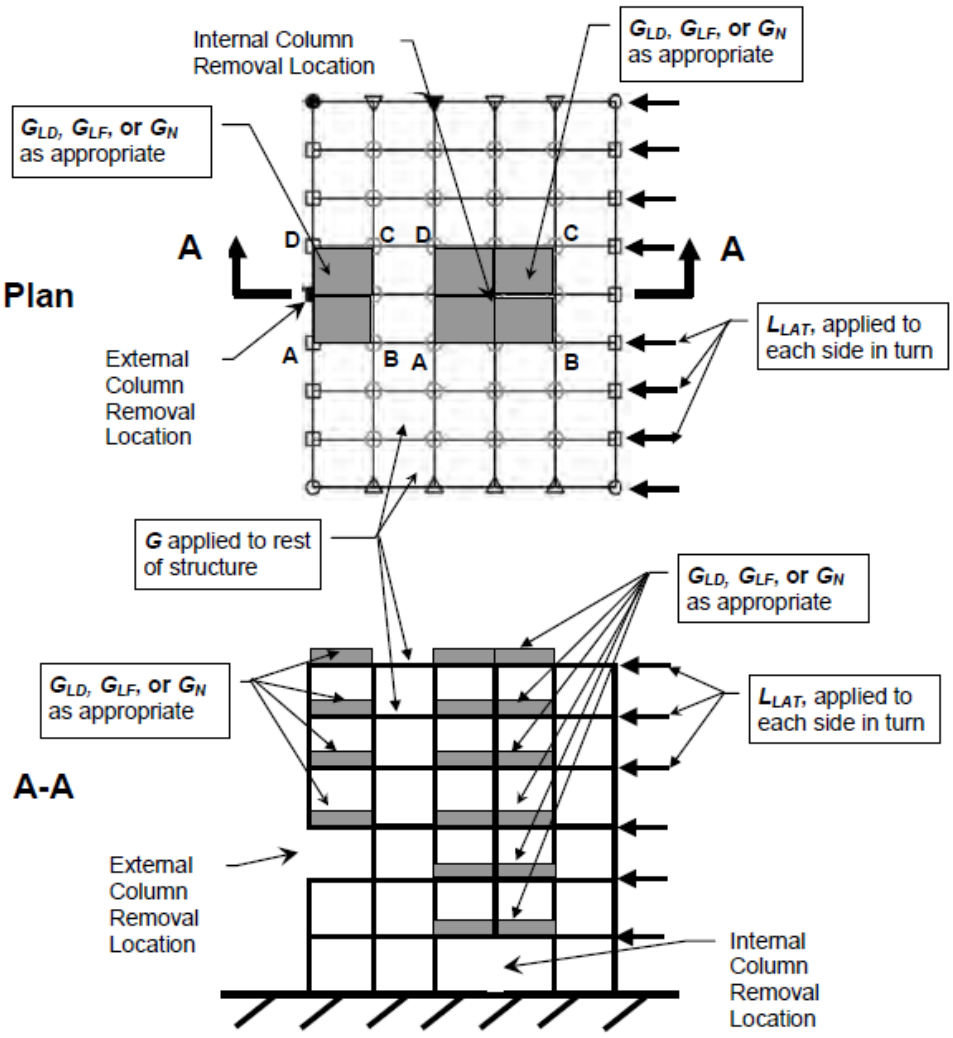

Figure 2-6 Load Arrangement for the AP Method (UFC 2010)

As can be seen in Figure 2-6, amplified loads (G_{LD}, G_{LF} and G_N) are applied to the bays adjacent to the lost column. Each bay above those bays also experiences amplified loads. Loads without any increase factors are applied to the rest of the structure. The level of amplification of loads depends on the type of analysis being conducted. The three cases where modified loads are utilized are as follows: Linear and force-controlled (G_{LF}), linear and deformation-controlled (G_{LD}), and nonlinear (G_N). The nonlinear

amplification is only applied for the NSP and does not differentiate between force-controlled or deformation-controlled behavior. The reason for this uniformity is that the NSP, by explicitly accounting for nonlinearity, only requires modification for dynamic effects. Since the NDP explicitly accounts for both nonlinear and dynamic effects, it uses the unmodified load combination (G) for all bays. In the linear static procedure, load amplification factors must be implemented that account for both nonlinear and dynamic effects. However, this modification differs between components with ductile responses and those that behave in a more brittle manner. For deformation-controlled behavior, both inertial effects and expected ductility are accounted for in the load modifier. However, for force-controlled behavior, only inertial effects are taken into consideration (Stevens 2008). In addition to gravity loads, lateral loads (L_{LAT}) are applied to every story and each side of the structure, one side at a time. This lateral load is, in effect, a notional load to account for the effects of stability and the influence of the inherent out-of-plumbness that is present in all structures. This lateral load is defined in UFC 4-023-03 as follows (UFC 2010):

$$L_{LAT} = .002\Sigma P \qquad [2.7]$$

where

L_{LAT} = Applied lateral load

$.002\Sigma P$ = Notional lateral load applied at each floor.

ΣP = Sum of the gravity loads (both dead and live) acting on only the floor considered. No increase factors are applied.

The other direct design method described in UFC 4-023-03 is the Enhanced Local Resistance method. The ELR method, unlike the previous two methods described, is considered a threat-dependent approach. In other words, the effectiveness of the ELR method is directly derived from the initial event that causes damage to one (or more) of the columns. Furthermore, the ELR method arrests collapse by hardening columns to prevent failure. A structure designed in this manner may or not be able to redistribute loads upon the potential failure of a column. For these reasons, the ELR method is not looked upon favorably as a primary design measure (CPNI 2011). Subsequently, as can be seen from Table 2-3, the ELR method is only applied in UFC 4-023-03 as a supplementary method in conjunction with either the TF method or the AP method.

2.2.4 General Services Administration Progressive Collapse Analysis and Design Guidelines (GSA 2003)

One of the two initially prominent design guidelines that arose in the US to address the issue of progressive collapse was the General Services Administration (GSA) document *Progressive Collapse Analysis and Design Guidelines* (GSA 2003). GSA (2003) was developed for use in federal office buildings, but not those associated with the Department of Defense (here UFC 4-023-03 applies). GSA (2003) differs from UFC 4-023-03 in that it features a more direct and comprehensive method of assessing the risk factors involved in whether or not a structure should be considered for progressive collapse analysis and design (CPNI 2011). However, this document has not been revised and updated in the manner of UFC 4-023-3. It has been noted that certain principals and concepts from this document, such as demand-capacity ratios, have begun manifesting in

updated versions of UFC 4-023-03 (CPNI 2011). Since this trend is currently indicative of GSA (2003) ultimately being replaced by UFC 4-023-03, further details of this document will not be discussed in this thesis.

2.2.5 Blast and Progressive Collapse (AISC)

In order to clarify the behavior of steel structures under extraordinary loading conditions and discuss appropriate design considerations for these circumstances, the American Institute of Steel Construction (AISC) has released Facts for Steel Buildings #2: *Blast and Progressive Collapse* developed by Marchand and Alfawakhiri (2004). The document is divided into eight sections: general behavior of blast loading, threats and acceptable risk, resistance of steel structures to extreme loads, mitigation of progressive collapse, best practices to mitigate blast load effects, best practices to mitigate progressive collapse, a history on blast and collapse, and a discussion on current research and future needs (Marchand and Alfawakhiri, 2004). Since this study is concerned with the behavior of steel structures under progressive collapse scenarios, the fourth and sixth sections are of particular interest. The fourth section presents the guidelines relating to structural integrity available in ASCE 7 and discusses the basic concepts behind both the TF and the AP methods. Also provided in this section is a discussion on the importance of connection capacity and ductility when subjected to a combination of moment and axial force. The sixth section goes into more detail regarding the specific design guides (GSA and UFC) available at the time of the document's publication (Marchand and Alfawakhiri, 2004). However, since the release of *Blast and Progressive Collapse*, UFC 4-023-03 has undergone several major revisions. Consequently, the main use of this

document lies in its ability to introduce the basic concepts of progressive collapse as it applies to steel structures and to orient its reader with the available design guides used in the mitigation of this type of behavior.

2.3 Review of Recent Research

Although the area of progressive collapse research is still relatively new, there have been several recent investigations that have significantly contributed to the body of knowledge surrounding the topic. This section will contain a concise review of those investigations pertaining to steel structures that connect more clearly with the direction of this thesis.

Of primary interest in the area of progressive collapse is the behavior and resiliency of steel connections during collapse. The reason for this is that much of the information related to connection behavior published in design codes was obtained under seismic loading conditions (Sadek et al. 2009). Since progressive collapse conditions are characterized by monotonic loading and the potential for substantial axial force development in affected beams, connection behavior might be significantly influenced. Consequently, several investigations have been carried out that have attempted to clarify this behavior.

Kim and Kim (2009) conducted an analytical investigation into the collapse potential of moment frames with a variety of seismic connections: The reduced beam section connection (RBS), welded cover plated flange (WCPF) connection, and the welded unreinforced flange-welded web (WUF-W) connection. Within this study, structures were analyzed that had been designed for both moderate and high seismicity.

The results of the investigation indicated that while the RBS connections analyzed had a larger ductility capacity than the other connection types, there was also a substantial increase in the ductility demand in the models which included RBS connections. Moreover, while the WCPF and WUF-W connections performed in a similar manner for their respective structures, the WCPF connection, by virtue of its larger ductility capacity, was deemed more resilient for progressive collapse applications (Kim and Kim 2009).

As part of an extensive and ongoing research effort by the National Institute of Standards and Technology (NIST) into structural robustness, Sadek et al. (2009) conducted an experimental and analytical investigation into the behavior of two steel beam-column assemblies under the monotonic loading conditions typical of a column-removal scenario. The two connections studied were a welded, unreinforced flange, bolted web connection (WUF-B) and an RBS connection. The major finding of the study was that these connections exhibited greater rotational capacity under the loading conditions sustained in the experiment than anticipated by existing design provisions (Sadek et al. 2009).

A study similar to Sadek et al. (2009) was conducted by Kim et al. (2010) into the collapse resistance of WUF-B moment connections designed to resist gravity loads. Two identical connections were tested: one for monotonic testing and one for cyclic testing. As in the study by Sadek et al. (2009), it was shown that the tested connection design exhibited greater rotational capacity under monotonic conditions. However, in this experiment, the influence of a potential axial load in the beam was not considered (Kim et al. 2010).

Investigations into semi-rigid and simple shear connection behavior under progressive collapse conditions have also been pursued. Examples of such investigations include: Gong (2010), Pirmoz (2011), Pirmoz et al. (2011), and Xu and Ellingwood (2011).

Due to the inherent complexity involved in progressive collapse behavior, many researchers utilize three-dimensional, nonlinear, dynamic micro models when analyzing structural systems. However, this approach is time-consuming and computationally expensive. Consequently, there have been many attempts to create and validate macro model based approaches that might be more easily employed. Examples of such attempts are seen in the work of Main et al. (2009) and Alashker et al. (2011). Once such approaches are validated, they may be used to explore the influence of various factors on progressive collapse behavior.

Khandelwal et al. (2008A) investigated the behavior of seismically-designed steel structures subjected to column-loss scenarios using two-dimensional finite element macro models. Two 10-story structures were considered: One designed with intermediate moment frames (IMFs) located in Atlanta (GA) and one designed with special moment frames (SMFs) located in Seattle (WA). Both structures were designed by NIST for progressive collapse investigations. The study concluded that the structure designed for high-seismic activity exhibited larger potential to resist progressive collapse through its general layout and system strength rather than the activation of improved seismic detailing (Khandelwal et al. 2008A). A separate investigation was conducted by Khandelwal et al. (2008B) for the same two structures with braced frame systems, one with special concentrically braced frames (SCBFs) and one with eccentrically braced

frames (EBFs). The study concluded that the EBF system designed for high seismic activity showed greater potential to resist progressive collapse when compared to the SCBF system. Similar to the investigation involving the structures with moment frames, the conclusion in this study was that this additional resiliency was primarily due to the improved layout of one system versus the other rather than from the utilization of ductile detailing (Khandelwal et al. 2008B).

Kim and An (2008) investigated the impact of including catenary behavior in analytical models of structures with steel moment-resisting frames. The analysis was conducted according to the AP method outlined in GSA (2003); both nonlinear static and nonlinear dynamic analyses were included. The study found that those models which allowed catenary behavior to occur in the beams formed an upper bound in terms of load resistance to those models which did not consider catenary behavior. Moreover, it was also concluded that the degree of catenary force development increased with a corresponding increase in those variables which improved lateral restraint. However, the same correspondence was not seen as the number of stories was varied. The investigation was qualified by the statement that the analyses conducted assumed the joint conditions were such that full catenary force development would be allowed to occur (Kim and An 2008).

Kim et al. (2009) investigated the impact of various factors on the progressive collapse resistance of steel moment frames using two-dimensional nonlinear static finite element analysis; however, only flexural behavior in the beams was considered. Loads were applied in the push-down analysis according to GSA (2003) guidelines. The primary factors studied included: the number of bays in the lateral load resisting system,

the number of stories, the span length of the beams, and the level of design earthquake load. The results of the nonlinear static push-down analysis indicate that the progressive collapse resistance of the systems seemed to increase with the number of bays and the number of stories. Conversely, the collapse resistance seemed to decrease with increasing span length. The collapse-resistance of the studied structures was higher for those that were designed for higher earthquake loads. Finally, the study concluded that, when compared to nonlinear dynamic analyses, the nonlinear static pushdown analysis seemed to overestimate the collapse resistance of structures (Kim et al. 2009).

Khandelwal and El-Tawil (2011) compared a variety of push-down methods for the evaluation of progressive collapse resistance for structures designed for moderate and high seismic activity. The methods included in the investigation were the uniform pushdown method, the bay pushdown method and the incremental dynamic pushdown method. In the first method, gravity loads are increased uniformly throughout the structure. The bay pushdown method increases the gravity loads in the affected bays alone. The incremental dynamic method conducts a series of dynamic analyses while increasing the gravity loads in the bays of interest. A variety of conclusions were drawn from this investigation. First, it was determined that while the incremental dynamic analysis produced the most realistic results, the bay pushdown method produced results which closely agreed with the former. Second, it was concluded that the development of catenary forces in certain parts of the structure resulted in the development of compressive forces in other parts of the structure associated with frame action. Finally, the investigation proposed the concept of implementing ‘fuses’ to prevent the propagation of collapse in the event that the structure in question loses its capacity to

bridge over a damaged element (Khandelwal and El-Tawil 2011). These concepts will be explored further in the development of the investigations present in this thesis.

Many of the analytical techniques used to investigate structures for progressive collapse, such as the AP method specified UFC 4-023-03, use the extreme event load combination detailed in ASCE 7 [2.2]. Consequently, these methods ignore the potential impact of a co-existing wind load. The influence of this was examined by Gerasimidis and Baniotopoulos (2011). The conclusion of this investigation was that, while negligible for relatively low-rise structures, the presence of wind load could influence the behavior of taller structures significantly. However, the nature of this influence depends heavily on the specific structural system being considered (Gerasimidis and Baniotopoulos 2011).

In addition to the publications discussed above, there have been many other investigations into various aspects of progressive collapse. Since these investigations relate somewhat more remotely to the direction of this thesis, they will be discussed in brief. For more information relating to these topics, the reader is encouraged to seek out the corresponding source(s) provided in the references section. In order to better understand the behavior of actual structures, Song et al. (2010) conducted two experimental and analytical investigations of full-scale buildings undergoing collapse. Quiel and Marjanishvili (2011) discussed the impact of structural fires associated with extreme events on the progressive collapse resistance of structures. Vlassis et al. (2009) explored the consequence of falling floors (from higher stories) on the progressive collapse of multi-story structures. The influence of random imperfections on the load transfer response under a column removal scenario was explored by Szyniszewski

(2010). Finally, in order to quantify the effect of variability in design parameters, Kim et al. (2011) conducted a sensitivity analysis on a variety of parameters including: yield strength, live load, elastic modulus and damping ratio.

2.4 Theoretical Background

In this section, the theoretical concepts supporting the ideas being developed in this thesis are explained. Since understanding the cross-sectional behavior of W-sections under combined axial force and moment is necessary for developing theories and discussions related to the catenary response of ductile steel beams, this behavior is examined briefly first. In the second part of this section a discussion is presented on the behavior of ductile steel beams transitioning to catenary behavior with idealized boundary conditions. The latter was the work of Alp (2009) and formed the fundamental basis behind the concepts being discussed in later chapters.

2.4.1 M-N Interaction at the Cross-Sectional Level

Steel beams subjected to transverse loads initially resist the applied loads through the use of flexural action. However, under large displacements, significant axial components may develop, which will influence the member's ability to resist the imposed vertical loads. Structures subjected to the notional column-loss scenarios indicative of progressive collapse analyses will contain beams under the double-span condition. The result of this increase in span length is a corresponding increase in moment demand within the steel beams. Consequently, there is a significant possibility that one or more of these beams will reach flexural capacity under the imposed loading. Subsequently, the

beams must make use of catenary behavior in order to provide the reserve capacity necessary to sustain the loads. After flexural yielding, the beams achieve this through a ductile transition from moment (M) to axial force (N) (Marchand and Alfawakhiri, 2004). Details regarding the specific nature of this transition will differ depending on the type of cross-section being considered. However, for the sake of brevity, the formulas being presented in this section will be limited to those applicable for steel W-sections.

At the cross-sectional level, the distributions associated with the various states of stress may be integrated over the cross-section in order to obtain the corresponding moments and axial forces. Total yielding of the cross-section may be achieved under a variety of combinations of axial force and moment. Since the wide-flange W-sections conventionally used in steel structures are symmetric, the plastic neutral axis (PNA) location associated with full yielding of the cross-section under conditions of pure moment will be through the centroid of the cross-section. However, the presence of an axial force will cause a migration of the neutral axis away from the centroid and towards one of the outer flanges (depending on the orientation of the associated moments and axial forces). For W-sections, M-N interaction equations describing the yield surface, obtained from Horne (1979), are shown in Equations [2.7] and [2.8].

When the PNA is located in the web,

$$\frac{M}{M_P} = 1 - \left[\frac{N}{N_P}\right]^2 \frac{A^2}{4t_w Z_x} \qquad M, N \geq 0 \qquad [2.7]$$

When the PNA is located in the flange,

$$\frac{M}{M_P} = \left(1 - \frac{N}{N_p}\right)\left[1 - \left(1 - \frac{N}{N_p}\right)\frac{A}{2b_f d}\right]\frac{Ad}{2Z_x} \qquad M, N \geq 0 \qquad [2.8]$$

where:

M = Applied moment

M_P = Plastic moment

N = Applied axial force

N_P = Plastic axial force

A = Cross-sectional area

t_w = Web thickness

Z_x = Plastic section modulus

2.4.2 Behavior of Ductile Steel Beams Transitioning to Catenary Action (Alp 2009)

Alp (2009) conducted a rigorous investigation on the behavior of ductile steel beams as they transition from flexural to cable behavior. Since this thesis discusses the behavior of these beams in actual steel framed structures, Alp (2009) served as a foundation for the major investigations presented in the remaining chapters. The following topics were addressed by this document:

- Development of theoretical models to predict the response of beams transitioning from flexural to catenary behavior for rectangular and W-shaped cross-sections
- Verification of theoretical models through FE analysis techniques

- Development of equations to predict the mid-span deflection at the onset of catenary behavior
- Investigation on the effect of elastic boundary conditions on beam behavior
- Correlation of beam models to full steel framed structures

In this study, theoretical models were developed to establish the load-deflection and force-deformation responses of various idealized systems. The following cases were examined: a simply-supported beam with a concentrated load at mid-span, a fully fixed beam with a concentrated load at mid-span, and a fully fixed beam with a uniformly distributed load applied along the length. A unique approach was utilized in the development of these relationships that considered two bounding theories: rigid-plastic theory and cable-theory.

Rigid-plastic theory assumes that there is no deformation response associated with elastic behavior. In other words, the beam does not begin to deflect until yielding begins to occur. Since an idealized, elastic-perfectly plastic moment-curvature relationship was assumed concurrently, the beam exhibited no flexibility until the plastic moment capacity had been reached. Conversely, cable-behavior assumes that the beam has no flexural rigidity. According to this assumption, the beam is unable to develop moment capacity and all vertical loads must be carried by the development of axial tension within the member. These two types of behavior are ideal and indicative of either infinitely short or infinitely long beams. Figure 2-7, displayed below, depicts the M-N response for the two idealizations in conjunction with curves illustrating the potential behavior of actual steel beams (Alp 2009).

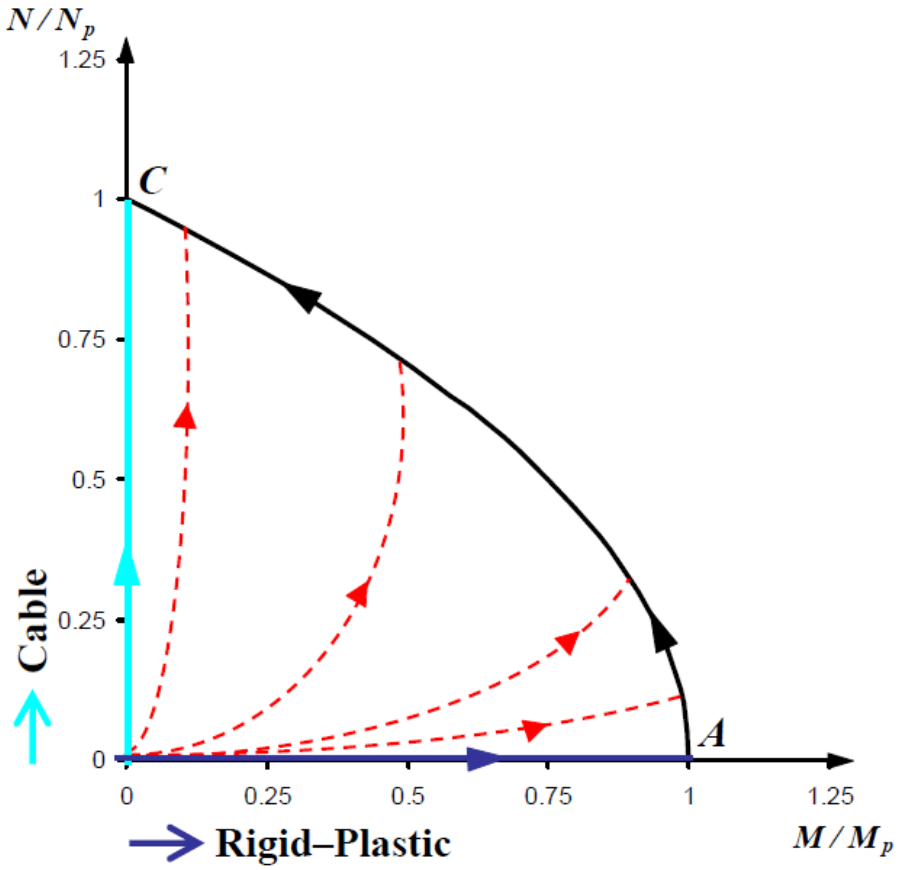

Figure 2-7 M-N Relationships for Actual Steel Beams (Alp 2009)

From Figure 2-7, it can be seen that actual steel members will exhibit some amount of axial force development prior to reaching the yield surface. However, once full yielding of the cross-section has been achieved, the beam will follow along the yield surface as it continues to deflect until it reaches a state of pure cable behavior (N = Np).

After developing theoretical models to predict the response of the various systems under the two bounding theories, Alp (2009) verified these models with analytical results. The principal of superposition was then applied with results from the two theories in order to develop equations to predict the onset of catenary action for various systems.

However, in order to restrict this discussion to topics more explicitly relevant to this thesis, a full review of these topics will not be provided.

Alp (2009) also investigated the influence of elastic boundary conditions on the behavior of ductile steel beams under combined moment and axial force. The investigation considered the effects of both translational and rotational restraint and their combined effects. The three idealized beam models used in this study are shown below in Figures 2-8, 2-9 and 2-10.

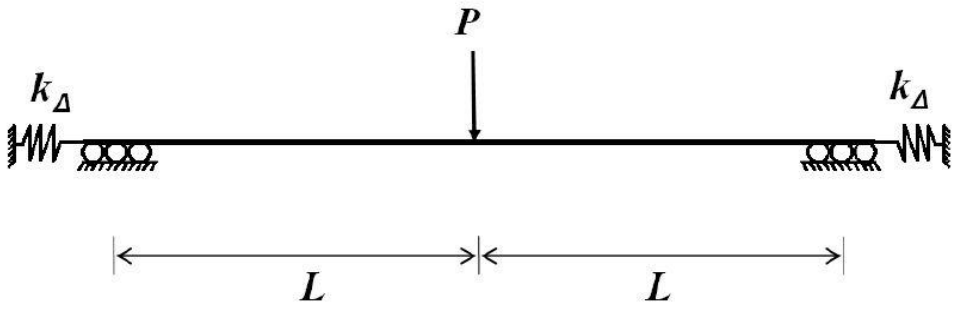

Figure 2-8 Beam with Translational Springs Only (Alp 2009)

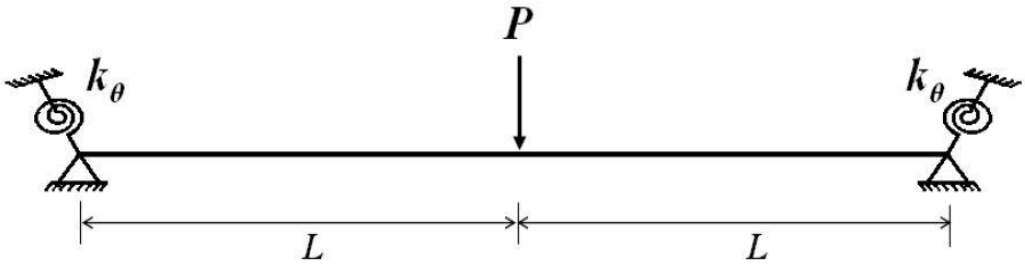

Figure 2-9 Beam with Rotational Springs Only (Alp 2009)

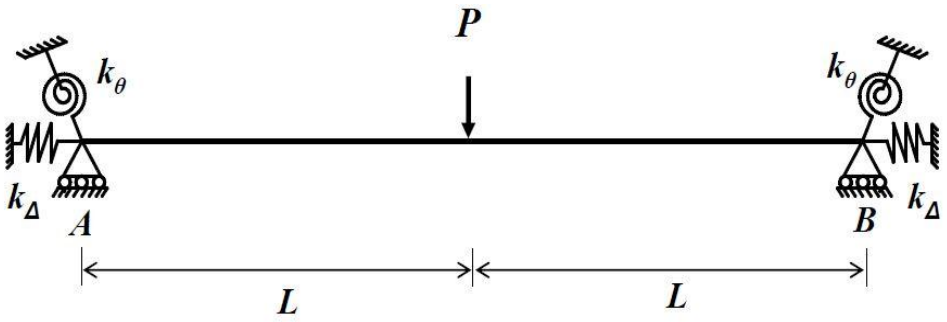

Figure 2-10 Beam with Combined Springs (Alp 2009)

Through the course of this study, Alp (2009) found that significant axial restraint profoundly influenced the beam's ability to resist higher levels of load at lower levels of deflection. This result is shown below in Figure 2-11. Note that in this figure, the load is normalized with the equivalent plastic collapse load of a fixed-fixed beam (P_c) and the mid-span deflection underneath the concentrated load is normalized with respect to the beam depth (d). Levels of axial restraint increase from the lowest level (TR1) to the highest level (TR10).

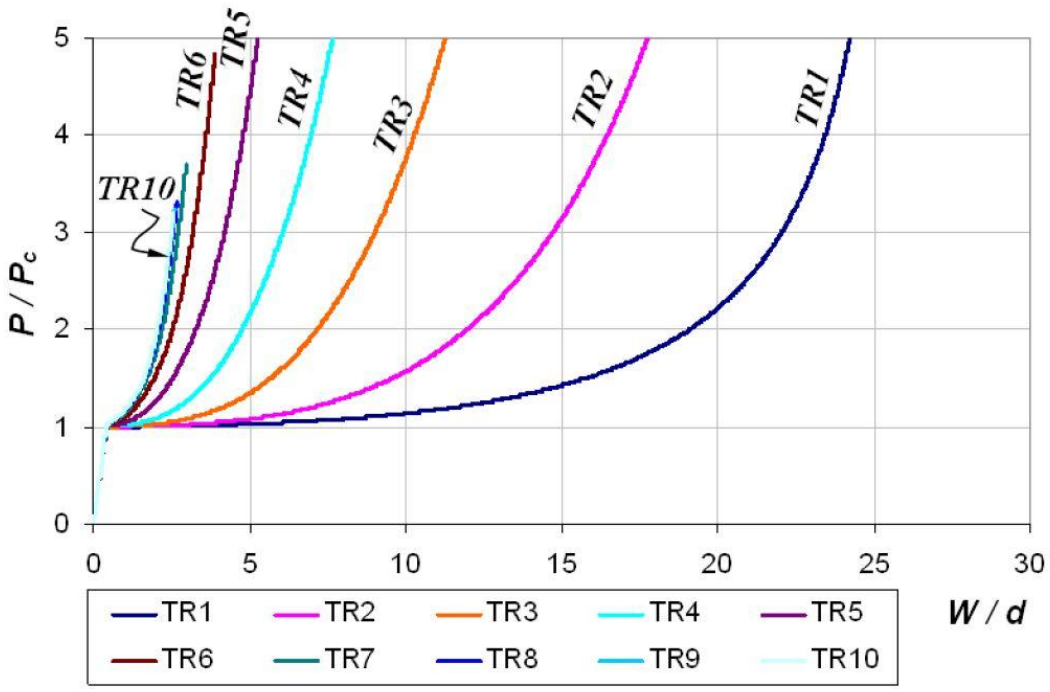

Figure 2-11 Load-Deflection Plot for Beams with Translational Springs (Alp 2009)

Moreover, beams with higher axial restraint were shown to transition from flexural to cable behavior faster and at lower levels of deflection. Correspondingly, the deflection at the onset of pure cable behavior was seen to be lower in these beams (Alp 2009).

However, Alp (2009) found that varying the level of rotational restraint yielded results significantly more complicated than the case with translational springs alone. The outcome was that the deflection at the onset of catenary behavior initially increased with increasing rotational restraint up until a specific level of resistance. For lower levels of restraint, hinge formation at the ends could occur under a predominantly flexural response and significant axial force needed to be allowed to develop in order for a hinge to form under a combination of moment and axial force. Consequently, prior to hinge

formation, these systems exhibited a response more indicative of a simply-supported beam. Once hinge formation occurred, these beams approached the behavior exhibited by the fixed-fixed case (Alp 2009).

In comparing the influence of both types of restraint, it was discovered that the level of axial restraint was significantly more influential on the behavior of the beam at the onset of catenary action. Table 2-5 shows the results of the investigation containing beams with both types of springs with respect to the mid-span deflection at the onset of catenary behavior (W_{cat}).

Table 2-5 Results for Beam Models with Combined Springs (Alp 2009)

Group No	Name	k_{Δ} (kip/in)	k_{θ} (k-in/rad)	W_{cat} (in)	W_{cat}/d
1	**K11**	1	1	345.67	24.87
	K12	1	5000	353.58	25.44
	K13	1	500000	349.90	25.17
	K14	1	50000000	349.85	25.17
2	**K21**	24	1	147.66	10.62
	K22	24	5000	154.89	11.14
	K23	24	500000	152.40	10.96
	K24	24	50000000	152.27	10.95
3	**K31**	400	1	49.27	3.54
	K32	400	5000	56.89	4.09
	K33	400	500000	54.70	3.94
	K34	400	50000000	54.23	3.90
4	**K41**	25600	1	29.34	2.11
	K42	25600	5000	39.11	2.81
	K43	25600	500000	36.92	2.66
	K44	25600	50000000	36.12	2.60

From Table 2-5, it can be seen that the mid-span deflection at the onset of catenary behavior varies significantly with changes in the translational spring stiffness. The level of rotational restraint provided smaller variations within each of the groups. Figures 2-12, 2-13 and 2-14 show the normalized load-deflection, axial force-deflection and moment-deflection plots for each group.

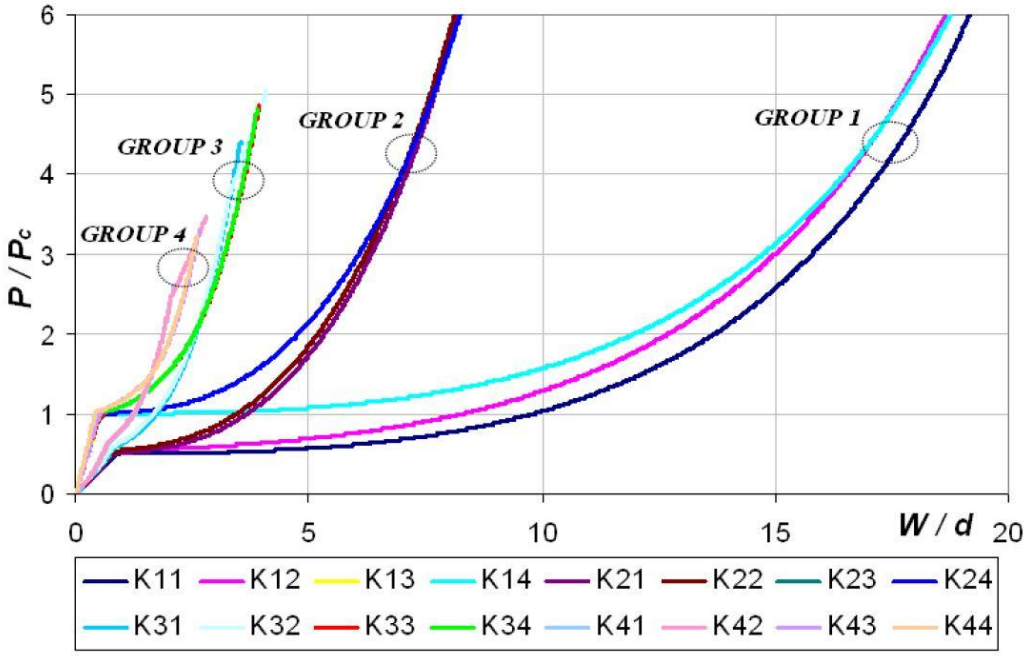

Figure 2-12 Normalized Load-Deflection Plot for Combined Spring Cases (Alp 2009)

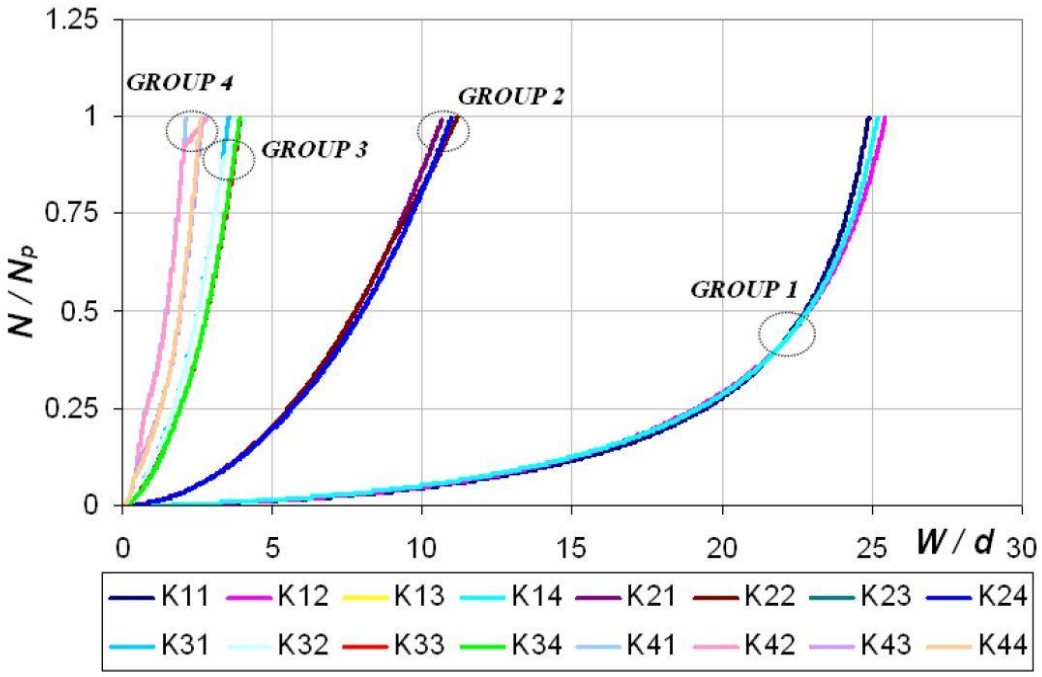

Figure 2-13 Axial Force-Deflection Plot (Mid-span) for Combined Spring Cases (Alp 2009)

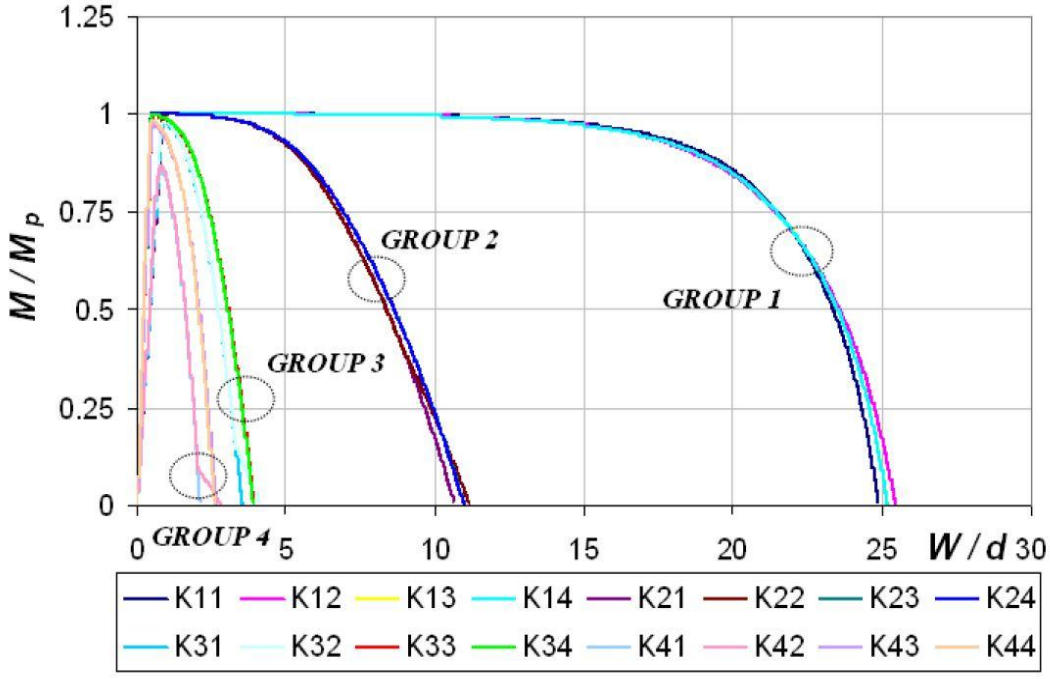

Figure 2-14 Moment-Deflection Plot (Mid-span) for Combined Spring Cases (Alp 2009)

Similar to the behavior indicated in Table 2-5, it can be seen from Figure 2-12 that the level of translational restraint profoundly influenced the beam's ability to sustain higher levels of load at correspondingly lower levels of mid-span deflection. The level of rotational restraint provided relatively small variations in the load-deflection response within each group. Moreover, from Figures 2-13 and 2-14, it can be seen that it is primarily translational restraint that influences the rate at which a beam transitions from flexural to pure cable behavior. This faster transition corresponds to the increased capacity at relatively lower deflection levels which was previously mentioned.

After investigating the behavior of beams with idealized support conditions, Alp (2009) then provided some correlation of these results with an FE analysis of a simple steel-framed structure. The structure used for this comparison is shown below in Figure 2-15 in conjunction with the idealized beam.

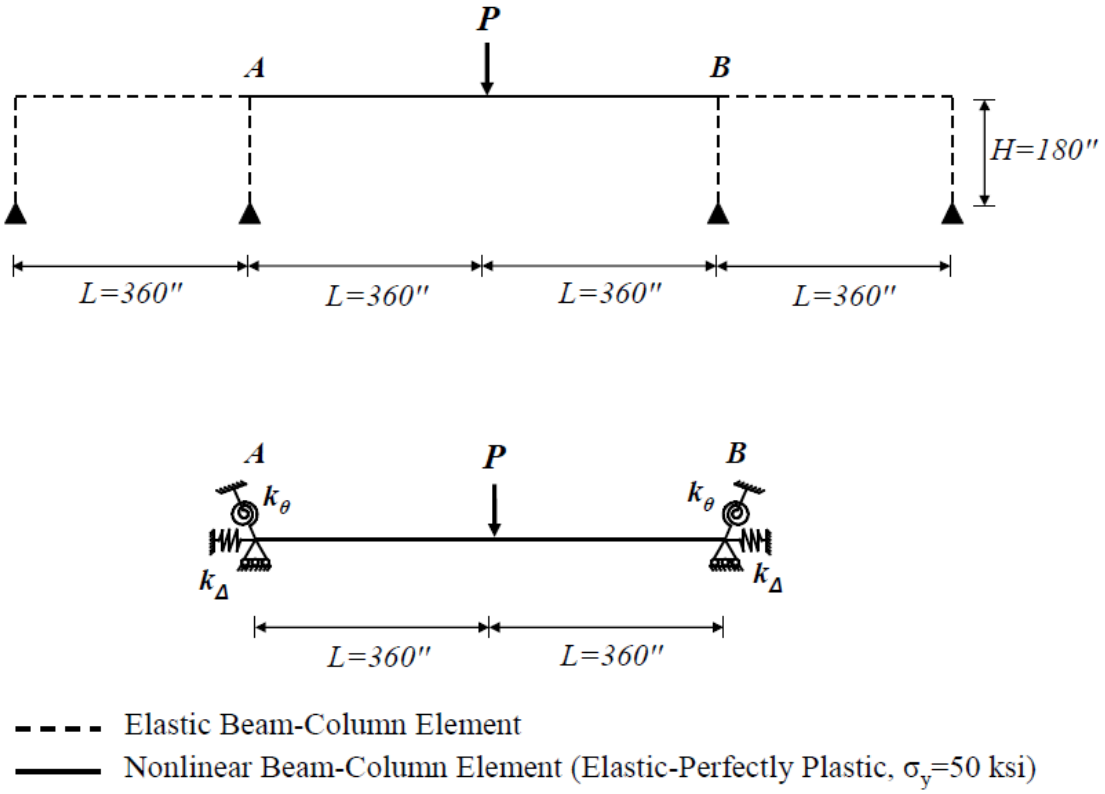

Figure 2-15 Beam and Frame Models used in Comparison (Alp 2009)

As noted in Figure 2-15, the side frames that correlate with the translational and rotational springs were restricted to linear-elastic behavior. Sources of material and geometric nonlinearity in the structure were limited to the beam transitioning from flexural to catenary behavior. The stiffness values associated with the side frames were obtained by taking the slope of the load-deflection curve resulting from an OpenSees analysis of an individual frame with a unit force or moment applied. These values were then used to quantify the spring constants for the beam model. The behavior of the beam

was then monitored as it transitioned into full catenary action under the applied concentrated load (Alp 2009).

The results of the study showed an excellent correlation between the beam and frame models. The normalized load-deflection plot produced from the analysis is shown below in Figure 2-16.

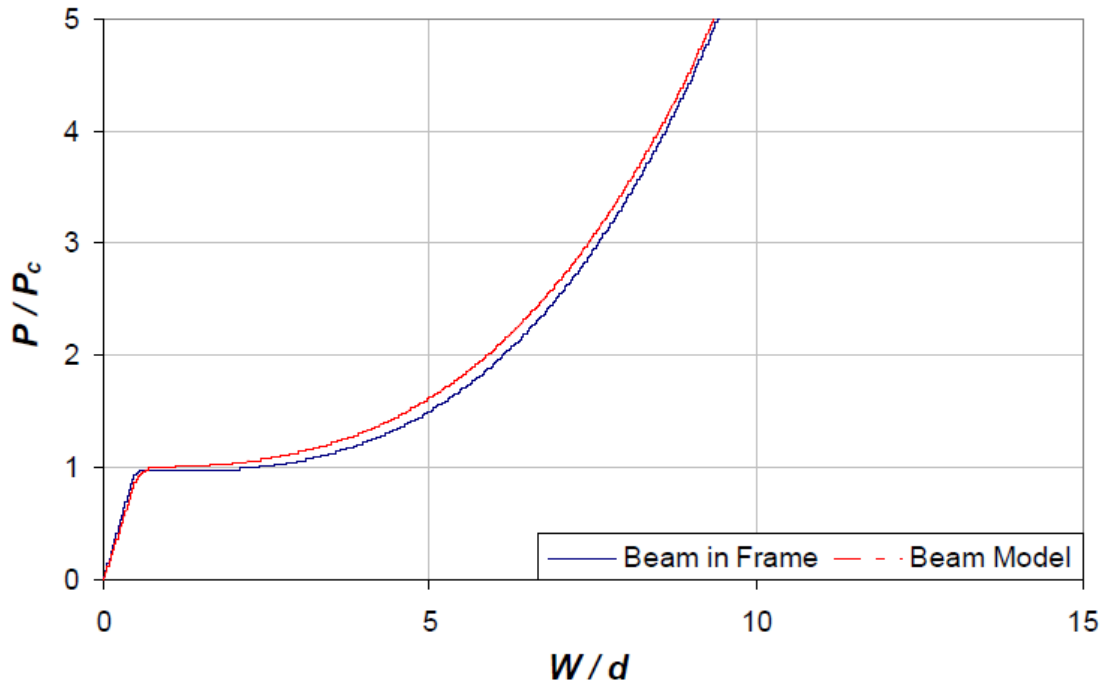

Figure 2-16 Load-Deflection Plot for the Beam and Frame Models (Alp 2009)

As indicated by Figure 2-16, there were some small differences between the beam and frame models, but there was a very close overall correlation. These differences can be attributed to the development of initial compressive forces in the elastic region for the beam in the full frame model (Alp 2009).

2.5 FE Modeling

All finite element analyses performed as a part of this study were conducted using the *Open System for Earthquake Engineering Simulation* (OpenSees) finite element software package (McKenna et al. 2000). This software was selected based upon its historic use here at Auburn University and its applicability to the problems being considered in this study. While OpenSees has the capability to produce three-dimensional (3D) models, its use was restricted to two-dimensional (2D) macro-models for the purposes of this research. Within this finite element modeling section, the basic aspects of OpenSees are discussed with a particular focus on the components that were the most essential for this investigation.

2.5.1 Material Models

OpenSees has the capability to integrate a variety of material models into each analysis. However, the two most important for this thesis research were the linear-elastic and elastic-perfectly plastic material models. These models are depicted below in Figures 2-17 and 2-18.

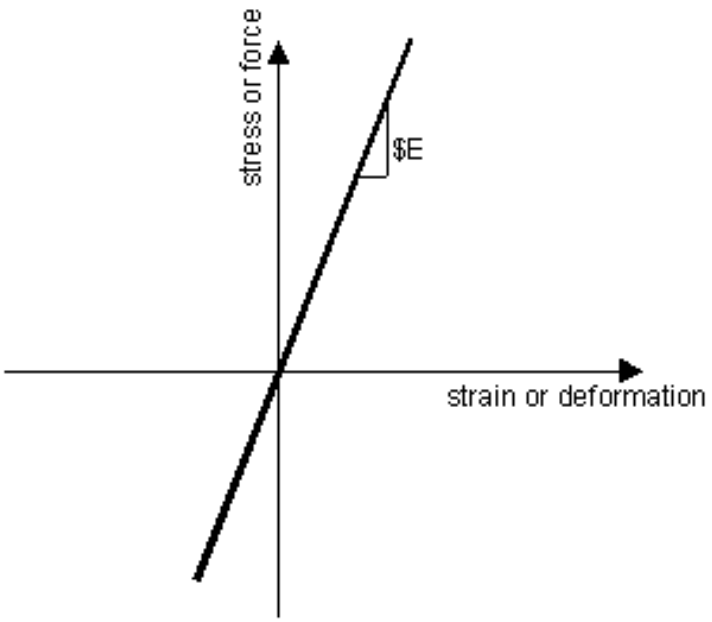

Figure 2-17 Linear-Elastic Material Model (McKenna et al. 2000)

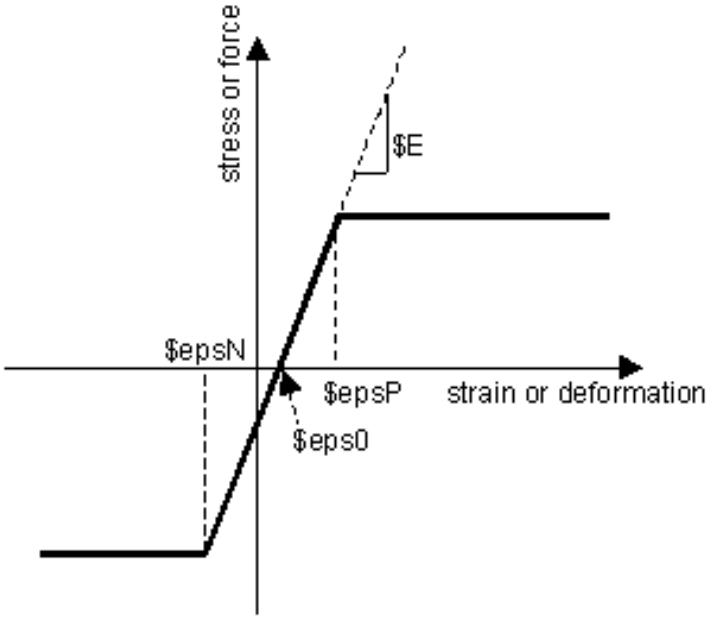

Figure 2-18 Elastic Perfectly-Plastic Material Model (McKenna et al. 2000)

From the preceding figures, it can be seen that all that is required to define these two materials in OpenSees is the specification of an elastic modulus ($E), and for the

elastic perfectly-plastic material model, the inclusion of a strain that defines the onset of plastic behavior in tension and compression ($epsP, $epsN). Note that the inclusion of an initial elastic strain ($eps0) is optional and was not utilized in this research study.

2.5.2 Element Types

Among the variety of element types available for use in OpenSees, beam-column elements are particular useful for fast-running, 2D frame analyses. Consequently, this general element type was used for all frame models. The specific beam-column elements utilized in this study were the elastic beam-column element and the non-linear, force-based beam-column element.

For simplicity, the elastic beam-column element may be utilized in lieu of defining an elastic section with the nonlinear beam-column element. Defining this element type only requires inputting a modulus of elasticity, cross-sectional area and moment of inertia (about the major axis of bending). Due to its simplicity, this element was utilized to define members for areas where linear-elastic behavior was desired.

When nonlinear material behavior must be considered, the two best options available in OpenSees are the displacement-based beam-column and the force-based beam column. The difference in these two element types is inherent in their formulations. In other words, the formulation of the displacement-based beam-column is based upon expressions of displacement, whereas the formulation of the force-based beam-column is based upon expressions of force (this may be iterative or non-iterative). The behavior of these two element types differs significantly. The displacement beam-column is based upon a cubic shape function. As a result, its curvature distribution is

linear within an element. Consequently, the displacement beam-column will yield results that show greater element stiffness than its force-based counterpart. Because of this behavior, in order to obtain results of a reasonable level of accuracy, it is necessary to utilize more elements than if the force beam-column was used. Additionally, using a substantial amount of displacement beam-columns in an analysis will occasionally cause complications with global system convergence. However, this element type has an advantage over the force beam-column in that it rarely has difficulties with compatibility between forces and deformations at the local element level. Both element types consider the spread of plasticity along the element and are capable of considering equilibrium in the deformed shape, which is important for progressive collapse applications.

Unlike the elastic beam-column element, it is necessary to specify a section in the definition of a displacement-based or force-based beam-column. This is essential in order to consider the effects of plasticity on the element's behavior. Integration points must also be specified in order to numerically evaluate the integrals associate with the element using Gauss-Lobatto quadrature.

2.5.3 Section Definitions

Section definitions are used in OpenSees in conjunction with certain element types in order to ascertain the properties of a specific element and/or its general response. There are several options available for doing this. For the purposes of this investigation, it was determined that an approach involving fiber sections was optimal.

Utilizing fiber-sections in a 2D analysis is imperative for capturing the transition from flexural to catenary behavior. The reason for this is that, by definition, beam

elements are not able to capture the spread of plasticity through a cross-section. Consequently, they are unable to represent the upward migration of the neutral axis that occurs during the transition to catenary behavior. By discretizing a cross-section into local "fibers" that will be integrated to determine the cross-sectional response and using this section definition for the beam elements, it is possible to obtain element forces and deformations comparable to what would be obtained from a more sophisticated micro model comprised of elastic-plastic shell elements. The main advantage of this approach is that a significant amount of computational effort is saved by using a simplified macro model with beam elements. Additionally, an appreciable amount of time can be saved during construction and optimization of the model. Finally, macro models are substantially easier to modify in the event that multiple analyses need to be conducted for comparison purposes.

In OpenSees, fiber sections can be constructed using several different methods. Individual fiber locations may be specified, or fibers may be specified using layer or patch commands. In this particular analysis, the patch command was utilized for simplicity. This approach involves specifying four nodal locations for the quadrilateral patch and the number of element subdivisions for both in-plane directions over the cross-section. Figure 2-19 shows a depiction of a general quadrilateral patch.

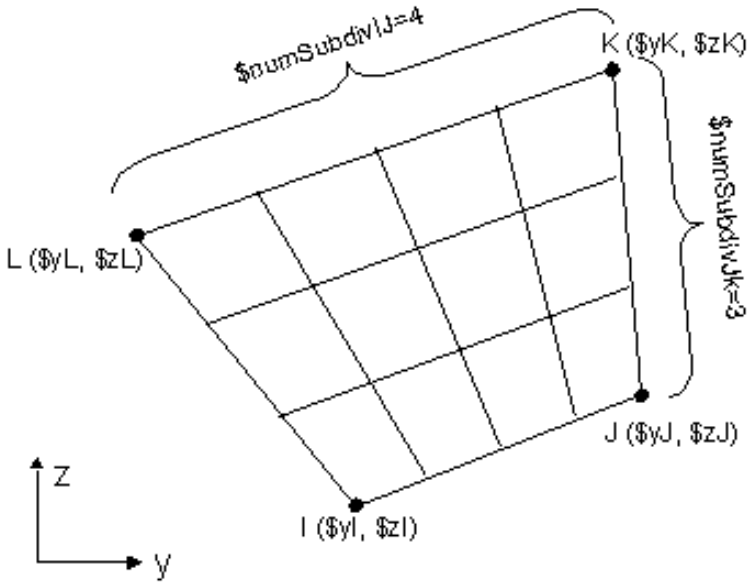

Figure 2-19 General Quadrilateral Patch (McKenna et al. 2000)

For the W-sections used in this investigation, three quadrilateral patches were utilized to represent each cross-section: one for the web and one for each flange. 200 fiber divisions were utilized for each vertical inch of the cross-section in order to achieve reasonable accuracy. Note that this approach ignores the contribution of the fillets to the cross-sectional behavior. This was accounted for throughout this thesis research.

2.5.4 Geometric Transformations

In addition to material and section definitions, a geometric transformation type is also specified in OpenSees when defining elements. These transformations change element stiffnesses and their associated forces from the local coordinate system to the global coordinate system. Depending on how this transformation is accomplished, it is possible to include the effects of geometric non-linearity on the element being

constructed. Throughout the course of this research, three geometric transformations were utilized: the "linear transformation", the "corotational transformation" and the "p-delta transformation." The information contained herein related to these transformations was developed by De Souza (2000).

The first translation type, the linear transformation, assumes simplifications with respect to the behavior of the element in order to convert stiffness and resisting force from one reference frame to the other. These simplifications include infinitesimal displacements and rotations and small values of strain within the element. Consequently, this transformation type is only useful for applications where large displacements and deformations are not anticipated.

The second transformation type, the corotational transformation, accounts for arbitrarily large rotations and displacements by attaching a coordinate system that will displace and rotate along with the element. Rigid body motion is then separated from element deformations. Due to the nature of the formulation, there are no limitations on the range of these rigid body motions. Consequently, using the corotational transformation, it is possible to consider problems that include large rotations and displacements. However, this approach does not account for large strains along an element. This contingency may be bypassed by using proper finite element discretization.

The third transformation type, the p-delta transformation, performs a linear transformation of stiffness and force, but considers the influence of second-order effects. This transformation type was utilized in lieu of the corotational transformation with beams not expected to experience catenary behavior in the situation where element loads

were being implemented. This was because the formulation of the corotational transformation ignores the influence of element loads.

2.5.5 Loads

Loads may be applied in OpenSees according to a variety of load patterns and types. For the purposes of the research contained in this thesis, the "plain" load pattern from OpenSees was sufficient. This load pattern allows for the application of nodal loads, element loads and single-point constraints. Within a single pattern, multiple loads of different (or identical) types may be specified. These loads are then applied according to a specified time series, which defines the relationship between the load factor and the time domain. The "linear" time series was used consistently for every model constructed as a part of this thesis. This specific time series increases the load factor linearly according to a specified slope. The default slope of 1.0 was maintained for each model.

2.5.6 Analytical Methodology

Following construction of a model, in addition to designation of the analysis type, it is necessary to specify information that will determine how the analysis will be conducted. Topics associated with these parameters are as follows: constraint enforcement, numbering of degrees of freedom, non-linear solution procedure, the method of storing and solving the system of equations, the method of advancement for each time-step and the convergence criterion.

In all OpenSees models contained within this investigation, constraints were enforced using Lagrange multipliers. For efficiency, the reverse Cuthill-Mckee

numbering algorithm was utilized to reduce the bandwidth of the matrices. The non-linear solution method chosen for all models in this investigation was the Newton-Raphson method. The system of equations were stored and solved as general banded matrices. For simplicity in post-processing, each time step was advanced according to an incremental displacement. Finally, convergence of each solution was determined according to an energy increment test.

Chapter 3 – Baseline System

3.1 Overview

In this chapter, the study of the baseline system is described in detail. First, the concept of the baseline system is explained and its pertinence to this thesis is clarified. Following this, a brief outline of the frame design procedure is provided. Next, details of the FE model are given. Finally, the results of the FE analyses are provided for four column-removal scenarios; discussions of points of interest are supplied throughout the presentation of results with a more comprehensive discussion given at the end of the chapter.

3.2 Concept

The baseline system was developed in order to investigate the effects of multiple perimeter column-removal scenarios on the behavior of a realistic structural system considering varying levels of nonlinearity in the lateral load-resisting system (LLRS). The baseline system also served as a control for the parametric study presented in Chapter 4. Of primary interest in this investigation are: the effect of the model type (level of nonlinearity considered in the LLRS) on the system behavior, the effect of catenary behavior on the load-carrying capacity of the structure, and the potential impact of connection ductility demands. Due to the nature of catenary behavior in steel beams, each analysis was conducted as non-linear static; appropriate load modifiers were

implemented from UFC 4-023-03 to account for inertial effects. Plan and elevation views of the structure and one of its perimeter moment frames are shown below in Figures 3-1 and 3-2 respectively.

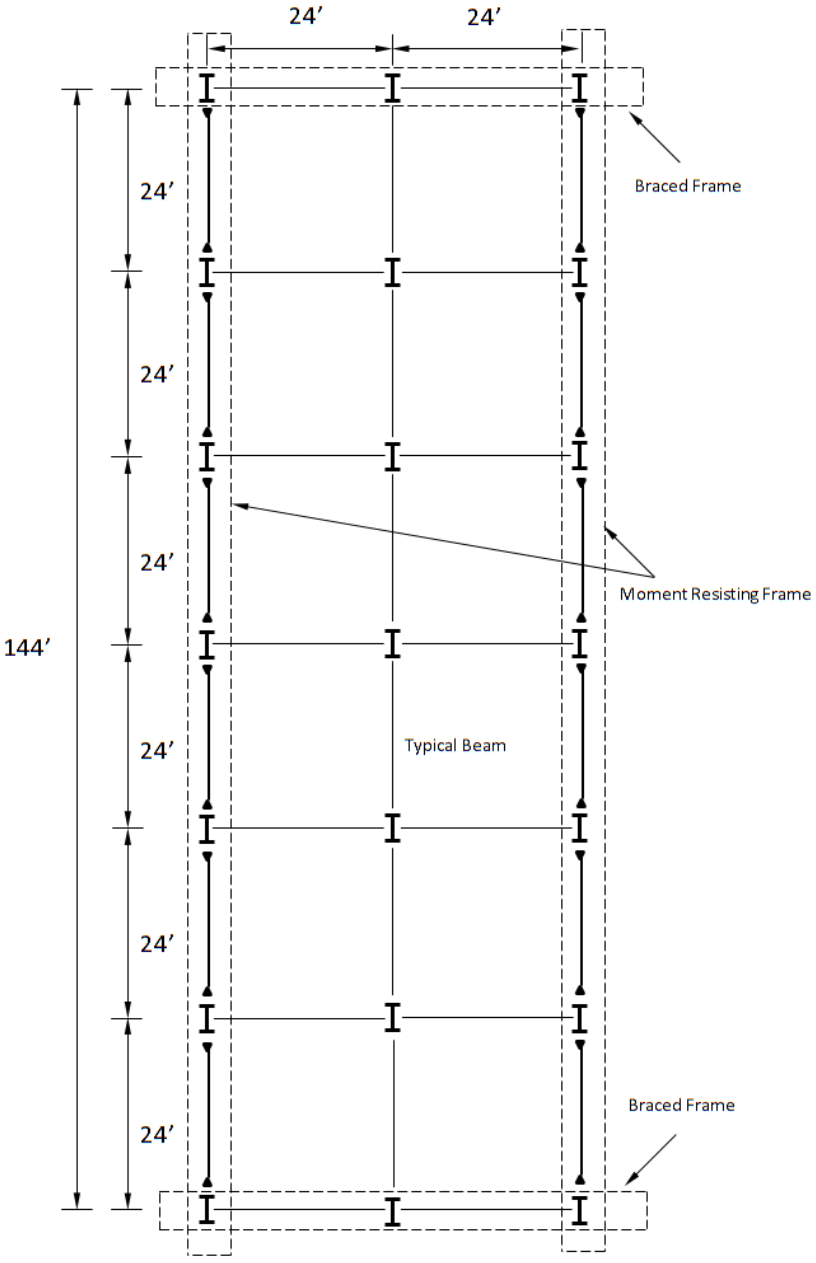

Figure 3-1 Plan View of the Baseline System

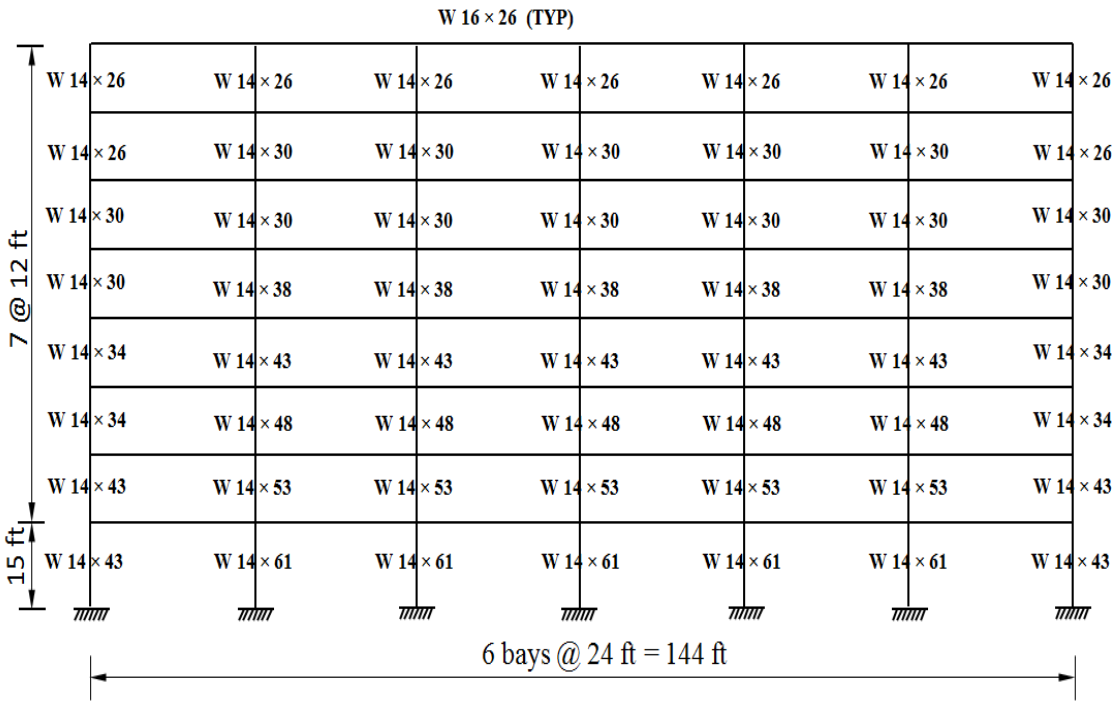

Figure 3-2 Elevation View of the Baseline System's Perimeter Moment Frame

As seen in Figures 3-1 and 3-2, the structure was designed as an eight-story, two-bay steel-framed structure. Bay widths were uniformly taken as 24 ft. The bottom story height was selected to be 15 ft; other stories have a height of 12 ft. The footprint of the structure has dimensions of 144 ft x 48 ft. The total height of the building is 99 ft. The structure was dimensioned to reflect a realistic, but not necessarily typical, multi-story office building. Moreover, the dimensioning allows for variations in several characteristics that were investigated as a part of the parametric study, such as the number of bays included in the LLRS and the number of stories. Further details relating to these effects are discussed in Chapter 4. Finally, as indicated in Figure 3-1, the baseline system utilizes perimeter moment frames along the longer sides and braced frames along the shorter sides for stability considerations. Internal bays were designed to

resist gravity loads alone. The focus of this thesis is on the response within the perimeter moment frames. As such, all discussions herein relate to the collapse-resistance of these frames.

A major part of the baseline study was exploring the influence of various perimeter column-removal scenarios on the response within the corresponding moment frame. Four different column-removal locations were considered, in the following order: The central column, the column directly adjacent to the central column, the penultimate column, and the corner column. These locations are shown below in Figure 3-3.

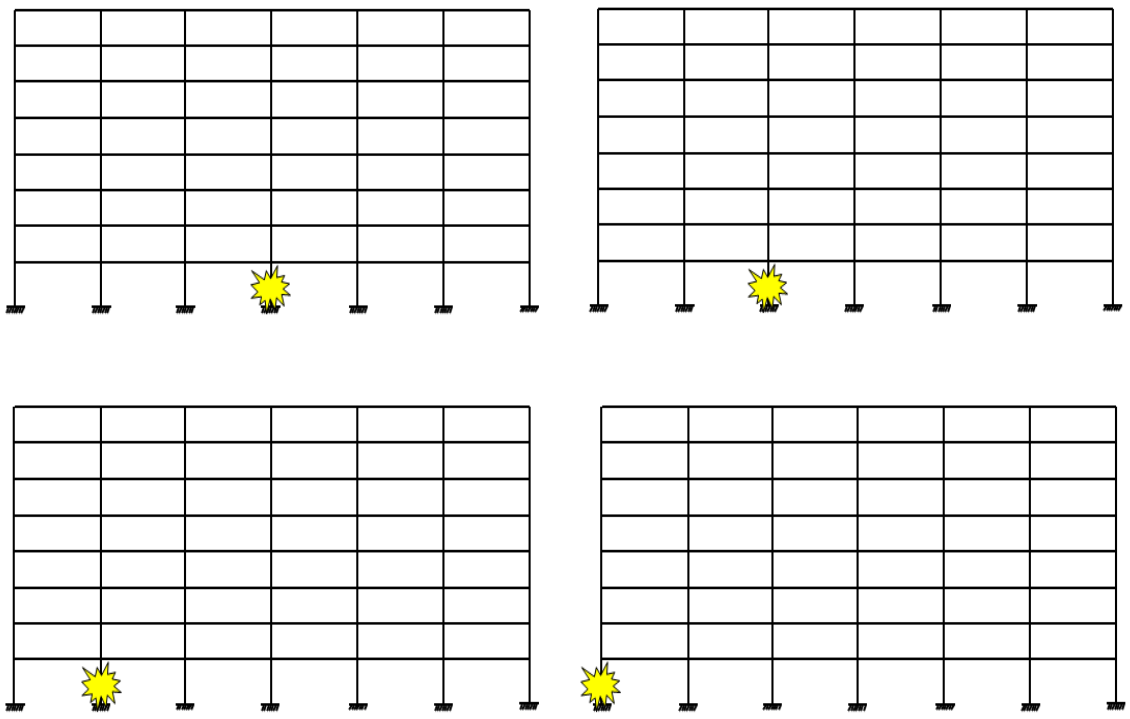

Figure 3-3 Column-Removal Scenarios Considered in the Baseline Study

All columns were removed notionally, as discussed in UFC 4-023-03. In addition to assumptions relating to the manner and location of column-removal, several other simplifying assumptions were used throughout the course of the baseline study:

- Non-composite action was assumed for all beams in both the design and FE analysis procedures.
- The presence of the floor slab was ignored in the FE analysis models, but its weight was accounted for.
- Fully-ductile connection behavior was assumed in each model. However, the implications of potential connection ductility limitations are discussed throughout this thesis.
- The beams were assumed to be sufficiently braced out-of-plane such that lateral-torsional buckling was not a concern. Local buckling was also not considered as a limit state in the FE analyses.
- The influence of shear deformations and inelastic panel zone behavior were not considered.
- 3-D Effects were not considered.
- All modeled structures were assumed to have fixed bases.

3.3 Design

In this section, the load selection and design procedure for the baseline system is explained in further detail.

3.3.1 Loading

As previously mentioned, the baseline system was designed as a multi-story office building; the building location was chosen to be Atlanta, GA. Loads were obtained from ASCE 7-05. The vertical (gravity) loads chosen for the structural design are as follows:

- Concrete Slab Weight - 50 psf
- Superimposed Dead Load (Floor) – 50 psf
- Superimposed Dead Load (Roof) – 60 psf
- Live Load (Floor and Roof) – 50 psf

Additionally, the baseline system was designed for both wind and seismic loads, chosen based upon the building's location.

3.3.2 Member Selection

The commercial software package SAP2000 (CSI 2012)was utilized for the design of the structure, which was conducted according to the specifications in AISC (2005). In the design process, all beams were restricted to the same section for simplicity in the comparisons of catenary force development. Column sections were restricted by floor location, with one exception: the two outermost column sections at each floor were allowed to differ. The moment frames were designed as ordinary moment frame (OMF)

systems, since this produced the most economical design. The resulting sections are shown in Figure 3-2.

3.4 FE Model Description

Within this section, details related to the development of the baseline frame FE model are discussed. General modeling concepts and considerations were described in Chapter 2.

In order to capture the influence of catenary behavior in the beams directly above the removed columns, an approach was utilized that was previously developed by Scott et al. (2008) and implemented by Alp (2009). In this approach, fiber-section discretization is utilized in conjunction with the force-based beam column and the corotational transformation. The contributions of each to developing catenary behavior were described in the corresponding sections in Chapter 2. To account for the influence of large strains, 100 element divisions were used along the length of each beam being considered for this type of behavior.

Loads for each pushdown analysis were applied according to the NSP outlined in UFC 4-023-03, but without consideration for the notional lateral load. Since the consideration of initial imperfections was not included in the scope of this study, exclusion of this notional lateral load was desired in order to prevent its influence from obscuring the results of the analyses. The loading arrangements utilized for each column-removal scenario are shown below in Figure 3-4.

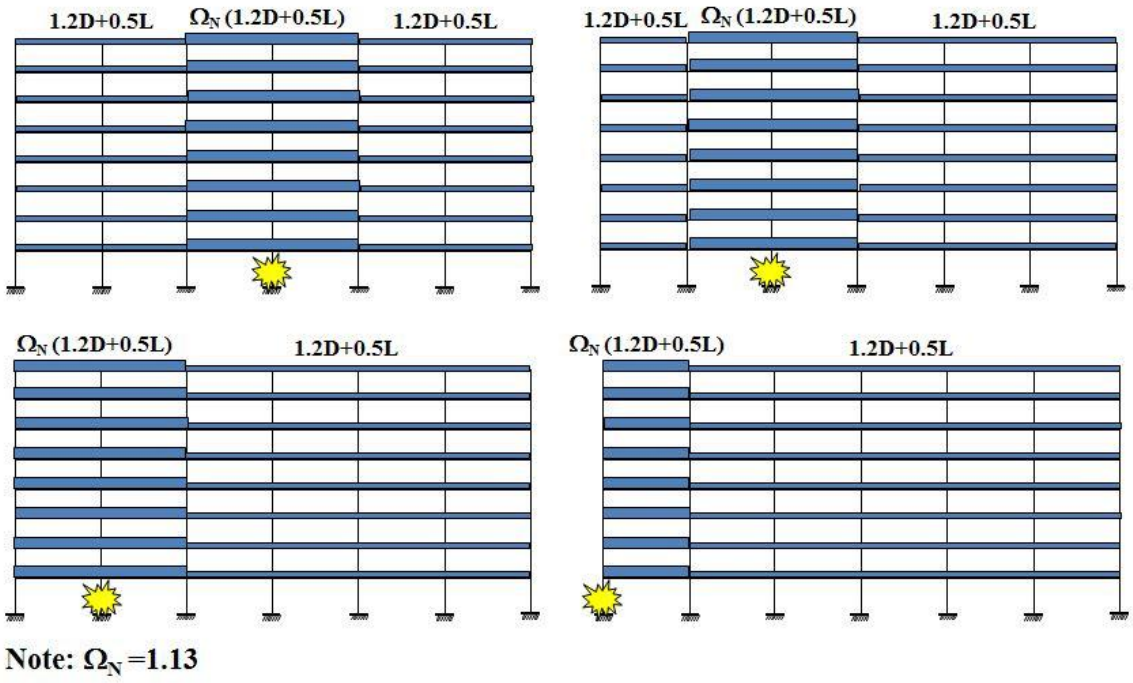

Figure 3-4 Loading Arrangements for FE Analyses

The NSP dynamic amplification factor from UFC 4-023-03, labeled Ω_N in Figure 3-4, was applied to loads in the bays directly above the removed column. This factor was determined by using the following equation:

$$\Omega_N = 1.08 + \frac{0.76}{\left(\frac{\theta_{pra}}{\theta_y} + 0.83\right)} \quad [3.1]$$

Where

Ω_N = Dynamic increase factor for nonlinear static analysis

θ_{pra} = Plastic rotation angle

θ_y = Yield rotation angle

The value of θ_y in [3.1] was calculated from equation 5-1 in ASCE 41-06 and found to be 0.0134 (rad). UFC 4-023-03 TF requirements state that the steel beams and their connections must be capable of a total rotation capacity of 0.2 (rad) in order to be considered for TF development. Therefore, since there has been insufficient research on fully-restrained connection behavior under these loading conditions, and since the consequences of potential connection fracture were not considered implicitly in the models, 0.2 (rad) was selected as the total rotation capacity for load-calculation purposes. Subsequently, θ_{pra} was determined to be 0.1866 (rad); the load-increase factor applied to the amplified bays, Ω_N, was then found to be 1.13. Details related to implementation of the load patterns into Opensees and the analytical methodology used in all analyses were described in sections 2.5.5 and 2.5.6 respectively.

Each column-removal scenario contained three distinct analyses. In the first analysis, the columns and beams in the frames adjacent to the beams in the double-span condition, hereafter called "side-frame" beams and columns, were modeled with the linear geometric transformation and elastic material model discussed in Chapter 2. The second analysis considered material nonlinearity in the side-frames. To model this, an elastic perfectly-plastic material model was used for the pertinent members. Since A992 steel was used in the structural design, a yield stress of 50 (ksi) was defined in the material model; this corresponded to a yield strain of .001724 (in/in). In the third analysis, both material and geometric nonlinearity were considered in the side-frames. As in the second analysis, the elastic perfectly-plastic material model was utilized for all beams and columns within the side-frames. Geometric nonlinearity in the columns was

accounted for by using the corotational geometric transformation. Since the beams in the side-frames were being subjected to distributed loading along the element length, the corotational transformation could not be used to account for geometric nonlinearity. Instead, the p-delta transformation was implemented to consider this effect. However, in preliminary analyses, it was determined that, unlike for the columns, the consideration of geometric nonlinearity for the beams in the side-frames should not significantly influence the system behavior.

3.5 FE Model Results

In this section, the results of each column-removal scenario are discussed sequentially, in the following order: The central column (scenario 1), the column directly adjacent to the central column (scenario 2), the penultimate column (scenario 3), and the corner column (scenario 4).

3.5.1 Presentation of Results

Results are presented in a format that most clearly highlights the concepts being investigated in this thesis. The following topics are addressed within the subsections of each scenario: The influence of the model type, the general response of the system, the response of the beams exhibiting catenary behavior, and the development of connection ductility demands.

As previously discussed, in order to ascertain the effects of considering material and geometric nonlinearity in the side-frame models, three different model types were developed. For simplicity, the three model types are classified in the following manner

for the remainder of this thesis: linear-elastic (includes no geometric or material nonlinearity in the side-frames), linear-inelastic (accounts for material nonlinearity alone), and nonlinear-inelastic (accounts for both material and geometric nonlinearity).

In all column-removal scenarios, the results indicated that both geometric and material nonlinearity significantly influenced both the behavior of the side-frames and the behavior of the beams developing catenary behavior. Thus, in order to draw conclusions more representative of a realistic structural response, all detailed discussions in the sections involving the general response, catenary action demands, and connection ductility demands for all column-removal scenarios are developed using the nonlinear-inelastic side-frame model. For clarity, all plots associated with these discussions have been truncated at the point of maximum load factor (LF).

In all plots, load is represented in terms of a LF, the vertical load applied at a specific time step of the analysis normalized with the total vertical load. As previously described in section 2.5.6, all increases in load corresponded to an incremental increase in displacement located at the mid-span of the first-floor beam, for convenience in post-processing. In the case of column-removal scenario 4, this location was moved to the unsupported external end of the first-floor beam.

Horizontal and vertical deflections at nodes (Δ_v and Δ_h) are shown in inches. Values of vertical deflection in all plots correspond to the deflection of the beam for the floor being considered at the location directly above the removed column; a negative value of vertical deflection indicates downward movement. Values of horizontal deflection in all plots correspond to the movement of the nodes at the interface between

the beam for that floor and its side-frames; a positive value of horizontal deflection indicates inward movement.

Beam section forces are shown normalized with respect to the plastic moment or the plastic axial force for the section. Inter-story drift is described as a drift index that is normalized with respect to the story height under consideration. Finally, connection ductility demands are shown in terms of plastic rotation at the beam ends. Rotations associated with the joint and with elastic behavior were accounted for in the calculation of these values.

For column-removal scenarios with asymmetric side-frames (scenarios 2 and 3), the values of force and horizontal deflection presented are associated with the side that contains fewer frames, since the stiffness and strength of that side controlled the collapse-resistance of the system. Moreover, with the exception of scenario 4, it was also seen that the level of catenary force development on this side was greater. This was primarily due to the orientation of the column forces being transmitted from the higher stories.

3.5.2 Scenario 1

The first column-removal scenario considered the reaction of the system to the notional removal of the central column in one of the perimeter moment frames. In this scenario, both side-frames had identical stiffness characteristics and strength levels.

3.5.2.1 Effect of Model Type

Load-deflection plots comparing the results of the three model types for scenario 1 are provided below in Figures 3-5 and 3-6; a comparison of axial force development

with LF is shown in Figure 3-7. These figures show results for the first-floor beam only. This was allowed for brevity, since the most relevant behavioral differences can still be explained using these simplified plots.

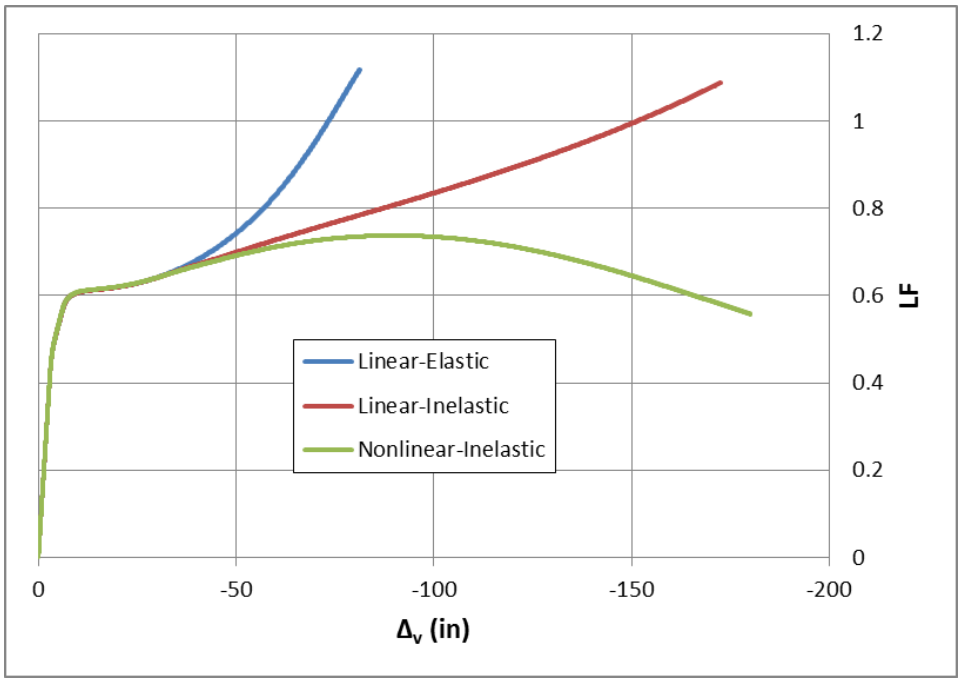

Figure 3-5 Comparison of LF vs. Vertical Deflection by Model Type (Scenario 1)

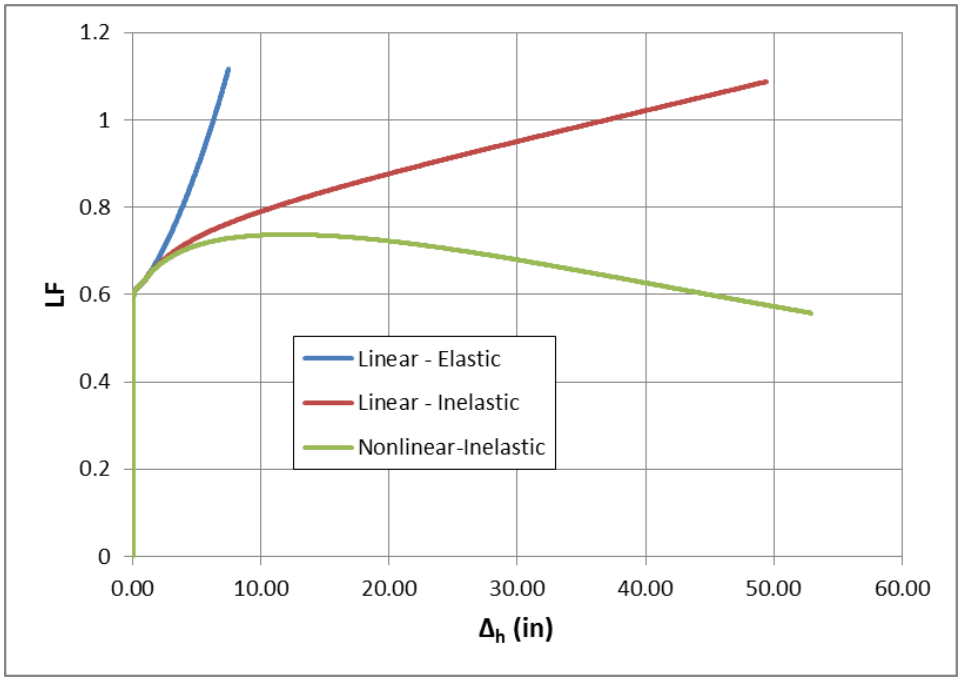

Figure 3-6 Comparison of LF vs. Horizontal Side-Frame Displacement by Model Type (Scenario 1)

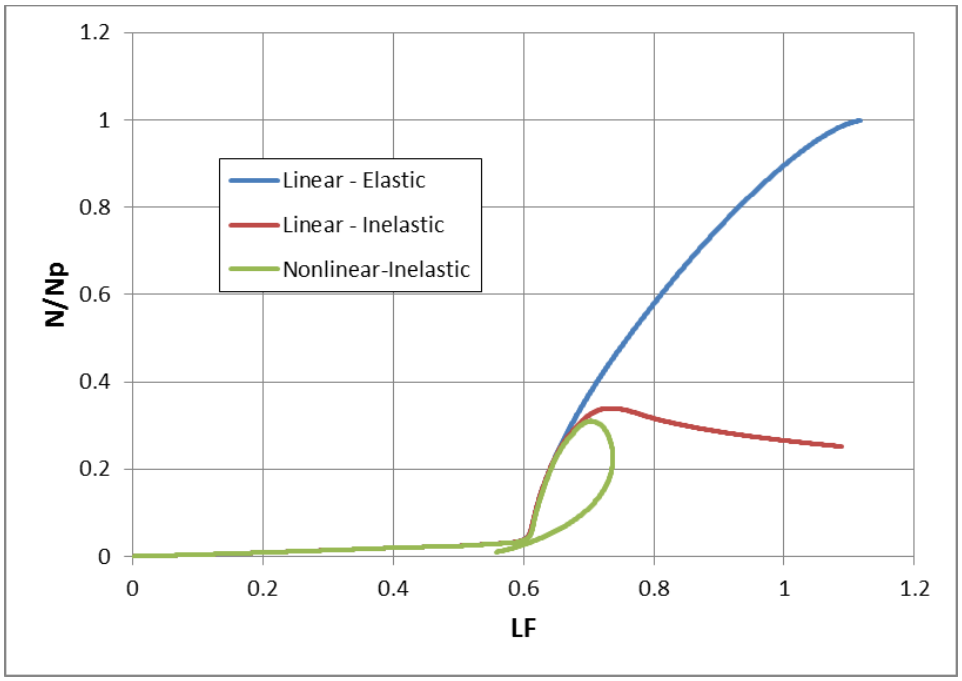

Figure 3-7 Comparison of N/Np vs. LF by Model Type (Scenario 1)

The trends for each model show a point at which the system needed to deflect more substantially in order to increase the LF. This is the point at which the flexural plastic collapse load was reached for all beams in the double-span condition. In each model run under this column-removal scenario, this threshold corresponded to a LF near 0.6, verified by using the upper-bound theory of plastic analysis. After the point of flexural plastic collapse, catenary force development began to occur in the associated beams. This is indicated by a sharp increase in axial force development, shown in Figure 3-7.

Comparing the trends shown above, it can be seen that significant differences in load-carrying behavior existed between the three model types. By including successively higher levels of nonlinearity in the side-frames, successively lower LFs were maintained for similar values of deflection. For example, Figure 3-5 show that at about 75 in of vertical deflection, the LF for the linear-elastic case was near 1.0. However, for this same level of deflection, it lowered to 0.77 when material nonlinearity was modeled in the side-frames. When both geometric and material nonlinearity were jointly considered, the corresponding LF dropped again to 0.73. The same trend can be seen in Figure 3-6 for values of horizontal displacement. Additionally, as deflections increased, the influence of higher-order effects became increasingly profound. The ultimate result was that the nonlinear-inelastic side-frames seemed to exhaust their capacity comparatively early and began to drop load, indicating failure.

Maximum catenary force development was generally more influenced by the effects of material nonlinearity. From Figure 3-7, it can be seen that without any level of nonlinearity considered in the side-frames, the first-floor beam reached its plastic axial

force. However, by including inelastic behavior in the side-frames, flexibility in the boundaries associated with plasticity caused significant slowing of catenary force development. When the side-frames adjacent to the first-floor beam neared fully-plastic behavior, the beam began to partially transition back into flexural behavior. Concurrent with this response, slightly more catenary force development began to occur in the upper-floor beams as the structure tried to avert collapse. This response will be described in more detail in section 3.5.2.3. Allowing the influence of higher-order effects caused the side-frames adjacent to the first-floor beam to reach their capacities more quickly. Consequently, the behavior previously described occurred at an accelerated pace.

3.5.2.2 General Response

The load-deflection response of the baseline system to column-removal scenario 1 is shown below in Figures 3-8 and 3-9. Plots of base shear and drift index versus LF are shown in Figures 3-10 and 3-11 respectively.

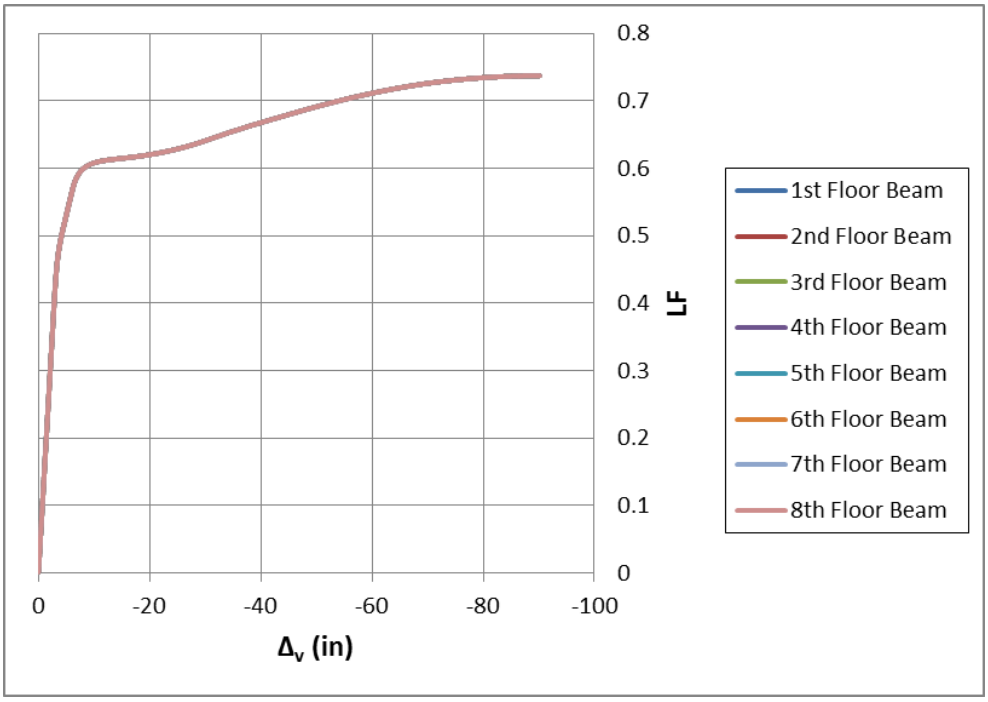

Figure 3-8 LF vs. Vertical Deflection (Scenario 1)

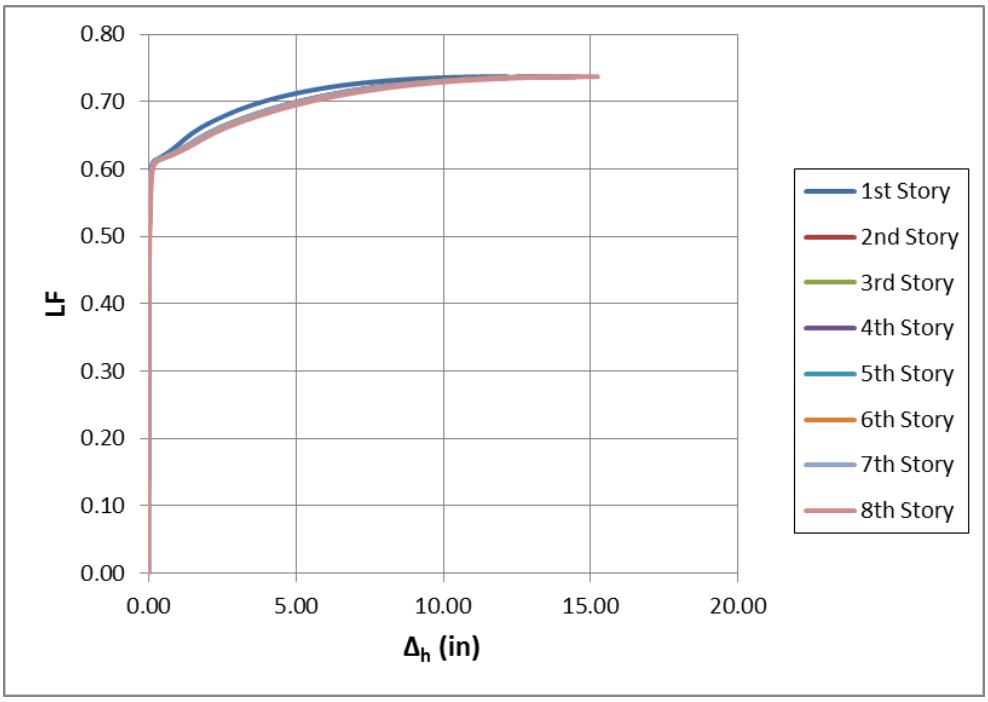

Figure 3-9 LF vs. Horizontal Side-Frame Displacement (Scenario 1)

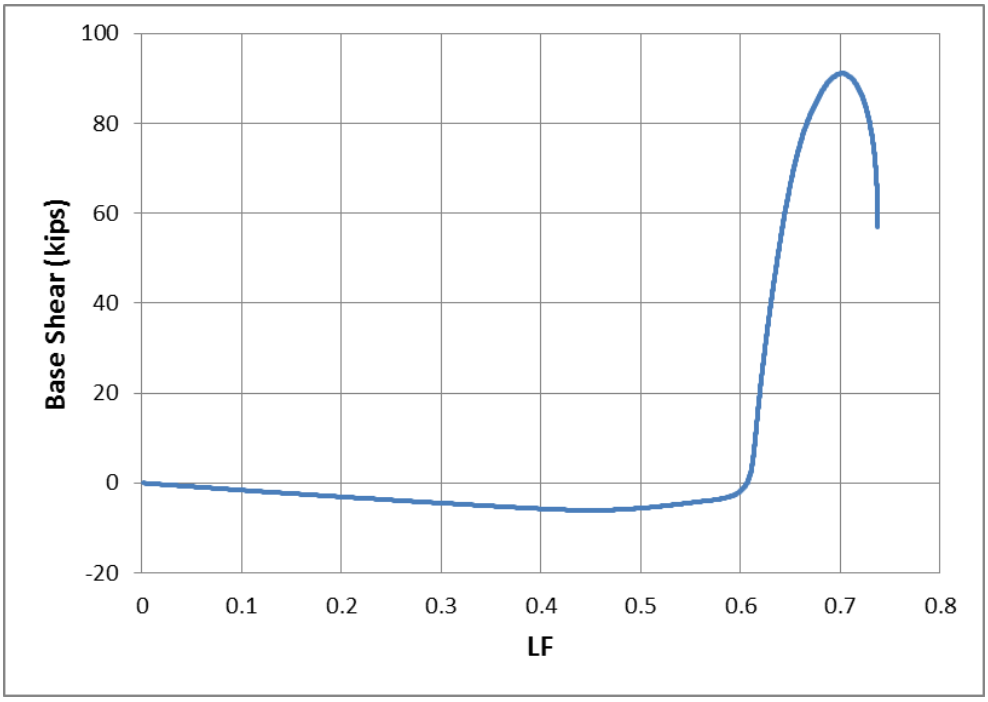

Figure 3-10 Base Shear vs. LF (Scenario 1)

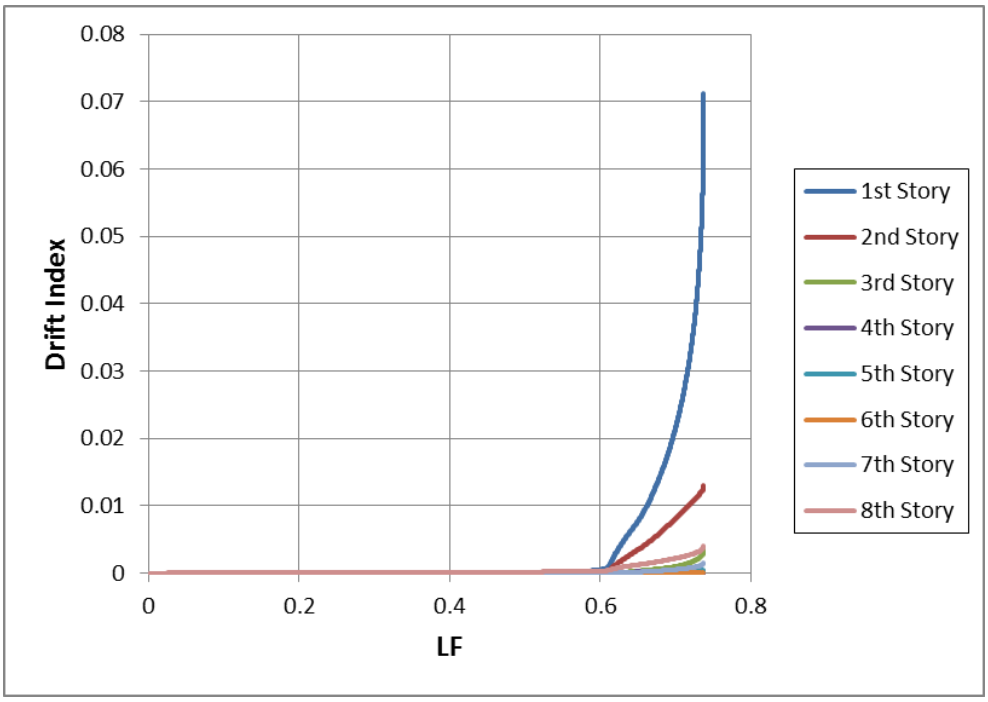

Figure 3-11 Drift Index vs. LF (Scenario 1)

In Figures 3-8 through 3-11, it can be seen that the maximum LF achieved under the central column-removal scenario was about 0.74. Additionally, as seen in Figures 3-8 and 3-9, the maximum vertical mid-span deflection of the beams and maximum horizontal side-frame displacement were about 90 in and 15 in respectively.

Figure 3-11 indicates that the maximum relative drift occurred in the first story of the side-frames. Past the point of flexural plastic collapse in the beams at a LF near 0.6, the amount of vertical and horizontal deflection required to sustain additional load substantially increased.

Figure 3-10 indicates that the base shear, the sum of the lateral forces being imposed on the side-frames by the adjacent beams, increased quickly past the point of flexural plastic collapse to a maximum value of about 91 kips. However, once a LF near 0.7 was reached, the base shear demand began to drop until the point of system failure, when the LF began to drop. This is a result of the behavioral change in the first-floor beam identified in the previous section.

Failure in this column-removal scenario was defined by the formation of a plastic sway mechanism in the adjoining side-frames. This failure mode is shown below in Figure 3-12.

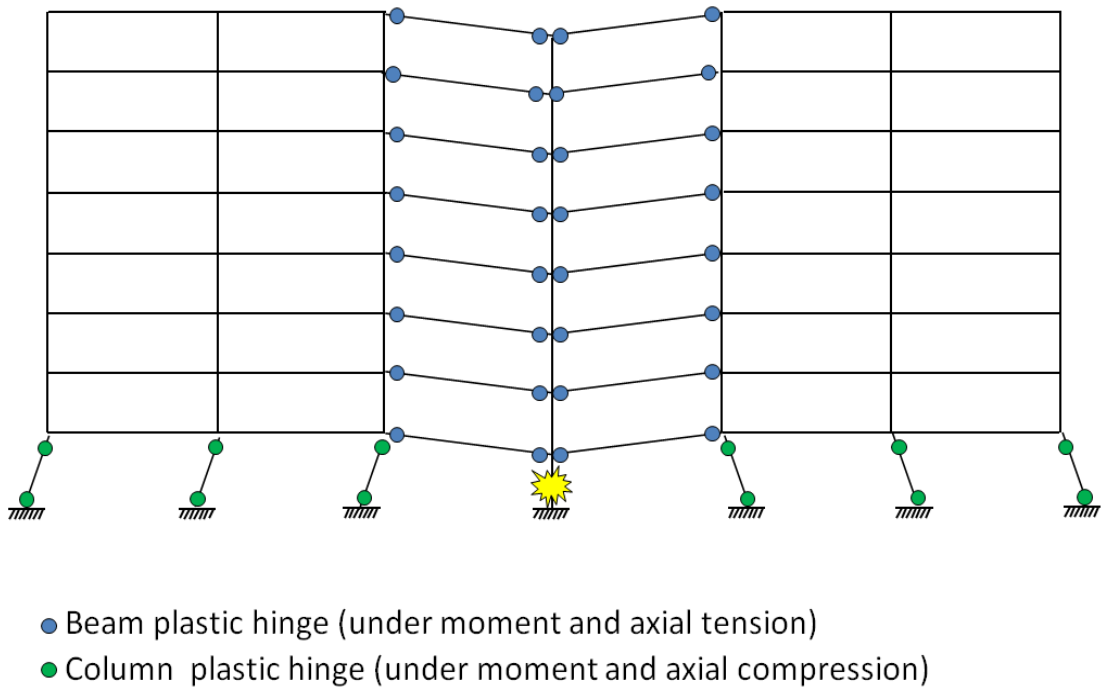

Figure 3-12 Baseline System Failure Mode (Scenario 1)

3.5.2.3 Catenary Action Demands

Figures 3-13 through 3-17 show the catenary action demands in the first– eighth floor beams. In the figures below, point A identifies the point where a flexural plastic mechanism formed in the beams and point B identifies the point of maximum catenary force development in the first-floor beam.

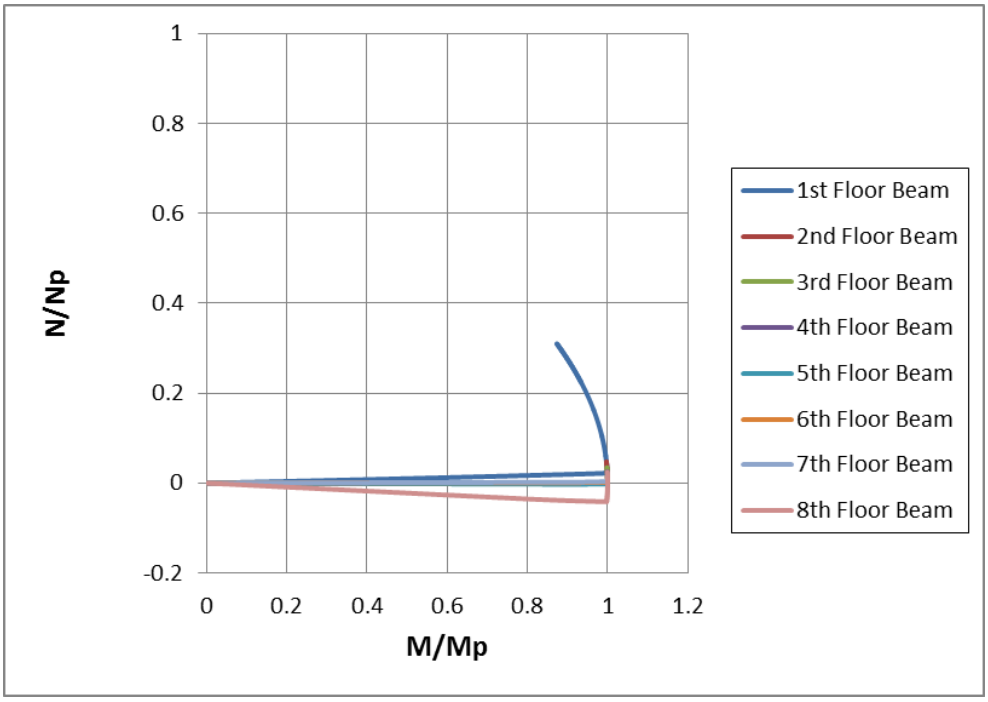

Figure 3-13 N/Np vs. M/Mp (Scenario 1)

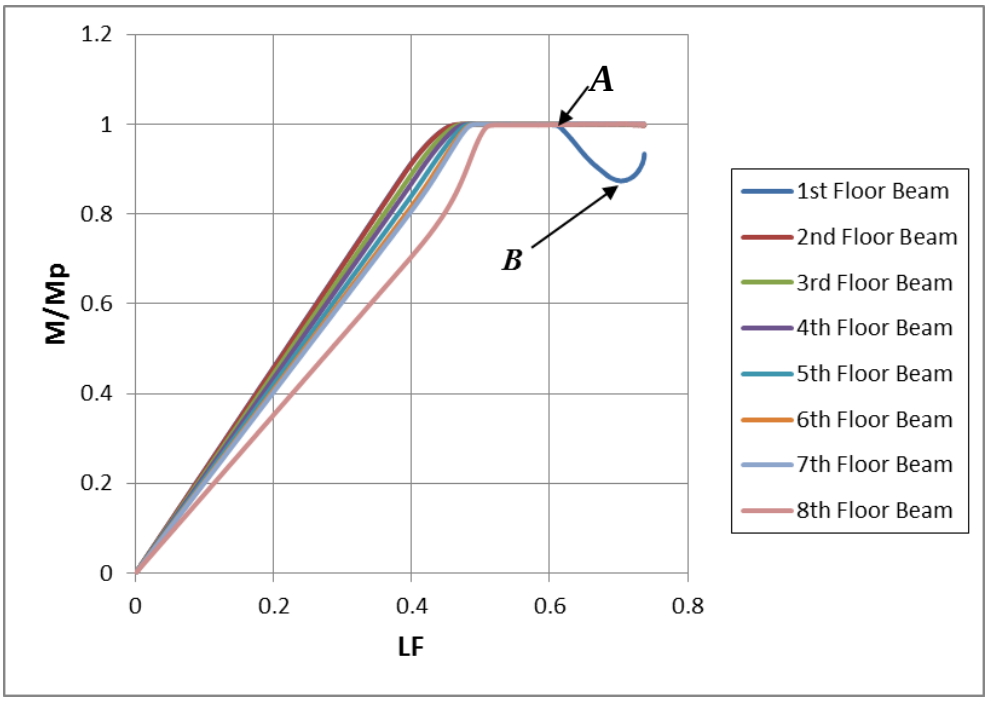

Figure 3-14 M/Mp vs. LF (Scenario 1)

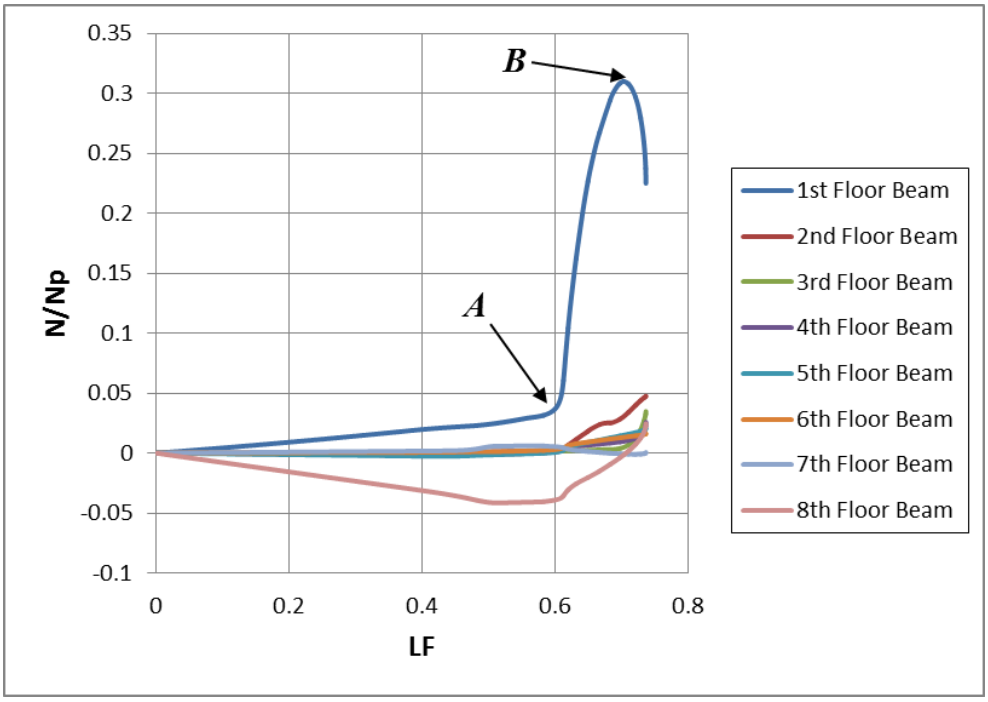

Figure 3-15 N/Np vs. LF (Scenario 1)

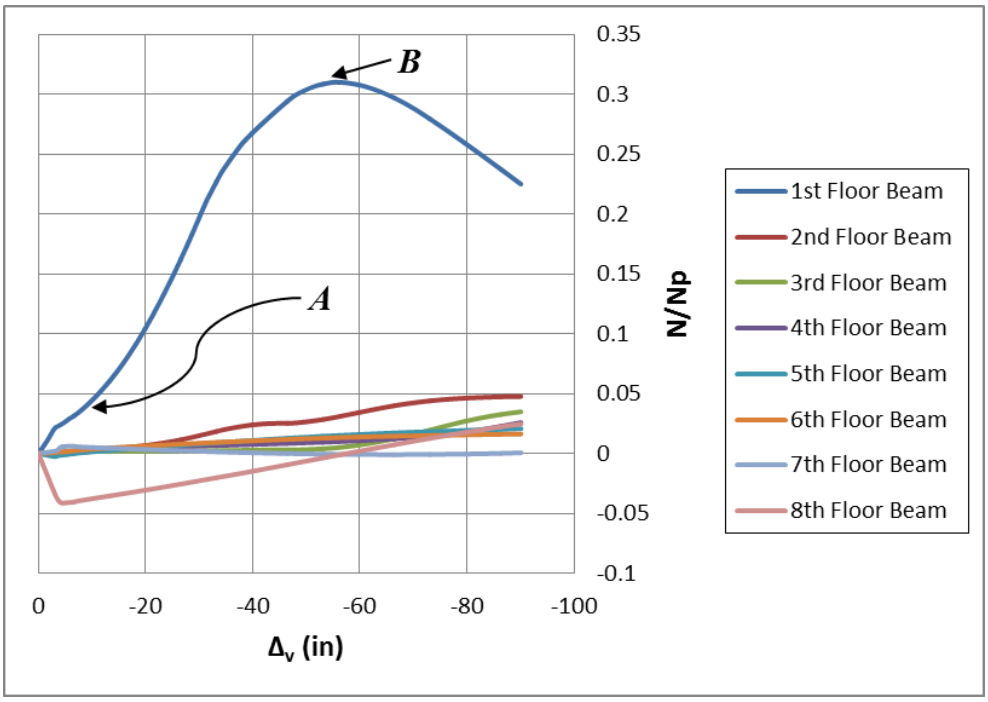

Figure 3-16 N/Np vs. Vertical Deflection (Scenario 1)

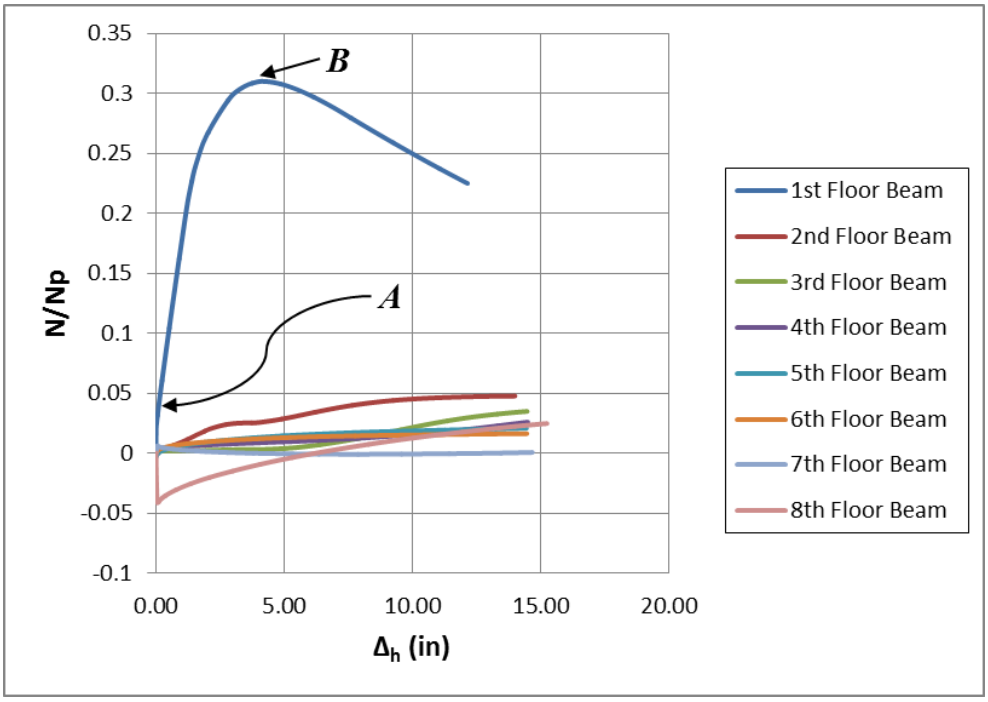

Figure 3-17 N/Np vs. Horizontal Side-Frame Displacement (Scenario 1)

When beams transition from flexural to catenary behavior and develop axial tension, they resist additional load by using the vertical component of the axial force. This method of resistance is shown clearly in Figure 3-10. Moreover, when catenary behavior is developed, it requires a ductile response in the beam and is accompanied by relatively large vertical displacements compared to flexural behavior; this correlation is shown in Figure 3-15.

The lateral forces associated with catenary behavior impose both force and ductility demands on the side-frames. The ductility demands associated with this scenario are indicated by the substantial increase in horizontal displacement from point A to the point of failure, shown in Figure 3-12. Alp (2009) showed that these demands depend on the strength and stiffness levels of both the anchoring system (side-frames)

and the beam itself. As shown in Figures 3-14 – 3-17, the majority of catenary force development prior to failure occurred in the first-floor beam. This corresponded to a maximum catenary force of 117 kips (31% of Np). Subsequently, the majority of the base shear demand shown in Figure 3-10 was contributed by the lateral force being transferred to the side-frames by this beam. This increased level of catenary force development can be attributed to the higher level of restraint offered to the first-floor beam by the adjoining side-frames and the additional portion of load transferred to the beam from higher stories.

As the lateral force demands on the side-frames increased with load, they began to cause yielding and plasticity in the side-frame members. This loss of stiffness, coupled with geometric effects, seemed to cause a distinct change in the response of the various beams (identified by point B) that was initially mentioned in section 3.5.2.1. At this point, the levels of deflection could have been substantial enough that the vertical component of force in the first-floor beam was able to resist the applied loads without further catenary force development. As deflections increased, successively lower levels of catenary force were needed. This caused the first-floor beam to partially transition back into flexural behavior prior to system failure (identified by the region from point B to the point of failure). This response was not seen from the beams in higher floors, where significantly smaller portions of axial tension were developed.

As the structure reached various limit states and approached failure, it attempted to redistribute load among the various floors. This process is best observed by examining the portion of the total floor load applied to the amplified bays that was resisted by each beam as the LF increased. This distribution is show in Figure 3-18.

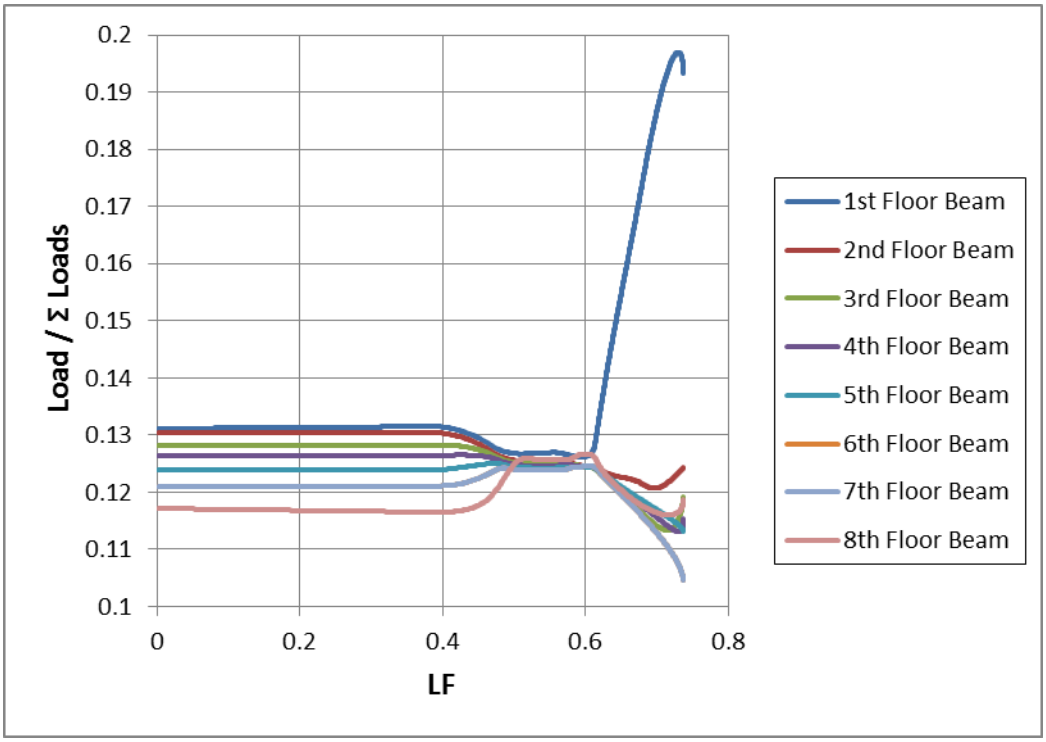

Figure 3-18 Normalized Beam Floor Load vs. LF (Scenario 1)

Figure 3-18 shows that prior to plastic hinge formation in all beams, larger portions of load were resisted by the beams closer to ground level. After the formation of a flexural plastic mechanism, when the first-floor beam began to develop considerable levels of axial tension, significantly more load was resisted by this beam. This trend continued until system failure, when a very small amount of load-redistribution was seen among the various beams just prior to collapse.

3.5.2.4 Connection Ductility Demands

The levels of plastic rotation developed in each beam resulting from column-removal scenario 1 are shown in Figure 3-19. The maximum plastic rotation demands prior to failure are shown in Table 3-1.

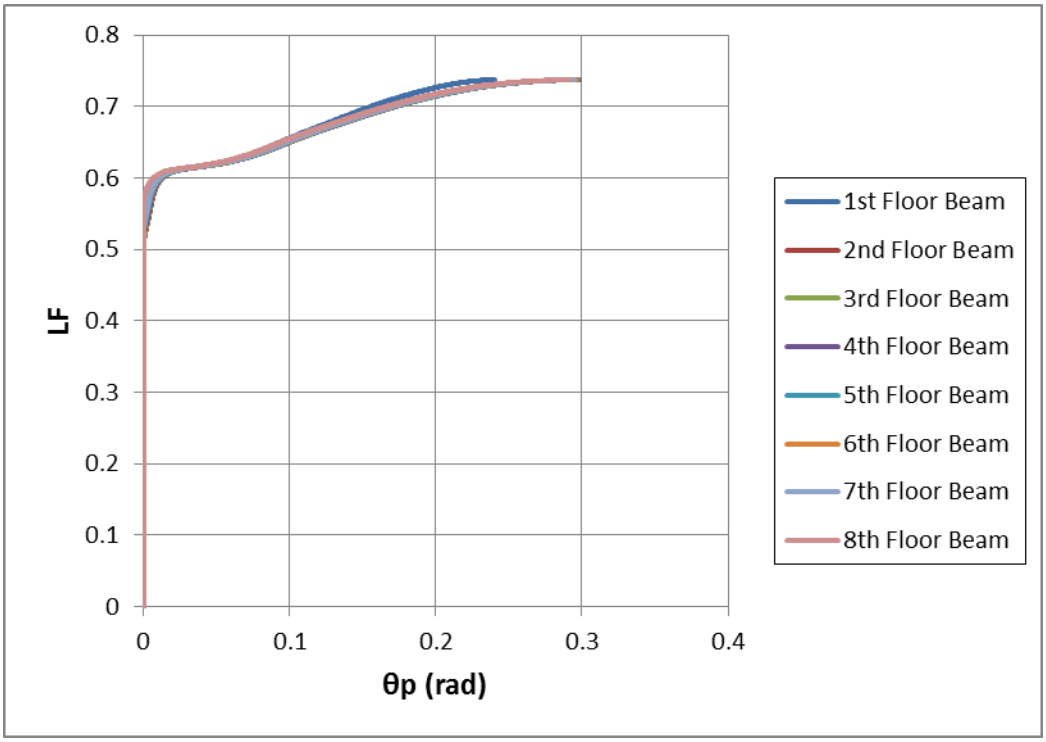

Figure 3-19 Plastic Rotation Demands (Scenario 1)

Table 3-1 Plastic Rotation Demands at Maximum LF (Scenario 1)

Beam Location	θp (rad)
1st Floor	0.240
2nd Floor	0.292
3rd Floor	0.297
4th Floor	0.298
5th Floor	0.297
6th Floor	0.296
7th Floor	0.294
8th Floor	0.291

Figure 3-19 indicates that plastic rotation demands were generally consistent among all beams. However, most likely due to large joint rotations at the ends of the first-floor beam resulting from plasticity induced by catenary forces, maximum plastic rotation demands at these locations were smaller.

3.5.3 Scenario 2

The second column-removal scenario considered the reaction of the system to the notional removal of the column directly adjacent to the central column. In this scenario, the left side of the system had fewer side-frames, which resulted in lower overall strength and stiffness levels.

3.5.3.1 Effect of Model Type

Load-deflection plots comparing the results of the three model types for scenario 2 are provided below in Figures 3-20 and 3-21; a comparison of axial force development with LF is shown in Figure 3-22. As with the previous scenario, these figures show results for the first-floor beam only.

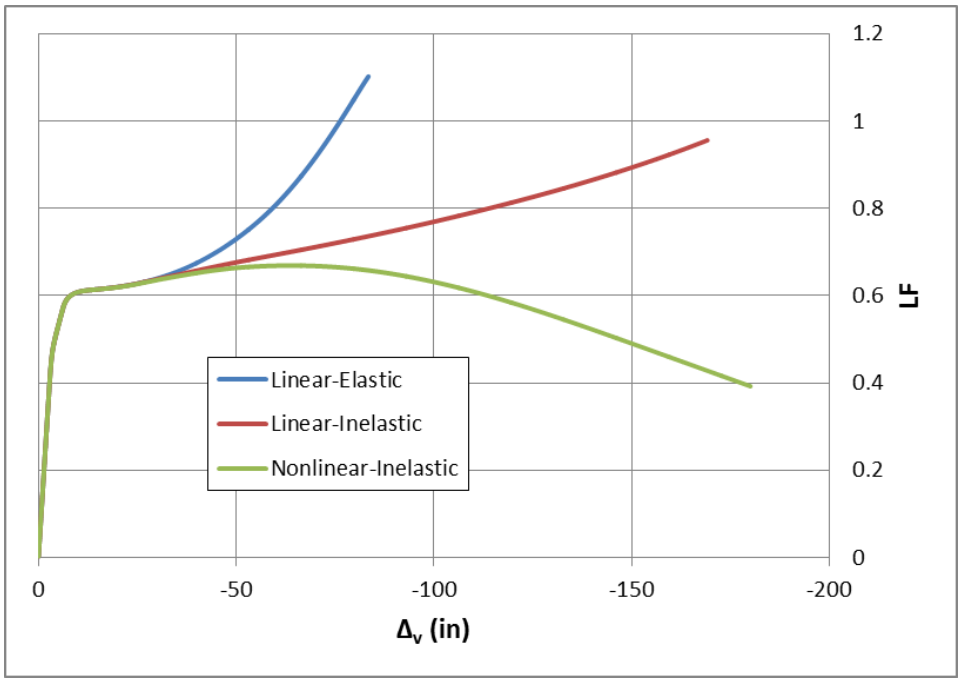

Figure 3-20 Comparison of LF vs. Vertical Deflection by Model Type (Scenario 2)

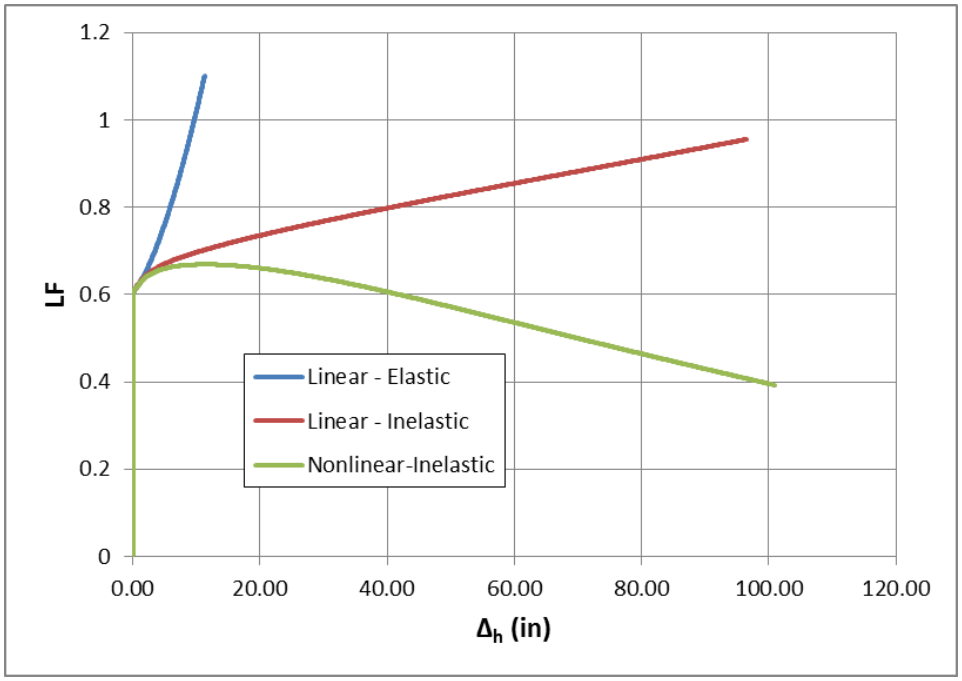

Figure 3-21 Comparison of LF vs. Horizontal Side-Frame Displacement by Model Type (Scenario 2)

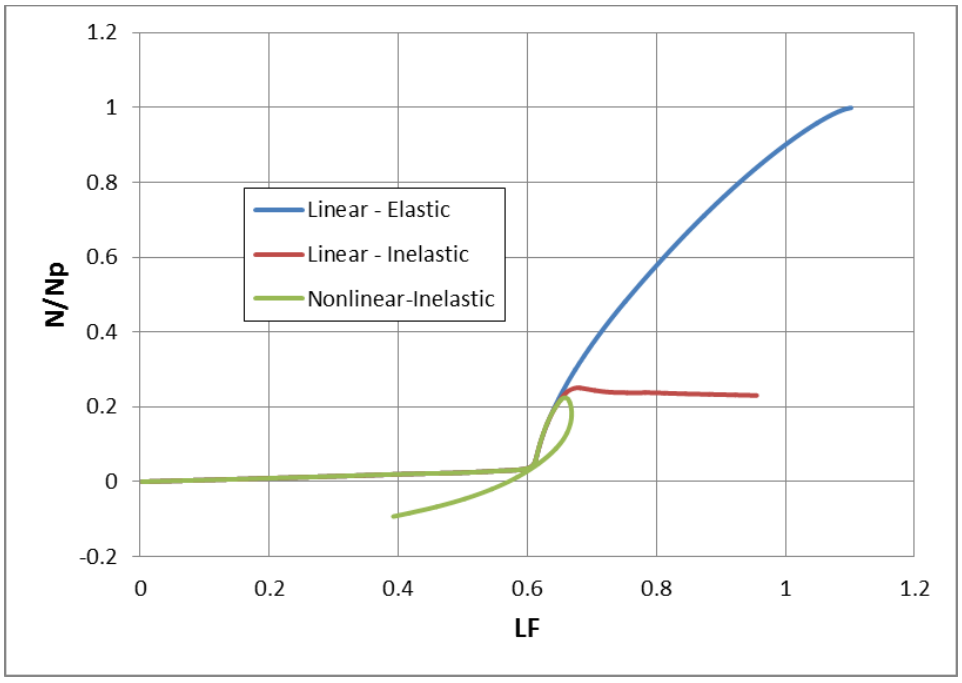

Figure 3-22 Comparison of N/Np vs. LF by Model Type (Scenario 2)

The results for all three models in scenario 2 closely mimic the trends described for the central column-removal scenario. As seen previously, the proposed point of flexural plastic collapse seemed to occur near a LF of 0.6. Significant catenary force development began after this point.

Near the maximum capacity of the nonlinear-inelastic system, at 64 in of vertical deflection, the LF was 0.67. The LFs at this same level of vertical deflection were 0.70 and 0.84 for the linear-inelastic and linear-elastic models respectively, showing the same reduction in strength identified in scenario 1.

Maximum catenary force development, shown in Figure 3-22, was even more severely influenced by the effects of material nonlinearity in this column-removal scenario. This was most likely due to the decreased strength and stiffness levels of the side-frames to the left of the beams, which resulted in failure of the system prior to significant catenary force development. Despite this, the general behavioral influence of material and geometric nonlinearity on catenary force development remained consistent for scenario 2.

Overall, the influence of both types of nonlinearity was more apparent in this column-removal scenario than in the case where the central column was removed. This can be correlated with the lower stiffness and strength levels of the side-frames on the left side of the beams.

3.5.3.2 General Response

The load-deflection response of the baseline system to column-removal scenario 2 is shown below in Figures 3-23 and 3-24. Plots of base shear and drift index versus LF are shown in Figures 3-25 and 3-26 respectively.

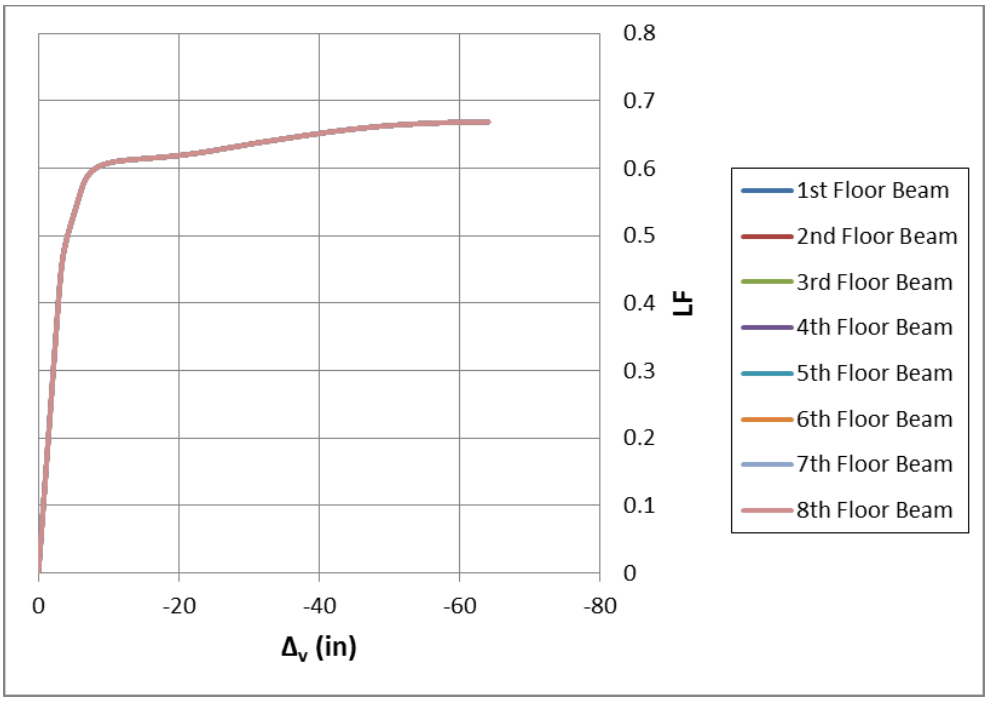

Figure 3-23 LF vs. Vertical Deflection (Scenario 2)

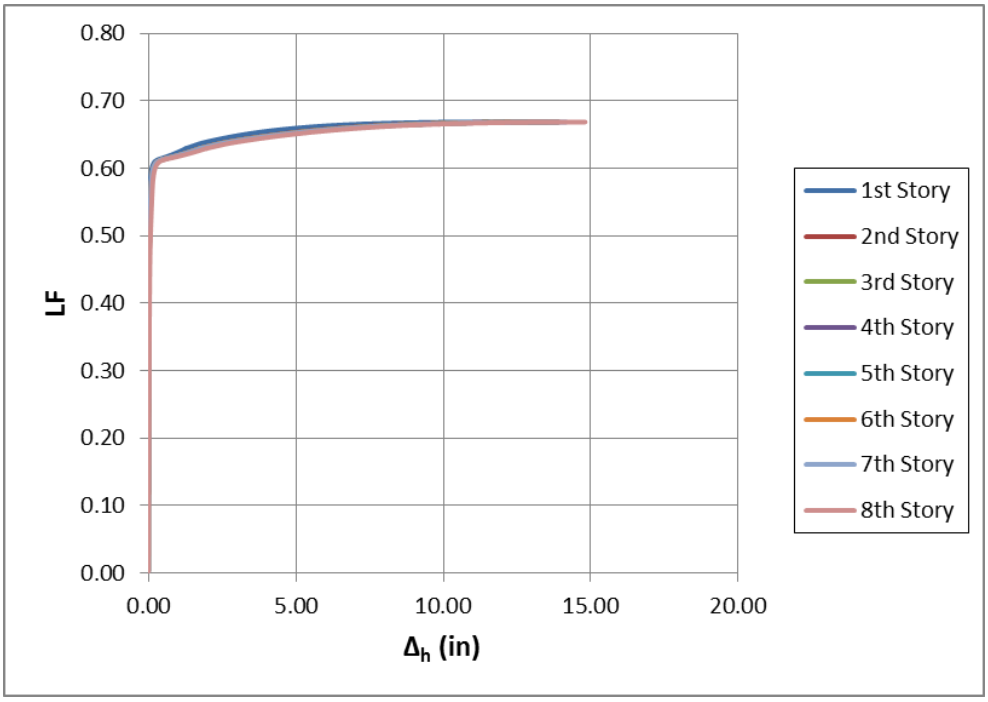

Figure 3-24 LF vs. Horizontal Side-Frame Displacement (Scenario 2)

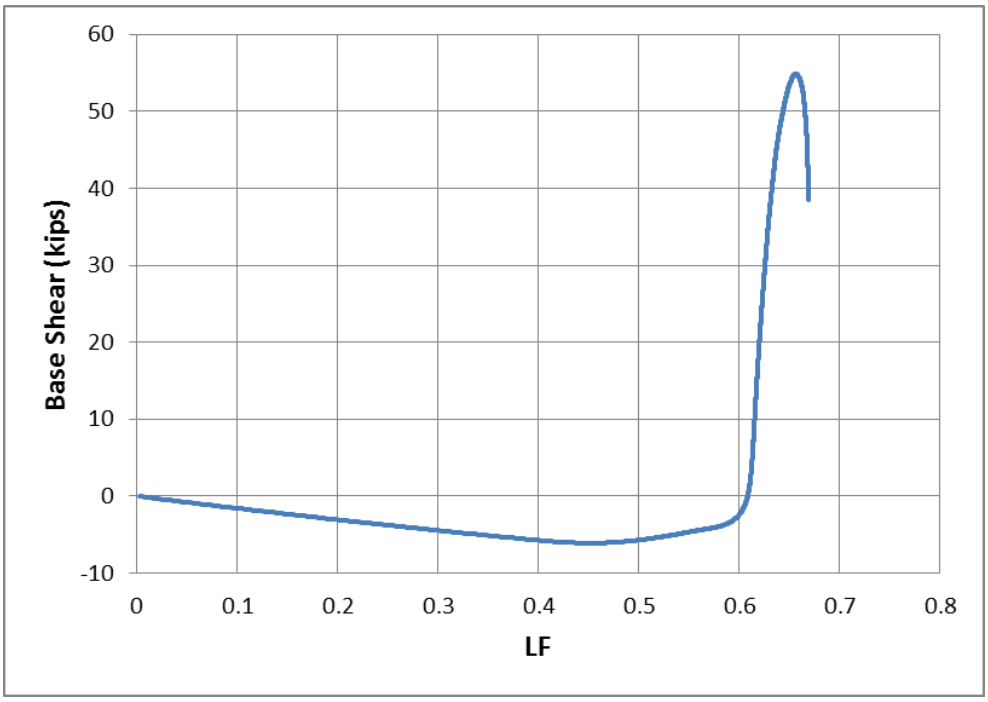

Figure 3-25 Base Shear vs. LF (Scenario 2)

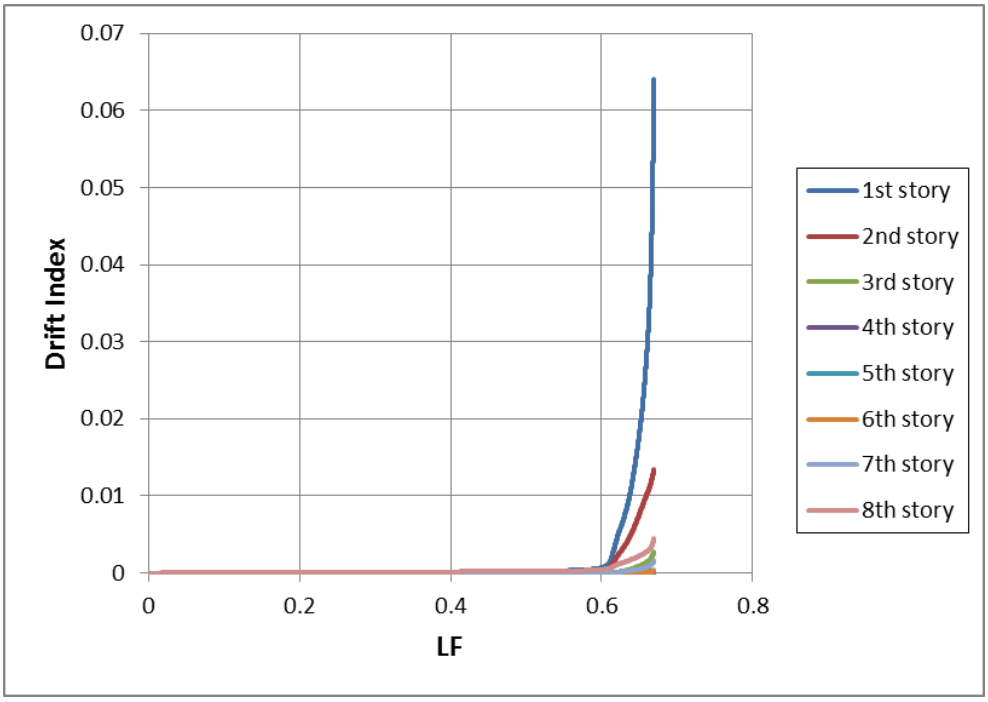

Figure 3-26 Drift Index vs. LF (Scenario 2)

Figures 3-23 through 3-26 show that the maximum LF achieved under column-removal scenario 2, approximately 0.67, is lower than the corresponding LF from the central column-removal scenario. The amount of vertical deflection required to fail the system, approximately 64 in, is also somewhat lower. However, the maximum values of horizontal displacement at failure were ostensibly equivalent to the values associated with column-removal scenario 1. This can be attributed to the lower stiffness and strength levels of the system, which result in larger deformations at lower levels of force, but limit the amount of force and deformation that can be sustained.

Figure 3-26 indicates that, similar to the preceding scenario, the maximum relative drift occurred in the first story of the side-frames where catenary development was highest. Past the point of flexural plastic collapse, the amount of vertical and

horizontal deflection required to sustain additional load, shown in Figures 3-23 and 3-24, substantially increased.

The maximum base shear developed in this scenario was 55 kips. Figure 3-25 shows that the base shear followed the same trend that was established in scenario 1: it increased quickly past the point of flexural collapse, but began to drop prior to failure. As described previously, this most likely resulted from the response of the first-floor beam to excessive flexibility in the side-frames associated with plasticity.

Unlike the failure mode observed in scenario 1, system failure in this column-removal scenario was defined by instability in the column adjacent to the notionally removed column; some plasticity was exhibited in the side-frames prior to collapse. This failure mode is illustrated in Figure 3-27.

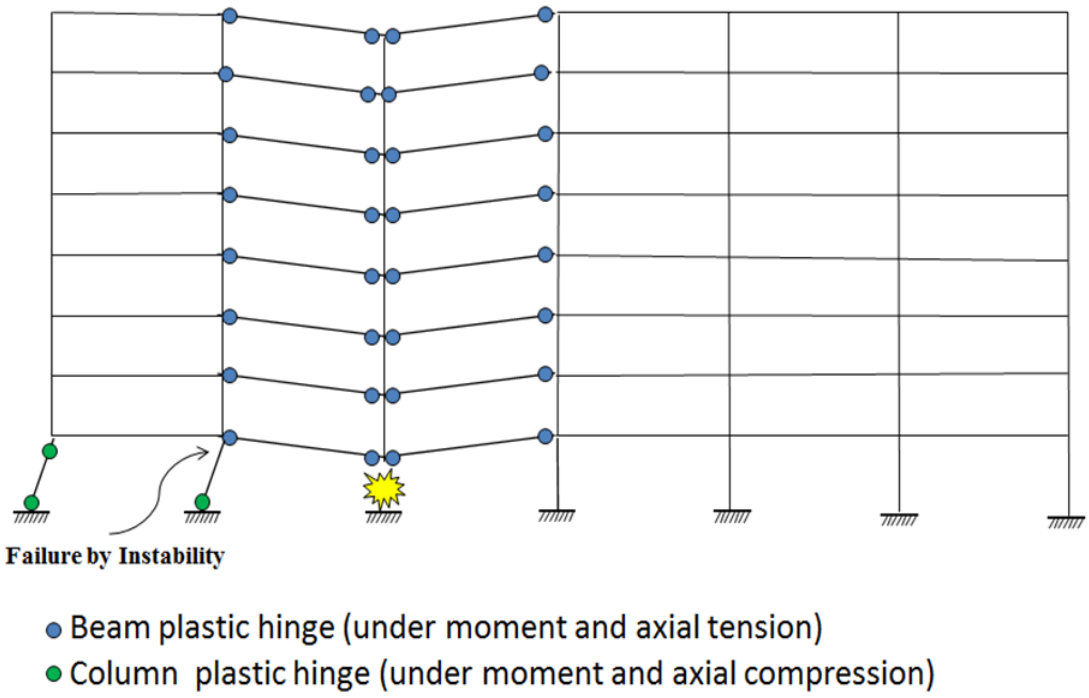

Figure 3-27 Baseline System Failure Mode (Scenario 2)

3.5.3.3 Catenary Action Demands

Figures 3-28 through 3-32 show the catenary action demands in the first – eighth floor beams for scenario 2. Points A and B correspond to the same points defined previously.

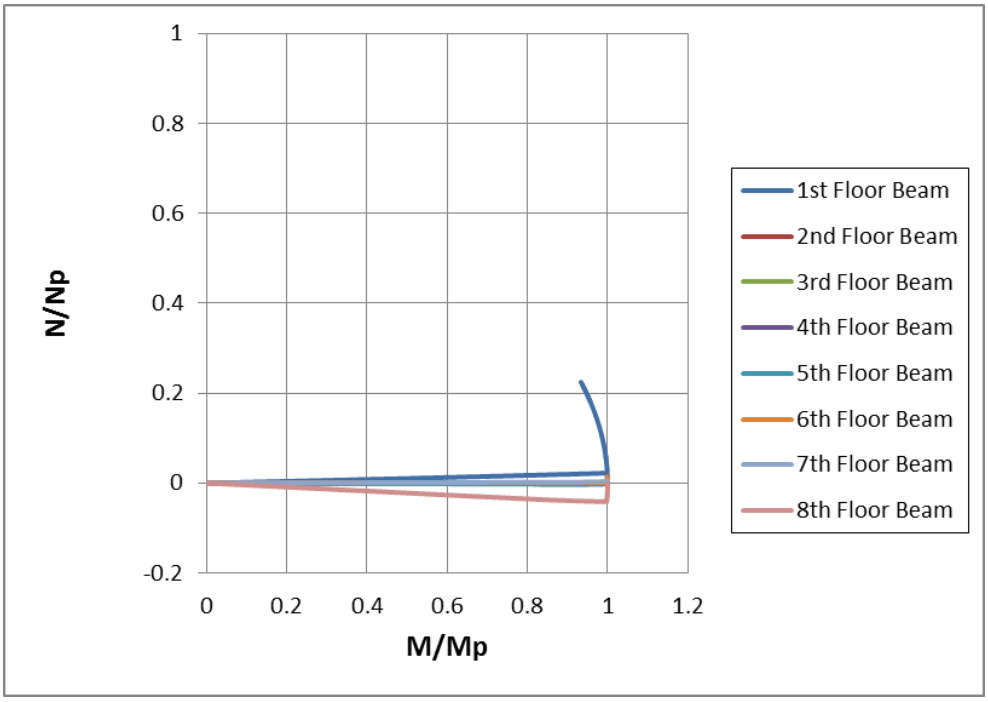

Figure 3-28 N/Np vs. M/Mp (Scenario 2)

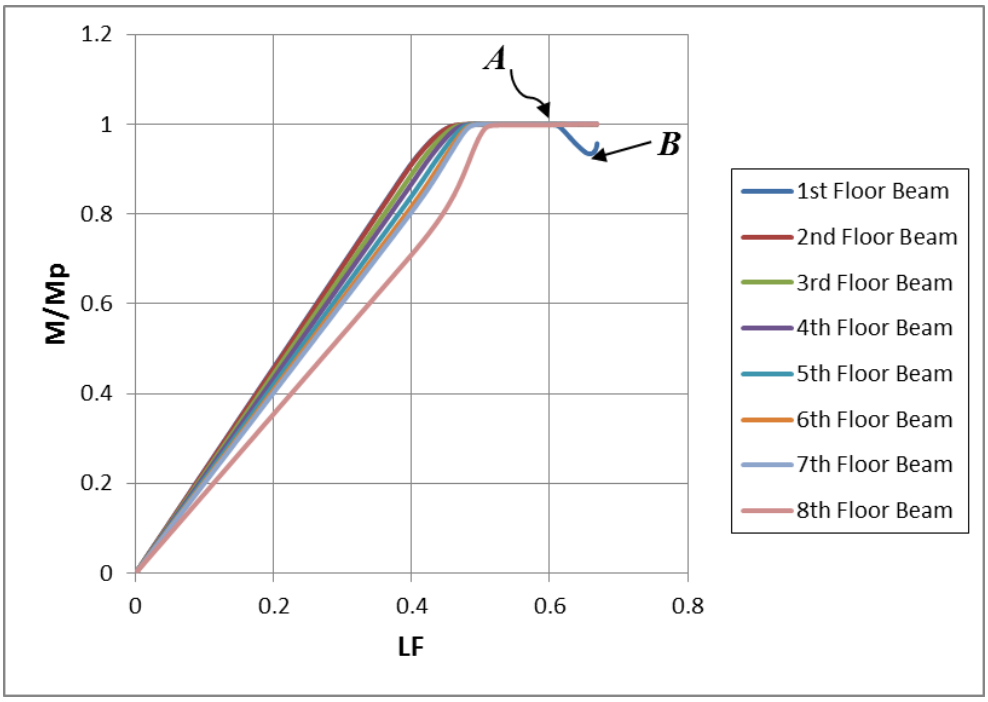

Figure 3-29 M/Mp vs. LF (Scenario 2)

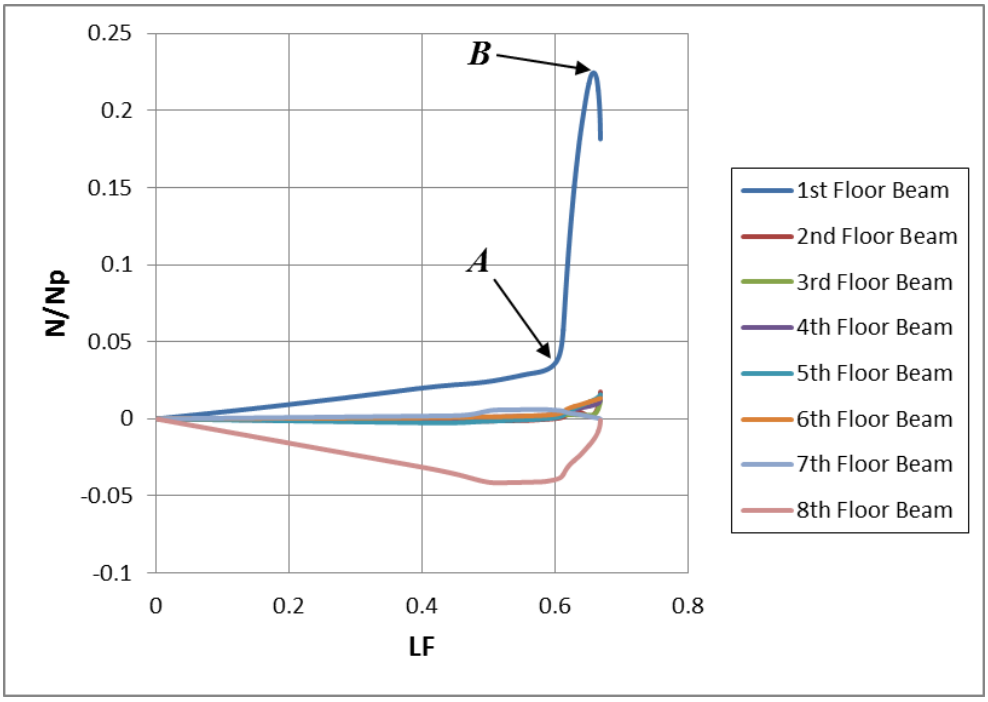

Figure 3-30 N/Np vs. LF (Scenario 2)

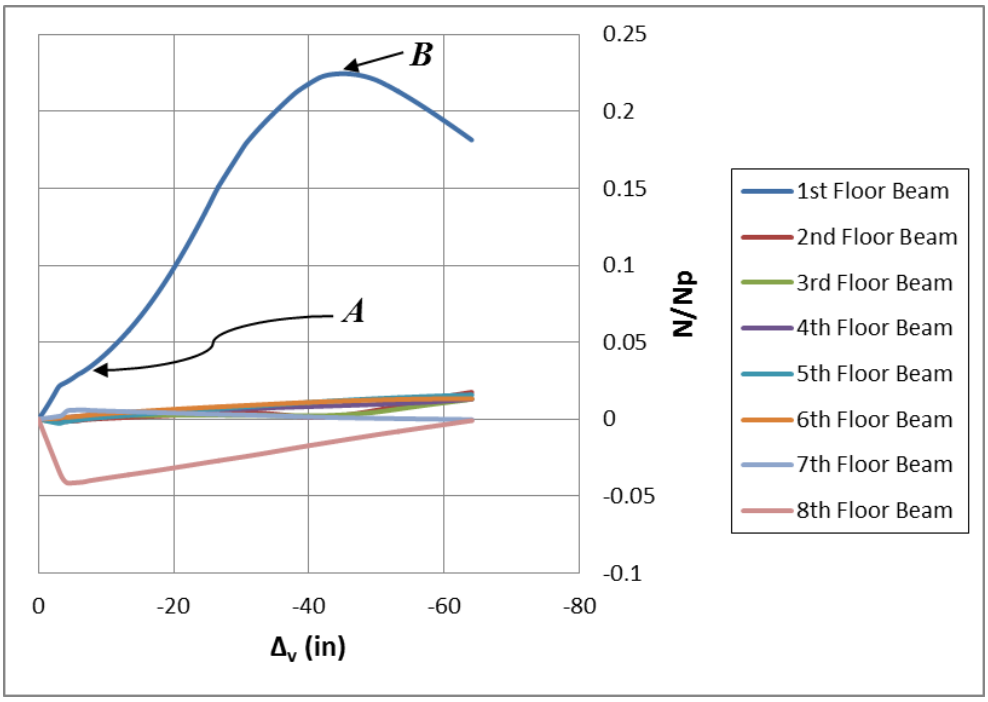

Figure 3-31 N/Np vs. Vertical Deflection (Scenario 2)

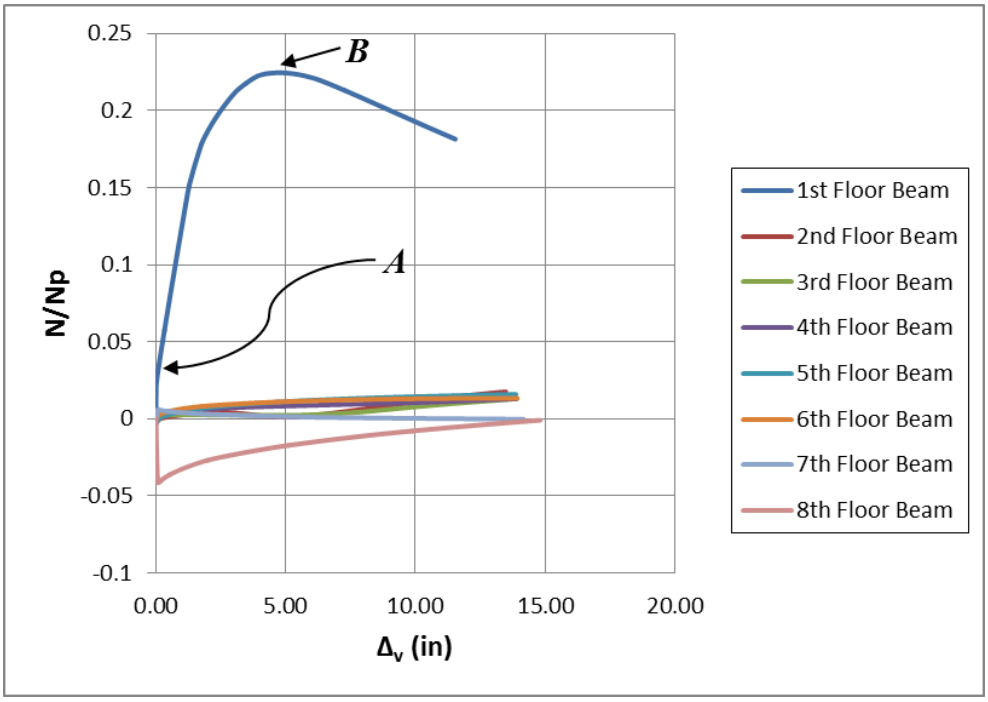

Figure 3-32 N/Np vs. Horizontal Side-Frame Displacement (Scenario 2)

Correlative with the general response, the response of the beams in the baseline system to column-removal scenario 2 mirrored the results from the central column-removal scenario, with minor differences. Likely due to the decreased strength and stiffness levels of the system, which were limited by the side-frames to the left of the beams, the maximum catenary force in the first-floor beam was reduced to 79.3 kips (about 21% of Np). However, since almost all catenary force development occurred in the first-floor beam, the general trend for this development remained unchanged.

Likewise, the same behavior associated with plasticity and large deflections, shown in Figures 3-31 and 3-32, was observed between the three key points (A, B, and the point of failure). This behavior remained consistent despite the somewhat smaller values of deflection concordant with the reduced LF at collapse.

3.5.3.4 Connection Ductility Demands

The levels of plastic rotation developed in each beam resulting from column-removal scenario 2 are shown in Figures 3-33 and 3-34. The maximum plastic rotation demands prior to failure at the ends of each beam are shown in Table 3-2.

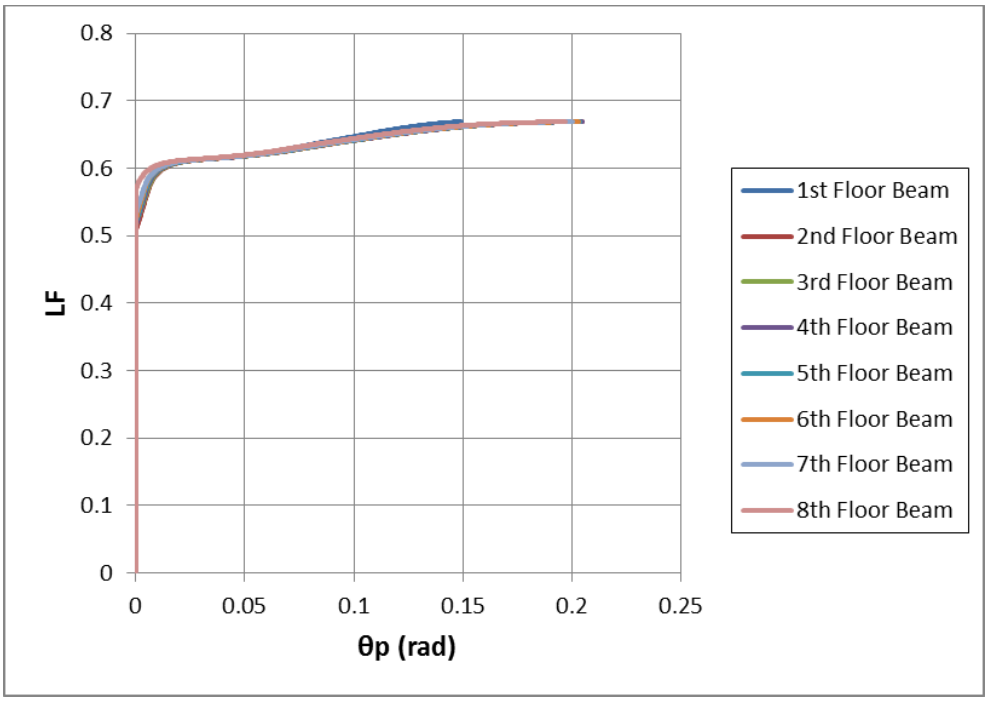

Figure 3-33 Plastic Rotation Demands (Scenario 2 – Left End)

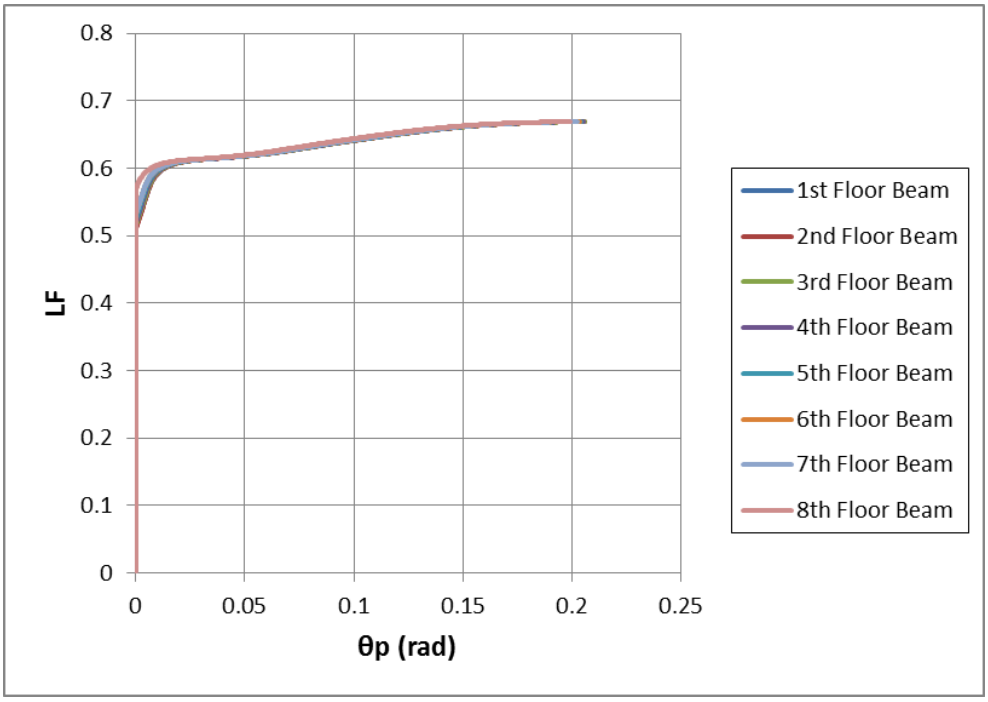

Figure 3-34 Plastic Rotation Demands (Scenario 2 – Right End)

Table 3-2 Plastic Rotation Demands at Maximum LF (Scenario 2)

Beam Location	θp, Left End (rad)	θp, Right End (rad)
1st Floor	0.15	0.203
2nd Floor	0.205	0.206
3rd Floor	0.204	0.206
4th Floor	0.205	0.205
5th Floor	0.204	0.204
6th Floor	0.203	0.203
7th Floor	0.201	0.203
8th Floor	0.197	0.199

The beams in scenario 2 are anchored by three bays to the right and one to the left. This asymmetric restraint, combined with plastic behavior in the first-story columns to the left of the beams, resulted in large joint rotations at the left end of the first-floor beam. The outcome of this was that the plastic rotation demands at this end of the beam

were substantially smaller than the values seen at the opposing end. Overall, likely due to the lower load levels at failure, the plastic rotation demands associated with scenario 2 were smaller than those associated with scenario 1.

3.5.4 Scenario 3

The third column-removal scenario considered the reaction of the system to the notional removal of the penultimate column. As in scenario 2, the left side of the system had fewer side-frames, which resulted in lower overall strength and stiffness levels. Moreover, as shown in Figures 3-3 and 3-4, the left set of side-frames in scenario 3 had only one first-story column.

3.5.4.1 Effect of Model Type

Load-deflection plots comparing the results of the three model types for scenario 2 are provided below in Figures 3-35 and 3-36; a comparison of axial force development with LF is shown in Figure 3-37. Consistent with the previous methods of presentation, these figures show results for the first-floor beam only.

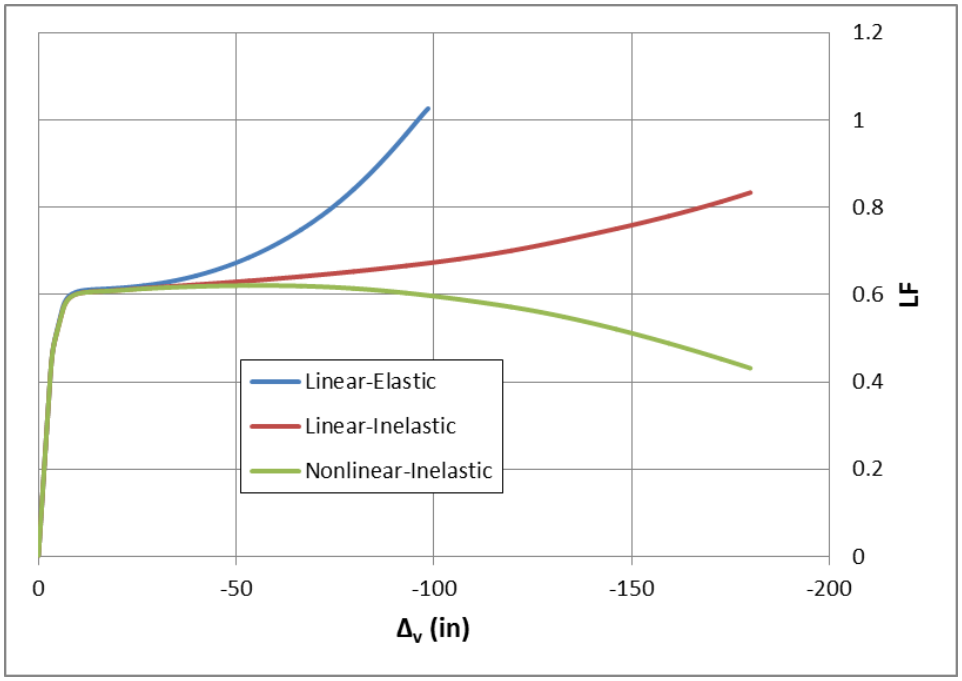

Figure 3-35 Comparison of LF vs. Vertical Deflection by Model Type (Scenario 3)

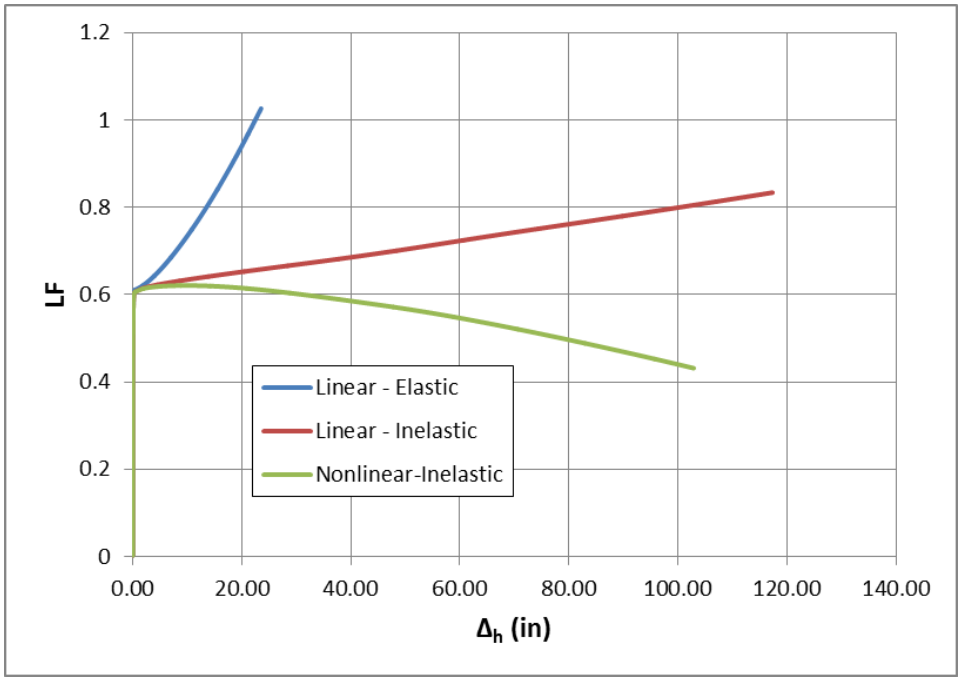

Figure 3-36 Comparison of LF vs. Horizontal Side-Frame Displacement by Model Type (Scenario 3)

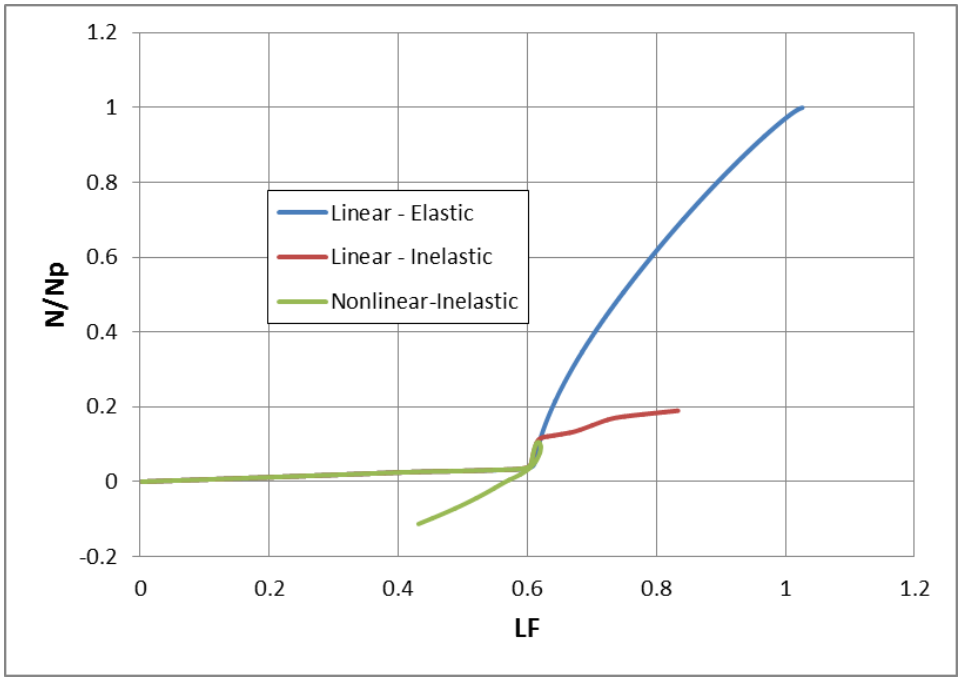

Figure 3-37 Comparison of N/Np vs. LF by Model Type (Scenario 3)

The results from the three models in scenario 3 show similar behavioral differences to what was previously established in scenarios 1 and 2, with slight differences. As seen before, a LF near 0.6 marked a distinct change in the behavior of the system; namely, the first-floor beam began to develop more significant levels of axial tension. However, in the models that allowed plasticity in the side-frames for scenario 3, the eighth-floor beam did not form a plastic hinge at its left end. Instead, a hinge was formed at the top of the column framing into this beam. This was a consequence of the eighth-story column being weaker than the eighth-floor beam.

Near the maximum capacity of the nonlinear-inelastic system, at 56 in of vertical deflection, the LF was 0.62. The LFs at this same level of vertical deflection were 0.63 and 0.70 for the linear-inelastic and linear-elastic models respectively, once again showing the same downward trend of resistance identified in the previous scenarios.

However, the relative magnitude of difference between the LFs for the three models is notably smaller in this column-removal scenario, due to the early onset of failure in the nonlinear-inelastic model.

Compared to the trend observed in scenario 2, the maximum catenary forces developed during scenario 3 diminished more significantly with successively higher levels of nonlinearity. The left side of the system in scenario 3 consisted exclusively of corner columns which framed directly into the ends of the beams. By implementing material nonlinearity and establishing a strength level for this side of the system, catenary development became severely restricted. Moreover, since this side of the system had only one first-story column, including higher-order geometric effects seemed to result in the system promptly failing by instability in this column. These impacts are discussed further in the ensuing discussions.

3.5.4.2 General Response

The load-deflection response of the baseline system to column-removal scenario 3 is shown below in Figures 3-38 and 3-39. Plots of base shear and drift index versus LF are shown in Figures 3-40 and 3-41 respectively.

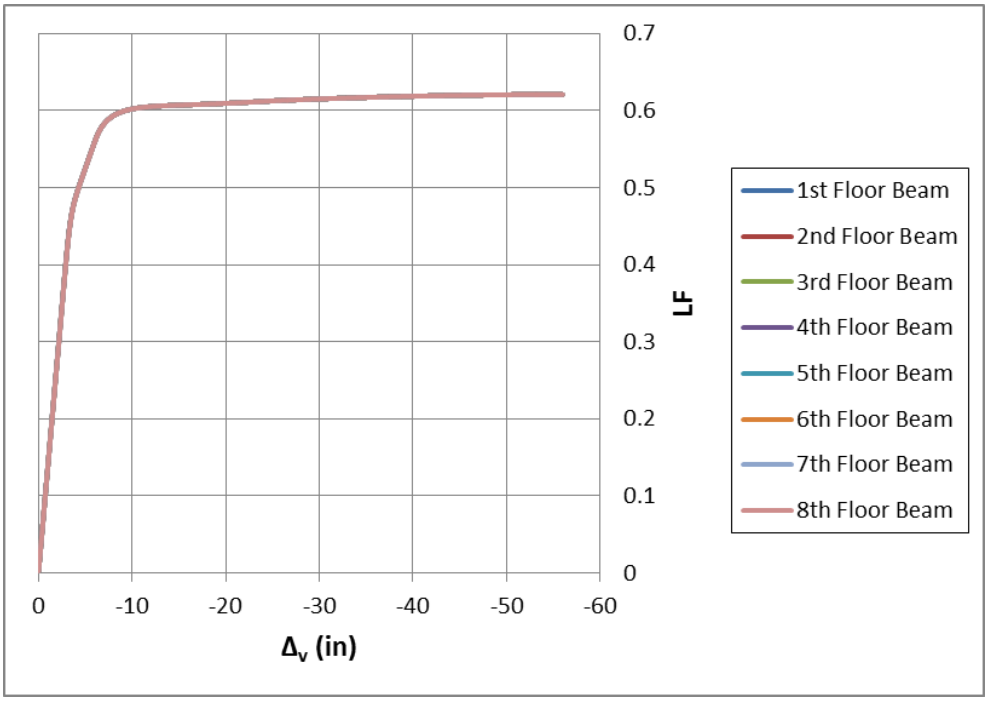

Figure 3-38 LF vs. Vertical Deflection (Scenario 3)

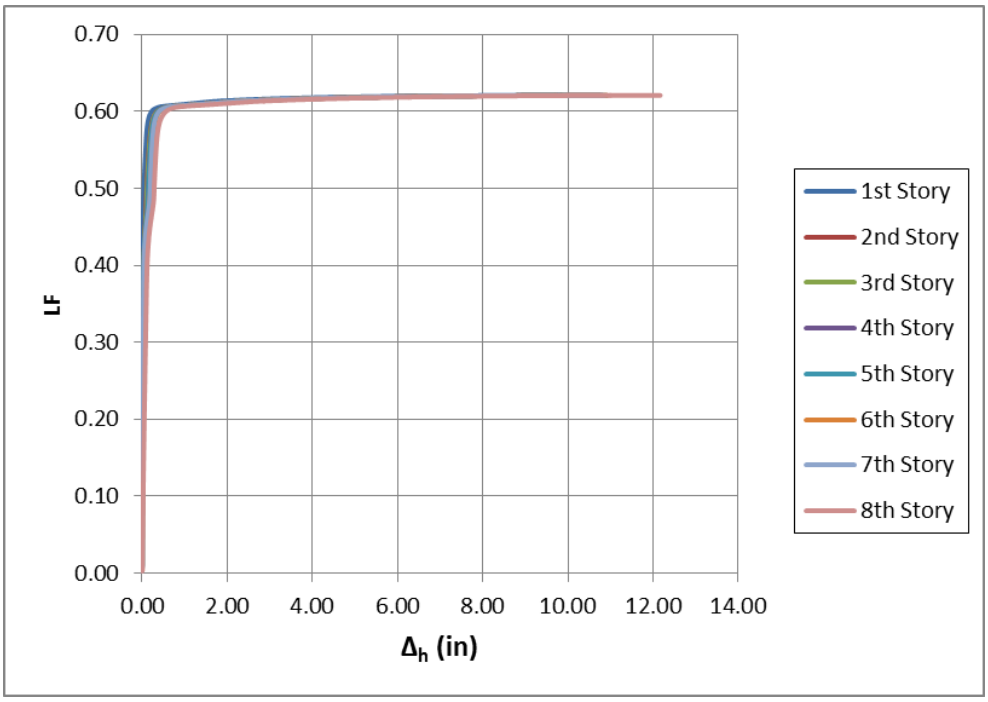

Figure 3-39 LF vs. Horizontal Side-Frame Displacement (Scenario 3)

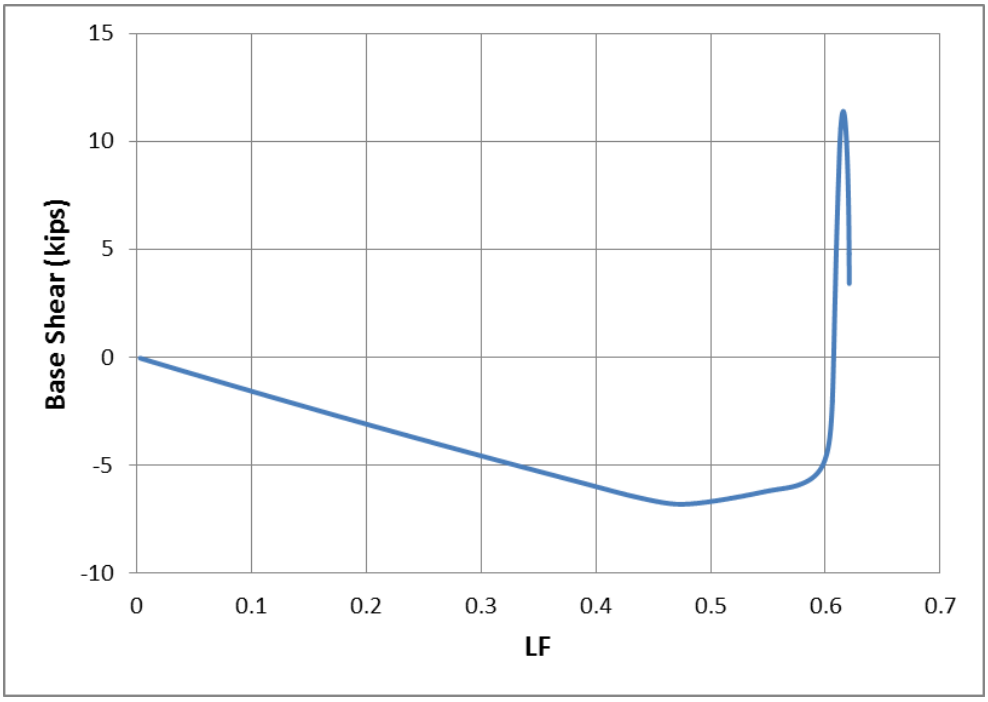

Figure 3-40 Base Shear vs. LF (Scenario 3)

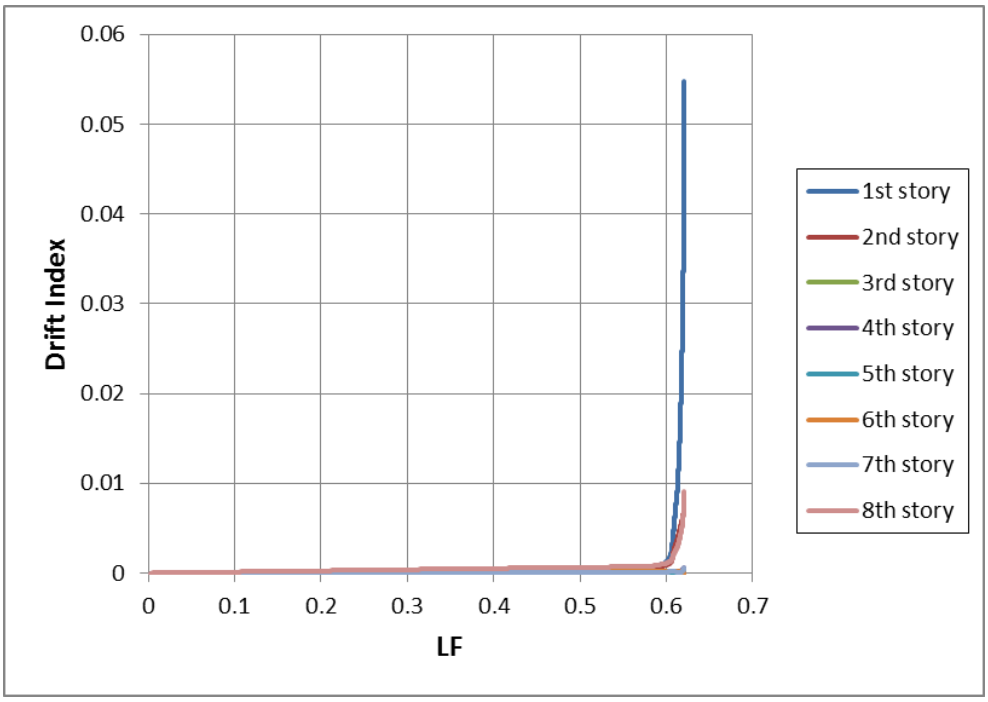

Figure 3-41 Drift Index vs. LF (Scenario 3)

The analytical results from scenario 3 show that the maximum LF achieved by the system was approximately 0.62. The maximum vertical mid-span deflection of the beams and maximum horizontal side-frame displacement were about 56 in and 12 in respectively. These values augment the trend established by scenario 2's results: as the left side of the baseline system became weaker, despite the increased flexibility, overall deflection levels went down.

The levels of horizontal drift exhibited by the system, shown in Figure 3-41, were notably smaller than what was seen prior. However, the same deflections associated with the onset of catenary behavior are seen in Figures 3-38 and 3-39.

The maximum base shear developed in this scenario was about 11.5 kips. The trend for base shear, provided in Figure 3-40, shows little deviation from the other column-removal scenarios. However, the difference between the LF at the maximum level of base shear (0.616) and the LF at failure (0.62) is somewhat smaller.

Failure in column-removal scenario 3 was characterized by instability in the first-story column within the left side-frame. As indicated by Figure 3-42, system failure coincided with plastic hinge formation at the column's fixed base.

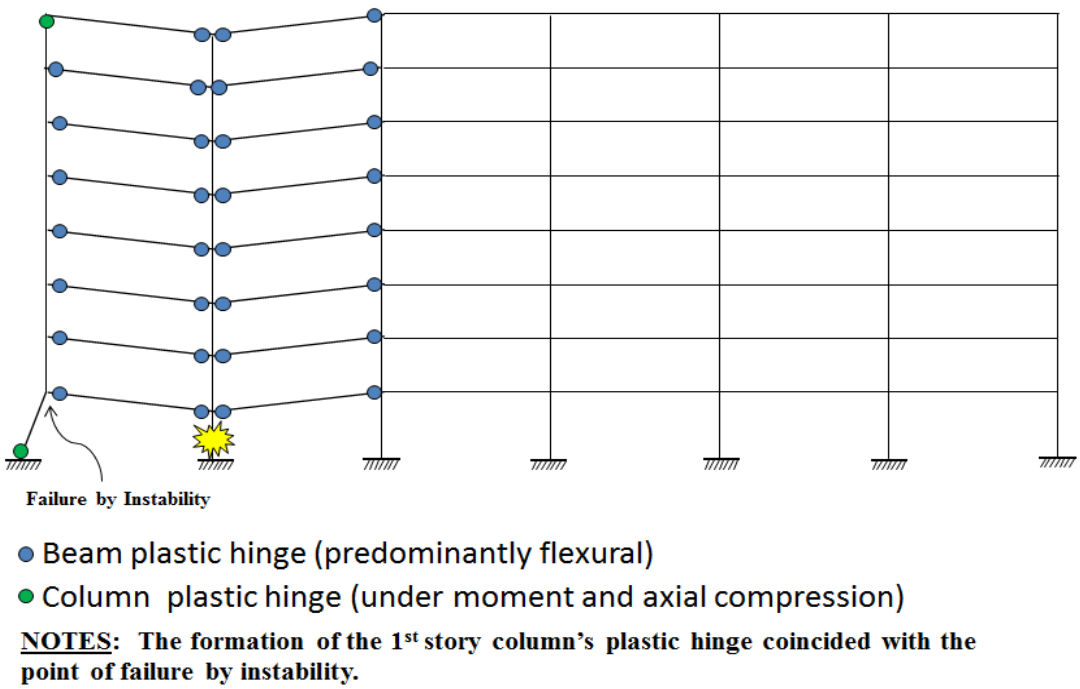

Figure 3-42 Baseline System Failure Mode (Scenario 3)

3.5.4.3 Catenary Action Demands

Figures 3-43 through 3-47 show the catenary action demands in the first – eighth floor beams for scenario 3. Points A and B correspond to the same points defined previously.

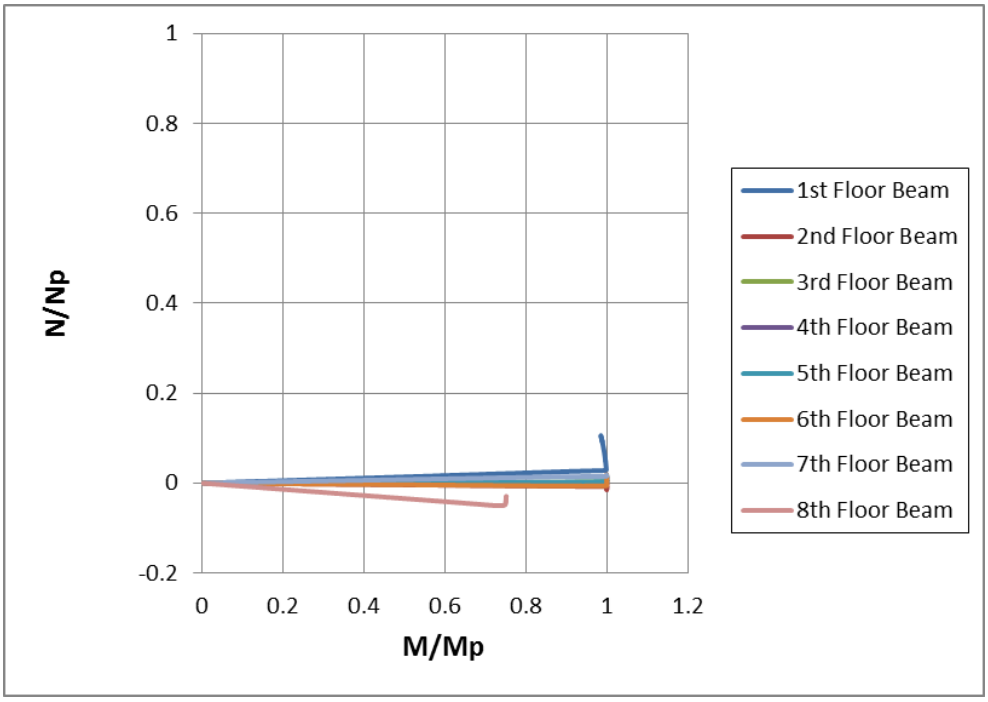

Figure 3-43 N/Np vs. M/Mp (Scenario 3)

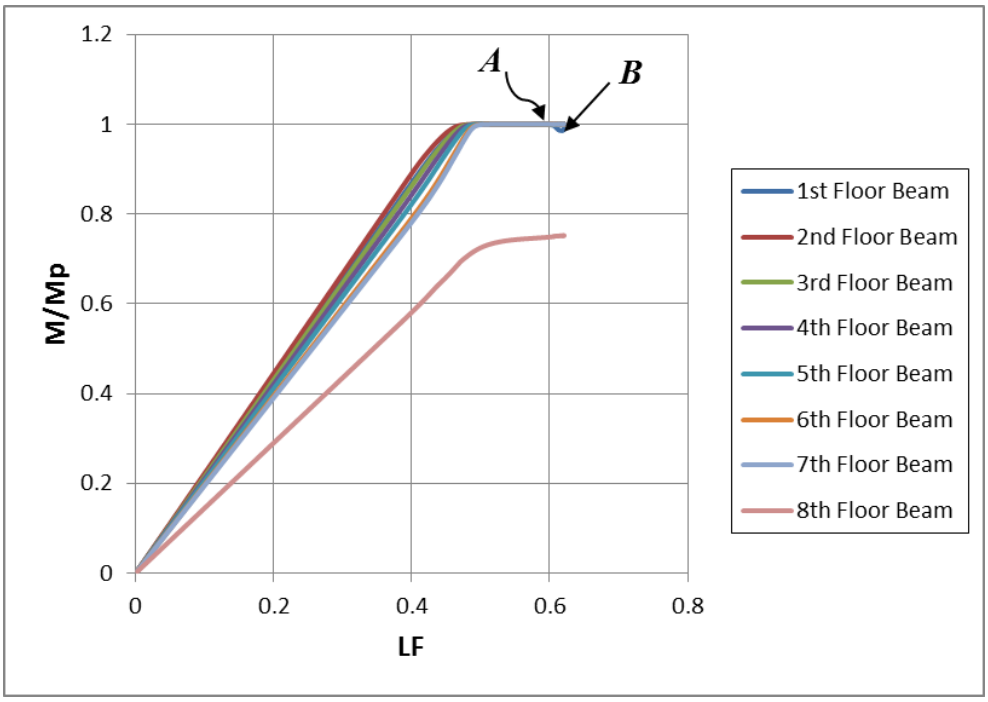

Figure 3-44 M/Mp vs. LF (Scenario 3)

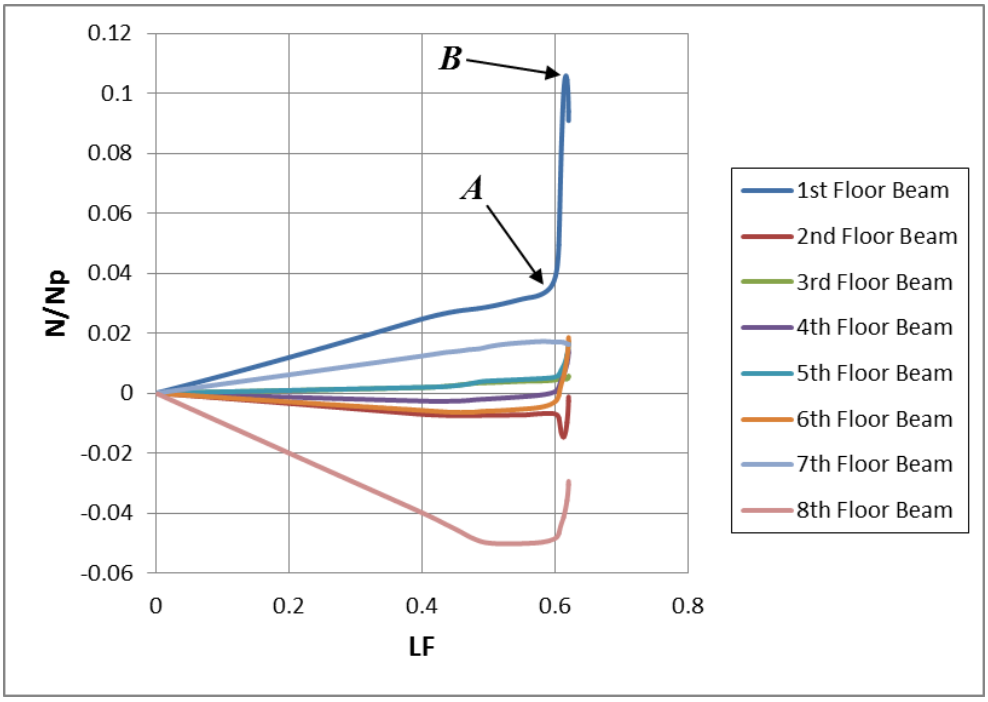

Figure 3-45 N/Np vs. LF (Scenario 3)

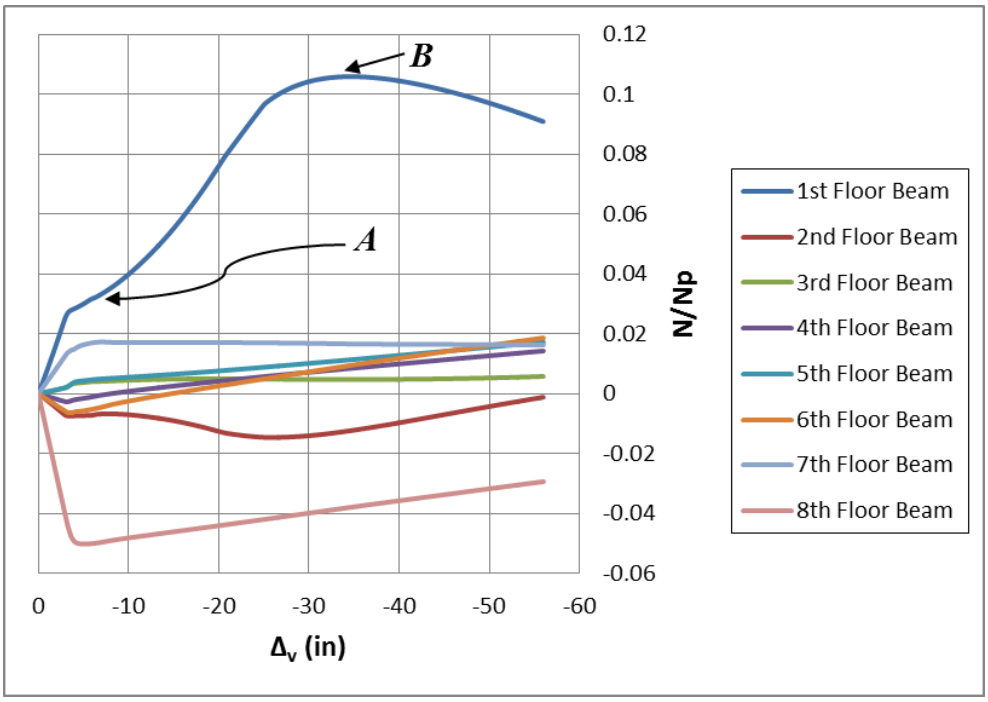

Figure 3-46 N/Np vs. Vertical Deflection (Scenario 3)

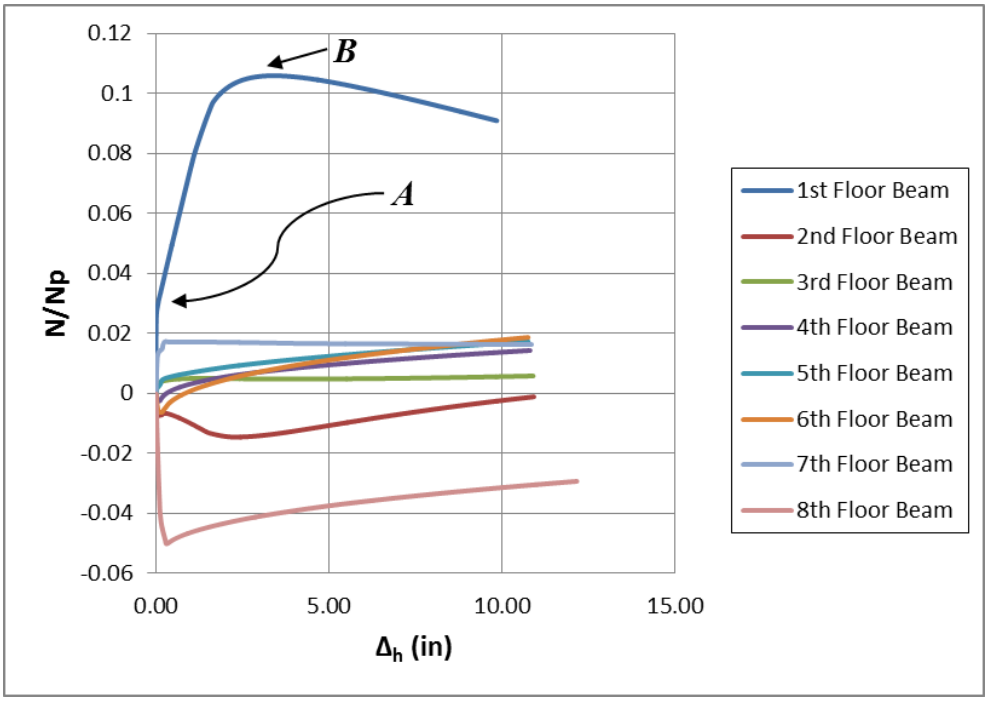

Figure 3-47 N/Np vs. Horizontal Side-Frame Displacement (Scenario 3)

Several conclusions can be drawn from examining Figures 3-43 through 3-47 in detail. In this scenario, the first-floor beam developed a maximum value of 40 kips (about 10.6% of Np) in axial tension. This value is significantly smaller than the corresponding maximums from both preceding scenarios. Additionally, the eighth-floor beam only formed plastic hinges at its right end and at its center. Moreover, this beam remained in axial compression throughout the entire analysis. A similar behavior, with a slight difference, was exhibited by the second-floor beam. While this beam also remained in compression for the duration of the analysis, it formed all plastic hinges contributing to flexural plastic collapse within its span, as identified in Figure 3-44.

In scenario 3, the difference between the LF at which the maximum catenary force was achieved (point B) and the LF at total collapse is fairly negligible; as seen before, this outcome can be identified by a similar trend for base shear.

3.5.4.4 Connection Ductility Demands

The levels of plastic rotation developed in each beam resulting from column-removal scenario 3 are shown in Figures 3-48 and 3-49. The maximum plastic rotation demands at each beam end prior to failure are provided in Table 3-3.

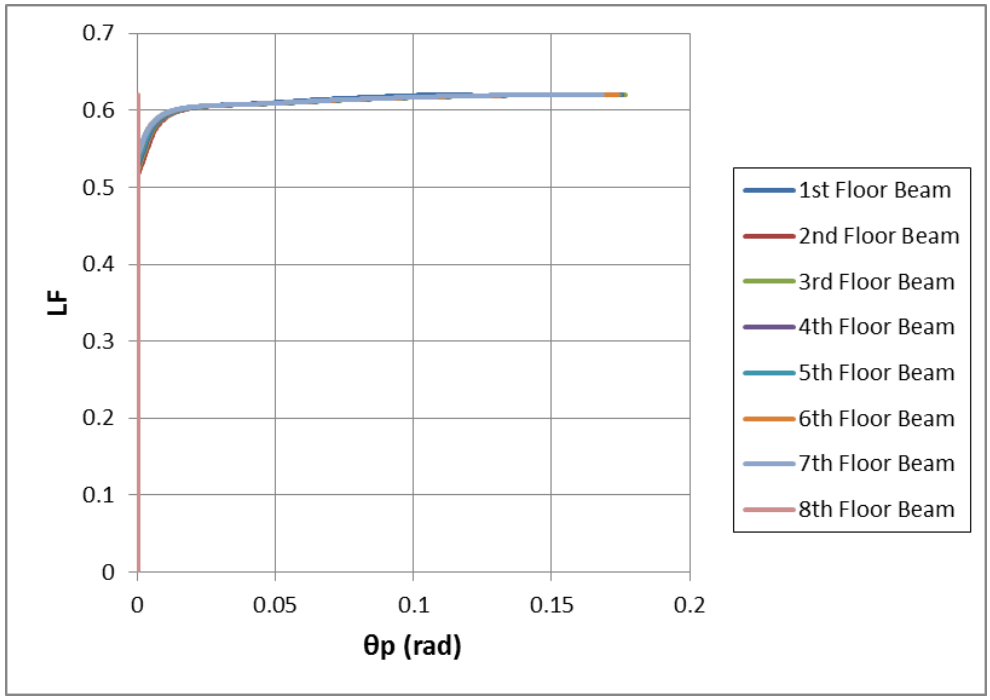

Figure 3-48 Plastic Rotation Demands (Scenario 3 – Left End)

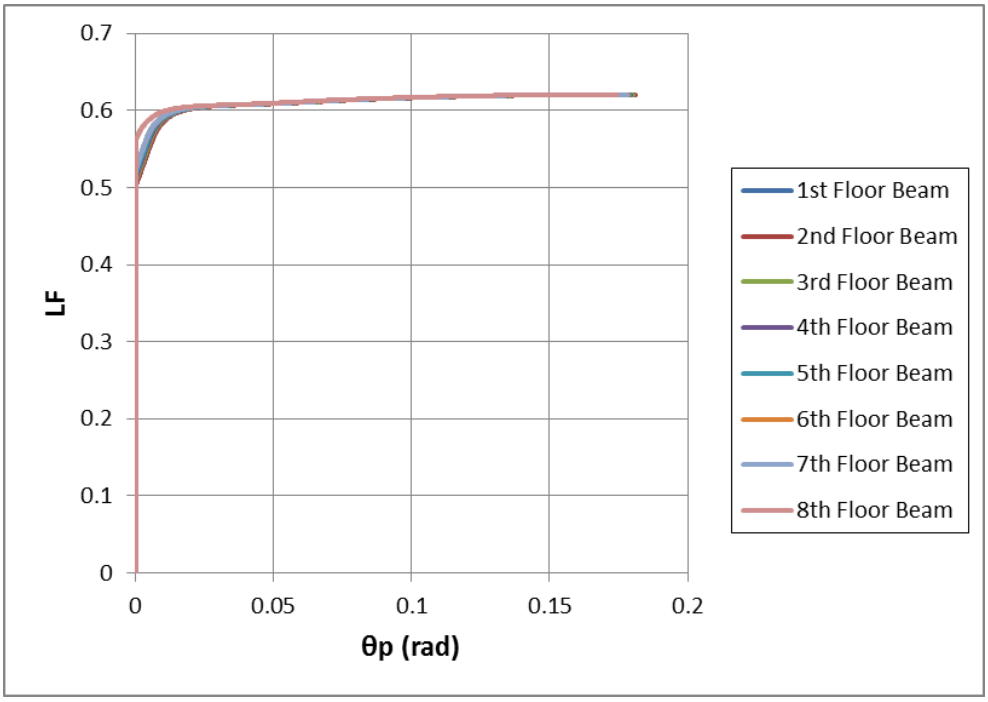

Figure 3-49 Plastic Rotation Demands (Scenario 3 – Right End)

Table 3-3 Plastic Rotation Demands at Maximum LF (Scenario 3)

Beam Location	θp, Left End (rad)	θp, Right End (rad)
1st Floor	0.121	0.180
2nd Floor	0.174	0.181
3rd Floor	0.177	0.18
4th Floor	0.176	0.179
5th Floor	0.175	0.179
6th Floor	0.174	0.178
7th Floor	0.168	0.178
8th Floor	0	0.175

The maximum plastic rotation demands associated with scenario 3 were comparatively smaller than the values attained in the previous two scenarios. However, these demands still remained relatively constant among the beams. Once again, an

exception was seen at the left end of the first-floor beam attributed to joint flexibility associated with plasticity in the first-story column anchoring this end.

3.5.5 Scenario 4

The fourth column-removal scenario considered the reaction of the system to the notional removal of the corner column. In this scenario, the first-floor beam had no column anchoring its left end; this lack of restraint noticeably influenced the behavior of the system. Due to its significant departure from the catenary response exhibited in the other three scenarios, which is the main focus of this thesis, the analysis of column-removal scenario 4 is limited and recommended for future study.

3.5.5.1 Effect of Model Type

Load-deflection plots comparing the results of the three model types for scenario 4 are provided below in Figures 3-50 and 3-51; a comparison of axial force development with LF is shown in Figure 3-52. Consistent with the previous methods of presentation, these figures show results for the first-floor beam only.

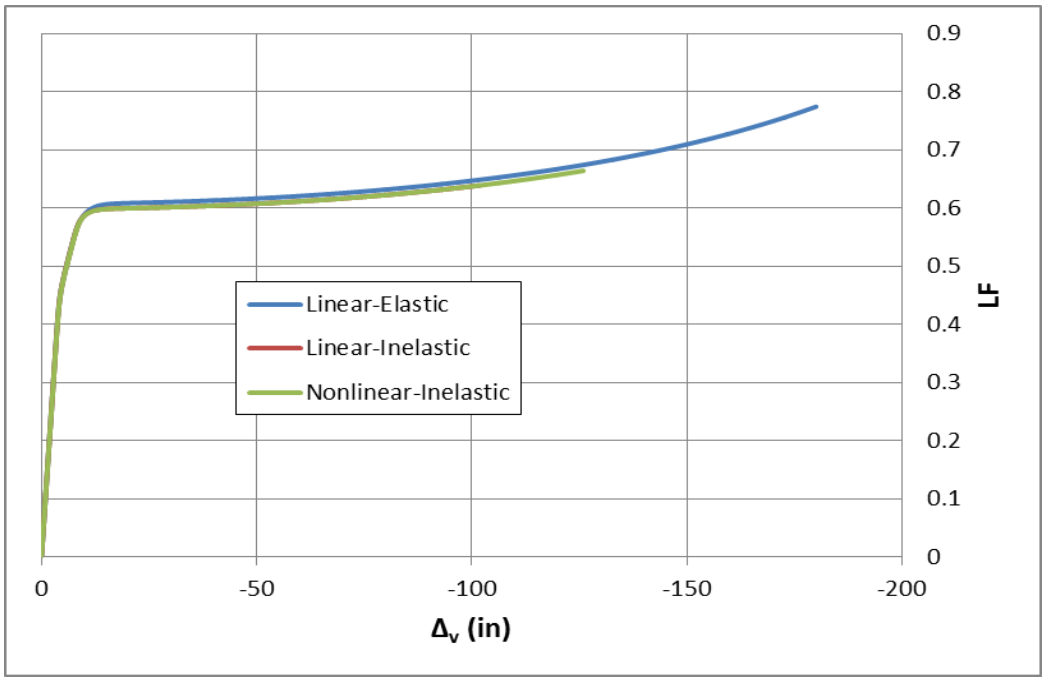

Figure 3-50 Comparison of LF vs. Vertical Deflection by Model Type (Scenario 4)

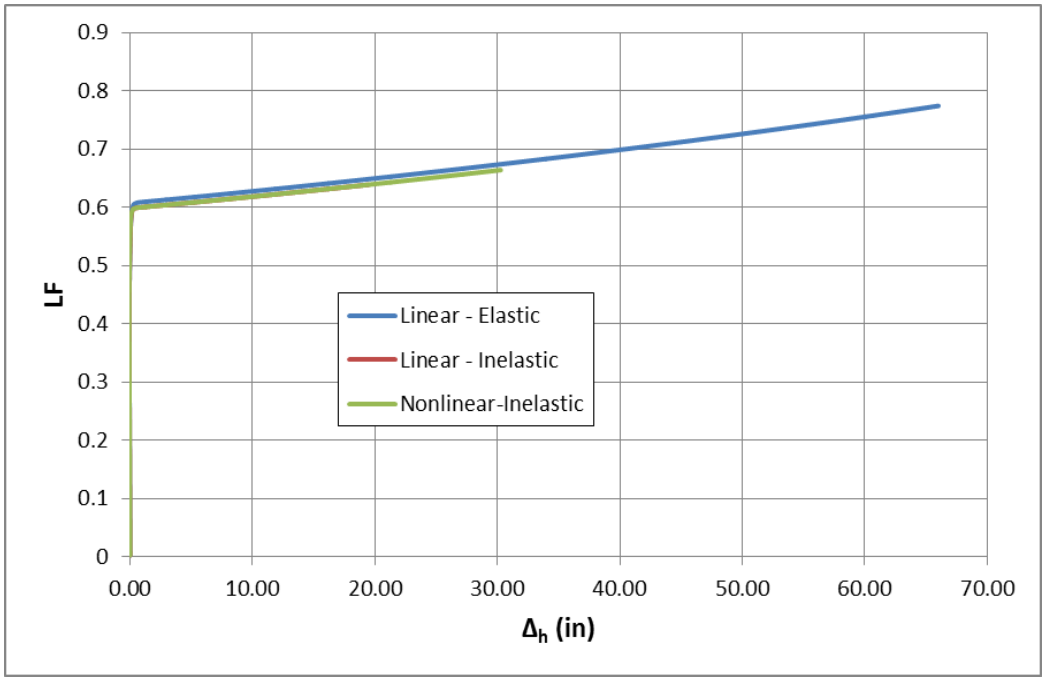

Figure 3-51 Comparison of LF vs. Horizontal Side-Frame Displacement by Model Type (Scenario 4)

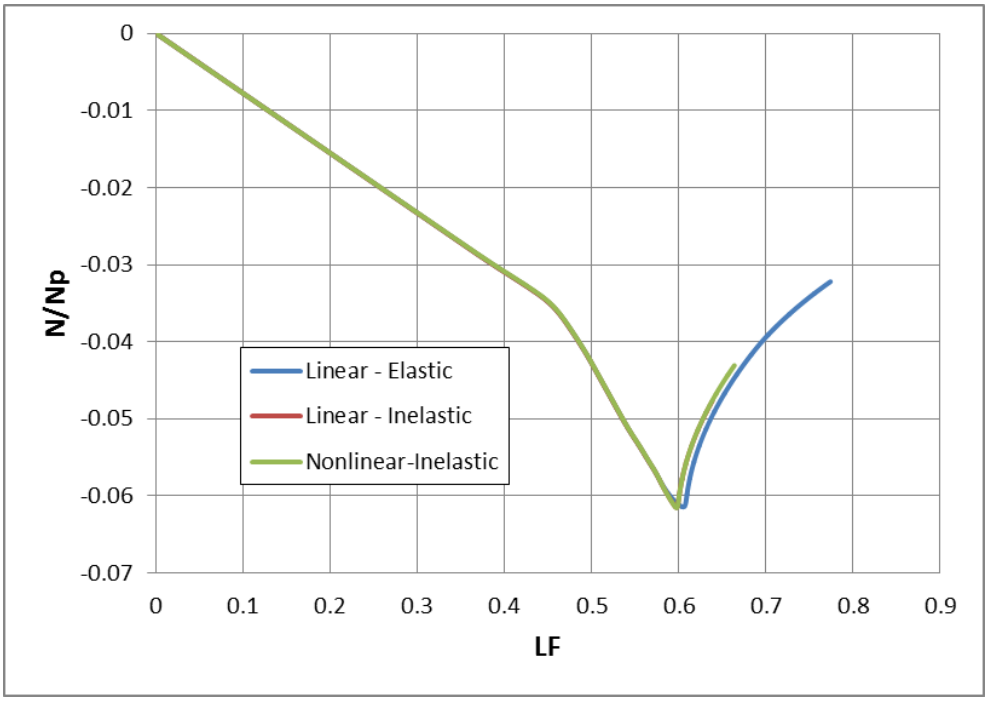

Figure 3-52 Comparison of N/Np vs. LF by Model Type (Scenario 4)

Figures 3-50 through 3-52 show noticeable differences from the trends identified in the previous column-removal scenarios. Specifically, the behavior of each model is nearly identical. The only perceivable variation between the three models can be seen in the trends for the linear-elastic model. This model, having no strength limitations associated with it, is able to show a more extended range of behavior.

Additionally, Figure 3-52 indicates that the first-floor beam remained in compression throughout the entire analysis, but did exhibit some reduction in the magnitude of this force following the point of flexural collapse.

3.5.5.2 General Response

The load-deflection response of the baseline system to column-removal scenario 4 is shown below in Figures 3-53 and 3-54. Plots of base shear and drift index versus LF are shown in Figures 3-55 and 3-56 respectively.

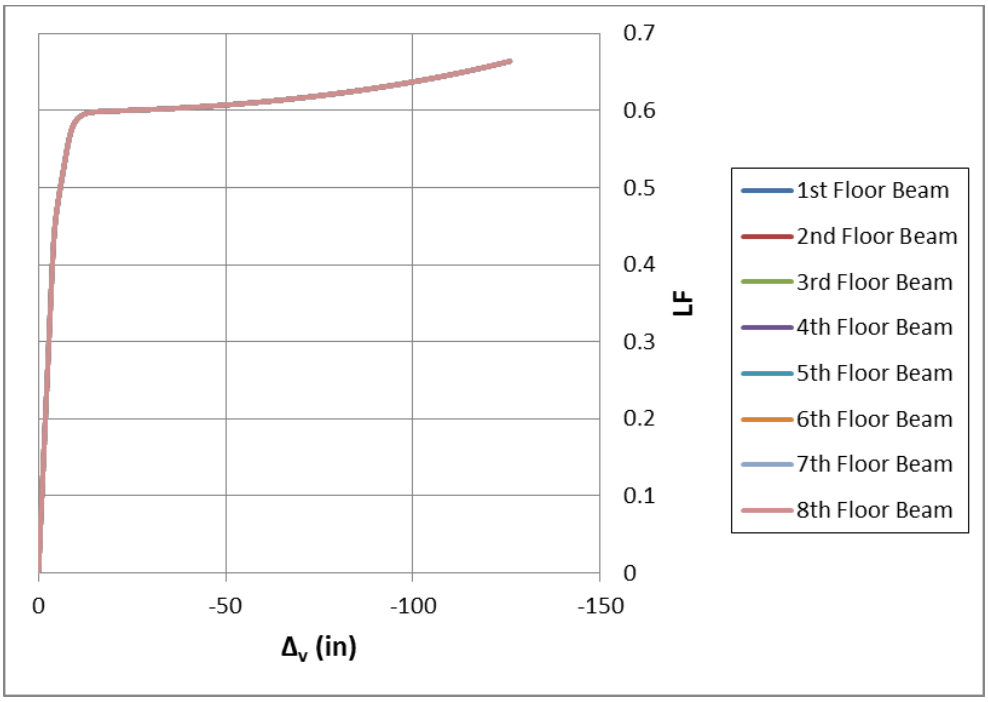

Figure 3-53 LF vs. Vertical Deflection (Scenario 4)

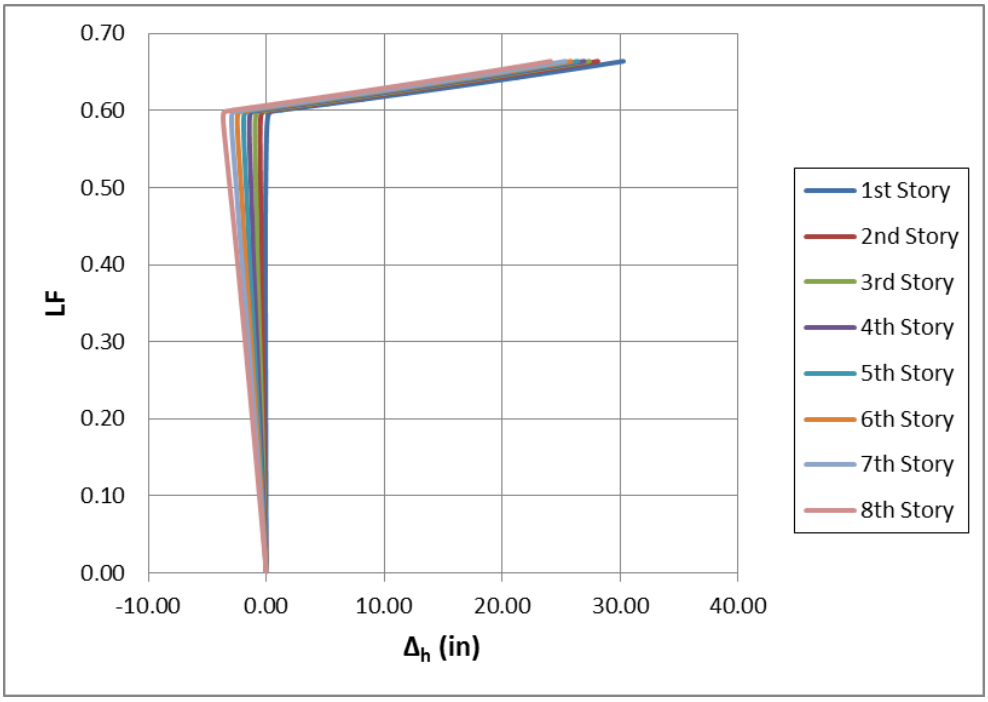

Figure 3-54 LF vs. Horizontal Side-Frame Displacement (Scenario 4)

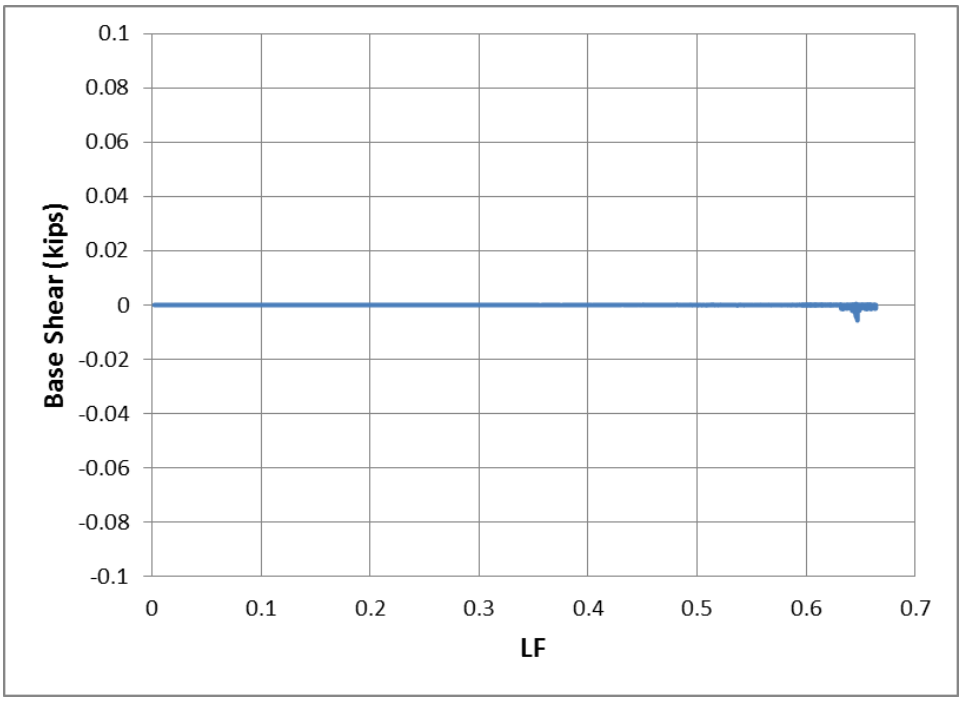

Figure 3-55 Base Shear vs. LF (Scenario 4)

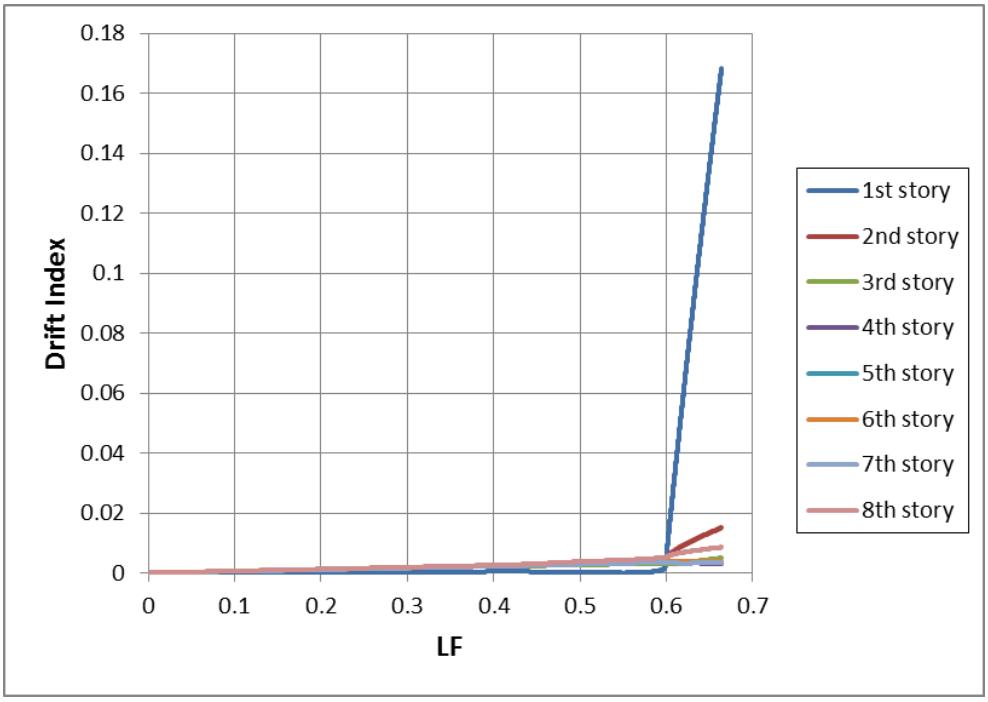

Figure 3-56 Drift Index vs. LF (Scenario 4)

The results from column-removal scenario 4 indicate different behavioral trends than what has been previously discussed. Of primary interest is that the baseline system achieved a maximum LF of 0.66 in this scenario before divergence occurred, a level closer to what the system achieved in scenario 2 than the lower level sustained during scenario 3.

Moreover, past the point of flexural plastic collapse, the trends depicted in Figures 3-53 through 3-56 show that the levels of load increased with deflection despite the lack of any significant development of base shear, which is not suggestive of catenary behavior. Examining Figure 5-56 in greater detail, it can be seen that the system showed some small fluctuations in base shear just prior to failure. Since the magnitudes of these

fluctuations were relatively negligible, this behavior might be attributed to numerical instability or small amounts of load-redistribution prior to failure.

3.5.5.3 Catenary Action Demands

The individual responses of the first-eighth floor beams to column-removal scenario 4 are shown in Figures 3-57 through 3-61. Since the results indicate that no true catenary forces developed in reaction to column-removal scenario 4, the behavioral trends shown in these figures cannot accurately be associated with catenary behavior. Consequently, the points designated on the corresponding plots from scenarios 1-3 are not utilized in this section. For consistency, the results depicted in these figures are from the beams' left ends.

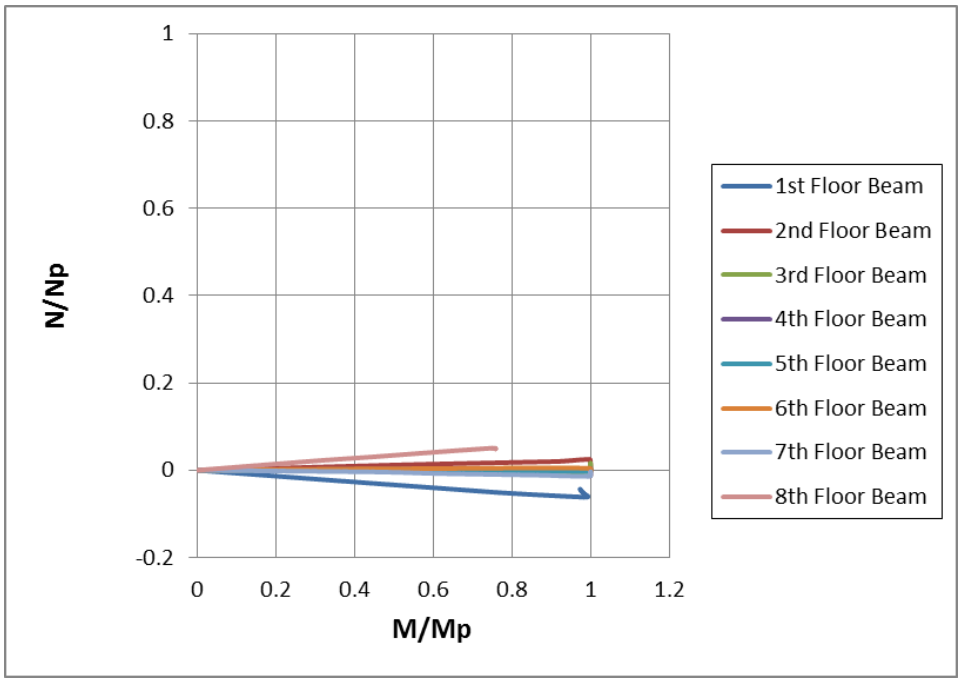

Figure 3-57 N/Np vs. M/Mp (Scenario 4)

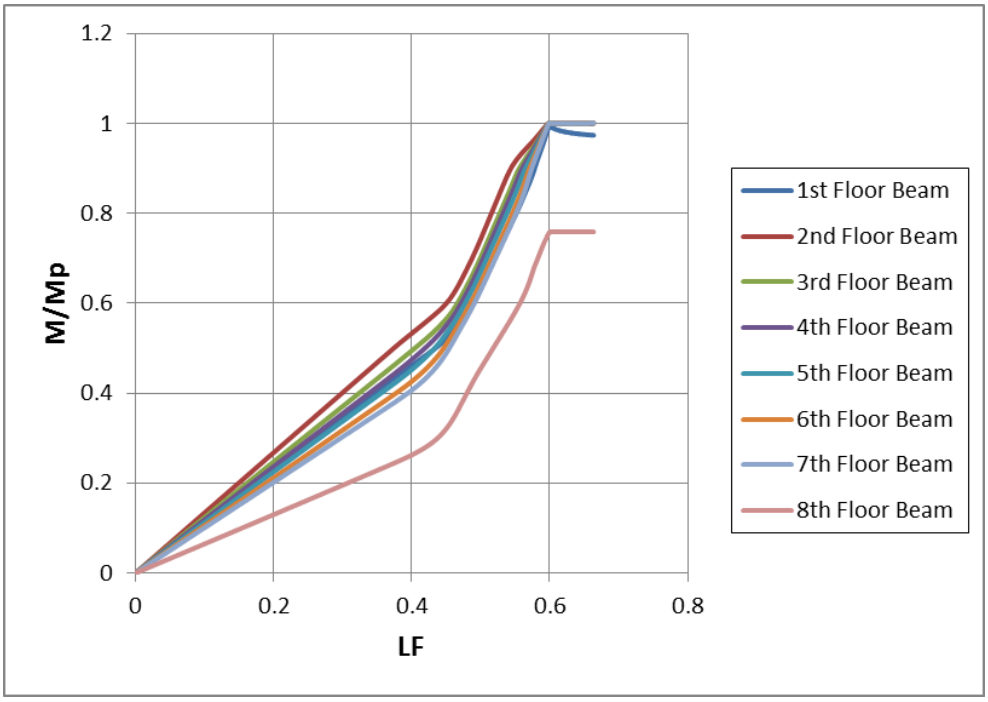

Figure 3-58 M/Mp vs. LF (Scenario 4)

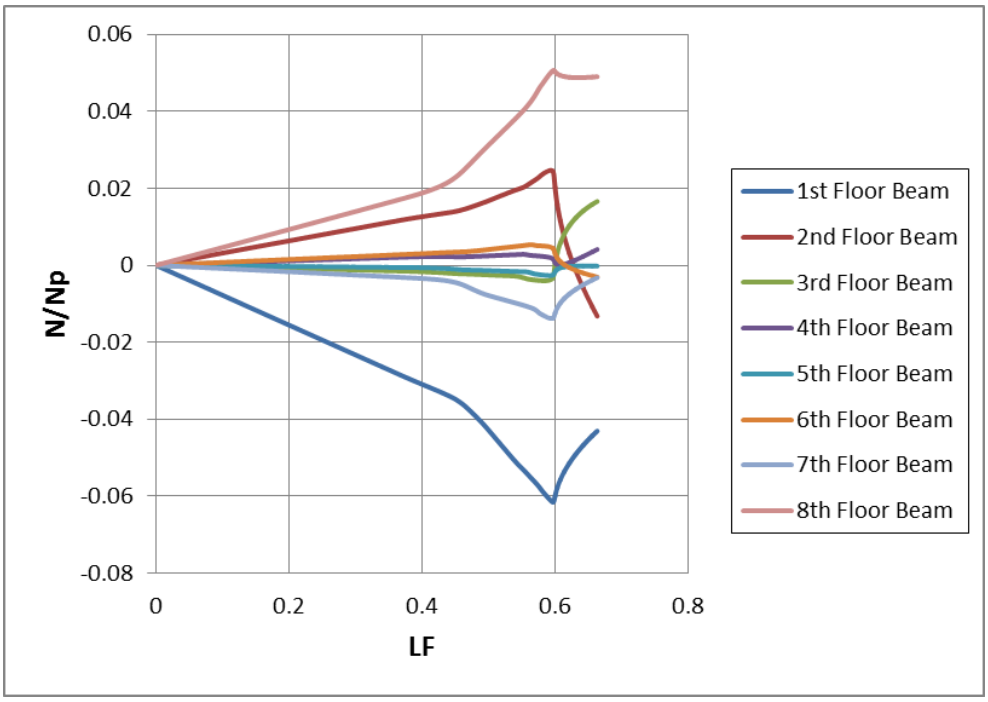

Figure 3-59 N/Np vs. LF (Scenario 4)

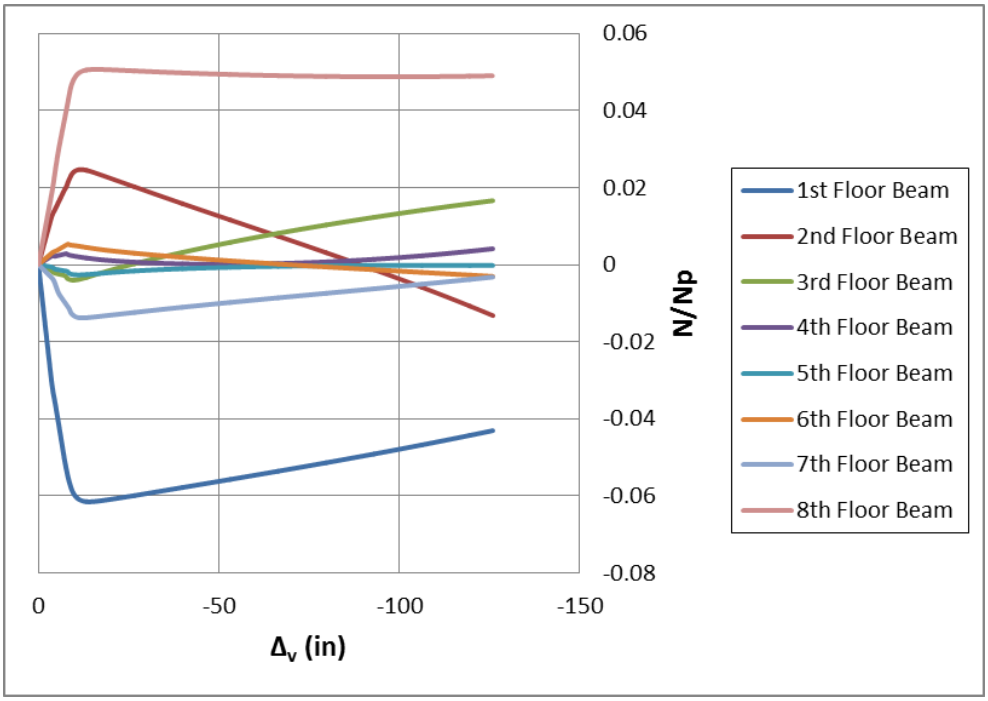

Figure 3-60 N/Np vs. Vertical Deflection (Scenario 4)

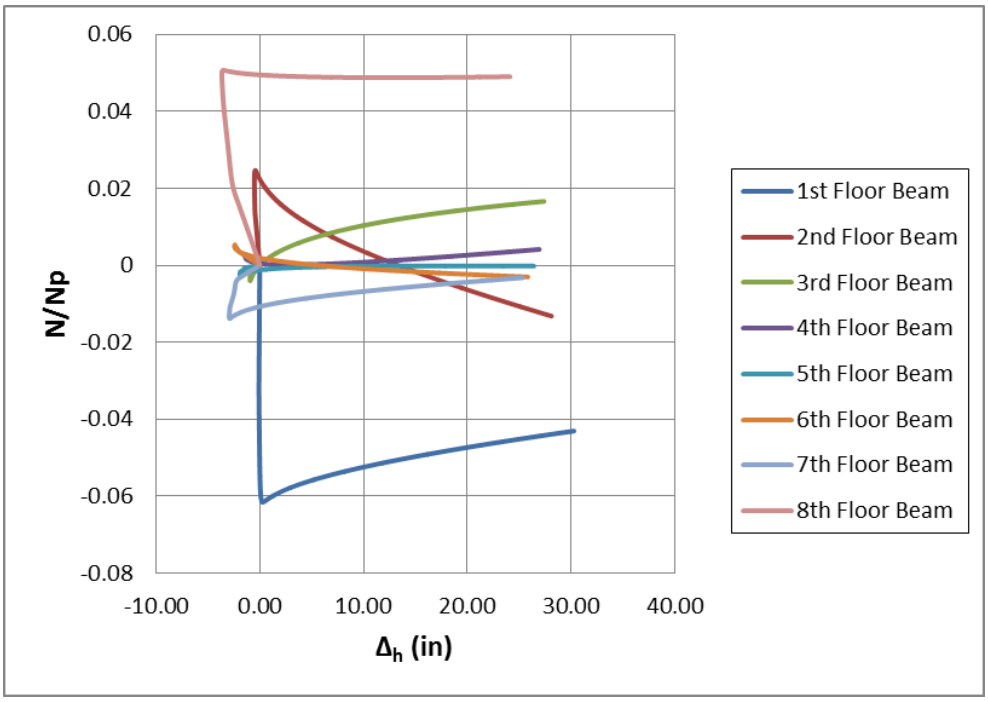

Figure 3-61 N/Np vs. Horizontal Side-Frame Displacement (Scenario 4)

Figures 3-57 through 3-61 show that while a change in behavior occurred past the point of flexural plastic collapse, it is not outwardly indicative of catenary behavior. This can be concluded by the development of both tension and compression in the beams, depending upon the member location. The net result was a base shear of negligible magnitude. This trend continued until the simulation failed to converge at vertical and horizontal deflections in the first-floor beam of about 126 in and 30 in respectively.

3.5.5.4 Connection Ductility Demands

The levels of plastic rotation developed in each beam resulting from column-removal scenario 4 are shown in Figures 3-62 and 3-63. The maximum plastic rotation demands at each beam end prior to failure are shown in Table 3-4.

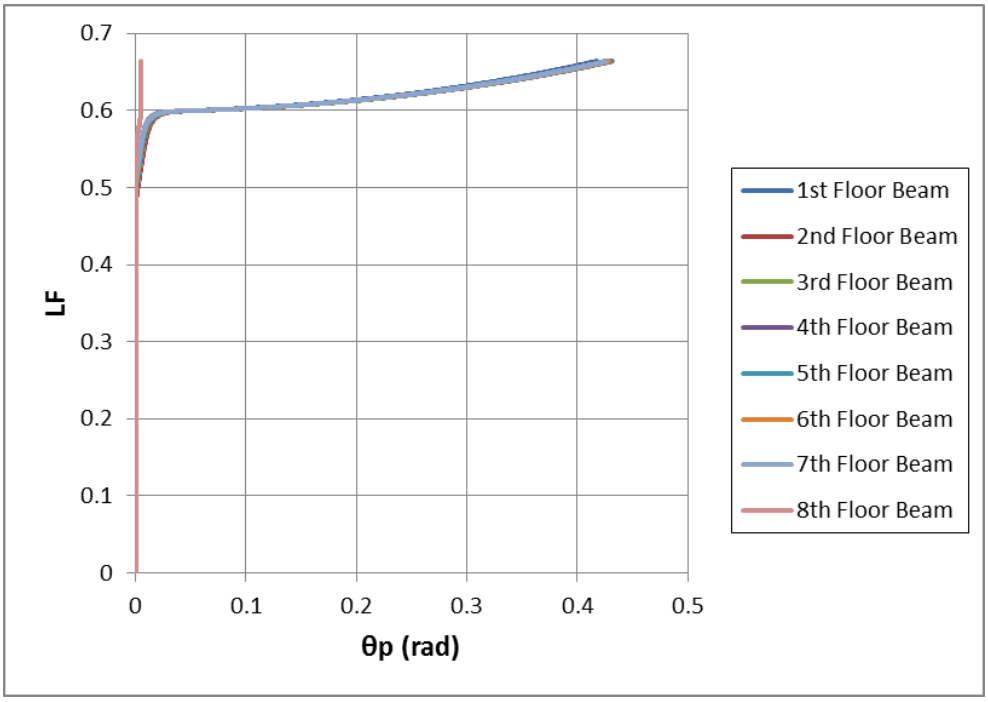

Figure 3-62 Plastic Rotation Demands (Scenario 4 – Left End)

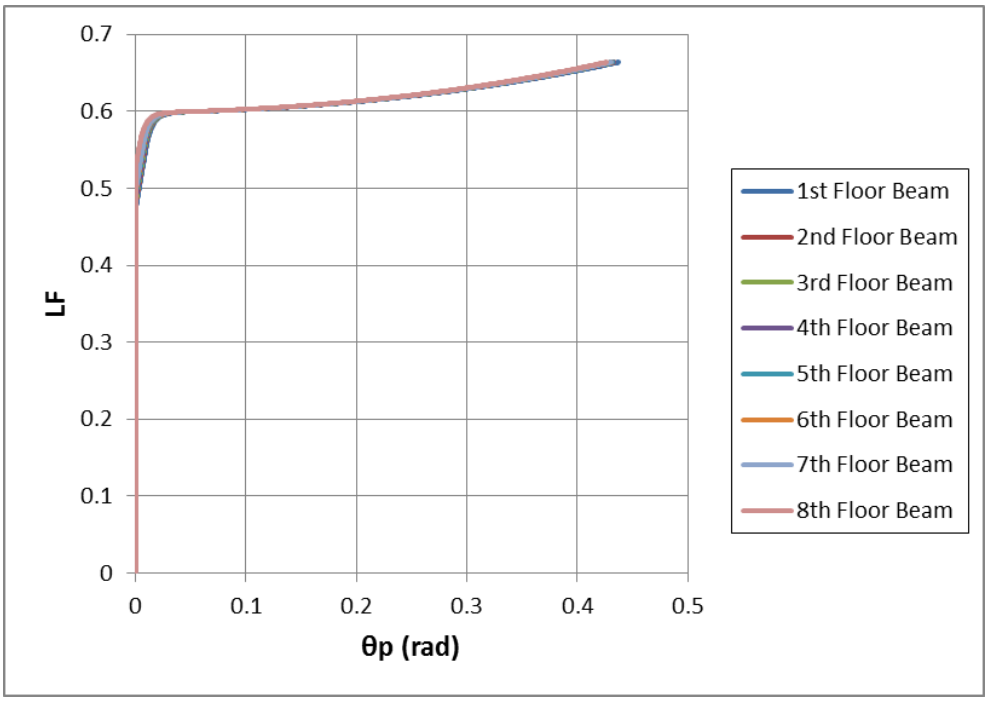

Figure 3-63 Plastic Rotation Demands (Scenario 4 – Right End)

Table 3-4 Plastic Rotation Demands at Maximum LF (Scenario 4)

Beam Location	θp, Left End (rad)	θp, Right End (rad)
1st Floor	0.418	0.438
2nd Floor	0.426	0.434
3rd Floor	0.432	0.433
4th Floor	0.431	0.433
5th Floor	0.43	0.432
6th Floor	0.429	0.431
7th Floor	0.427	0.431
8th Floor	0.005	0.427

The plastic rotation demands shown in Figures 3-62 and 3-63 are correlative with the large deflections undergone by the baseline system during scenario 4. The lowest demands were observed at the left end of the eighth-floor beam, where plastic hinge formation had occurred in the adjacent column. In general, the plastic rotation demands exhibited by the system during scenario 4 were significantly larger than the corresponding maximums from the other scenarios. In addition to the substantial levels of deflection and the lack of any relevant catenary force development, this behavior can be associated with lower levels of joint rotation.

3.6 Scenario Comparisons

In this section, comparisons are made between the first three column-removal scenarios concerning the differences in the load-carrying capacity of the baseline system, potential failure modes of the system, the extent of catenary force development observed in each case, and the trends for plastic rotation associated with catenary behavior. Due to the significant behavioral differences previously discussed, column-removal scenario 4 is

not included in these comparisons. At the end of the section, a general discussion emphasizing important concepts from the baseline study is then developed.

3.6.1 Comparison of Load-Carrying Capacity

Figures 3-64 and 3-65 show levels of deflection with increasing LF (until failure) for the nonlinear-inelastic model of each column-removal scenario. Maximum values are provided below in Table 3-5.

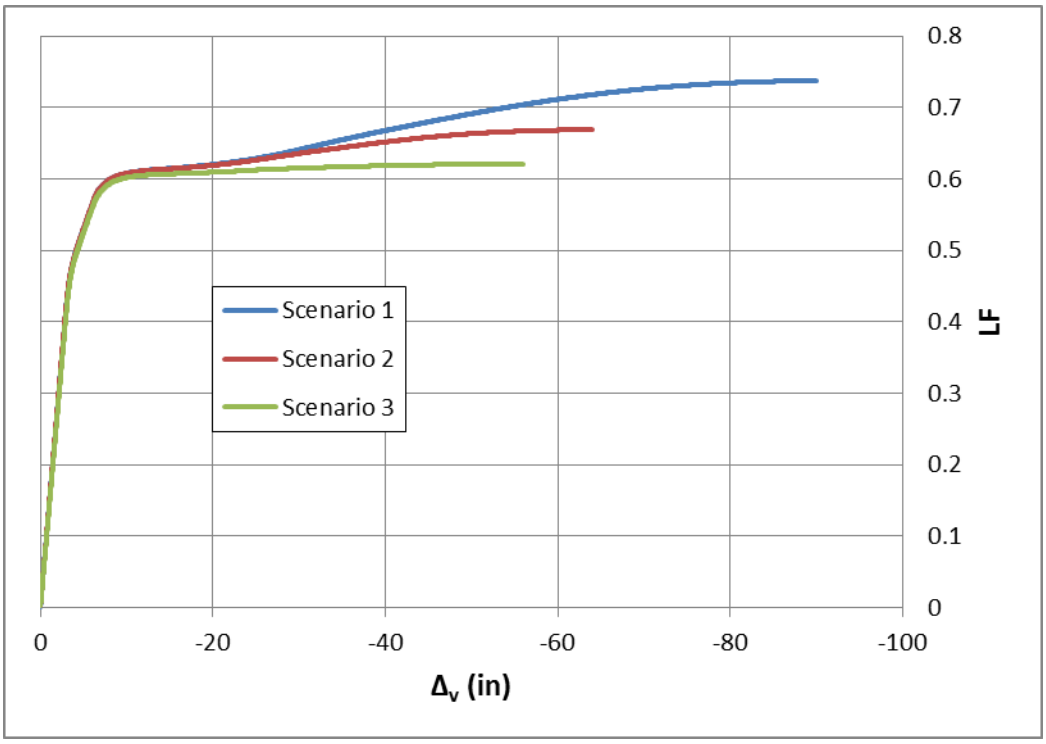

Figure 3-64 Scenario Comparison of LF vs. Vertical Deflection

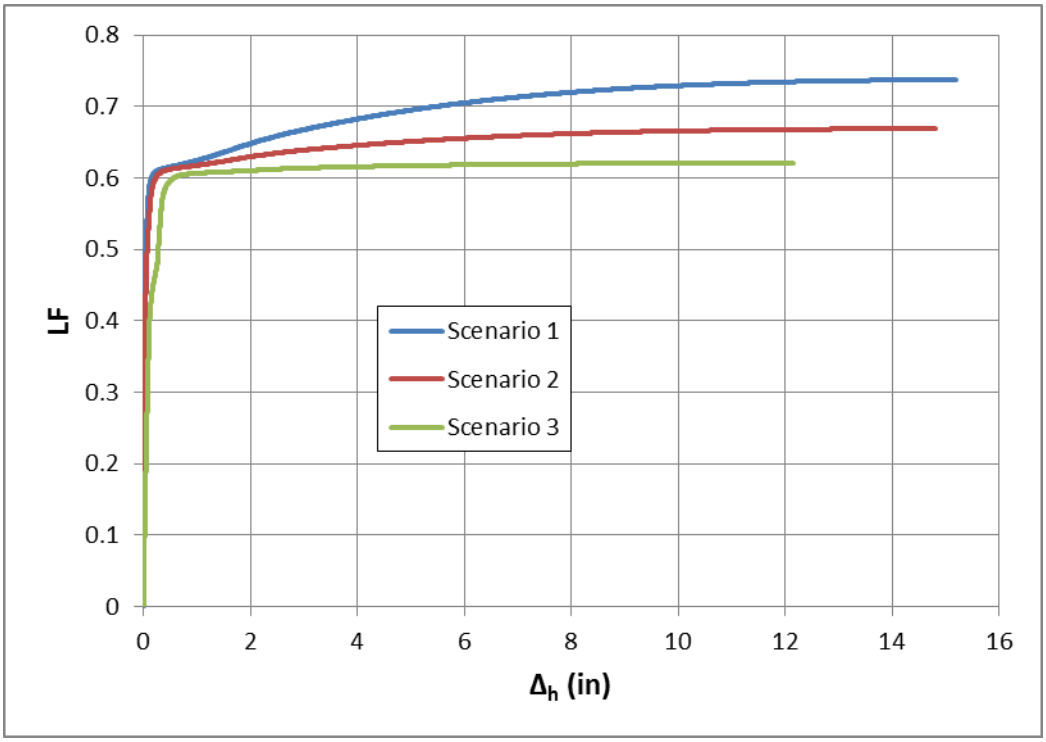

Figure 3-65 Scenario Comparison of LF vs. Horizontal Side-Frame Displacement

Table 3-5 Scenario Comparison of Maximum LFs and Deflection Levels

Column Removal Scenario	Maximum LF	Maximum Δ_h (in)	Maximum Δ_v (in)
1	0.737	15.2	90
2	0.669	14.8	64
3	0.621	12.2	56

The trends displayed in Figures 3-64 and 3-65 show the significance of the type of column-removal scenario considered to the response of the baseline system. As the removed column got closer to the corner, the lateral loads associated with progressive collapse caused significantly larger deflections in both the beam and the adjoining side-frames at the same level of vertical load. This behavior can be connected to the reduced levels of stiffness in the left side of the anchoring system. Moreover, the maximum LF

sustained became considerably lower, going from 0.737 in the first scenario to 0.621 in the third. This allowed the baseline system to reach larger magnitudes of deflection in scenarios 1 and 2, despite the increased levels of anchoring.

Furthermore, reducing the number of first-story columns in each side-frame seemed to change the mode of failure exhibited by the baseline system. In the first case, with equivalent levels of anchoring on either side of the beams, collapse was facilitated through a plastic sway mechanism. However, in scenarios 2 and 3, reductions in the number of columns present in the left side of the first-story seemed to cause failure modes characterized by instability.

Finally, Table 3-5 shows that the baseline system failed to reach the design loads in any of the column-removal scenarios, indicating a potential susceptibility of this particular structure to progressive collapse. However, the extent of failure differed between the three scenarios; scenario 1 resulted in the total collapse of the frame, while scenarios 2 and 3 resulted in partial collapse of the weaker side of the system.

3.6.2 Comparison of Catenary Force Development

Figure 3-66 shows a comparison of catenary force development in the first-floor beam with increasing LF for all scenarios. This beam has been chosen for comparison purposes, since it was the only beam to achieve any significant level of axial tension attributed to a catenary mode of response. Table 3-6 provides the maximum catenary forces (normalized with respect to Np) for all scenarios.

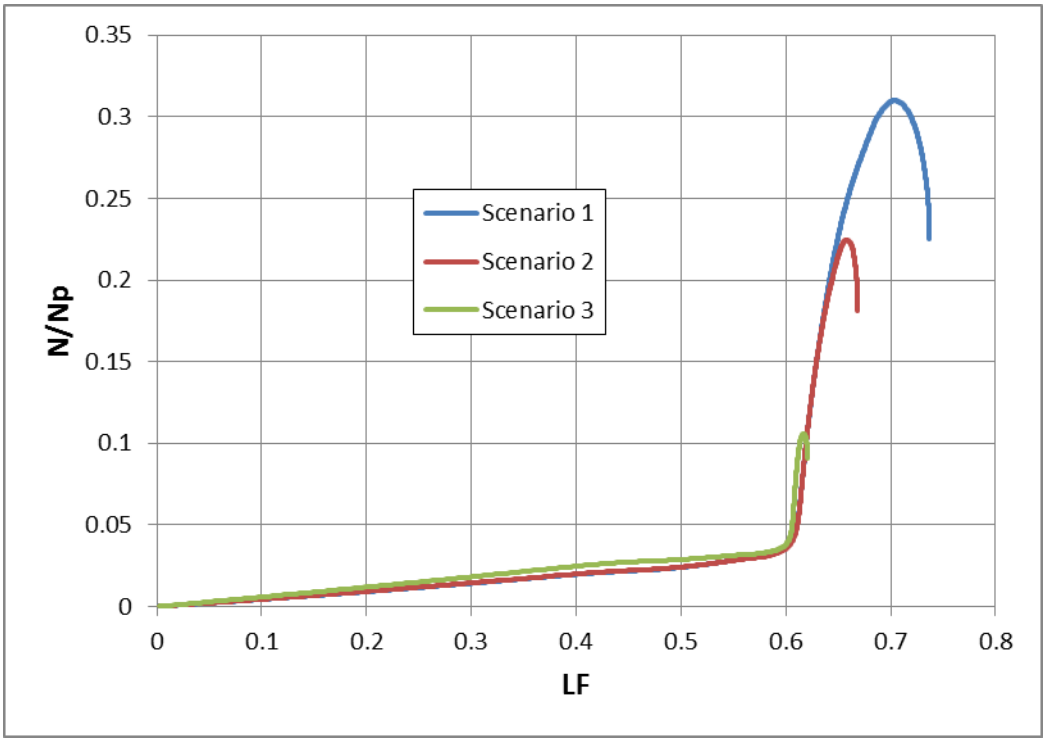

Figure 3-66 Scenario Comparison of N/Np vs. LF

Table 3-6 Scenario Comparison of Maximum Values of N/Np

Column Removal Scenario	Maximum LF	Maximum N/Np
1	0.737	0.310
2	0.669	0.224
3	0.621	0.106

Figure 3-66 shows that the behavioral patterns associated with catenary force development, which were discussed in the preceding sections, remained relatively similar, regardless of the column-removal scenario considered. However, Table 3-6 shows that the amount of catenary force developed in each scenario varied significantly. From scenario 1 to scenario 2, the maximum catenary force decreased 27.7%. From scenario 2 to scenario 3, it decreased53.6%. When compared to the corresponding

decreases in LF of 8.5% and 7.2%, it can be seen that the loss of anchoring members in the left side-frame seemed to more substantially influence the catenary demands. As previously explained, this difference can be attributed, in part, to the higher levels of deflection present in scenarios 2 and 3 which resulted in a larger vertical component for the axial force.

3.6.3 Comparison of Connection Ductility Demands

Table 3-7 displays both the location and the value of maximum plastic rotation for each column-removal scenario.

Table 3-7 Scenario Comparison of Maximum Plastic Rotation Demands

Column Removal Scenario	θp at Maximum LF (rad)	Beam Location
1	0.298	4th floor
2	0.206	2nd & 3rd floors
3	0.181	2nd floor

As indicated by Table 3-7, the maximum values of plastic rotation in the beams generally decreased as the column-removal location got successively closer to the corner of the structure. This was likely a consequence of the decreased level of force demand associated with failure in these scenarios. In other words, as the number of members in the left side-frame decreased, the overall strength level of the system decreased. This curtailed strength level seemed to result in a lower capacity for catenary force development and lower deflection and rotation demands related to this type of response.

Generally, plastic rotation demands seemed to be most influenced by joint rotations. These joint rotations can be associated with the natural elastic flexibility of the restraining members (eighth-floor) or extreme joint flexibility attributed to plasticity in the restraining members (first-floor). Consequently, maximum plastic rotation demands seemed to occur in locations with relatively stiff joints and low lateral force demands.

3.6.4 Conclusions

The correlations drawn from the baseline study indicate that a variety of aspects should be considered in order to investigate or mitigate progressive collapse in conventionally designed multi-story structures. The main conclusions drawn from the baseline study are summarized below:

- In all models, the effects of both geometric and material nonlinearity in the side-frames considerably influenced the system's behavior, demonstrating the significance of both in progressive collapse modeling techniques.

- The catenary forces developed in each scenario were greatest in the first-floor beam, likely due to the higher level of restraint available at this location. This highlights the potential need for the lowest-floor beam's connections and anchoring side-frames to be capable of sustaining the increased force demands associated with collapse-resistance.

- Principally a result of the high level of lateral force transferred by the first-floor beam, the failure modes in all column-removal scenarios seemed to be characterized by high degrees of plasticity and instability in the first-story columns. In general, the closer the removed column was to the center of the LLRS, the greater the exhibited capacity for load-resistance; however, in the event of failure, the extent of collapse was more severe.

- As discussed in Chapter 2, the rotation capacities of moment-resisting connections under combinations of moment and axial tension have not been firmly established in published literature. Consequently, depending upon the column-removal location being considered, a highly ductile connection type may result in the propagation of collapse through one of the failure modes seen in this chapter. Conversely, while utilizing a less ductile connection may result in partial collapse of the structure, it could potentially mitigate the extent of collapse.

- The results of column-removal scenario 4 showed a deviation from the catenary response observed in the first three scenarios. For concision, this behavior was not thoroughly investigated and is recommended for future study.

- The provisions for the UFC 4-023-03 TF method state that "There are no structural strength or stiffness requirements to be applied to the structural

members that are anchoring these horizontal tie forces." However, the preceding conclusions indicate that, precluding the influence of connection strength and ductility levels, the catenary force demands are directly related to both the stiffness and strength levels of the restraining systems. This investigation indicates that ignoring these associations could result in more severe collapse mechanisms.

Chapter 4 – Parametric Study

4.1 Overview

This chapter describes the parametric study, which was conducted to explore the effects of various design and layout considerations on the collapse response of structural steel moment frames. First described is the approach used to investigate the chosen parameters. Next, the results from each portion of the parametric study are presented and compared to the results from the baseline system and any other systems developed in this chapter suitable for inclusion. Finally, at the end of each section, conclusions are drawn regarding the potential impacts of the parameter under consideration.

4.2 Approach

Four parameters were selected for inclusion in this study: the building location, the number of stories, the number of bays in the lateral load-resisting system, and the building aspect ratio. These parameters were chosen for their perceived effects on the lateral load-resisting capability of the structure and/or the design loads used in analysis and member selection. Each parameter is investigated separately and compared to the results from the baseline study, which are provided in Chapter 3. The studies on the effect of the number of bays in the lateral load-resisting system and the effect of the number of stories also include a system developed for studying the effect of building

location. This system is included in order to determine the relative impact of changing the associated parameter in different building locations.

All systems designed for use in the parametric study were developed using the same design process employed for the development of the baseline system. For consistency, the central column removal scenario was utilized for all analyses included in this investigation. Based upon the precedent established in Chapter 3, all analyses were run using the nonlinear-inelastic model type and with the same analytical methodology previously employed.

The results for each parameter investigated are presented and discussed in a format comparable to what was adopted for use in Chapter 3; the general response is discussed first, then the catenary action demands, and finally the connection ductility demands. The locations, sign conventions, and methods of normalization (if applicable) for all values of deflection and force correspond to what was used for scenario 1 of the baseline system.

Within each section that discusses a particular type of response or behavior, the results from all systems in consideration are provided on the same figure. Following the presentation format previously utilized, these trends are truncated at the maximum LF attained. For concision, only the response of the most significant beam or story is displayed. More detailed sets of plots, depicting the full range of results, are provided in the appropriate appendix referenced in the corresponding parameter's section.

4.3 Effect of Building Location

This section investigates the potential impacts of a structure's location on its progressive collapse response. While many different parameters could be utilized for such an investigation, this thesis will restrict the scope to two main effects: The design wind loads and the design seismic forces. Consequently, two locations were chosen for the purposes of this study: San Francisco (CA) and Miami (FL). The former was chosen because its location corresponded to high seismic design forces with relatively moderate design wind loads. Conversely, the latter was chosen because its location corresponded to sizable design wind loads with relatively minor seismic design forces.

4.3.1 System Descriptions

The systems used in the investigation of this parameter were based on the dimensioning and layout of the baseline system. Consequently, both structures have the same plan view identified in Figure 3-1. The load selection and design process used in the development of these additional structures was also identical to the one employed in the design of the baseline system, with the exception of the design lateral loads. Minimizing member self-weight caused OMFs to be utilized for the structure located in Miami. In contrast, special moment frame (SMF) systems were used for the structure located in San Francisco. The resulting elevation view for the building located in San Francisco is shown below in Figure 4-1; the elevation view for the building located in Miami is shown in Figure 4-2.

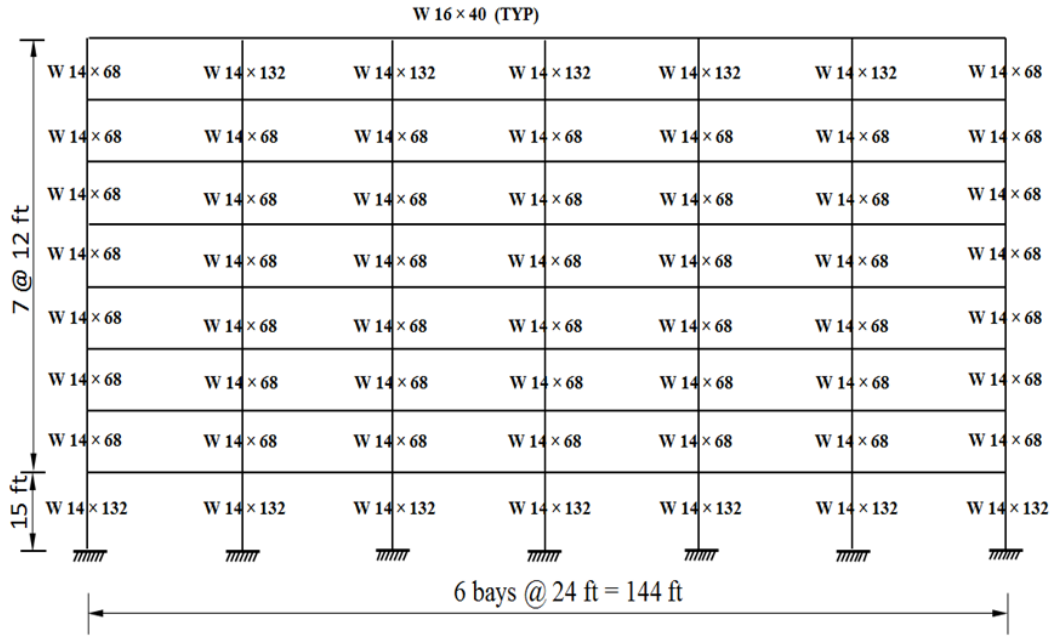

Figure 4-1 Elevation View of the Structure Located in San Francisco, CA

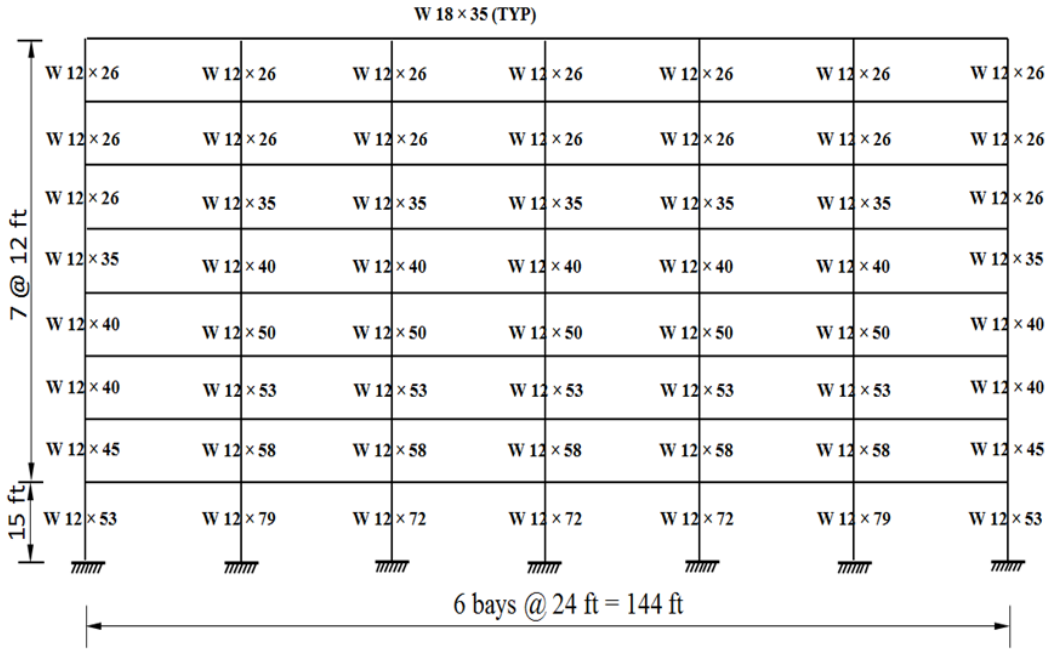

Figure 4-2 Elevation View of the Structure Located in Miami, FL

In order to facilitate discussions, pertinent characteristics and classifications for these structures are provided below in Table 4-1.

Table 4-1 System Classifications (Effect of Building Location)

System Label	Location	Frame Type	Number of Bays Included in LLRS	Number of Stories	Seismic Category	Design Wind Speed (mph)
P1-1	Miami	OMF	6	8	A	150
P1-2	San Francisco	SMF	6	8	E	85

4.3.2 FE Model Results and Comparisons

The results for systems P1-1 and P1-2 that are most critical for illustration are presented in this section and compared to the corresponding results from scenario 1 of the baseline study. Full sets of plots for these additional systems are located in Appendix A.

4.3.2.1 General Response

The general responses of systems P1-1 and P1-2 to a central column removal scenario are shown below in Figures 4-3 through 4-6 in conjunction with the results from the baseline system. Relevant maximums are listed in Table 4-2. Magnitudes of base shear and deflection at a LF of 1.0 are shown in Table 4-3 for each system (if applicable). Values of vertical deflection, horizontal deflection, and drift index are for the first-floor beam, eighth story, and first story respectively.

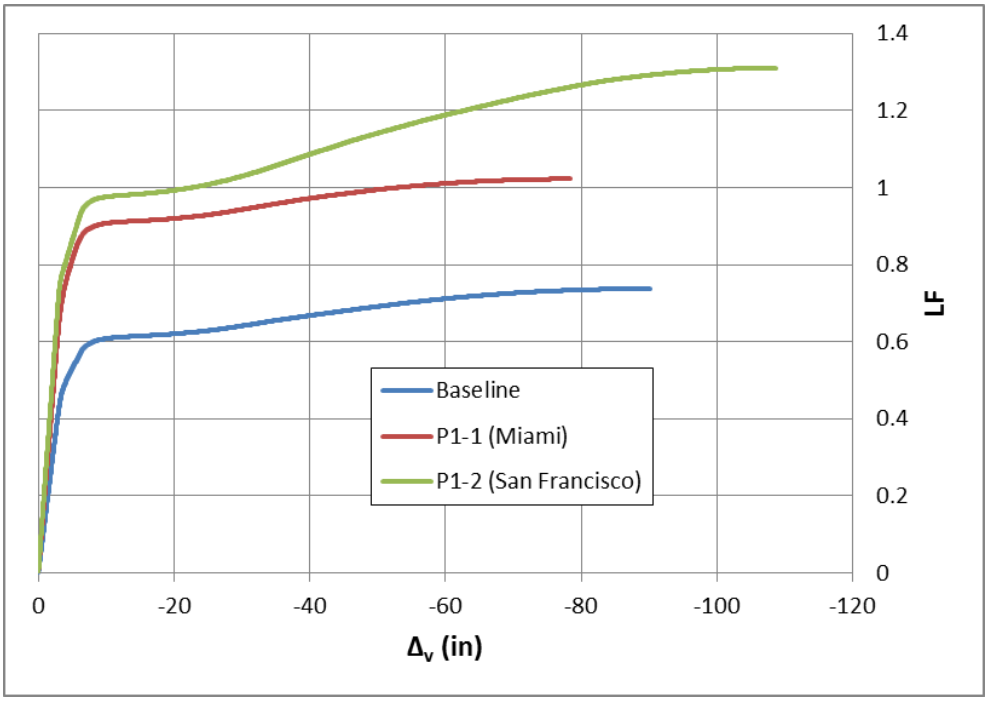

Figure 4-3 LF vs. Δ_v (Effect of Building Location)

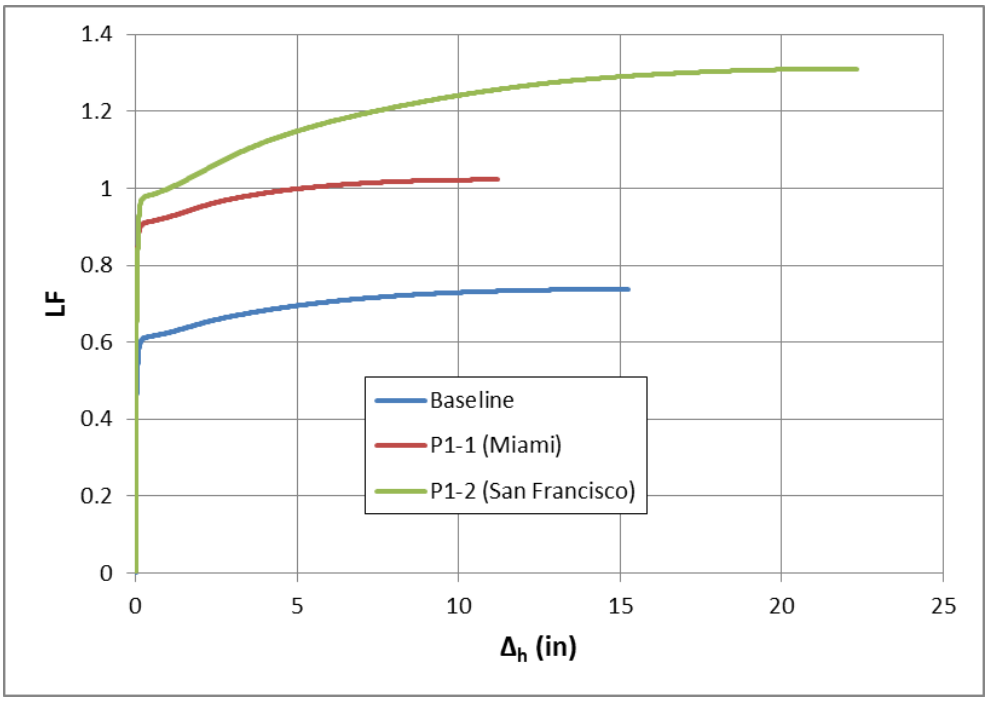

Figure 4-4 LF vs. Δ_h (Effect of Building Location)

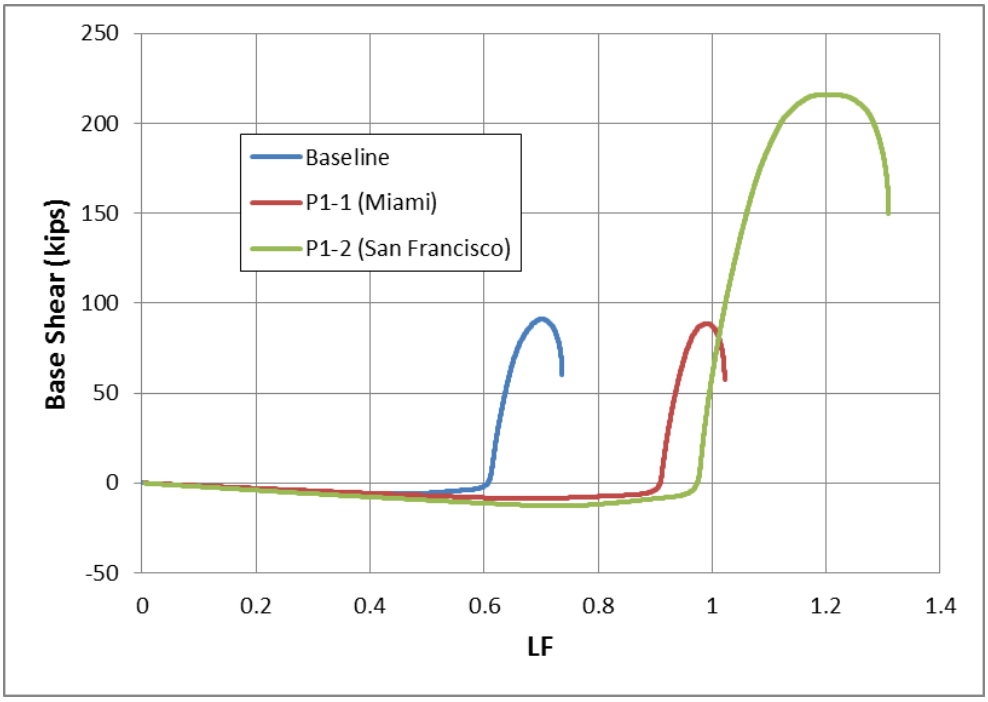

Figure 4-5 Base Shear vs. LF (Effect of Building Location)

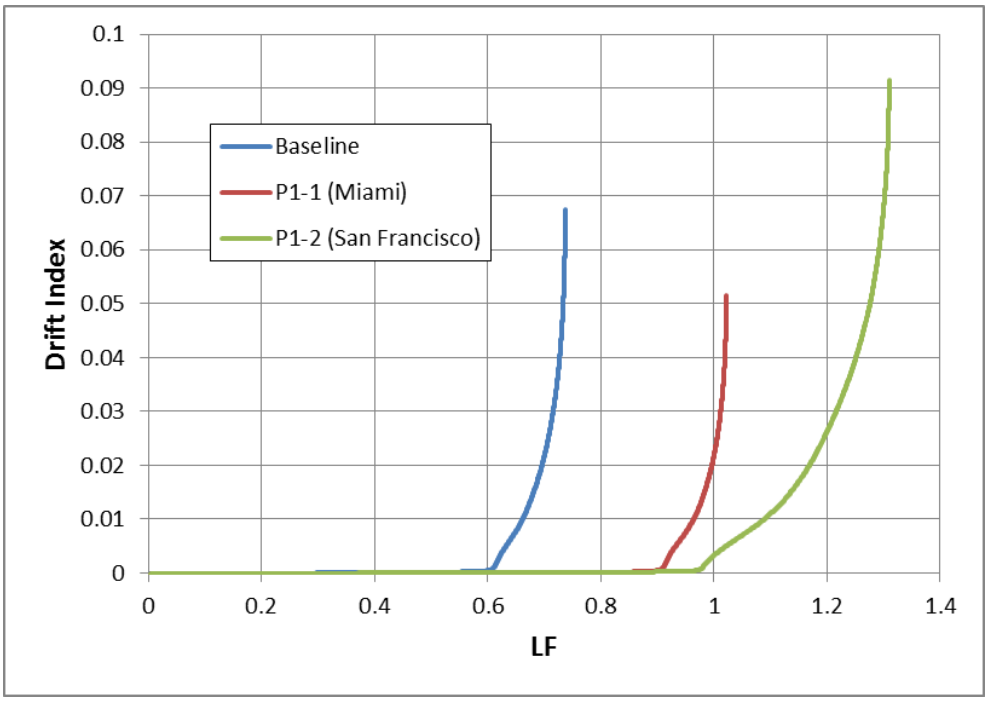

Figure 4-6 Drift Index vs. LF (Effect of Building Location)

Table 4-2 General Response Maximums (Effect of Building Location)

System	Maximum LF	Maximum Base Shear (kips)	Maximum Drift Index	Maximum Δ_h (in)	Maximum Δ_v (in)
Baseline	0.737	91.0	0.067	15.2	90.0
P1-1	1.02	88.6	0.051	11.2	78.3
P1-2	1.31	216	0.092	22.3	109

Table 4-3 General Response Values at LF = 1.0 (Effect of Building Location)

System	Base Shear at LF = 1.0 (kips)	Drift Index at LF = 1.0	Δ_h at LF = 1.0 (in)	Δ_v at LF = 1.0 (in)
Baseline	N/A	N/A	N/A	N/A
P1-1	84.0	0.02	5.10	52.7
P1-2	55.0	0.003	1.00	22.5
Note: The baseline system was unable to reach a LF of 1.0				

Table 4-2 shows that system P1-1 and P1-2, by sustaining LFs greater than 1.0, seemed to have sufficient capacity to sustain the full collapse loads. This potentially comes as a direct result of the increased level of lateral load used in the design of these systems. However, the values of base shear and deflection provided in Tables 4-2 and 4-3, in conjunction with the trends depicted in Figures 4-3 through 4-6, show that these systems have slight differences in their behavioral patterns.

While the formation of a flexural plastic mechanism in the beams directly above the removed column seemed to occur at higher LFs for both systems, system P1-2 was able to sustain a significant level of lateral force past this point. This is exhibited by the trend for base shear, depicted in Figure 4-5. However, as illustrated in Table 4-2, the maximum base shear sustained by system P1-1 was not substantially different than what was developed in the baseline system. This is likely a consequence of the design process used for each structure. Since system P1-2 was designed as an SMF in an area with high

seismic activity, the minimum required ratios of column strength to beam strength in conjunction with the large seismic design forces and drift requirements, resulted in substantially larger column sections with only slightly larger beam sections. Because of the increased level of anchoring, system P1-2 was able to generate significant amounts of catenary force and sustain these forces while undergoing the considerable levels of deflection shown in Figures 4-3, 4-4, and 4-6. This response is clarified further in the next section.

While system P1-1 was designed for higher levels of lateral force than the baseline system, it was not required to meet the same seismic strength and ductility requirements of system P1-2. As previously mentioned, this is a result of the structure being designed for a location with low seismic activity. Consequently, the forces used to design system P1-1 produced a structure with substantially smaller columns than system P1-2 with only slightly smaller beams. After the formation of a flexural plastic mechanism in the beams above the removed column, much of the capacity of the first-story columns seemed to be exhausted. Subsequently, the structure's capability to resist any additional load through catenary mechanisms was severely limited. The outcome was that the amount of lateral force (represented by the base shear) resisted by system P1-1 mimicked what was exhibited by the baseline system.

Finally, by examining Table 4-3, it can be seen that system P1-2 had significantly lower levels of deflection and base shear at a LF of 1.0 than system P1-1. As explained in the next section, this can be connected to the lower catenary action demands at this LF.

4.3.2.2 Catenary Action Demands

The catenary action demands associated with systems P1-1 and P1-2 are shown below in Figures 4-7 – 4-9, alongside the response from the baseline system. Table 4-4 displays the catenary action demands at the principal load levels for each system. Results are shown for the first-floor beam only.

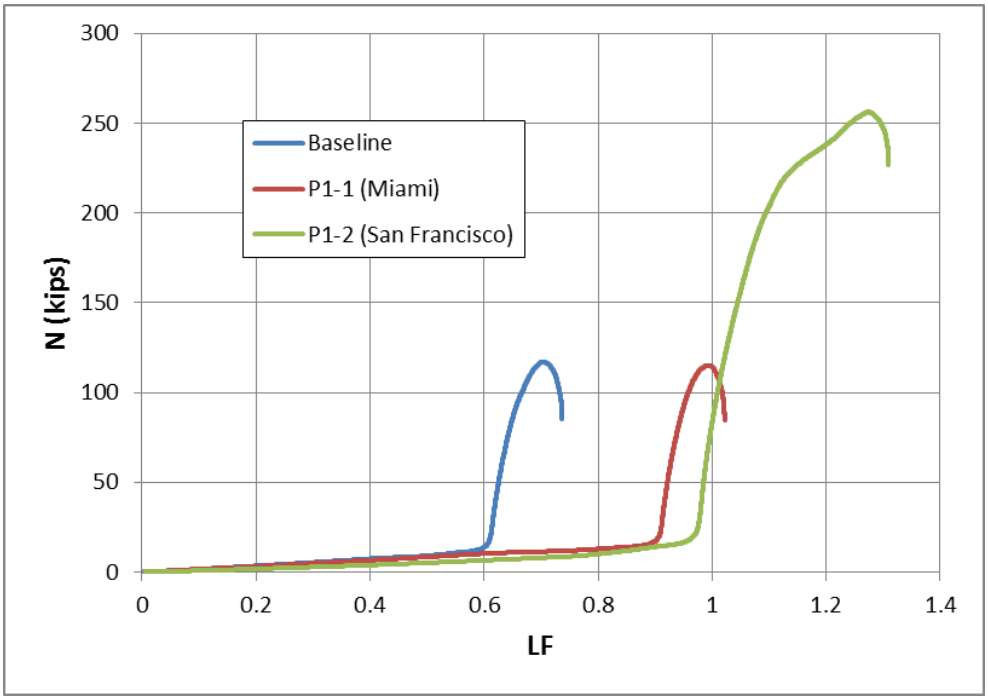

Figure 4-7 N vs. LF (Effect of Building Location)

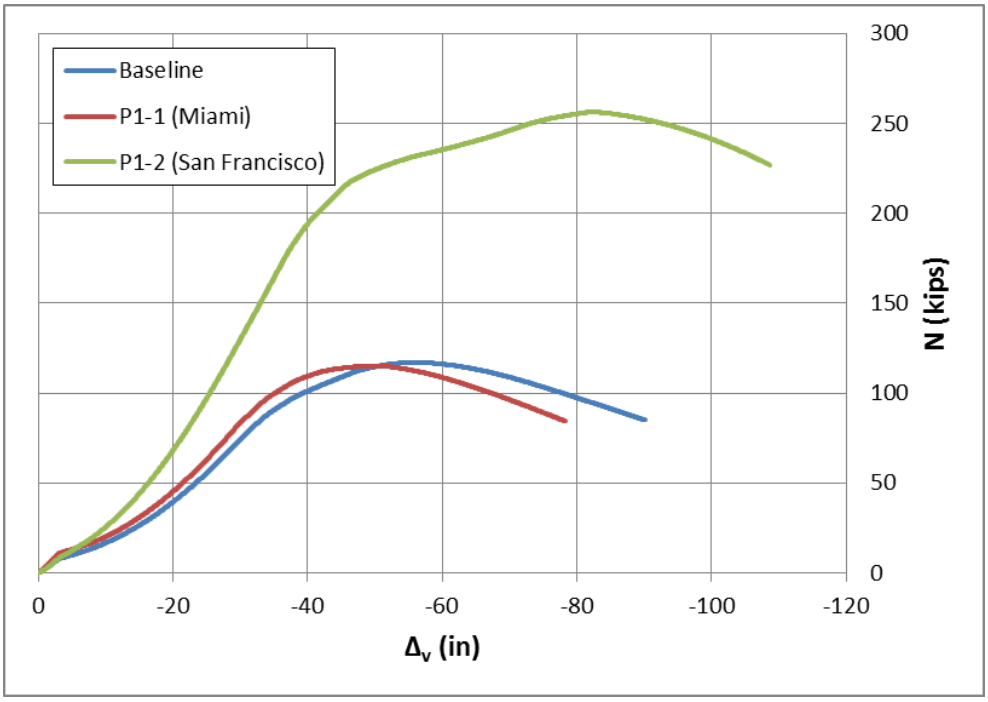

Figure 4-8 N vs. Δ_v (Effect of Building Location)

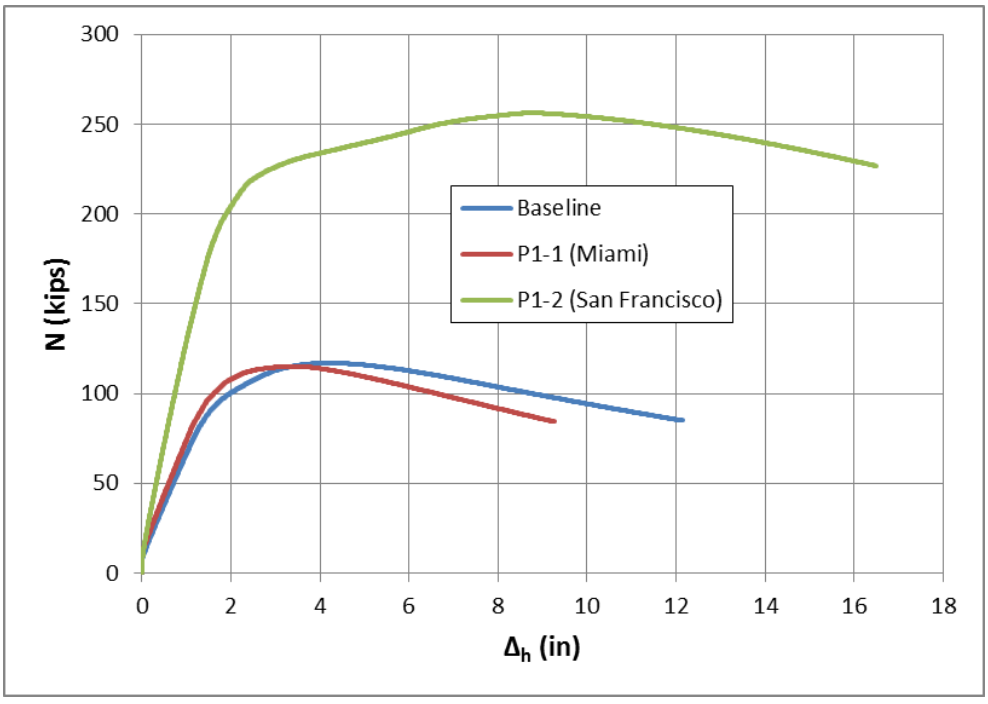

Figure 4-9 N vs. Δ_h (Effect of Building Location)

Table 4-4 Comparison of Catenary Action Demands (Effect of Building Location)

System	Maximum N (kips)	Maximum N/Np	N at LF = 1.0 (kips)	N/Np at LF = 1.0 (kips)	Percentage of LF Attributed to Catenary Behavior (%)
Baseline	117	0.310	N/A	N/A	18.6
P1-1	115	0.230	114	0.220	12.7
P1-2	256	0.440	83.0	0.140	26.0
Note: The baseline system was unable to reach a LF of 1.0					

The catenary action demands shown in Figures 4-7 through 4-9 support the discussion formulated in the previous section. System P1-1 developed similar magnitudes of catenary force to the baseline system, but at lower levels of overall deflection due to the larger beam and column sections. As previously mentioned, this behavior can be primarily associated with the ratio of column strength to beam strength.

By using a larger beam section and not significantly increasing the strength levels of the columns in the anchoring side frames, the residual capacity of these columns will be minimal after the formation of a flexural plastic mechanism in the adjoining beams. This can be most easily identified through the comparisons provided in Table 4-4. System P1-1 only used 23% of the first-floor beam's maximum axial tensile force prior to failure of the side frames; this corresponded to an increase in LF of 12.7%. The baseline system, facilitated through a more ductile response, made use of 31% of its first floor beam's maximum axial tensile force corresponding to a larger increase in LF of 18.6%.

However, by implementing appreciably stronger columns, particularly in the first story where it was indicated in Chapter 3 that anchoring is most needed, the structure can resist more significant portions of load through a catenary response mechanism. This seemed to be the case for system P1-2; the extensive ductility requirements and relatively

large seismic design forces resulted in this system being able to utilize about 44% of the 1st floor beam's maximum axial tensile force to increase the LF by 26%. This compares favorably to the percentages obtained from the baseline study and the analytical results of system P1-1.

Finally, unlike system P1-1, which needed almost all of its maximum catenary force in order to sustain the full collapse loads, system P1-2 needed significantly less catenary force development to reach a LF of 1.0. Despite its increased capability for employing a catenary response to resist loads, system P4-1 only needed to develop 83 kips of axial tensile force, or an N/Np ratio of 0.14, to achieve a LF of 1.0. As explained in the next section, this has implications related to potential connection ductility limitations.

4.3.2.3 Connection Ductility Demands

The levels of plastic rotation developed in the beams above the removed column for systems P1-1 and P1-2 are shown below in Figures 4-10 and 4-11. Comparisons of values of plastic rotation at the principal load levels and their locations in the three systems at these levels are provided in Table 4-5.

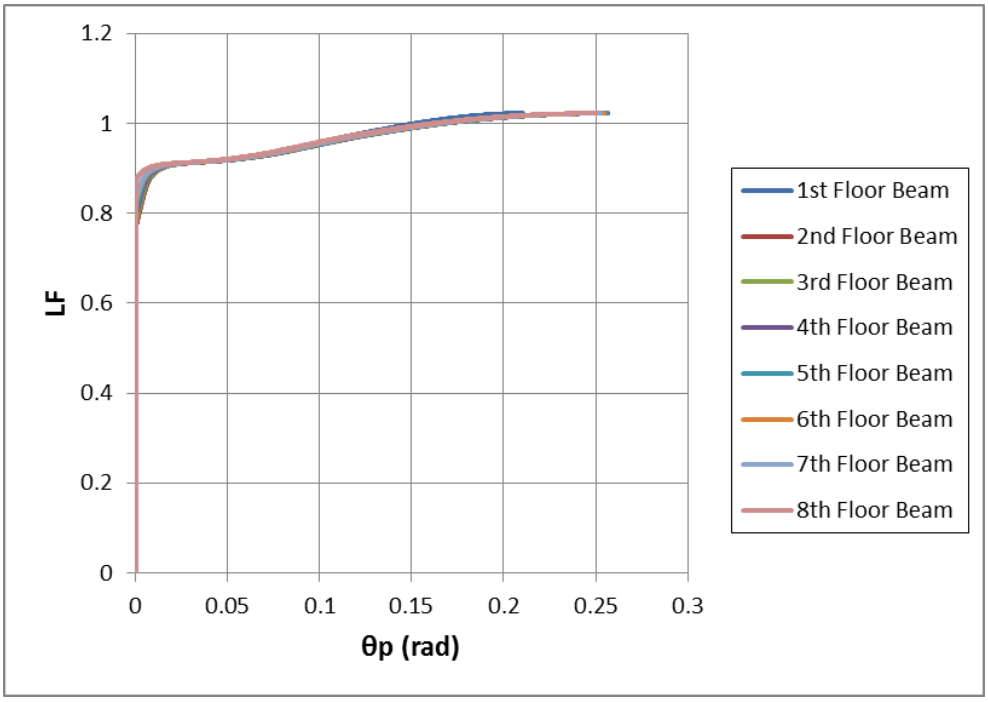

Figure 4-10 Plastic Rotation Demands for System P1-1

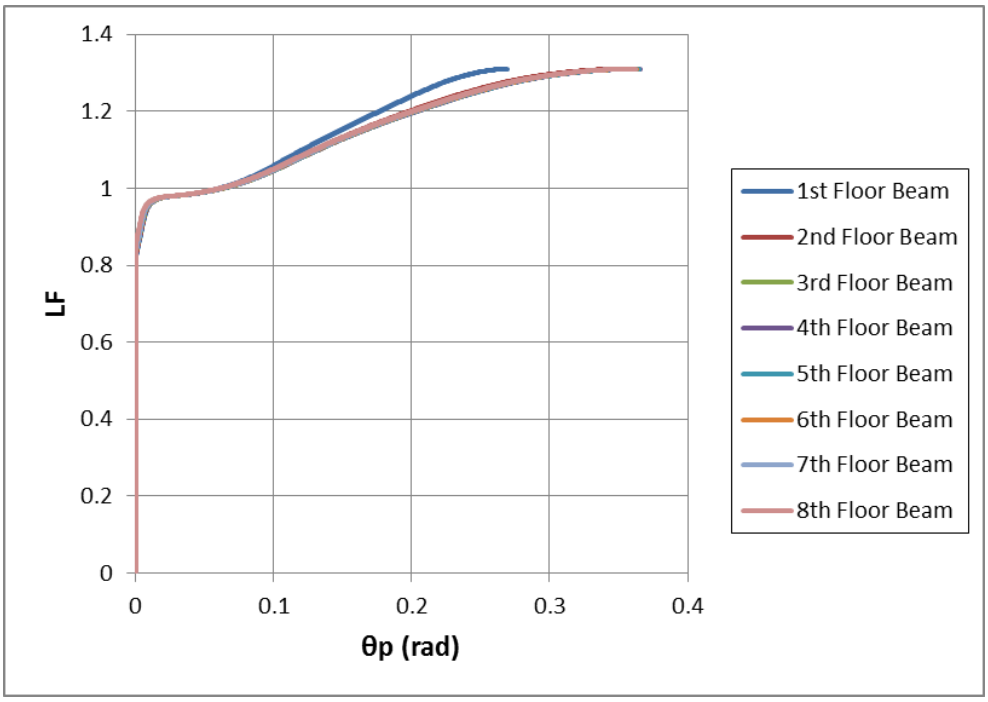

Figure 4-11 Plastic Rotation Demands for System P1-2

Table 4-5 Comparison of Plastic Rotation Demands (Effect of Building Location)

System	θp at Maximum LF (rad)	θp at LF = 1.0 (rad)	Beam Location
Baseline	0.298	N/A	4th floor
P1-1	0.257	0.153	3rd floor
P1-2	0.366	0.064	4th floor
Note: The baseline system was unable to reach a LF of 1.0			

The trends for maximum plastic rotation are relatively similar for systems P1-1, P1-2, and the baseline system (shown in Figure 3-18). As seen before, the plastic rotation demand was the lowest for the first-floor beam due to the effects of plasticity in the first story columns. The plastic rotation demands for the other stories remained relatively consistent within each individual system. However, the maximum plastic rotation demands associated with system P1-1 were lower than the corresponding maximums obtained from the baseline system. Conversely, the maximum plastic rotation demands associated with system P1-2 were higher than what was developed in the baseline system. Overall, these demands directly corresponded to the level of catenary force that was utilized by the systems as they attempted to resist collapse.

Despite the fact that system P1-1 was able to attenuate collapse through a catenary response, it needed to undergo substantial deformations in order to do so; potential connection ductility limitations could result in connection fracture and partial collapse of the structure prior to the full utilization of this resisting mechanism. Subsequently, at a LF of 1.0, system P1-2 had a maximum plastic rotation demand of 0.063 rad; this compares favorably to the .153 rad needed in system P1-1. The

implication of this is that, by efficiently and sparingly using a catenary response, system P1-2 could be more capable of averting both partial and total collapse.

4.3.3 Conclusions

Based upon the preceding discussions, and within the limitations imposed by the adopted assumptions, the following conclusions can be drawn from the study of a structure's location on its progressive collapse response:

- The structures in both locations that required larger design lateral loads had significantly higher overall resistance to progressive collapse caused by the removal of a first-story column. Moreover, the structure designed to resist large seismic forces showed greater potential to attenuate collapse than its counterpart designed for substantial wind loads. This implies that a structure's location, through the associated design lateral loads, could influence the structure's ability to resist the loading conditions indicative of a collapse scenario.
- System P1-2 was able to sustain greater portions of load attributed to catenary resistance than the baseline system and system P1-1. This indicates that the strength and ductility requirements of SMF systems designed for locations with high seismic activity can result in structures that more effectively resist additional load through the use of catenary mechanisms.
- It was seen that system P1-1 needed to attain large levels of plastic rotation in order to develop the catenary forces necessary to avert collapse. System P1-2, despite its greater potential for catenary behavior, needed significantly lower

levels of plastic rotation in order to sustain the same level of load. This implies that structures designed for certain locations may have sufficient capacity to resist collapse in the primary structural members, but be unable to do so because of limitations in the rotation capacities of their connections. Conversely, structures designed for locations with more considerable seismic requirements may be less affected by such limitations.

4.4 Effect of the Number of Stories

This section investigates the effect of the number of stories in a particular structure on its collapse response. By decreasing the number of stories in a structure, its overall design vertical load, seismic weight, and exposure to wind will all decrease, potentially resulting in smaller steel sections throughout the structure. Additionally, there will be fewer beams available for catenary force development. However, the total vertical load applied in the nonlinear pushdown analysis will decrease in opposition, due to the reduced number of stories supporting load. To investigate the overall impact of such changes, two three-story variants of the baseline system were laid out and designed: One in Atlanta (GA) and the other in San Francisco (CA). These two locations were chosen since the investigation on building location revealed that the eight-story structure located in San Francisco was substantially more resistant to collapse than the corresponding structures in Miami and Atlanta. Consequently, by including both Atlanta and San Francisco in the study of this parameter, its relative impact might be ascertained.

4.4.1 System Descriptions

As in the previous section, the systems used in the investigation of this parameter were based on the dimensioning and layout of the baseline system. Consequently, both structures have the same plan view identified in Figure 3-1. The load selection and design process used in the development of both structures was also identical to the one employed in the design of the baseline system, with the exception of the design lateral loads, which were altered by the reduction in stories. Minimizing member self-weight caused OMFs to be utilized for the structure placed in Atlanta. In contrast, special moment frame (SMF) systems were used for the structure placed in San Francisco. The resulting elevation view for the building located in Atlanta is shown below in Figure 4-12; the elevation view for the building located in San Francisco is shown in Figure 4-13.

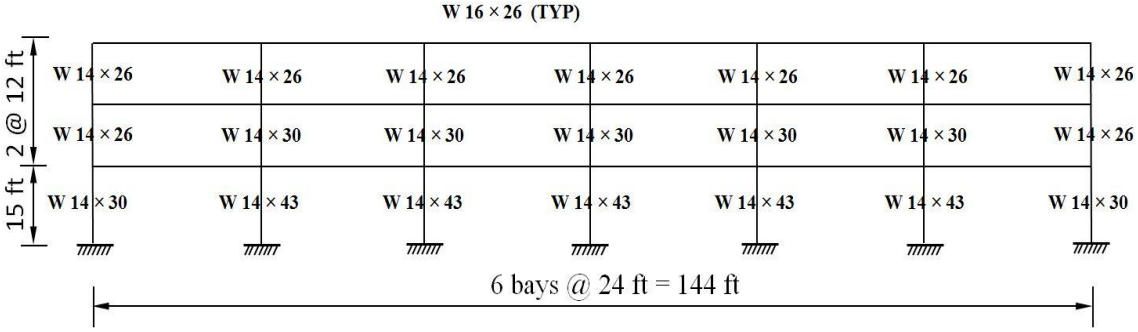

Figure 4-12 Elevation View of the Three-Story Structure in Atlanta

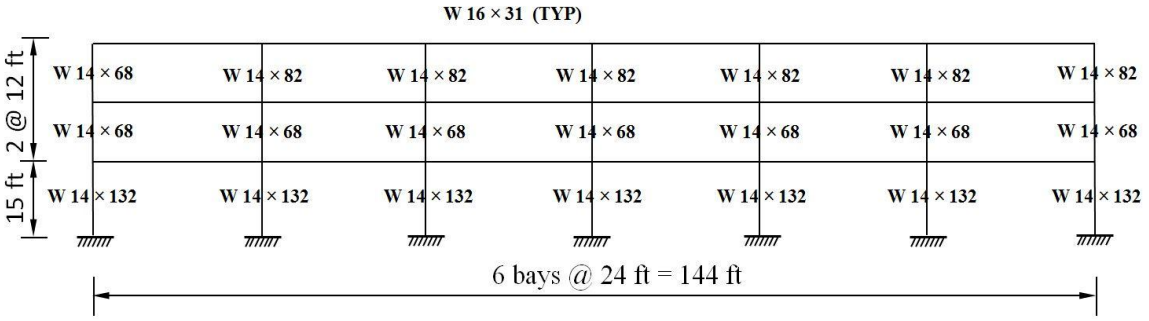

Figure 4-13 Elevation View of the Three-Story Structure in San Francisco

Of particular note is that system P2-2 retains the same first-story column section as system P1-2, but with smaller beams. This was a consequence of seismic compactness requirements, which limited the selection of W14s. Also of interest is that system P2-1 retains the same beam section as the baseline system, but with smaller columns. This is primarily a result of the building's location, which provides less influence to lateral loads.

In order to facilitate discussions, pertinent characteristics and classifications for these structures are provided below in Table 4-6.

Table 4-6 System Classifications (Effect of the Number of Stories)

System Label	Location	Frame Type	Number of Bays Included in LLRS	Number of Stories	Seismic Category	Design Wind Speed (mph)
P2-1	Atlanta	OMF	6	3	A	90
P2-2	San Francisco	SMF	6	3	E	85

4.4.2 FE Model Results and Comparisons

The results for systems P2-1 and P2-2 that are most critical for illustration are presented in this section and compared to the corresponding results from scenario 1 of the

baseline study and system P1-2 of the parametric study. Full sets of plots for these additional systems are located in Appendix B.

4.4.2.1 General Response

The general responses of systems P2-1 and P2-2 to a central column removal scenario are shown below in Figures 4-14 through 4-17 in conjunction with the results from the baseline system and system P1-2. Relevant maximums are listed in Table 4-7. Magnitudes of base shear and deflection at a LF of 1.0 are shown in Table 4-8 for each system (if applicable). Values of vertical deflection, horizontal deflection, and drift index are for the first-floor beam, top story, and first story respectively.

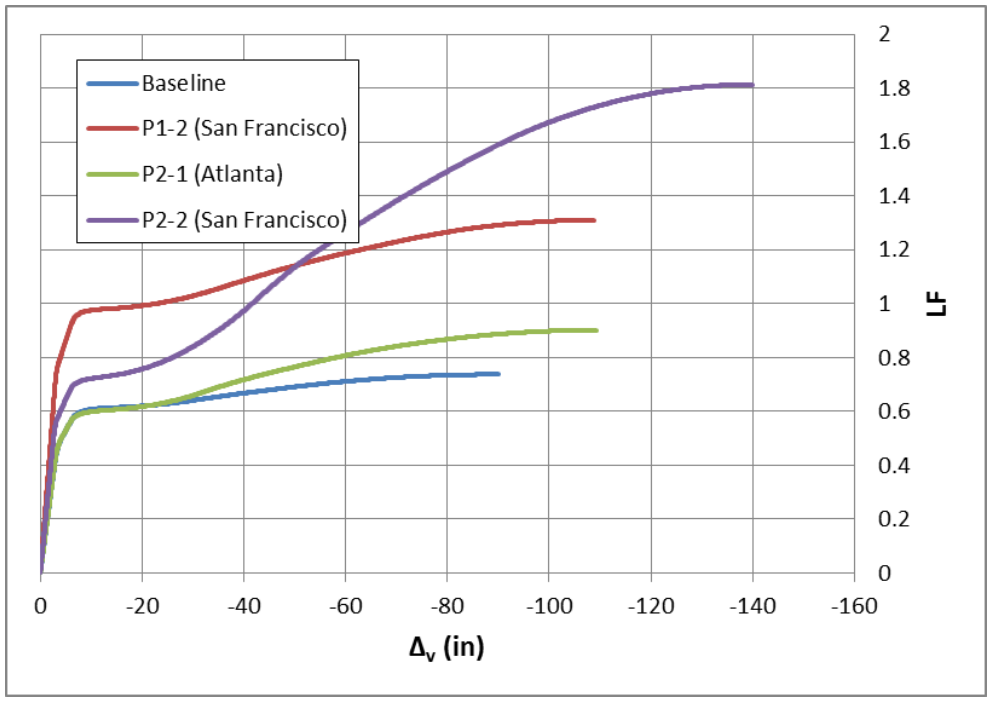

Figure 4-14 LF vs. Δ_v (Effect of the Number of Stories)

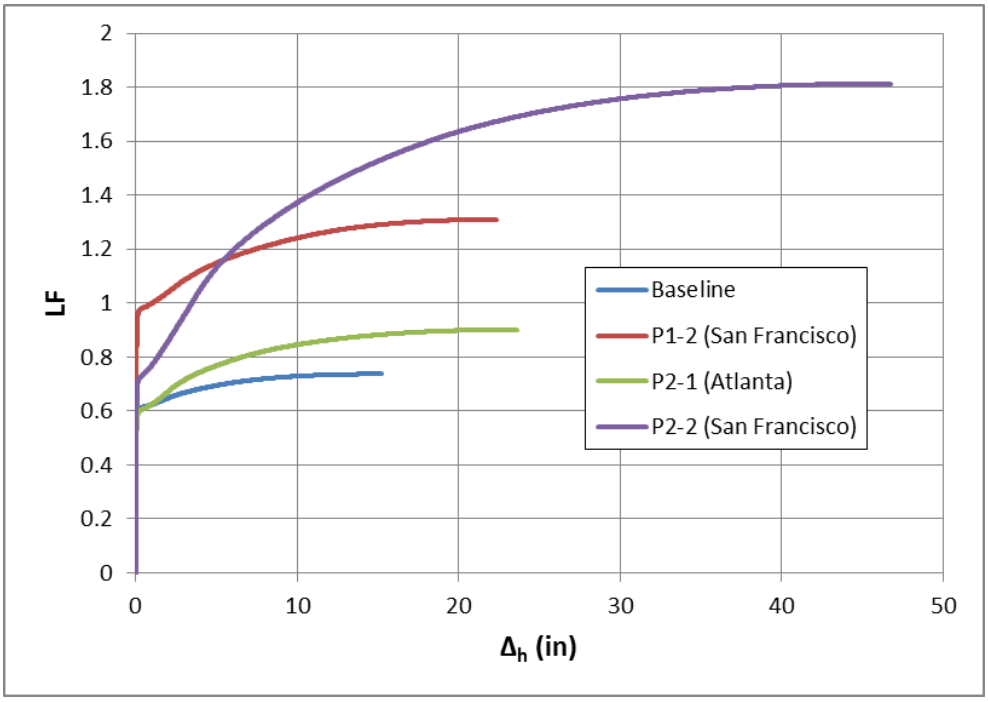

Figure 4-15 LF vs. Δ_h (Effect of the Number of Stories)

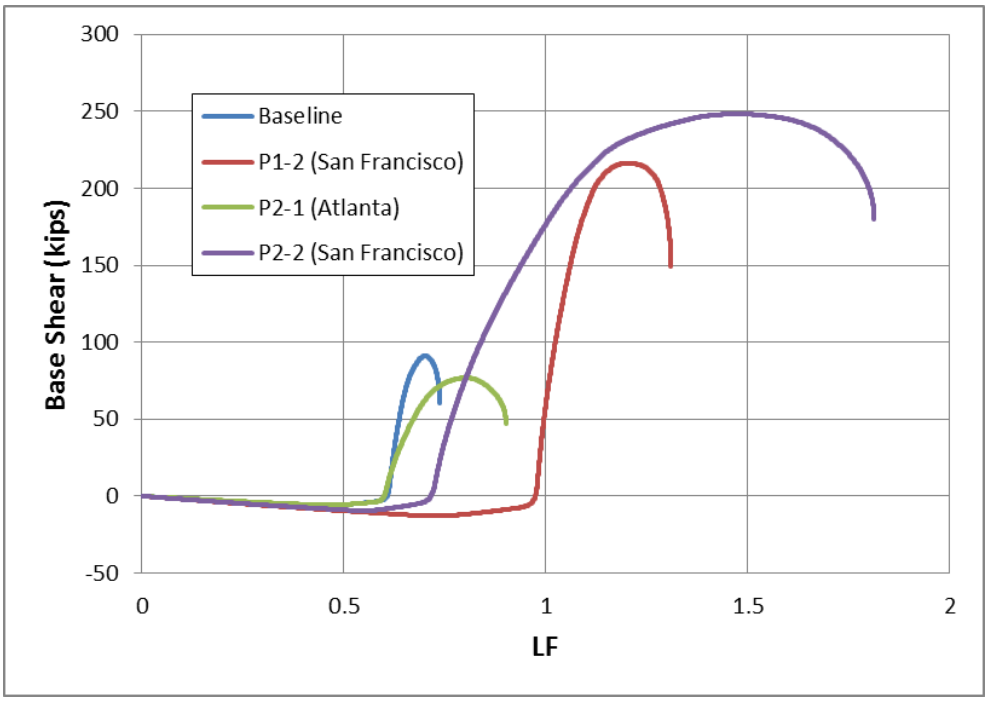

Figure 4-16 Base Shear vs. LF (Effect of the Number of Stories)

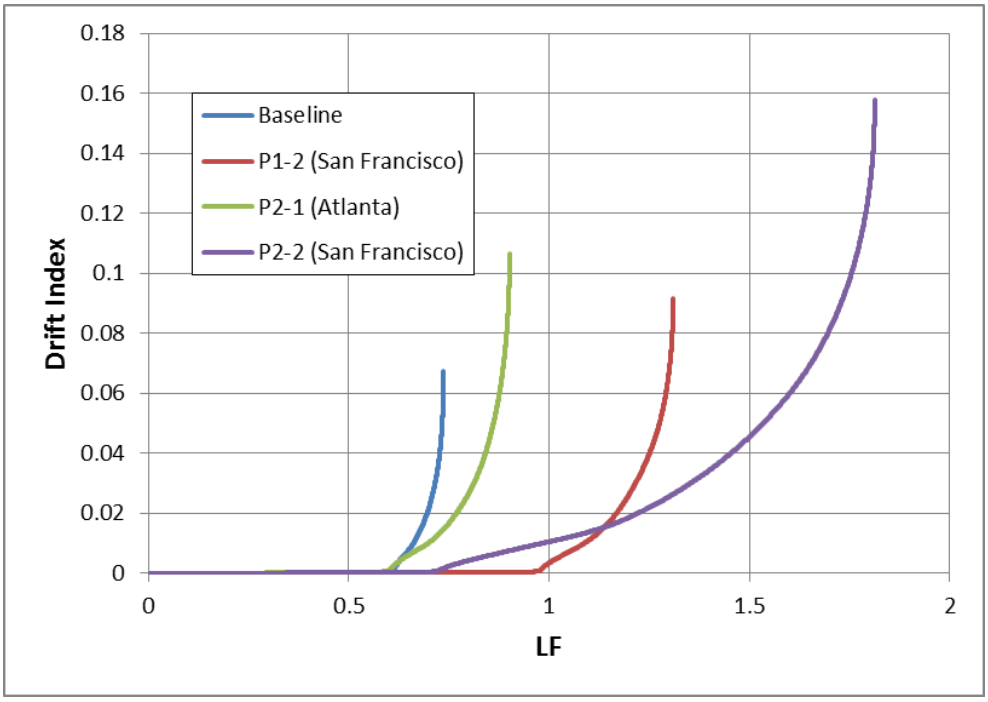

Figure 4-17 Drift Index vs. LF (Effect of the Number of Stories)

Table 4-7 General Response Maximums (Effect of the Number of Stories)

System	Maximum LF	Maximum Base Shear (kips)	Maximum Drift Index	Maximum Δ_h (in)	Maximum Δ_v (in)
Baseline	0.737	91.0	0.067	15.2	90.0
P1-2	1.31	216	0.092	22.3	108.7
P2-1	0.900	96.7	0.106	23.6	109.2
P2-2	1.81	248	0.158	46.8	140

Table 4-8 General Response Values at LF = 1.0 (Effect of the Number of Stories)

System	Base Shear at LF = 1.0 (kips)	Drift Index at LF = 1.0	Δ_h at LF = 1.0 (in)	Δ_v at LF = 1.0 (in)
Baseline	N/A	N/A	N/A	N/A
P1-2	55	0.003	1.00	22.5
P2-1	N/A	N/A	N/A	N/A
P2-2	177	0.01	3.50	41.6
Note: System P2-1 and the baseline system were unable to reach a LF of 1.0				

Table 4-7 shows that the systems located in San Francisco, P1-2 and P2-2, were able to sustain LFs greater than 1.0 and were thus able to attenuate collapse.

Similar to what has previously been seen, Figures 4-14 through 4-17 show that the formation of a flexural plastic mechanism in the beams seemed to occur around similar levels of deflection for all systems. The differences in each system's LF at this point are directly related to the flexural strength levels of the beams. Since the baseline system and system P2-1 had the same beam section, the LF corresponding to flexural plastic collapse of these systems coincides. However, since the beam section size of system P2-2 (W16 X 31) was smaller than the one used in system P1-2 (W16 X 40), the point of flexural plastic collapse occurred at a lower LF.

The overall deflection levels at system failure, the total LF resisted, and the portion of total load resisted by catenary mechanisms appear to be larger for the three-story systems than for the corresponding eight-story systems. The last two are most readily seen by examining Figure 4-16; the trends show that the lateral force demands imposed by the beams in systems P2-1 and P2-2 were retained, in some relative magnitude, for substantially larger portions of additional LF compared to the baseline system or system P1-2. Also, evident by the difference in LF between the point of flexural collapse and the point of system failure, in addition to the comparatively larger maximum base shear, system P2-2 exhibited the largest extent of catenary response. Subsequently, this system was able to sustain the highest LF (1.81) of all four systems.

However, by comparing the behavior of systems P1-2 and P2-2 at a LF of 1.0, provided in Table 4-8, it can be seen that while system P2-2 reached a higher maximum LF than system P1-2, it needed to deflect much more to reach a LF of 1.0; this can be

directly correlated with its increased utilization of catenary mechanisms for load resistance. These increased deflection levels coincided with more significant ductility demands in the beams.

4.4.2.2 Catenary Action Demands

The catenary action demands associated with systems P2-1 and P2-2 are shown below in Figures 4-18 through 4-20, alongside the response from the baseline system and system P1-2. Table 4-9 displays the catenary action demands at the principal load levels for each system. Results are shown for the first-floor beam only.

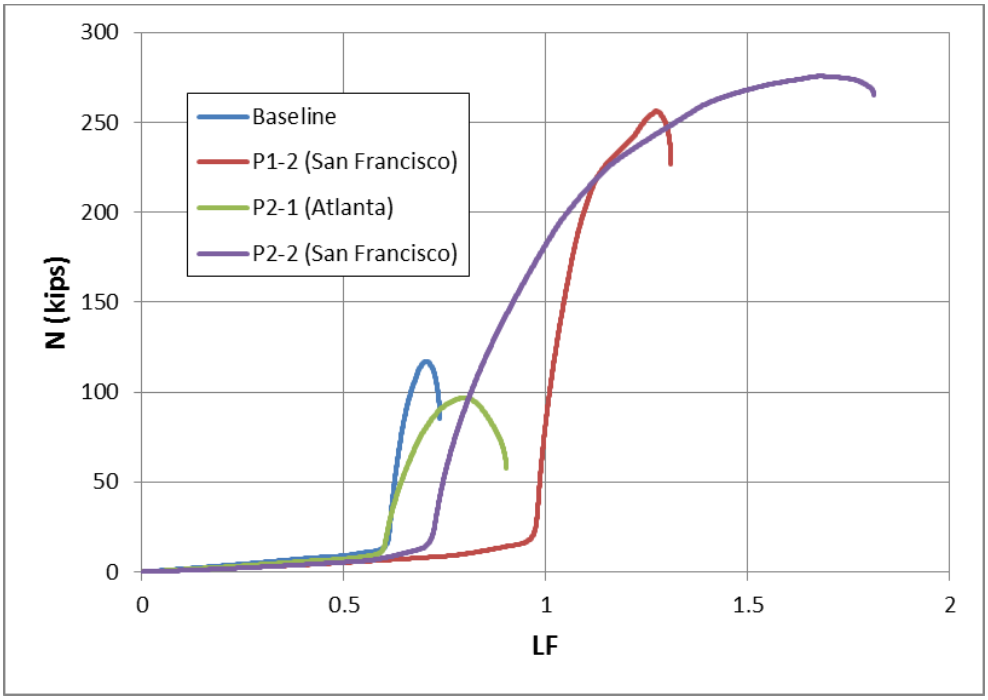

Figure 4-18 N vs. LF (Effect of the Number of Stories)

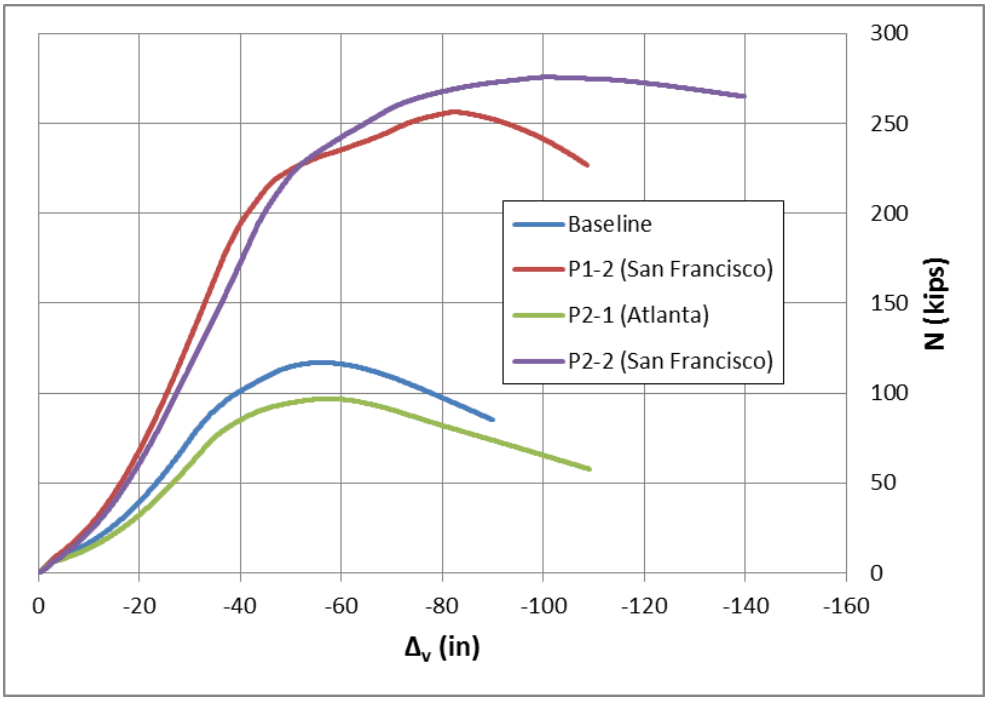

Figure 4-19 N vs. Δ_v (Effect of the Number of Stories)

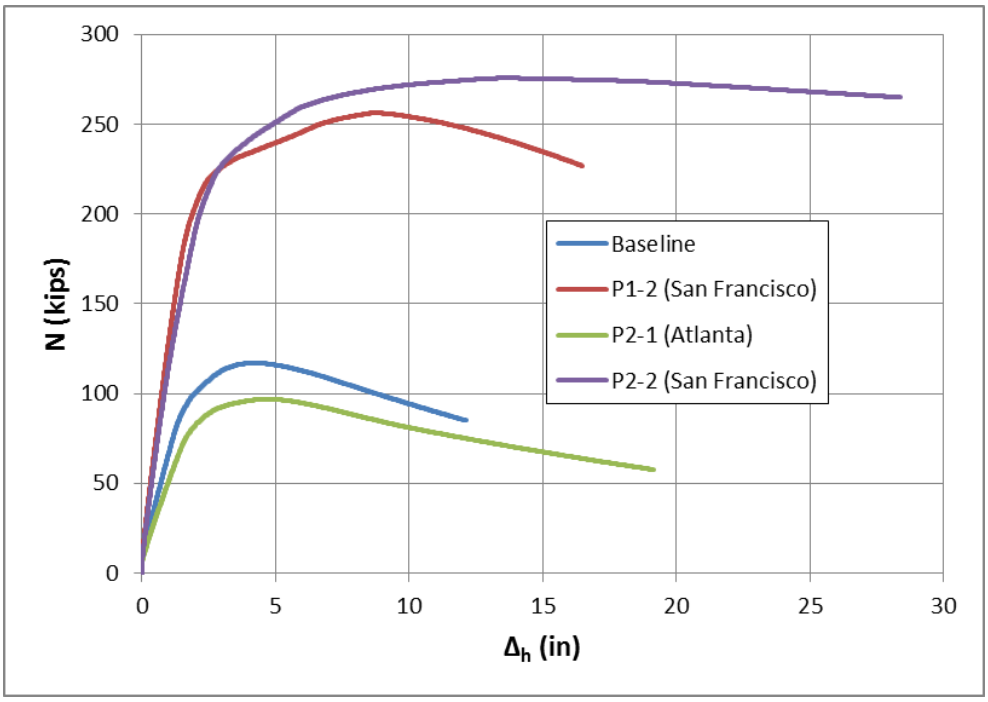

Figure 4-20 N vs. Δ_h (Effect of the Number of Stories)

Table 4-9 Comparison of Catenary Action Demands (Effect of the Number of Stories)

System	Maximum N (kips)	Maximum N/Np	N at LF = 1.0 (kips)	N/Np at LF = 1.0 (kips)	Percentage of LF Attributed to Catenary Behavior (%)
Baseline	117	0.310	N/A	N/A	18.6
P1-2	256	0.440	83.0	0.140	26.0
P2-1	96.7	0.260	N/A	N/A	34.8
P2-2	276	0.610	182	0.400	61.3
Note: System P2-1 and the baseline system were unable to reach a LF of 1.0					

Similar to the trends for base shear, the catenary action demands shown in Figures 4-18 through 4-20 indicate that systems P2-1 and P2-2 sustained catenary behavior longer than the eight-story structures. This concept can be quantified using Table 4-9. System P2-1, the three-story variant of the baseline system, used a catenary response to resist 34.8% of its maximum LF, a percentage substantially larger than the 18.6% used by the baseline system. Furthermore, system P2-2 used the same response to resist 61.3% of its maximum LF, compared to the smaller 26% used by system P1-2. There are several factors that could have contributed to the difference in behavior between the two types of system layouts.

As described in section 3.5.2.3, after the formation of a flexural plastic mechanism, the first-floor beam will carry the largest portion of additional load. Consequently, the beams in the first floor of the three-story structures experienced less overall vertical load with increasing LF than those in the eight-story structures; this was due to the smaller number of stories transferring load downward. Additionally, the three-story systems had lower levels of lateral stiffness at the first story, where catenary behavior was primarily concentrated. Likely a consequence of these factors, the first-

floor beams in these systems developed catenary force slower with each additional increase in LF, needing more deflection in order do so; this is verified by the trends depicted in Figures 4-18 through 4-20, which show a variation in slope with system layout.

The force and deformation demands on the side frames also differed substantially between the two layouts. The side frame columns in systems P2-1 and P2-2 were subjected to significantly smaller degrees of vertical force, potentially minimizing the influence of higher order effects. Despite this reduction, since system P2-1 had smaller first-story columns than the baseline system, it was still unable to sustain larger catenary forces in the first-floor beam, as evidenced by a comparison of the maximum values of N, provided in Table 4-9. However, likely due to the diminished vertical load levels on the side frame columns in the first story, which use the same section as the columns in system P1-2, system P2-2 was able to sustain more catenary force development in the first floor than system P1-2. This was also due, in part, to the smaller beam section utilized in system P2-2, which caused catenary behavior to occur earlier.

Because catenary force developed earlier in system P2-2, it utilized a greater portion of its first-floor beam's maximum axial tensile force at a LF of 1.0 (0.40 compared to 0.14 for system P1-2). However, as identified previously, heavy reliance on catenary mechanisms can correspond to more significant ductility demands.

4.4.2.3 Connection Ductility Demands

The levels of plastic rotation developed in the beams above the removed column for systems P2-1 and P2-2 are shown below in Figures 4-21 and 4-22. Comparisons of

values of plastic rotation at the principal load levels and their locations in the four systems at these levels are provided in Table 4-10.

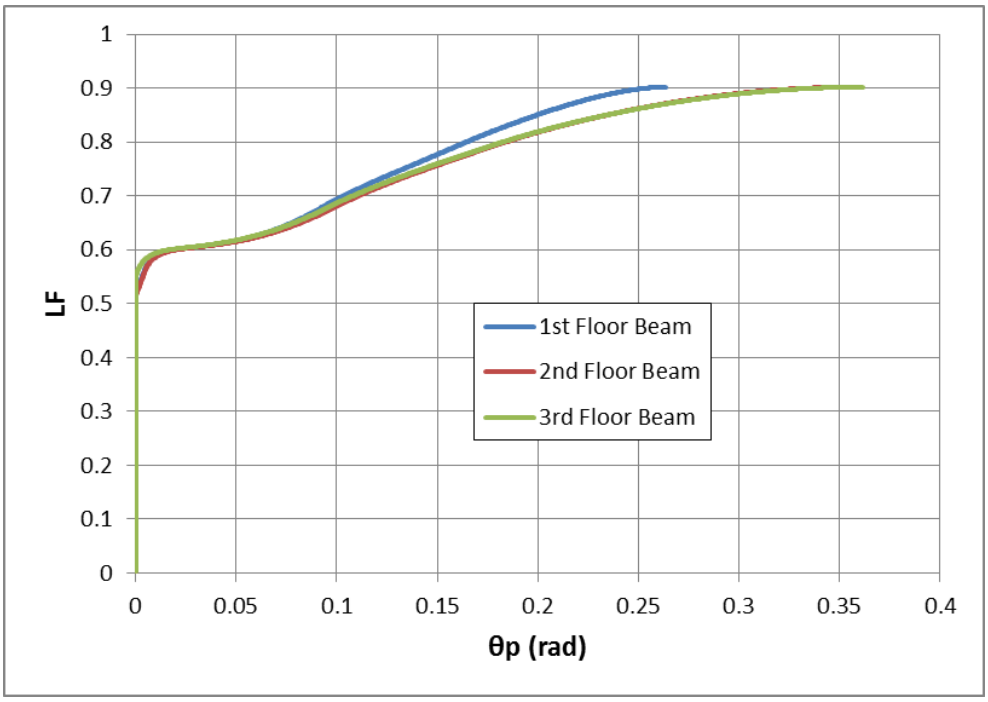

Figure 4-21 Plastic Rotation Demands for System P2-1

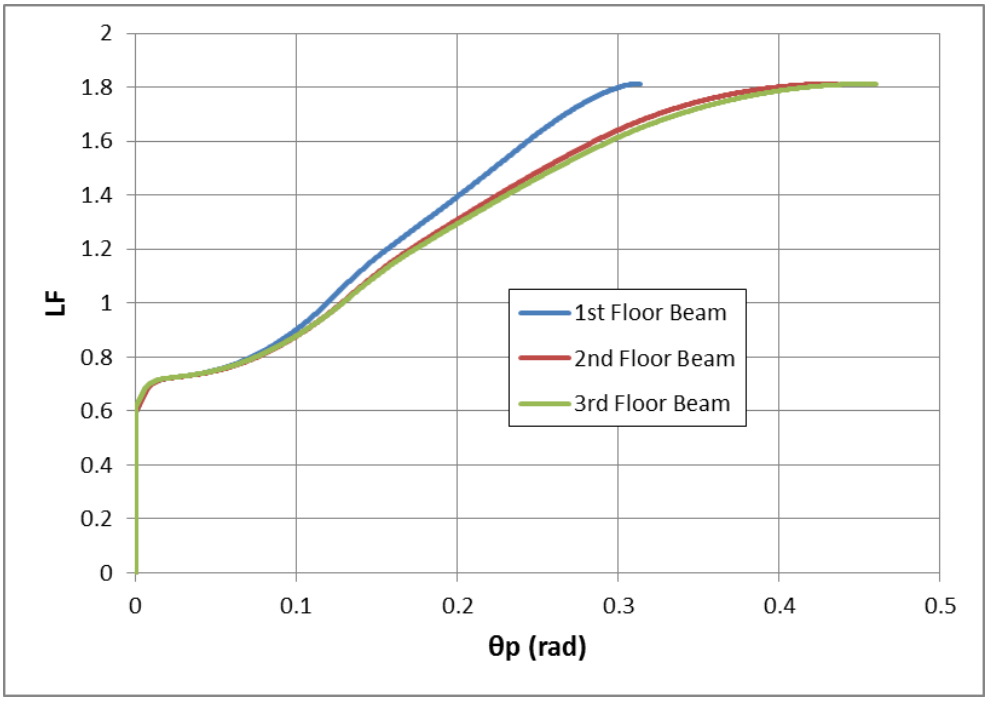

Figure 4-22 Plastic Rotation Demands for System P2-2

Table 4-10 Comparison of Plastic Rotation Demands (Effect of the Number of Stories)

System	θp at Maximum LF (rad)	θp at LF = 1.0 (rad)	Beam Location
Baseline	0.298	N/A	4th floor
P1-2	0.366	0.064	4th floor
P2-1	0.361	N/A	3rd floor
P2-2	0.460	0.129	3rd floor
Note: System P2-1 and the baseline system were unable to reach a LF of 1.0			

The plastic rotation demands shown in Table 4-10 indicate that the three-story structures had higher levels of maximum plastic rotation than their eight-story equivalents. Furthermore, as identified in the discussion on catenary action demands, these structures made more use of catenary mechanisms to resist the imposed loads. This continues to support the direct correlation between the utilization of catenary behavior

and plastic rotation demands. Further, this indicates a potential susceptibility of lower-rise structures to connection fracture associate with ductility limitations. In order to reach a LF of 1.0, system P2-2 required 0.129 rad of plastic rotation, over twice the maximum plastic rotation developed in system P1-2.

4.4.3 Conclusions

Based upon the previous discussions, and within the limitations imposed by the adopted assumptions, the following conclusions can be drawn regarding the effect of the number of stories in a structure on its overall progressive collapse response:

- At maximum capacity, systems P2-1 and P2-2 achieved LFs higher than their eight-story versions. This seems to indicate that as the number of stories in a structure decreases, its overall resistance to progressive collapse due to a central column removal scenario will increase. This response can be associated with a lower load demand on the first-floor beam and first-story columns, despite the smaller column section sizes utilized for the shorter structures.
- In the course of this study, it was seen that system P2-2 needed to attain higher levels of axial tension in its first-floor beam in order to reach a LF of 1.0. This indicates that having a fewer number of stories in a structure designed for significant seismic design forces can result in a system with higher overall collapse resistance, but a greater need to engage catenary behavior in order to sustain the anticipated loads.

- Potentially due to the decreased load demands and the curtailed influence of higher-order effects on the side frame columns, systems P2-1 and P2-2 made more use of catenary behavior to increase LF. Consequently, the conclusion can be drawn that structures with fewer stories are able to make more use of this type of response to redistribute load.
- In conjunction with their increased use of catenary mechanisms for load resistance, systems P2-1 and P2-2 exhibited higher overall levels of plastic rotation demand. This implies that lower-rise structures may be more susceptible to the limitations imposed by connection ductility levels.

4.5 Effect of the Number of Bays

This section investigates the effect of reducing the number of bays included in the LLRS of the baseline system and system P1-2 on their associated responses to progressive collapse. The loss of lateral load-resisting bays in the exterior frames will result in a greater concentration of strength in those bays remaining in the LLRS, which could profoundly influence the system's ultimate capacity and behavior during load-redistribution. As such, this investigation shall concentrate the lateral load-resisting bays at the center of the structures and remove the central column from those bays. The influence and response of the gravity bays were not considered in this investigation.

4.5.1 System Descriptions

Two additional systems, based upon the dimensioning and layout of the baseline system, were developed in order to study the influence of this parameter. As in the

investigation of the effect of the number of stories, two locations were considered in this study: Atlanta (GA) and San Francisco (CA). Both systems have the same plan view shown in Figure 3-1. However, the systems in this investigation restrict the lateral load-resisting bays to the center of the structure. Consequently, in the development of these structures, only the central sixteen bays were modeled and designed. This approach was employed for simplification of the design process, since the response of the gravity bays was not intended to be included in this investigation. However, to account for the presence of the load present on these beams, concentrated loads were assigned to the appropriate column joints in the LLRS. The magnitude of these loads corresponded to half the total load on the adjacent gravity beams. As previously seen, using OMFs in the structure located in Atlanta resulted in the most optimal design, whereas SMFs proved more optimal for the structure located in San Francisco. Elevation views of the final designs are shown in Figures 4-23 and 4-24 for the structures located in Atlanta and San Francisco respectively.

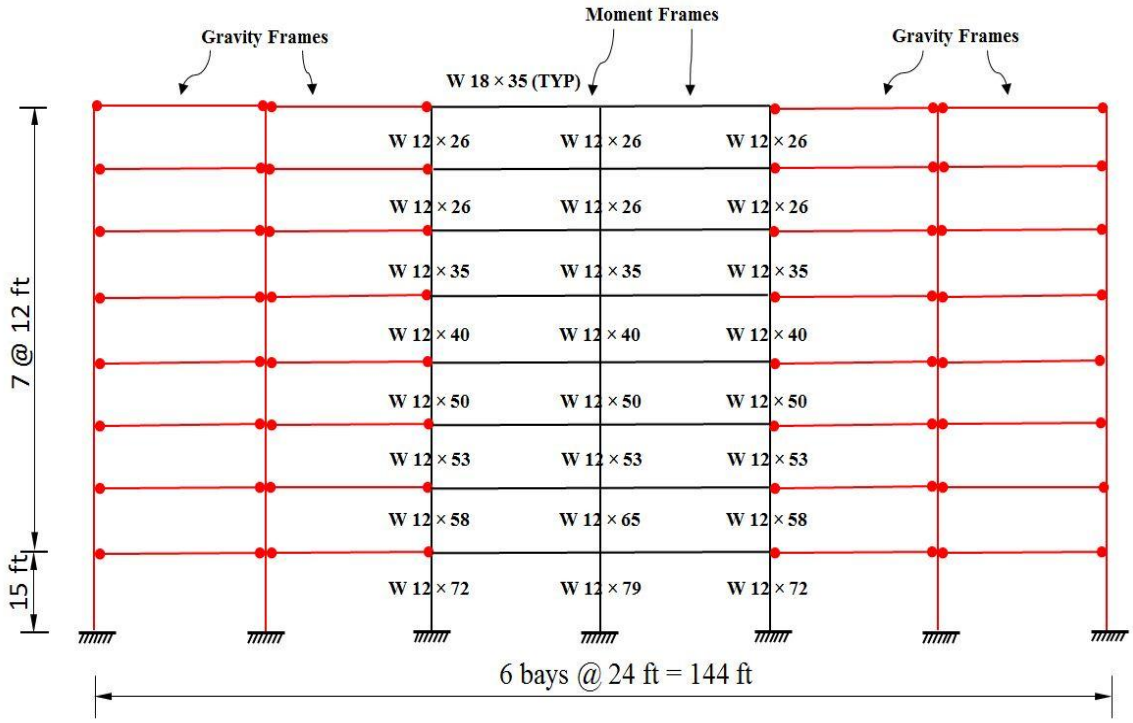

Figure 4-23 Elevation View of the Structure Located in Atlanta with Reduced Lateral Load-Resisting Bays

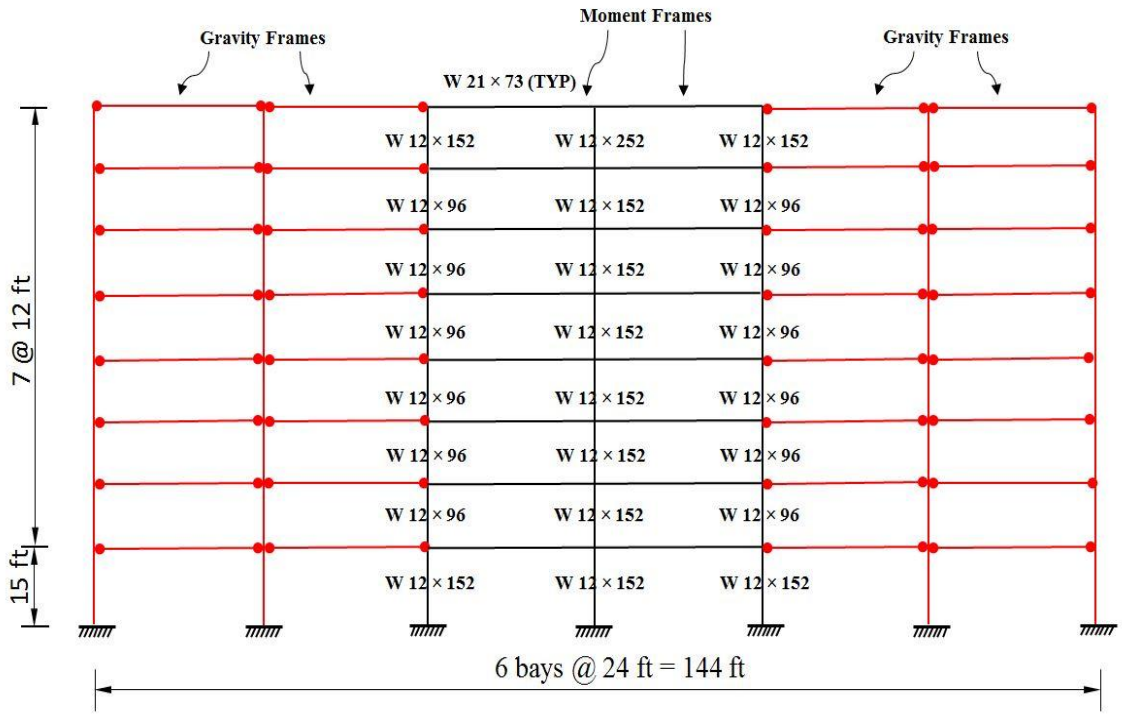

Figure 4-24 Elevation View of the Structure Located in San Francisco with Reduced Lateral Load-Resisting Bays

In order to facilitate discussions, pertinent characteristics and classifications for these structures are provided below in Table 4-11.

Table 4-11 System Classifications (Effect of the Number of Bays)

System Label	Location	Frame Type	Number of Bays Included in LLRS	Number of Stories	Seismic Category	Design Wind Speed (mph)
P3-1	Atlanta	OMF	2	8	A	90
P3-2	San Francisco	SMF	2	8	E	85

4.5.2 FE Model Results and Comparisons

The results for systems P3-1 and P3-2 that are most critical for illustration are presented in this section and compared to the corresponding results from scenario 1 of the

baseline study and system P1-2 of the parametric study. Full sets of plots for these additional systems are located in Appendix C.

4.5.2.1 General Response

The general responses of systems P3-1 and P3-2 to a central column removal scenario are shown below in Figures 4-25 – 4-28, in conjunction with the results from the baseline system and system P1-2. Relevant maximums are listed in Table 4-12. Magnitudes of base shear and deflection at a LF of 1.0 are shown in Table 4-13 for each system (if applicable). Values of vertical deflection, horizontal deflection, and drift index are for the first-floor beam, eighth story, and first story respectively.

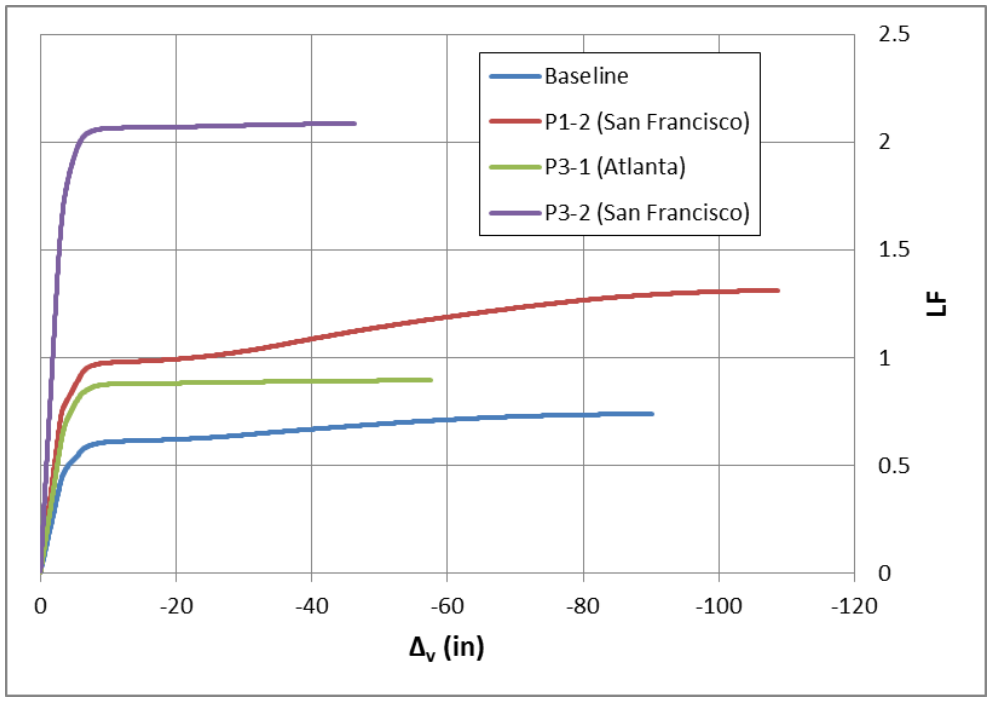

Figure 4-25 LF vs. Δ_v (Effect of the Number of Bays)

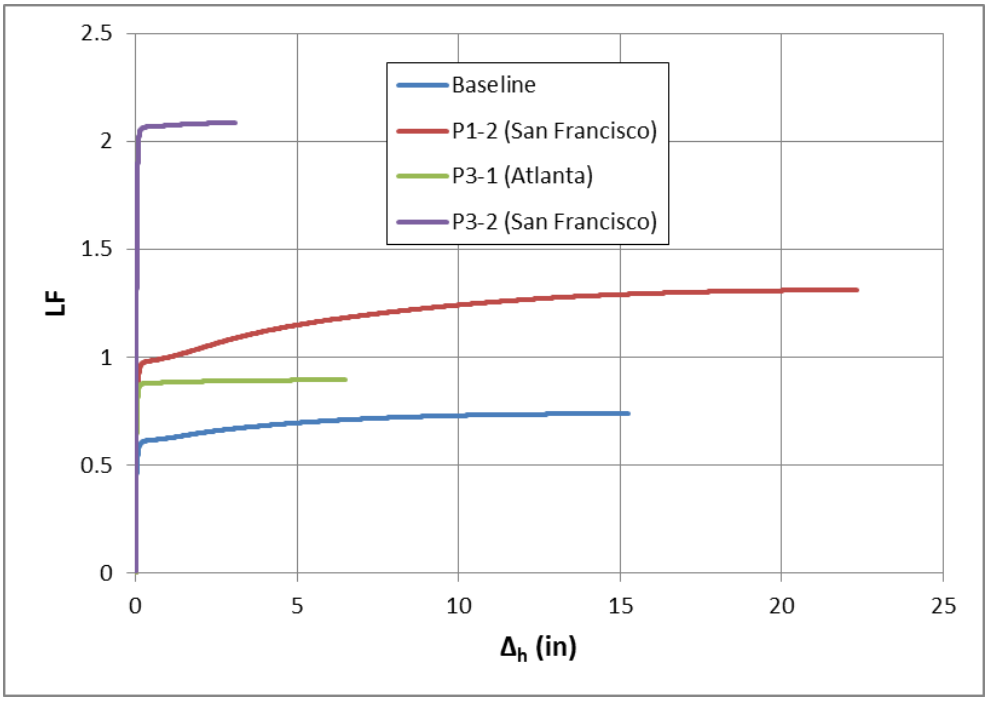

Figure 4-26 LF vs. Δ_h (Effect of the Number of Bays)

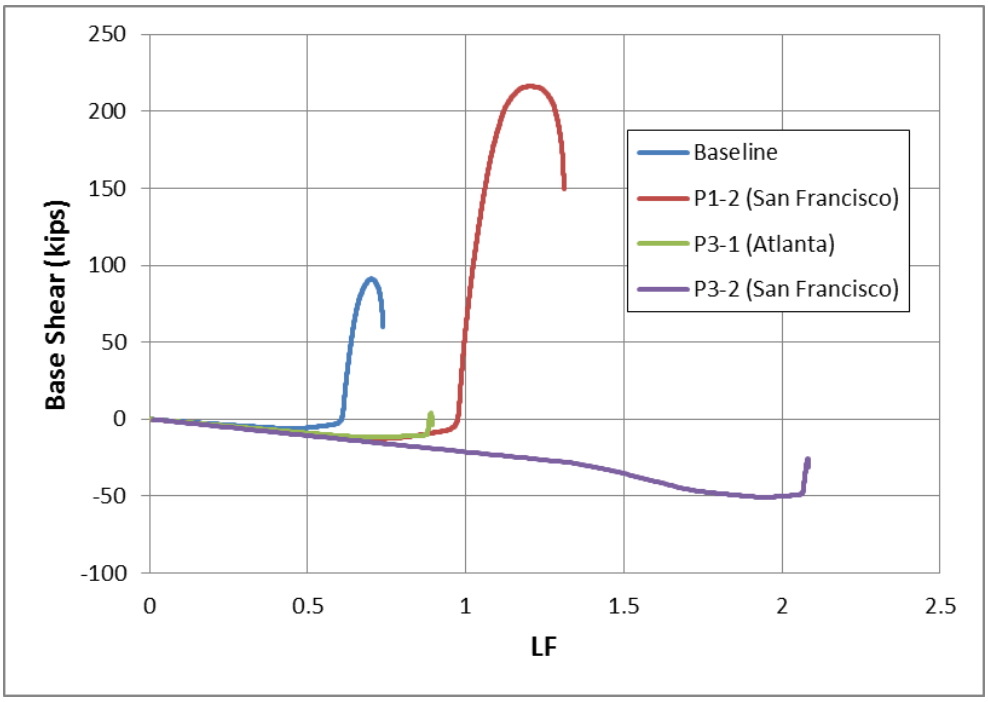

Figure 4-27 Base Shear vs. LF (Effect of the Number of Bays)

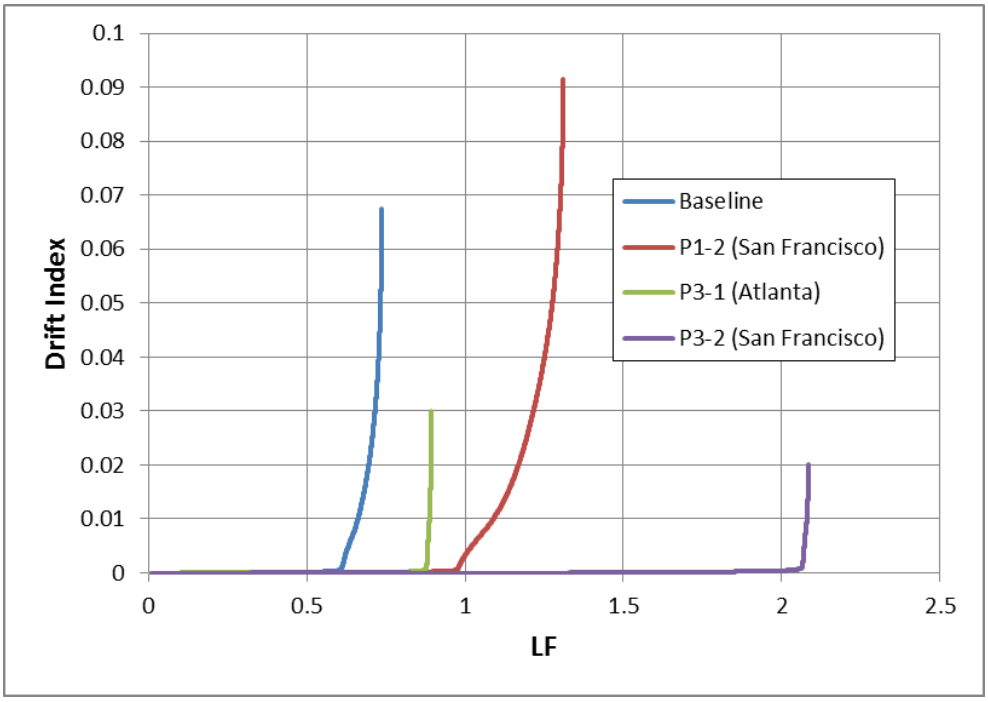

Figure 4-28 Drift Index vs. LF (Effect of the Number of Bays)

Table 4-12 General Response Maximums (Effect of the Number of Bays)

System	Maximum LF	Maximum Base Shear (kips)	Maximum Drift Index	Maximum Δ_h (in)	Maximum Δ_v (in)
Baseline	0.737	91.0	0.067	15.2	90.0
P1-2	1.31	216	0.092	22.3	109
P3-1	0.893	-11.0	0.030	6.50	57.6
P3-2	2.08	-50.7	0.020	3.63	46.4

Table 4-13 General Response Values at a LF of 1.0 (Effect of the Number of Bays)

System	Base Shear at LF = 1.0 (kips)	Drift Index at LF = 1.0	Δ_h at LF = 1.0 (in)	Δ_v at LF = 1.0 (in)
Baseline	N/A	N/A	N/A	N/A
P1-2	55.0	0.003	1.00	22.5
P3-1	N/A	N/A	N/A	N/A
P3-2	-21.4	<0.001	0.027	1.84
Note: System P3-1 and the baseline system were unable to reach a LF of 1.0				

Systems P3-1 and P3-2, as indicated by Table 4-12, were able to attain higher LFs than the corresponding systems with lateral load-resisting bays distributed across the entire length of the structure. This is most likely due to the concentration of lateral load-resistance in the immediate vicinity of the removed column, which results in larger beams and a subsequently larger flexural capacity. However, as in the previous cases, both structures located in Atlanta were unable to sustain the full collapse loads experienced at a LF of 1.0.

The load-deflection trends in Figures 4-25 and 4-26, in conjunction with the maximums provided in Table 4-12 show that systems P3-1 and P3-2 had significantly lower levels of deflection at their maximum LFs, which correlates with a predominately flexural response. Moreover, the trends for base shear in Figure 4-27 show little to no positive base shear development coincident with catenary behavior. This argument is further supported by the maximum values of base shear in Table 4-12, which are negative. This indicates that the maximum axial forces in these systems are associated with frame action.

Of the two systems that were able to sustain the full collapse loads, systems P1-2 and P3-2, the latter was able to do so while undergoing significantly lower levels of deflection due to its use of elastic frame action.

4.5.2.2 Catenary Action Demands

The catenary action demands associated with systems P3-1 and P3-2 are shown below in Figures 4-29 through 4-31 alongside the response from the baseline system and system P1-2. While system P3-2 did not make any significant use of catenary behavior,

and thus did not subsume demands associated with that type of response, its results have been included for comparison purposes. Table 4-14 displays the catenary action demands at the principal load levels for each system. Results are shown for the first-floor beam only.

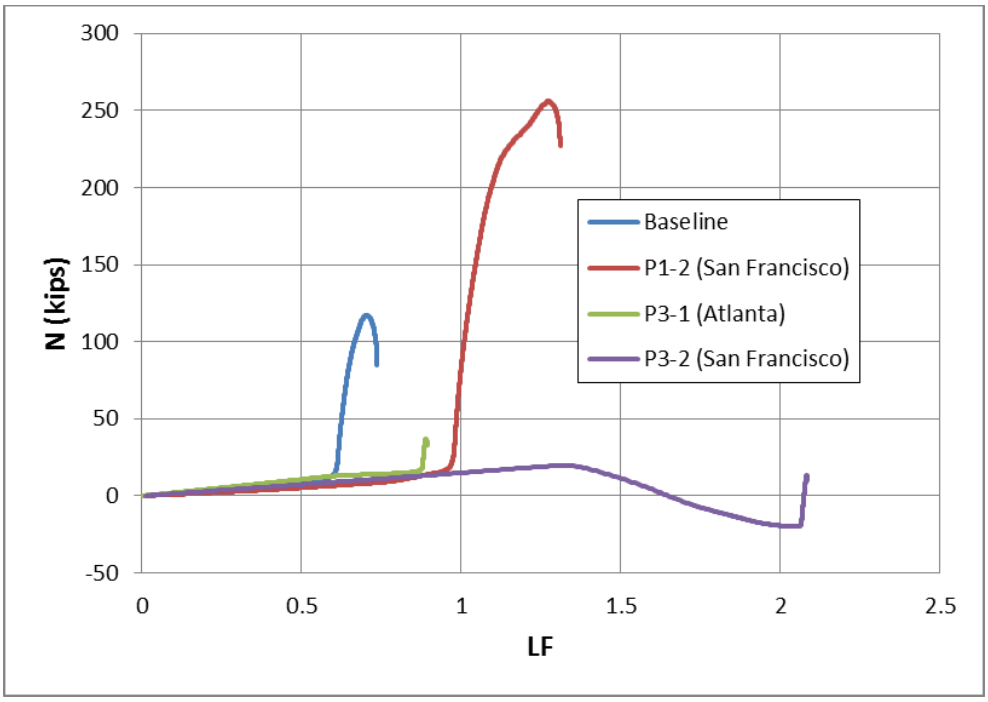

Figure 4-29 N vs. LF (Effect of the Number of Bays)

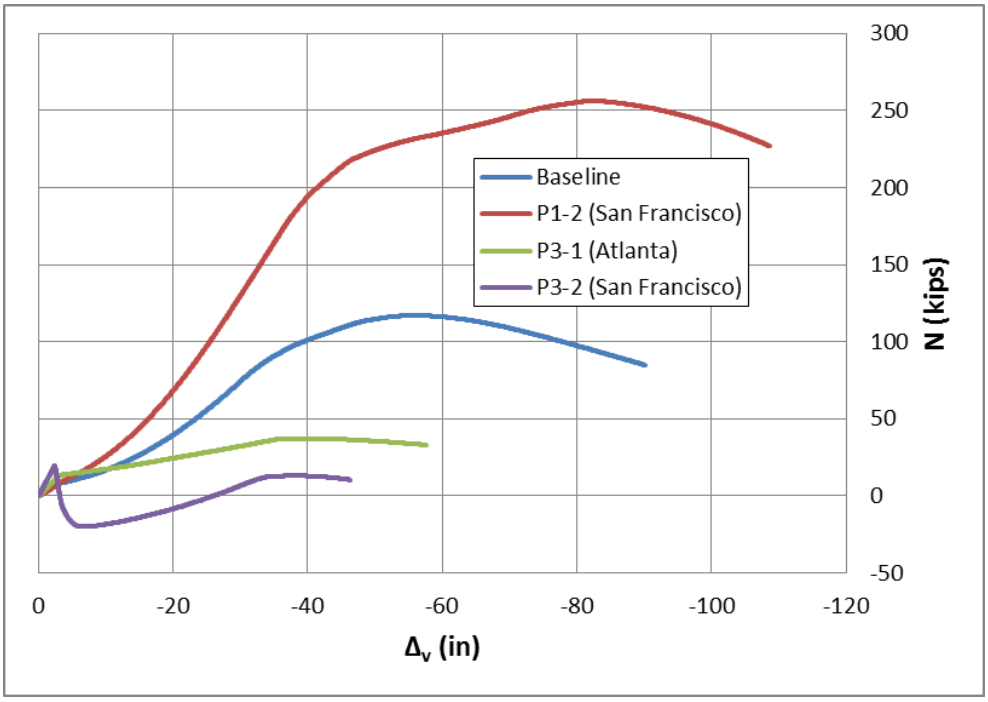

Figure 4-30 N vs. Δ_v (Effect of the Number of Bays)

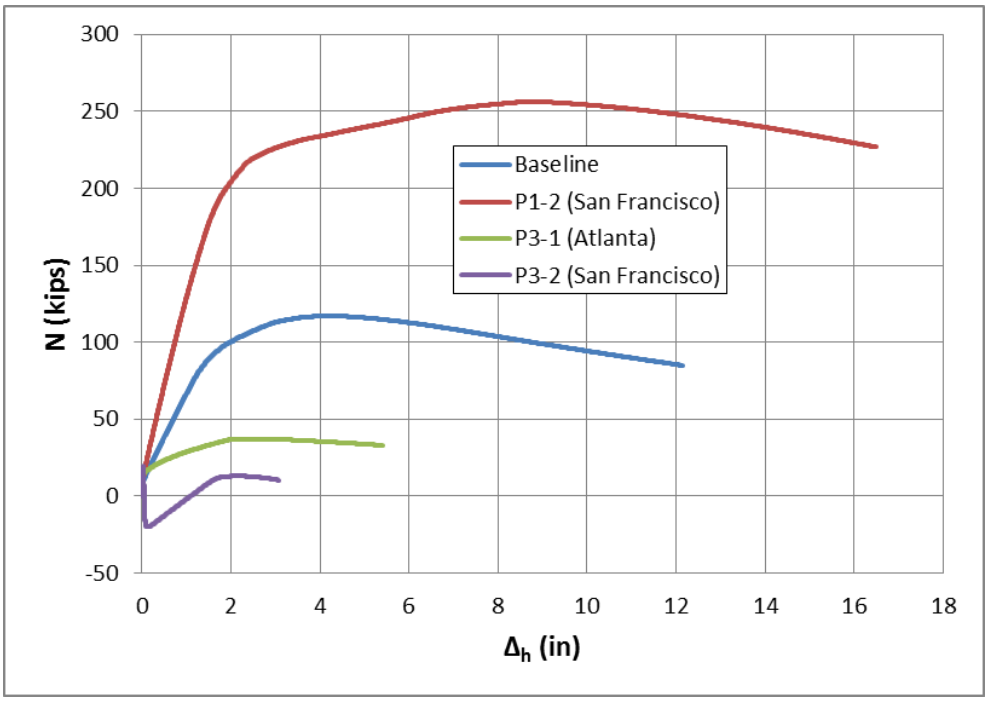

Figure 4-31 N vs. Δ_h (Effect of the Number of Bays)

Table 4-14 Catenary Action Demand Maximums (Effect of the Number of Bays)

System	Maximum N (kips)	Maximum N/Np	N at LF = 1.0 (kips)	N/Np at LF = 1.0 (kips)	Percentage of LF Attributed to Catenary Behavior (%)
Baseline	117	0.310	N/A	N/A	18.6
P1-2	256	0.440	83.0	0.140	26.00
P3-1	37.2	0.070	N/A	N/A	2.20
P3-2	47.2	0.040	21.0	0.020	Negligible

Notes: System P3-1 and the baseline system were unable to reach a LF of 1.0. For system P3-2, the maximum values of N were found in the seventh-floor beam and are considered a product of frame action.

Apparent by the relatively small values of N/Np in Table 4-14 and the extremely low percentages of maximum load resisted by catenary mechanisms, the systems with reduced lateral load-resisting bays made little use of catenary behavior. As previously mentioned, this response can be attributed to the consolidation of lateral load-resistance to the central bays, which increased the beam section sizes. This change had somewhat more of an impact on the structure located in San Francisco, as its overall capacity utilizing predominately flexural behavior more than doubled. This can be seen by comparing the curves for systems P1-2 and P3-2 in Figure 4-29; the onset of catenary behavior for system P3-2 almost coincides with its maximum LF.

Finally, when the full collapse loads were applied (LF of 1.0), system P3-2 remained elastic. In order to sustain the same load level, system P1-2 needed to develop 14% of its first-floor beam's maximum axial tensile force.

4.5.2.3 Connection Ductility Demands

The levels of plastic rotation developed in the beams above the removed column for systems P3-1 and P3-2 are shown below in Figures 4-32 and 4-33. Comparisons of

values of plastic rotation at the principal load levels and their locations in the four systems at these levels are provided in Table 4-15.

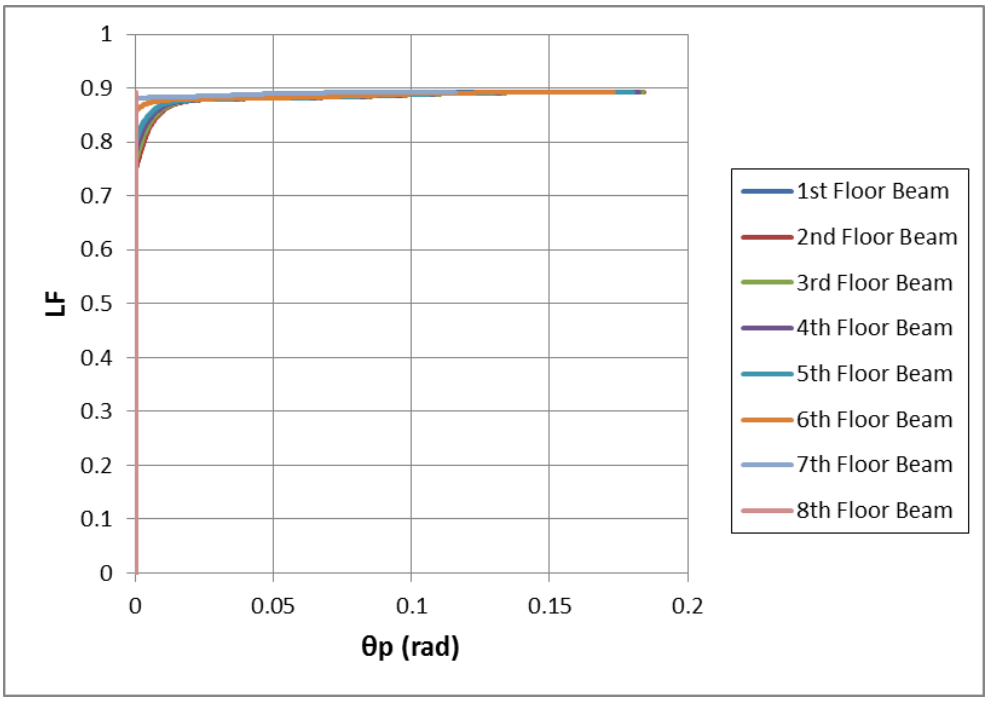

Figure 4-32 Plastic Rotation Demands for System P3-1

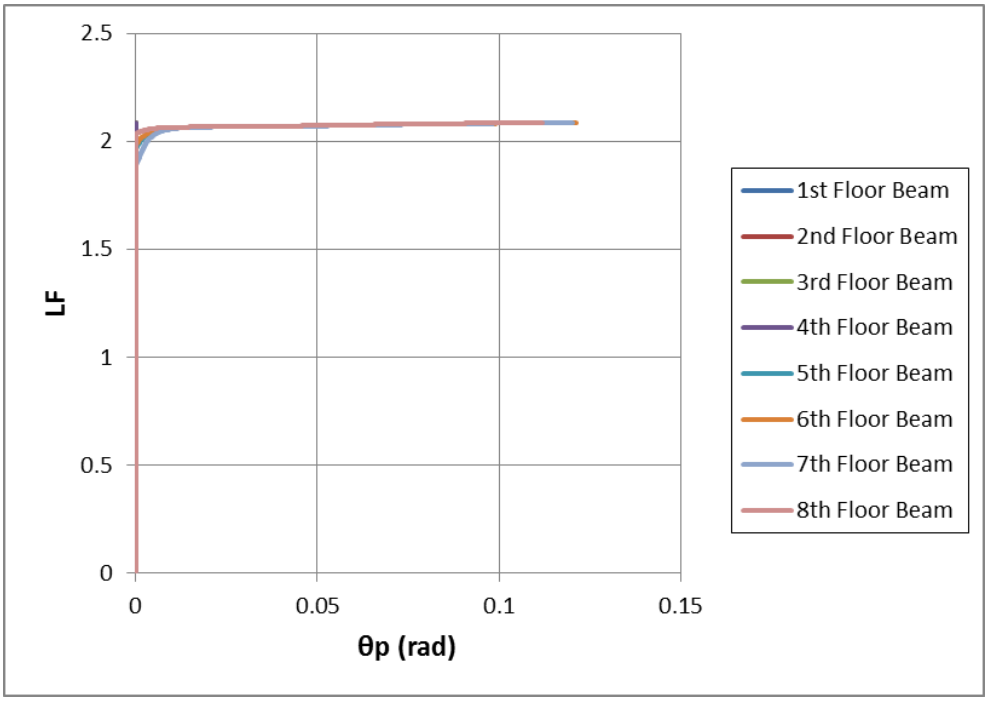

Figure 4-33 Plastic Rotation Demands for System P3-2

Table 4-15 Comparison of Plastic Rotation Demands (Effect of the Number of Bays)

System	θp at Maximum LF (rad)	θp at LF = 1.0 (rad)	Beam Location
Baseline	0.298	N/A	4th floor
P1-2	0.366	0.064	4th floor
P3-1	0.184	N/A	2nd floor
P3-2	0.121	0 (Elastic)	6th floor
Note: System P3-1 and the baseline system were unable to reach a LF of 1.0			

Concordant with predominately flexural behavior, the maximum plastic rotation demands developed in systems P3-1 and 3-2 were lower than the respective values observed in the baseline system and system P1-2.

Furthermore, at the full collapse load level, system P3-2 remained fully elastic, as indicated in Table 4-15. Consequently, the conclusion can be drawn that system P3-2, by

sustaining a LF of 1.0 and remaining elastic, would not be subject to full or partial disproportionate collapse.

4.5.3 Conclusions

Based upon the previous discussions, and within the limitations imposed by the adopted assumptions, the following conclusions can be drawn regarding the effect of reducing the number of lateral load-resisting bays in a structure with exterior moment frames:

- The analytical results showed that systems P3-1 and P3-2 were able to reach LFs higher than what the baseline system and system P1-2 respectively attained. This can be attributed to a considerable increase in the flexural capacity of the beams, which occurred as a result of constraining the number of lateral load-resisting bays.
- The catenary action demands indicated that neither system P3-1 nor system P3-2 developed any significant axial tension attributed to catenary behavior. This response correlates with the increased beam section size; at the point of plastic flexural collapse, the columns seemed to have expended most of their capacity and were unable to sustain significant catenary forces.
- The plastic rotation demands developed in each structure showed that systems P3-1 and P3-2 maintained lower levels of plastic rotation throughout the analysis. In particular, system P3-2 remained elastic at the full collapse load level. As with

the catenary action demands, this result likely occurred because the design of systems P3-1 and P3-2 provided larger beam sections.

As previously indicated, these conclusions are only relatable to systems with lateral load-resisting frames concentrated at the center of each exterior moment frame and analyses that consider the removal of the central column from the LLRS.

4.6 Effect of Building Aspect Ratio

This section investigates the potential impacts of a structure's aspect ratio on its progressive collapse response. As a building's aspect ratio changes, its seismic weight and exposure to wind-induced loads will correspondingly change. As shown in Figure 3-1, the baseline system was designed as a long, narrow structure with the short dimension being perpendicular to the moment frames. The analytical results presented in Chapter 3 revealed that, utilizing a fully ductile response, the baseline system was incapable of resisting the loading conditions associated with progressive collapse and experienced partial or full collapse, depending on the column removal scenario considered. An additional system is presented in this chapter; this system was developed to investigate the impacts of having an aspect ratio that increases both the seismic weight of the structure and the wind-exposure in the direction parallel to the moment frames. Due to the structure's location in Atlanta (GA), wind loads controlled the design of the system. Consequently, only the impacts of the latter are applicable for discussion Since altering this parameter involved no change in the dimensions of the two-dimensional FE model, but rather changed the magnitude of the design forces, it was not anticipated that

significantly behavioral differences would be seen between structures in different locations. Consequently, only one location was considered in the study of this parameter.

4.6.1 System Description

The system presented in this chapter was designed for a location in Atlanta, GA. It was designed for the same gravity loads that were used in the design of the baseline system and with the same design wind speed. However, unlike the baseline system, this system has two additional bays in the direction perpendicular to the moment frames. The plan view of this structure, called system P4-1, is shown in Figure 4-34. The structure's elevation view, including the resulting sections utilized in the moment frames, is depicted in Figure 4-35.

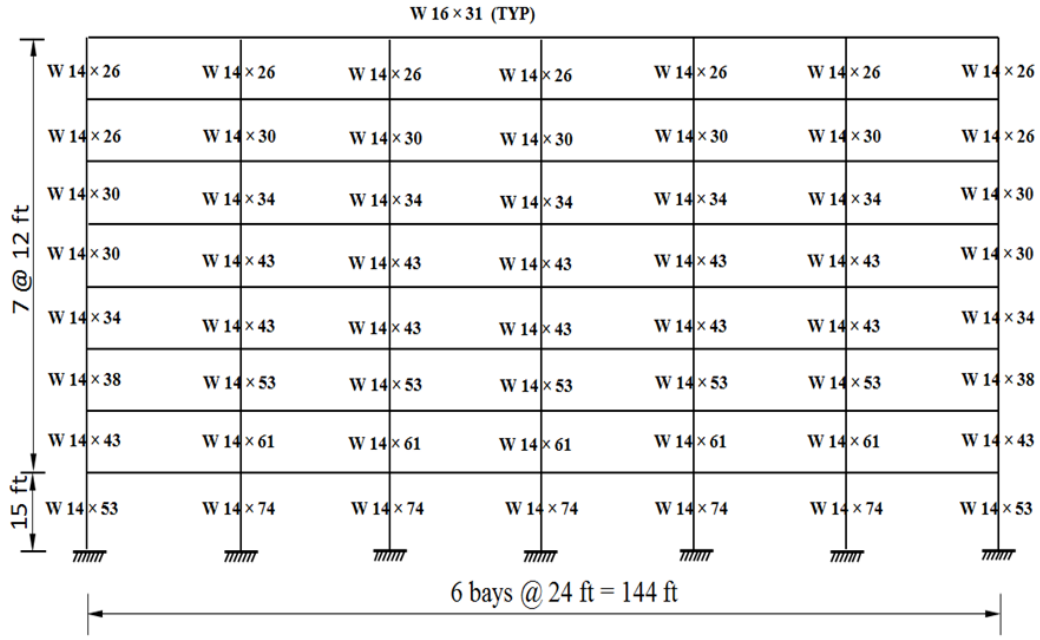

Figure 4-34 Elevation View of Structure with Alternate Aspect Ratio

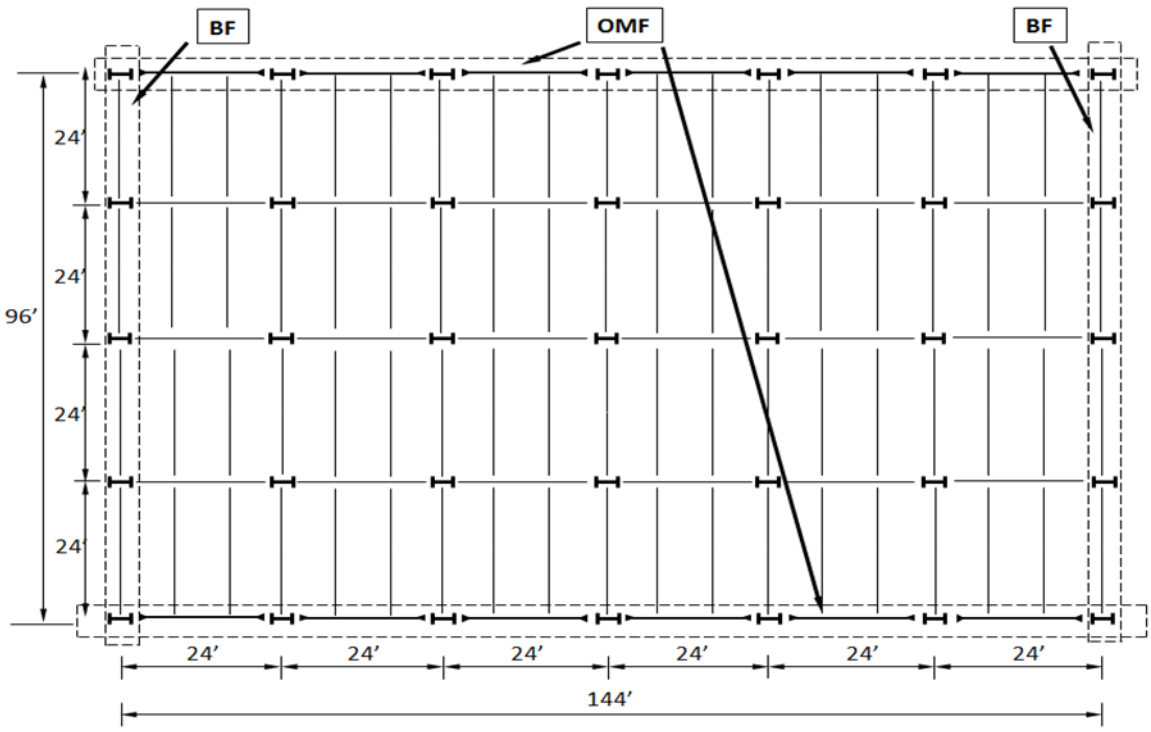

Figure 4-35 Plan View of Structure with Alternate Aspect Ratio

As indicated by Figure 4-35, system P4-1 contains two additional interior frames in the direction parallel to the OMFs. These frames were designed to resist gravity loads alone. Consequently, the only influence the changed aspect ratio had on the structural design process was in the magnitude of the lateral loads. In order to facilitate discussions, pertinent characteristics and classifications for this structure are summarized below in Table 4-16.

Table 4-16 System Classification (Effect of Building Aspect Ratio)

System Label	Location	Frame Type	Number of Bays Included in LLRS	Number of Stories	Seismic Category	Design Wind Speed (mph)
P4-1	Atlanta	OMF	6	8	A	90

4.6.2 FE Model Results and Comparisons

The results for system P4-1 that are most critical for illustration are presented in this section and compared to the corresponding results from scenario 1 of the baseline study. Full sets of plots for this additional system are located in Appendix D.

4.6.2.1 General Response

The general response of system P4-1 to a central column removal scenario is shown below in Figures 4-36 through 4-39 in conjunction with the results from the baseline system. Relevant maximums are listed in Table 4-17. Values of vertical deflection, horizontal deflection, and drift index are for the first-floor beam, eighth story, and first story respectively.

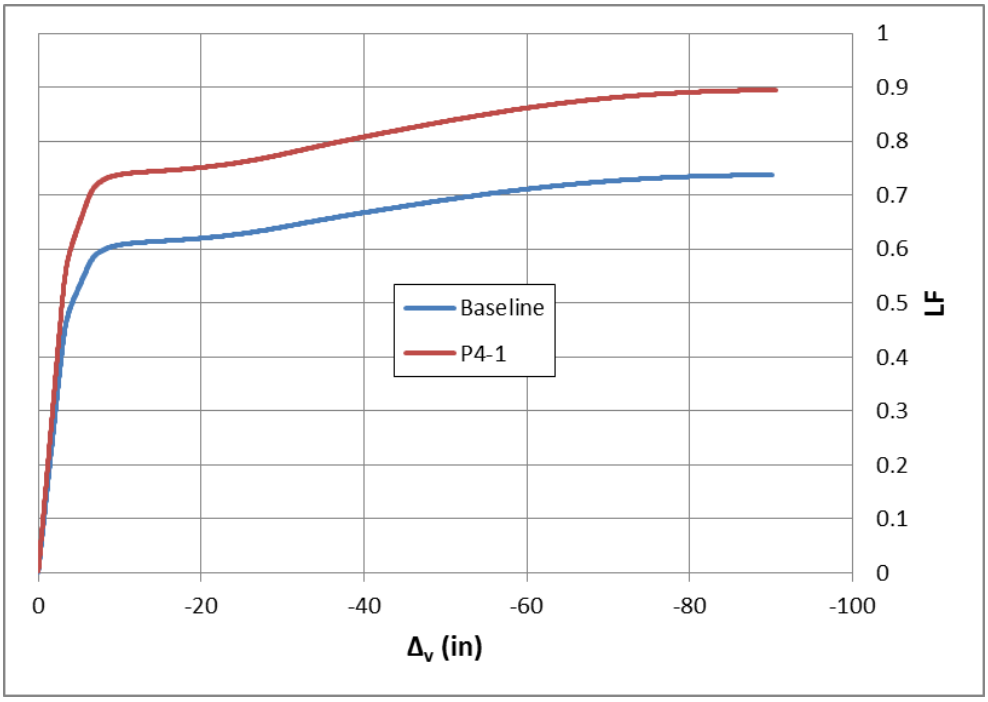

Figure 4-36 LF vs. Δ_v (Effect of Building Aspect Ratio)

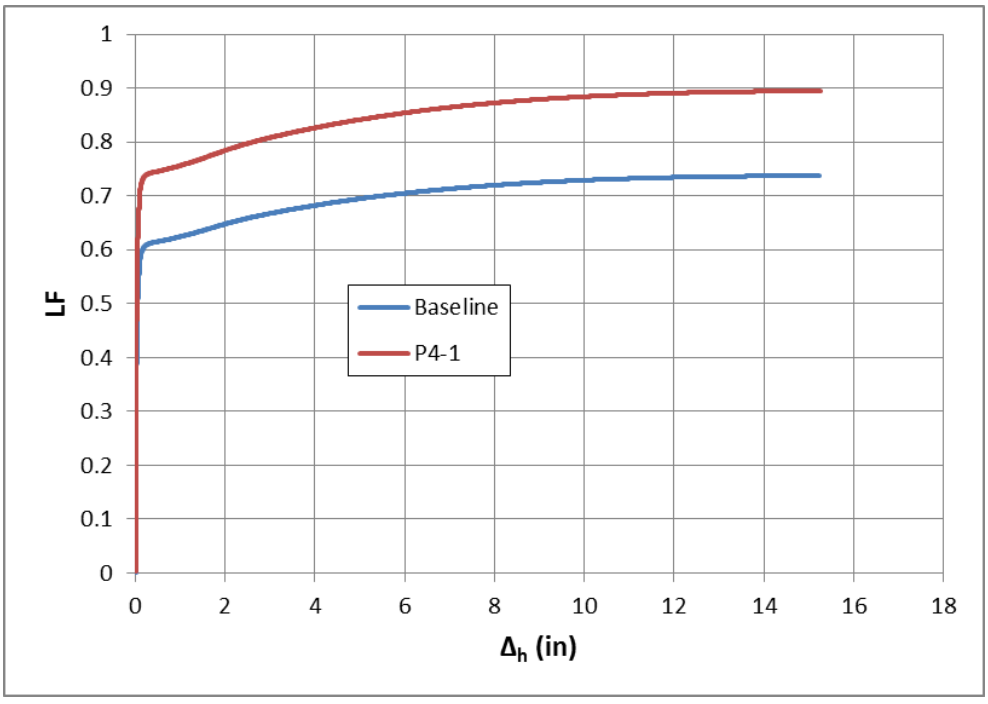

Figure 4-37 LF vs. Δ_h (Effect of Building Aspect Ratio)

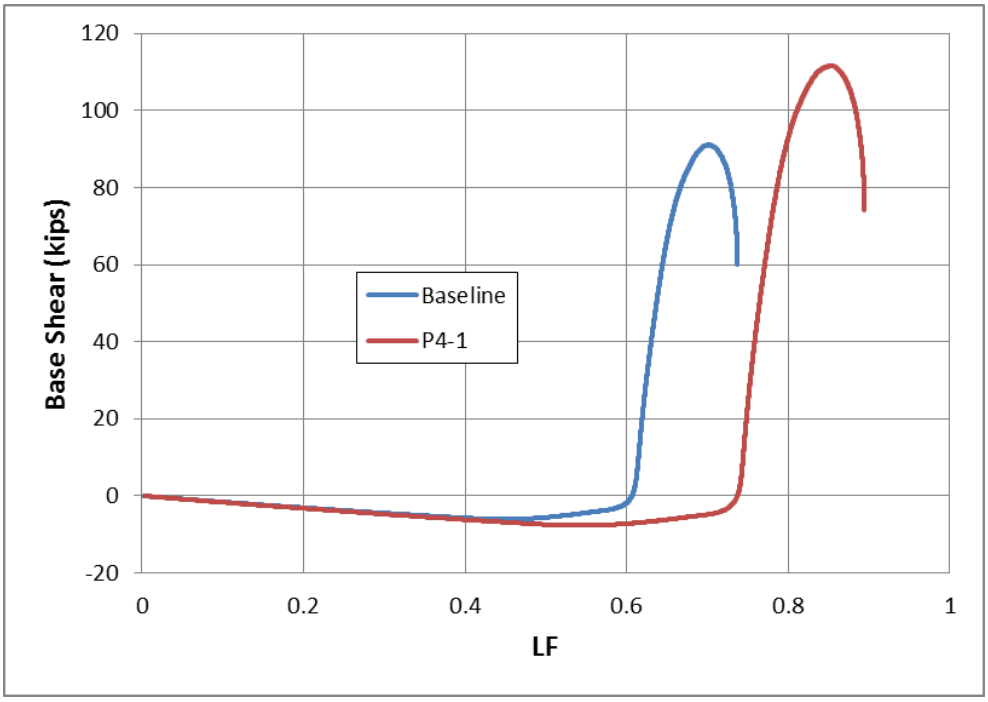

Figure 4-38 Base Shear vs. LF (Effect of Building Aspect Ratio)

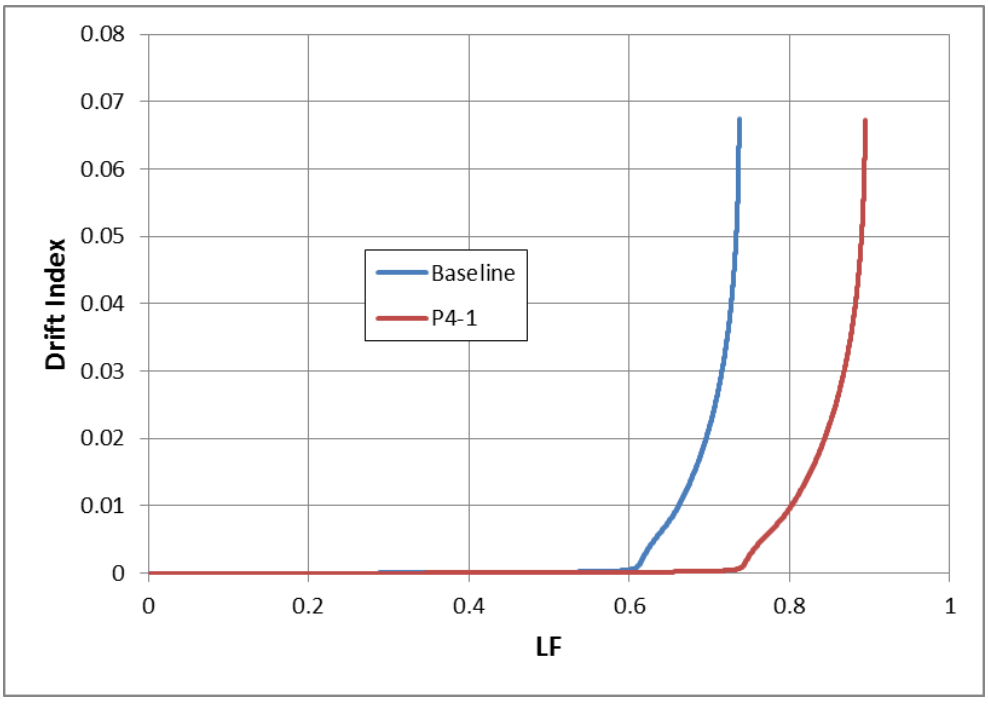

Figure 4-39 Drift Index vs. LF (Effect of Building Aspect Ratio)

Table 4-17 General Response Maximums (Effect of Building Aspect Ratio)

System	Maximum LF	Maximum Base Shear (kips)	Maximum Drift Index	Maximum Δ_h (in)	Maximum Δ_v (in)
Baseline	0.737	91.0	0.067	15.2	90.0
P4-1	0.894	112	0.067	15.3	90.5

Figures 4-36 through 4-39 display a consistent behavior that can be identified with system P4-1: Overall strength levels are increased over the baseline system's maximum levels with no change in the magnitudes of deflection experienced by the structure at the corresponding locations of these maximums. Moreover, while the maximum LF that was resisted by system P4-1, provided in Table 4-17, was larger than what was sustained by the baseline system, it was still lower than 1.0; this indicates that, much like the baseline system, system P4-1 was not able to avert collapse.

4.6.2.2 Catenary Action Demands

The catenary action demands associated with system P4-1 are shown below in Figures 4-40 through 4-42 alongside the response from the baseline system. Table 4-18 displays pertinent maximums for each system. Results are shown for the first-floor beam only.

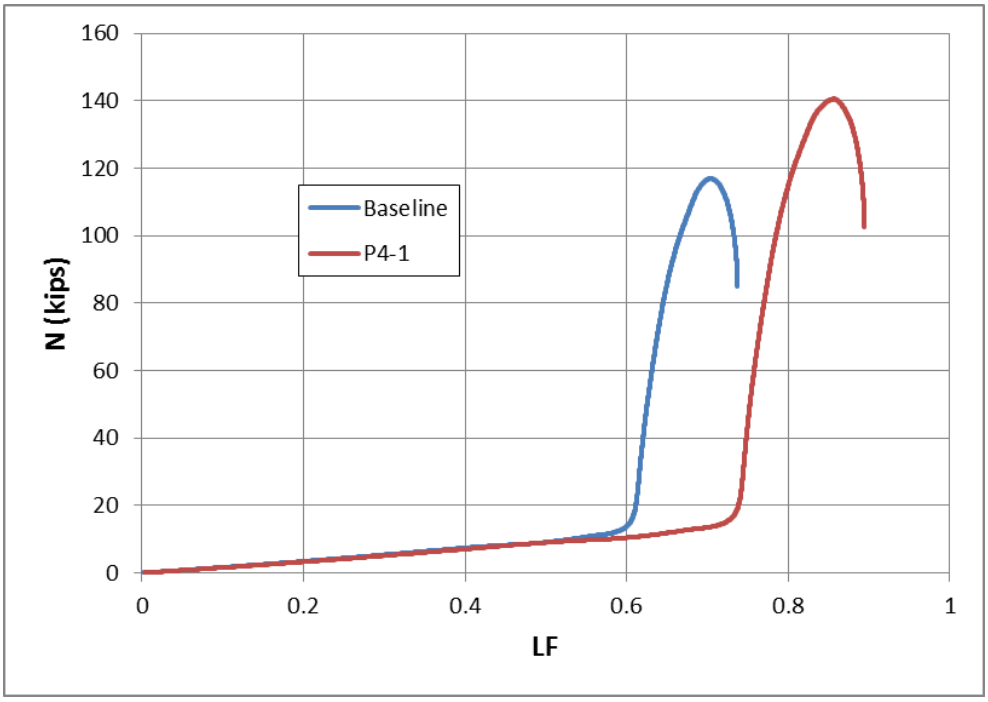

Figure 4-40 N vs. LF (Effect of Building Aspect Ratio)

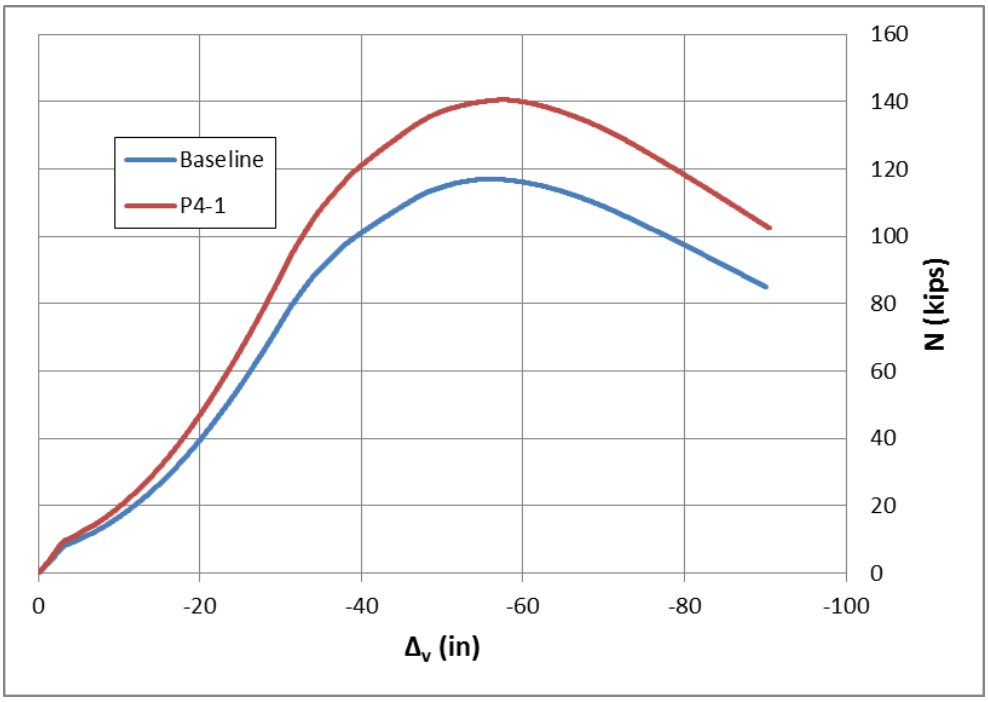

Figure 4-41 N vs. Δ_v (Effect of Building Aspect Ratio)

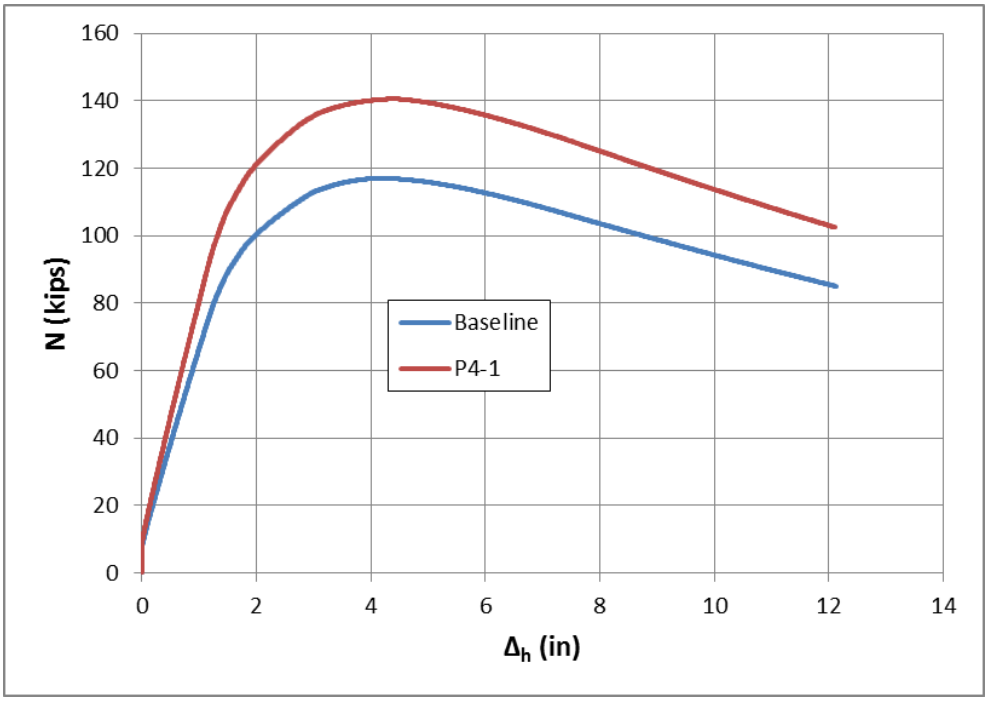

Figure 4-42 N vs. Δ_h (Effect of Building Aspect Ratio)

Table 4-18 Catenary Action Demand Maximums (Effect of Building Aspect Ratio)

System	Maximum N (kips)	Maximum N/Np	Percentage of LF Attributed to Catenary Behavior (%)
Baseline	117	0.310	18.6
P4-1	141	0.320	18.4

Supporting what was established in section 4.6.2.1, the catenary action demands associated with system P4-1 increased in absolute magnitude over the baseline system, but not in relative response. Thus, as indicated in Table 4-18, the maximum ratio of N/Np developed in the first-floor beam remained comparatively unchanged and the amount of additional load resisted by catenary mechanisms was identical. Moreover, Figures 4-41 and 4-42 show that the maximum values of catenary force were attained at

nearly identical values of deflection in both systems. By resisting higher levels of load utilizing a similar catenary response at matching deflection levels, system P4-1 should be less susceptible to potential connection ductility limitations than the baseline system.

4.6.2.3 Connection Ductility Demands

The levels of plastic rotation developed in the beams above the removed column for system P4-1 are shown below in Figure 4-43. Comparisons of maximum values of plastic rotation at the peak LF and their locations are provided in Table 4-19 for system P4-1 and the baseline system.

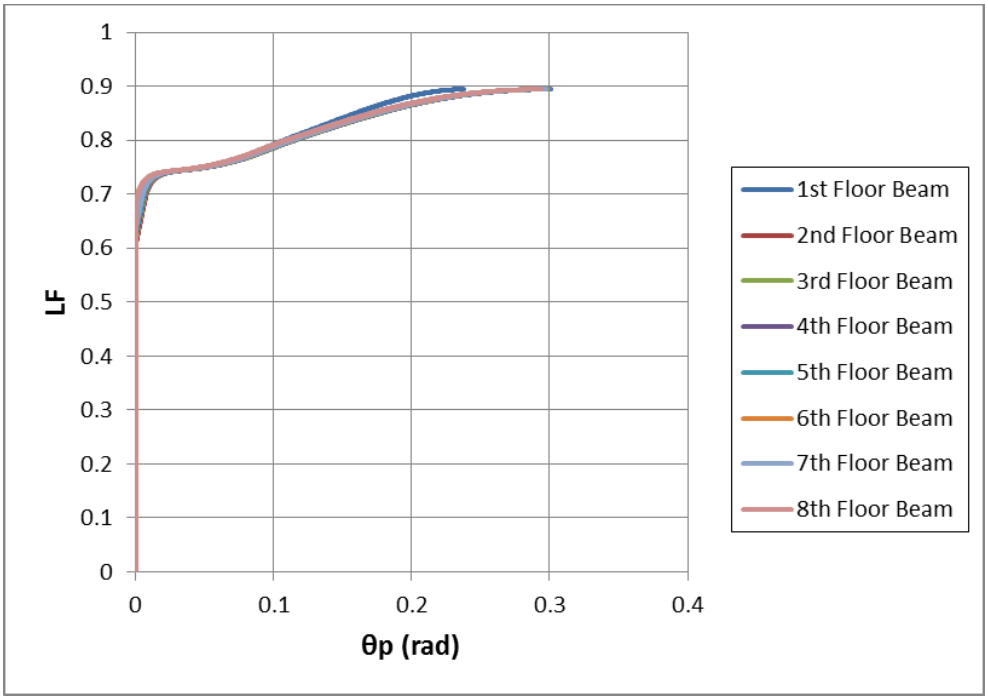

Figure 4-43 Plastic Rotation Demands for System P4-1

Table 4-19 Maximum Plastic Rotation Demands (Effect of Building Aspect Ratio)

System	θp at Maximum LF (rad)	Beam Location
Baseline	0.298	4th floor
P4-1	0.300	5th floor

From Figure 4-43, it is seen that the distribution of plastic rotation demand among the beams in system P 4-1 remained comparatively unchanged from the values obtained from the baseline system. Similarly, as can be seen in Table 4-19, the maximum values of plastic rotation at the peak LF in both systems are identical.

4.6.3 Conclusions

The comparisons between the baseline system and system P4-1 show that structures designed for similar levels of vertical load, but with different aspect ratios, can perform differently when subjected to the loss of a first story column in the lateral load resisting system. In particular, the results indicate that, for structures controlled by wind loads, increasing exposure in the direction of lateral load resistance for a specific exterior moment frame can correspondingly increase that frame's collapse resistance when subjected to the loss of a 1st story column. This increase can occur without substantially altering the type of response utilized.

Chapter 5 – Summary, Conclusions, and Recommendations

5.1 Summary

Historical precedent has established progressive collapse as a phenomenon characterized by the potential for extreme structural damage and loss of life. In an attempt to mitigate such behavior in conventional structures, several different approaches for analysis and design have been suggested. These methods include both threat-dependent and threat-independent procedures. Under the latter, a common approach is to subject the structure to a notional column-removal scenario and then check the ability of the structure to bridge over the removed member. The structure's response under such circumstances can involve the utilization of catenary or cable-like behavior to resist the imposed loads once the flexural capacity of the resisting members has been exhausted and sufficient levels of deflection have been attained.

Due to the unique combination of behavior displayed during progressive collapse, and the scale of such events, current research efforts have been aimed at a variety of topics. Foremost among these are analytical studies of various aspects of structural behavior exhibited during progressive collapse and experimental investigations aimed at quantifying the resiliency of structural elements and their associated connections.

Current design codes and guidelines within the United States, including ASCE 7 (2010), IBC (2009), GSA (2003), and UFC (2009), provide varying degrees of information and guidance regarding progressive collapse design. The most developed of

these, UFC (2009), includes a combination of threat-dependent methods (SLR method), prescriptive procedures (TF method), and analytical approaches (AP method).

In this thesis, an analytical investigation of various factors influencing the response of steel structures during progressive collapse was conducted using the FE program OpenSees and the loading conditions of the AP method, as outlined in UFC (2009). First, a baseline study was performed, which considered the response in the LLRS of a specifically designed, eight-story, six-bay, steel-framed structure. The notional removal of columns in 4 distinct locations throughout one of the perimeter moment frames was considered. Subsequently, the general response of the structure during each scenario, its catenary action demands, and connection ductility demands were recorded, discussed and compared. Following this, a parametric study was conducted, which considered the effects of changing various design parameters on the response of the system during collapse. The parameters investigated included: the building location, the number of stories, the number of bays in the lateral load-resisting system, and the building aspect ratio. The study found that each parameter can have a significant impact on overall system behavior and the development of catenary forces in particular.

5.2 Conclusions

Based upon the research presented in this thesis, and within the limitations imposed by the adopted assumptions, the following general conclusions can be drawn:

- In general, it was seen that the behavior exhibited by the beams was directly related to the characteristics of the adjacent side frames.

- When catenary mechanisms were used to resist load, the largest forces associated with this type of response were consistently found in the first-floor beam. This was believed to be primarily associated with the higher level of restraint at this location. This implies that, in order to sustain these forces, the beams in the lower stories of structural systems need to be properly anchored by side-frames and connections capable of resisting the imposed force demands.

- The column-removal scenarios simulated during the investigation revealed that column-removal locations closer to the center of structures can result in higher resistance to collapse, but more extensive failure modes in the event that the capacity of the side-frames is exhausted.

- It was seen that greater utilization of catenary behavior in the structures studied directly coincided with substantially increased ductility demands. Potential limitations on the ductile response of the moment connections could result in partial collapse. However, should the scenario under consideration result in the failure of the adjoining side-frames, such limitations could serve to prevent the propagation of collapse.

- The parametric study indicated that structures designed for locations with larger design lateral loads are more resistant to progressive collapse. This was also found to be true for structures with fewer stories, fewer bays in the lateral-load resisting system, and structures with aspect ratios that increase the design lateral loads. These conclusions are only applicable for central column-removal scenarios within the LLRS.

- It was seen that structures with fewer stories, more bays included in the LLRS, and those designed for highly seismic regions all displayed greater propensities for utilizing catenary behavior in order to avert collapse. However, the structures designed for larger seismic forces demonstrated less of a need to take advantage of such behavior.

- Many current design guidelines, such as the UFC 4-023-03 TF method, do not specify any strength or stiffness requirements for anchoring systems. The findings of this investigation indicate a potential need for the development of such provisions.

5.3 Recommendations

Because of the limitations associated with the assumptions used in this research, several topics and areas of investigation are recommended for further study:

- Due to the large forces and deformations observed during this investigation, which were associated with catenary behavior, it is recommended that detailed analytical and experimental investigations be conducted into the resiliency of steel connections during conditions indicative of progressive collapse

- It is recommended that studies explicitly considering the effect(s) of floor slabs, dynamic effects, strain-hardening, 3-D effects, and inelastic panel-zone behavior, be conducted to ascertain the relative impacts of such factors on the analyses presented in this thesis.

- It is recommended that theoretical relationships be established which predict the distribution of catenary force development in multi-story structures by story location.

- Finally, it is recommended that further study be conducted to verify the potential need to implement strength and stiffness considerations associated with anchoring systems into the UFC 4-023-03 TF requirements.

References

Agarwal, A., Haberland, M., Holicky', M., Sykora, M., and Thelandersson, S. "Robustness of Structures: Lessons from Faliures." *Structural Engineering International*, 22(1), 2012: 105-111.

Alashker, Y., Li, H., and El-Tawil, S. "Approximations in Progressive Collapse Modeling." *ASCE Journal of Structural Engineering*, 137(9), 2011: 914-924.

Alp, Y. *Combined Flexural and Cable-Like Behavior of Ductile Steel Beams.* MS Thesis, Auburn, AL: Auburn University, 2009.

American Institute of Steel Construction (AISC). *Seismic Design Manual.* Chicago, IL: American Institute of Steel Construction, 2005B.

American Institute of Steel Construction (AISC). *Steel Construction Manual, 13th Edition.* Chicago, IL: American Institute of Steel Construction, 2005A.

American Society of Civil Engineers (ASCE). *Minimum Design Loads for Buildings and other Structures (ASCE/SEI 7-05).* Reston, VA: American Soceity of Civil Engineers, 2005.

American Society of Civil Engineers (ASCE). *Minimum Design Loads for Buildings and other Structures (ASCE/SEI 7-10).* Reston, VA: American Society of Civil Engineers, 2010.

American Society of Civil Engineers (ASCE). *Seismic Rehabilitation of Existing Buildings (ASCE/SEI 7-06).* Reston, VA: American Society of Civil Engineers, 2006.

Centre for the Protection of National Infrastructure (CPNI). *Review of International Research on Structural Robustness and Disproportionate Collapse.* London, UK: Department for Communities and Local Government, 2011.

Computers and Structures Inc. *SAP2000.* 2012.

De Souza, R.M. *Force-Based Finite Element for Large Displacement Inelastic Analysis of Frames.* Phd Dissertation, Berkeley, CA: University of California, 2000.

Ellingwood, B.R., and E.V. Leyendecker. "Approaches for Design against Progressive Collapse." *Journal of the Structural Division*, 104(3), 1978: 413-423.

Ellingwood, B.R., Smilowitz, R., Dusenberry, D.O., Duthinth, D., Lew, H.S., and Carino, N.J. *Best Practices for Reducing Potential for Progressive Collapse in Buildings (NISTIR 7396).* Washington, D.C.: United States Department of Commerce, 2007.

General Services Administration (GSA). *Progressive Collapse Analysis and Design Guidelines for New Federal Office Buildings and Major Modernization Projects.* Washington, D.C.: GSA, 2003.

Gerasimidis, S., and Baniotopoulos, C.C. "Evaluation of Wind Load Integration in Disproportionate Collapse Analysis of Steel Moment Frames for Column Loss." *Journal of Wind Engineerig and Industrial Aerodynamics*, 99(11), 2011: 1162-1173.

Gong, Y. "Analysis and Design for the Resilience of Shear Connections." *Canadian Journal of Civil Engineering*, 37(12), 2010: 1581-1589.

Hamburger, R., and Whittaker, A. "Design of Steel Structures for Blast-Related Progressive Collapse Resistance." *North American Steel Construction Conference (NASCC).* Long Beach, CA: Conference Proceedings, AISC, 2004. 42-53.

Horne, M.R. *Plastic Theory of Structures.* Oxford, England: Pergamon Press, 1979.

International Code Council, Inc. *International Building Code.* Country Club Hills, IL: Delmar Cengage Learning, 2009.

Khandelwal, K., and El-Tawil, S. "Collapse Behavior of Steel Special Moment Resisting Frame Connections." *ASCE Journal of Structural Engineering*, 133(5), 2007: 646-655.

Khandelwal, K., and El-Tawil, S. "Pushdown Resistance as a Measure of Robustness in Progressive Collapse Analysis." *Engineering Structures*, 33(9), 2011: 2653-2661.

Khandelwal, K., El-Tawil, S., and Sadek, F. "Progressive Collapse Analysis of Seismically Designed Steel Braced Frames." *Journal of Constructional Steel Research*, 65(3), 2008B: 699-708.

Khandelwal, K., El-Tawil, S., Kunnath, S., and Lew, H.S. "Macromodel-Based Simulation of Progressive Collapse: Steel Frame Structures." *ASCE Journal of Structural Engineering*, 134(7), 2008A: 1070-1078.

Kim, J., and An, D. "Evalulation of Progressive Collapse Potential of Steel Moment Frames Considering Catenary Action." *The Structural Design of Tall and Special Buildings*, 18(4), 2008: 455-465.

Kim, J., Parl, J., and Lee, T. "Sensitivity Analysis of Steel Buildings Subjected to Column Loss." *Engineering Structures*, 33(2), 2011: 421-432.

Kim, T., and Kim, J. "Collapse Analysis of Steel Moment Frames with Various Seismic Connections." *Journal of Constructional Steel Research*, 65(6), 2009: 1316-1322.

Kim, T., Kim, J., and Park, J. "Investigation of Progressive Collapse-Resisting Capability of Steel Moment Frames Using Push-Down Analysis." *ASCE Journal of Performance of Constructed Facilities*, 23(5), 2009: 327-335.

Kim, T., Kim, U., and Kim, J. "Collapse Resistance of Unreinforced Steel Moment Connections." *The Structural Design of Tall and Special Buildings*, 2010: doi: 10.1002/tal.636, retreived from Wiley Online Library.

Main, J.A., Sadek, F., and Lew, H.S. "Assessment of Robustness and Disproportionate Collapse Vulnerability of Steel Moment-Frame Buildings." *Second International Workshop on Performance, Protection & Strengthening of Structures Under Extreme Loading (PROTECT2009).* Hayama, Japan: Conference Proceedings, 2009.

Marchand, K.A., and Alfawakhiri, F. *Facts for Steel Buildings, Number 2: Blast and Progressive Collapse.* Chicago, IL: American Institute of Steel Construction, 2004.

McKenna, F., and Fenves, G.L. *Open System for Earthquake Engineering Simulation (OpenSees).* Berkeley, CA: University of California, 2000.

Park, R., and Gamble, W. *Reinforced Concrete Slabs, 2nd Edition.* John Wiley and Sons, Inc., 2000.

Pirmoz, A. "Performance of Bolted Angle Connections in Progressive Collapse of Steel Frames." *The Structural Design of Tall and Special Buildings*, 20(3), 2011: 349-370.

Pirmoz, A., Danesh, F., and Farajkhah, V. "The Effect of Axial Beam Force on Moment–Rotation Curve of Top and Seat Angle Connections." *The Structural Design of Tall and Special Buildings*, 20(7), 2011: 767-783.

Quiel, S., and Marjanishvili, S.M. "Fire Resistance of a Damaged Steel Building that has been Designed to Resist Progressive Collapse." *ASCE Journal of Performance of Constructed Facilities*, 2011: doi:10.1061/(ASCE)CF.1943-5509.0000248, retreived from ASCE Library.

Sadek, F., Main, J.A., Lew, H.S., Robert, S.D., and Chiarito, V. "Testing and Analysis of Steel Beam-Column Assemblies under Column Removal Scenarios." *ASCE Structures Congress.* Austin, TX: Conference Proceedings, ASCE, 2009. 1708-1717.

Scott, M.H., Fenves, G.L., McKenna, F., and Filippou, F.C. "Software Patterns for Nonlinear Beam-Column Models." *ASCE Journal of Structural Engineering*, 134(4), 2008: 562-571.

Song, B.I., Sezen, H., and Giriunas, K.A. "Experimental and Analytical Assessment on Progressive Collapse Potential of Two Actual Steel Frame Buildings." *ASCE Structures Congress.* Orlando, FL: Conference Proceedings, ASCE, 2010. 1171-1182.

Stevens, D. *Assessment and Proposed Approach for Tie Forces in Framed and Load-bearing Wall Structures.* Draft Report, Dripping Springs, TX: Protection Engineering Consultants, 2008.

Szyniszewski, S. "Effects of Random Imperfections on Progressive Collapse Propagation." *ASCE Structures Congress.* Orlando, FL: Conference Proceedings, ASCE, 2010. 3572-3577.

The Instutition of Structural Engineers. *Paper RP/68/05: The Resistance of Buildings to Accidental Damage.* London, UK: IStructE, 1971.

Unified Facilities Criteria (UFC). *DoD Minimum Antiterrorism Standards for Buildings (UFC 4-010-01).* Washingon, D.C.: United States Department of Defense, 2007.

United Facilities Criteria (UFC). *Design of Buildings to Resist Progressive Collapse (UFC 4-023-03).* Washington, D.C.: United States Department of Defense, 2010.

United Facilities Criteria (UFC). *Structural Engineering (UFC 3-301-01).* Washington, D.C.: United States Department of Defense, 2011.

Vlassis, A.G., Izzuddin, B.A., Elghazouli, A.Y., and Nethercot, D.A. "Progressive Collapse of Multi-Storey Buildings Due to Failed Floor Impact." *Engineering Structures*, 31(7), 2009: 1522-1534.

Xu, G., and Ellingwood, B.R. "Disproportionate Collapse Performance of Partially Restrained Steel Frames with Bolted T-stub Connections." *Engineering Structures*, 33(1), 2011: 32-43.

Appendices

Appendix A – Supplementary Plots for Systems P1-1 and P1-2

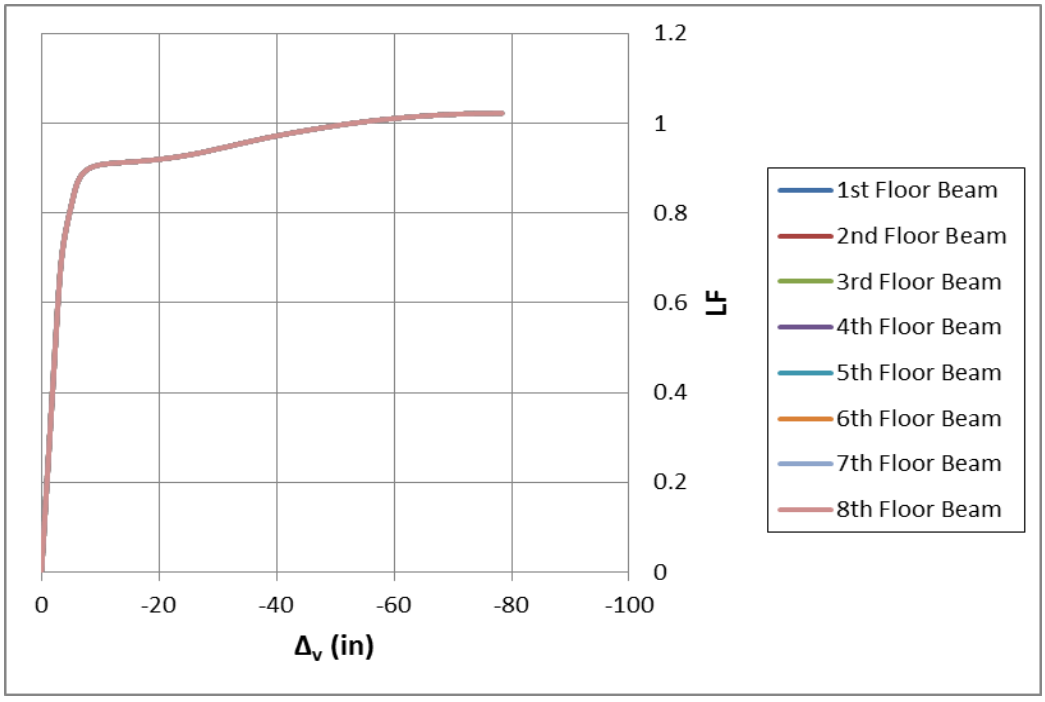

Figure A-1 LF vs. Vertical Deflection (System P1-1)

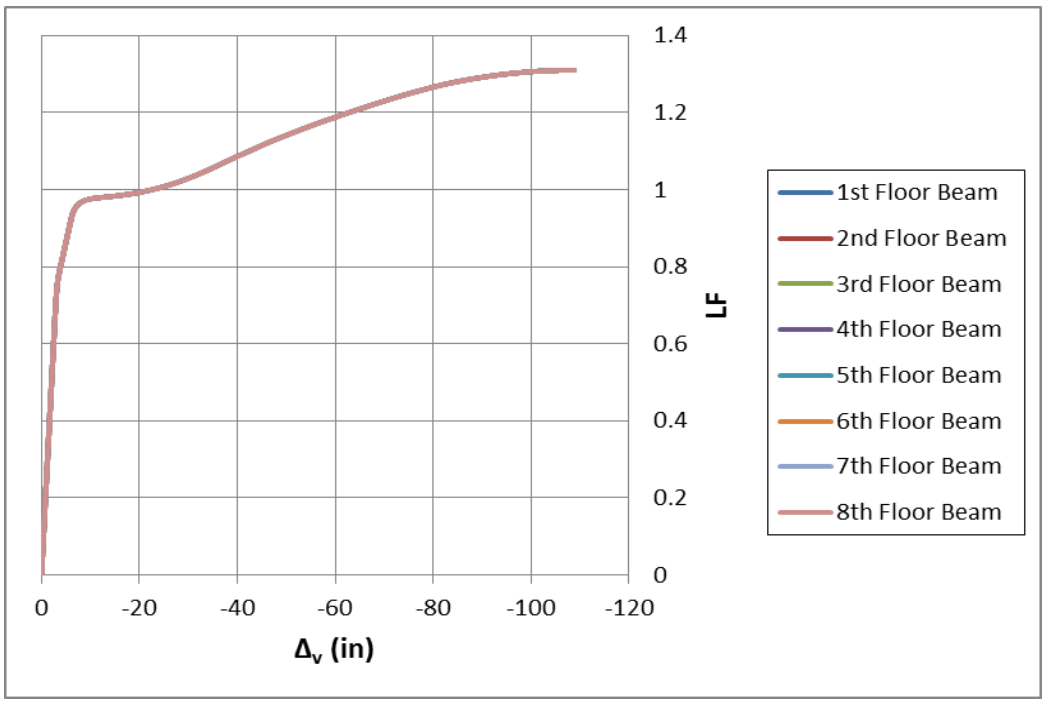

Figure A-2 LF vs. Vertical Deflection (System P1-2)

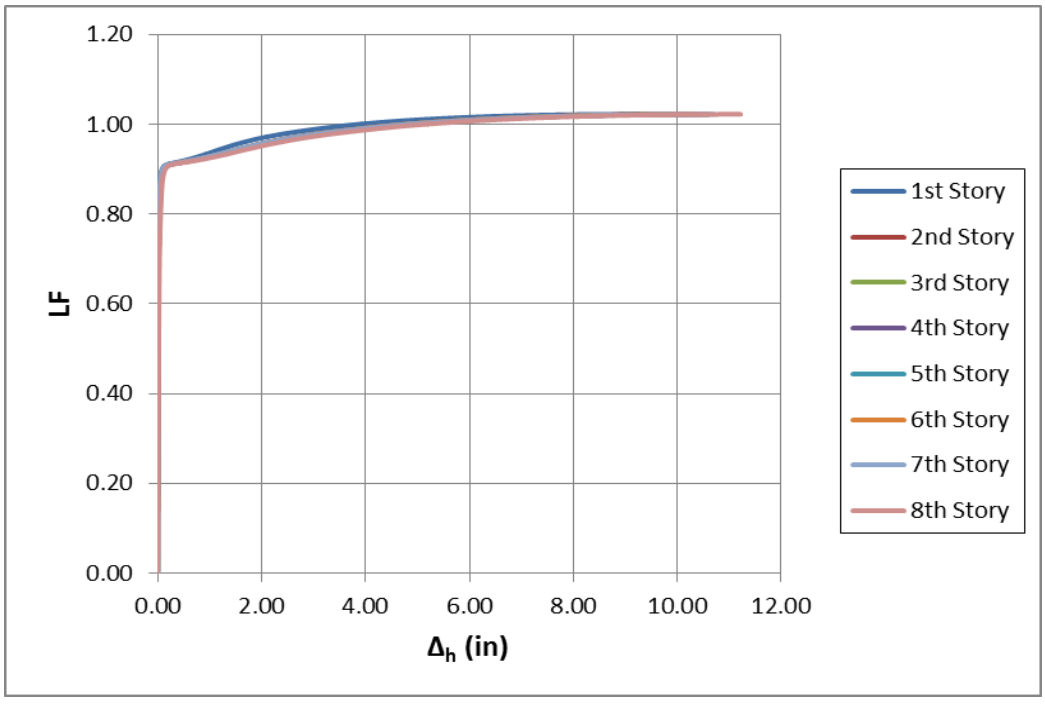

Figure A-3 LF vs. Horizontal Displacement (System P1-1)

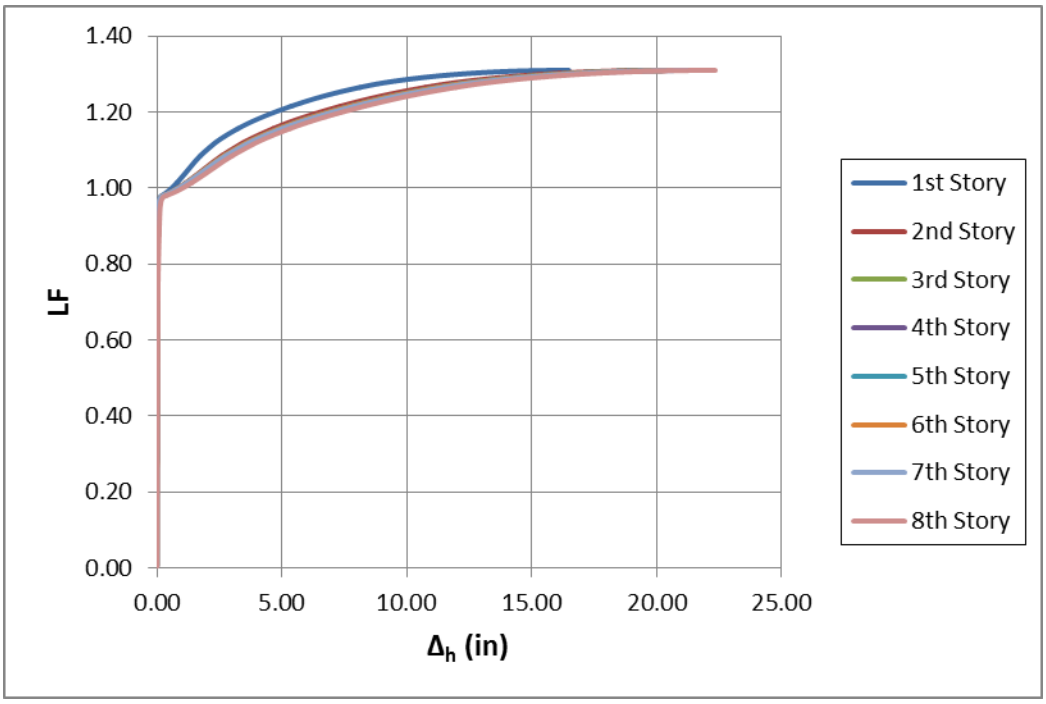

Figure A-4 LF vs. Horizontal Displacement (System P1-2)

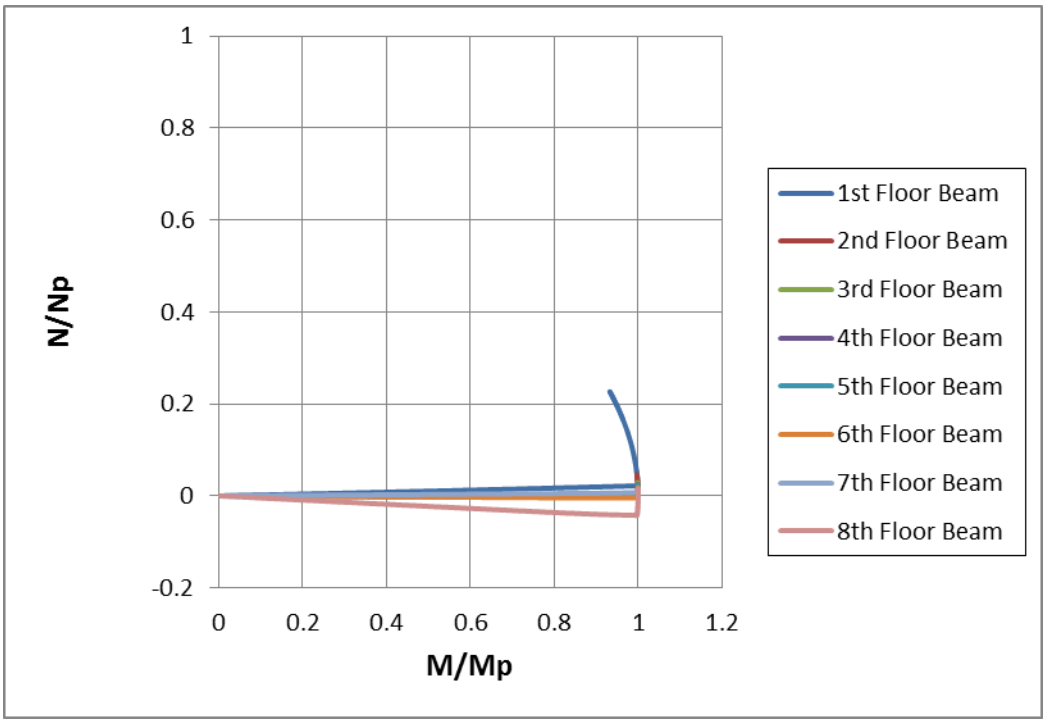

Figure A-5 N/Np vs. M/Mp (System P1-1)

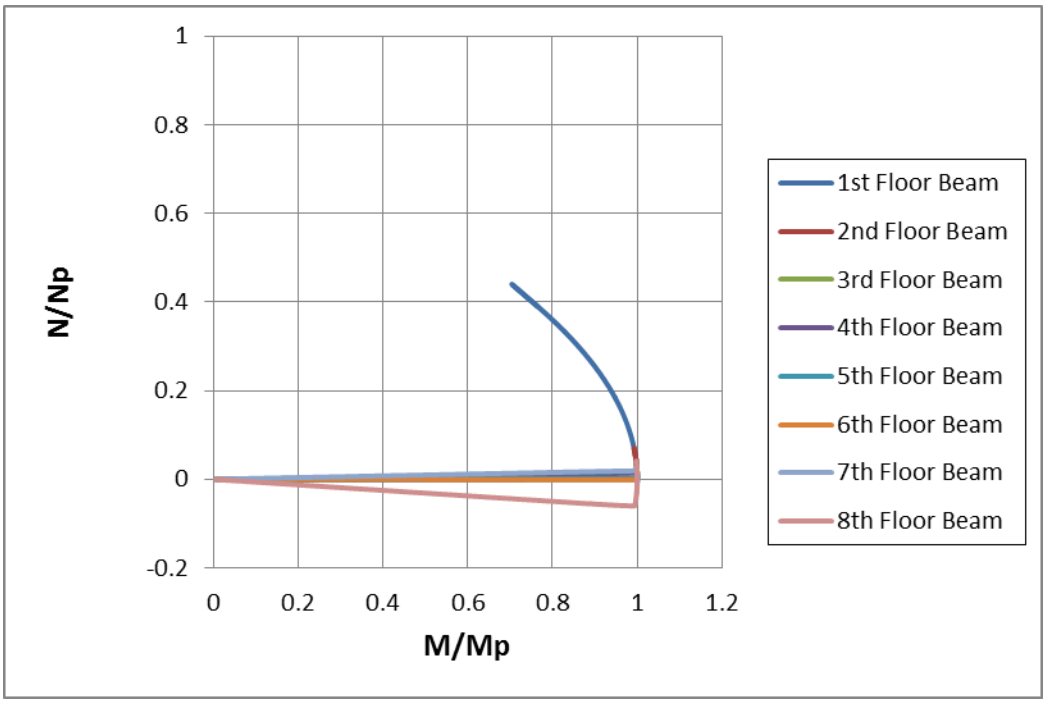

Figure A-6 N/Np vs. M/Mp (System P1-2)

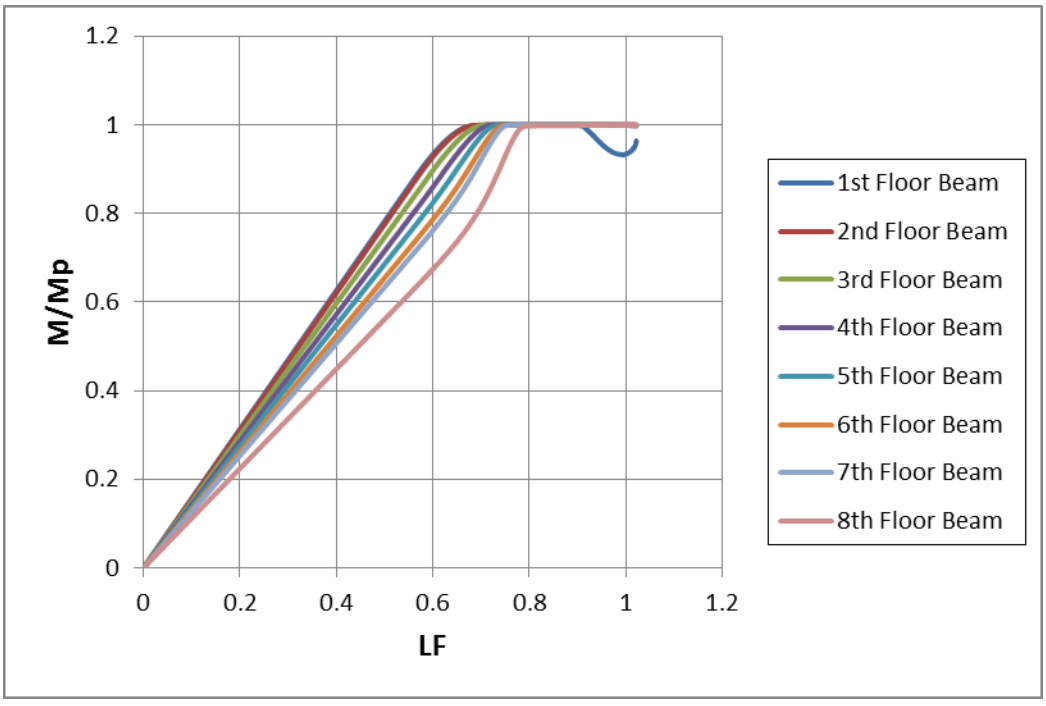

Figure A-7 M/Mp vs. LF (System P1-1)

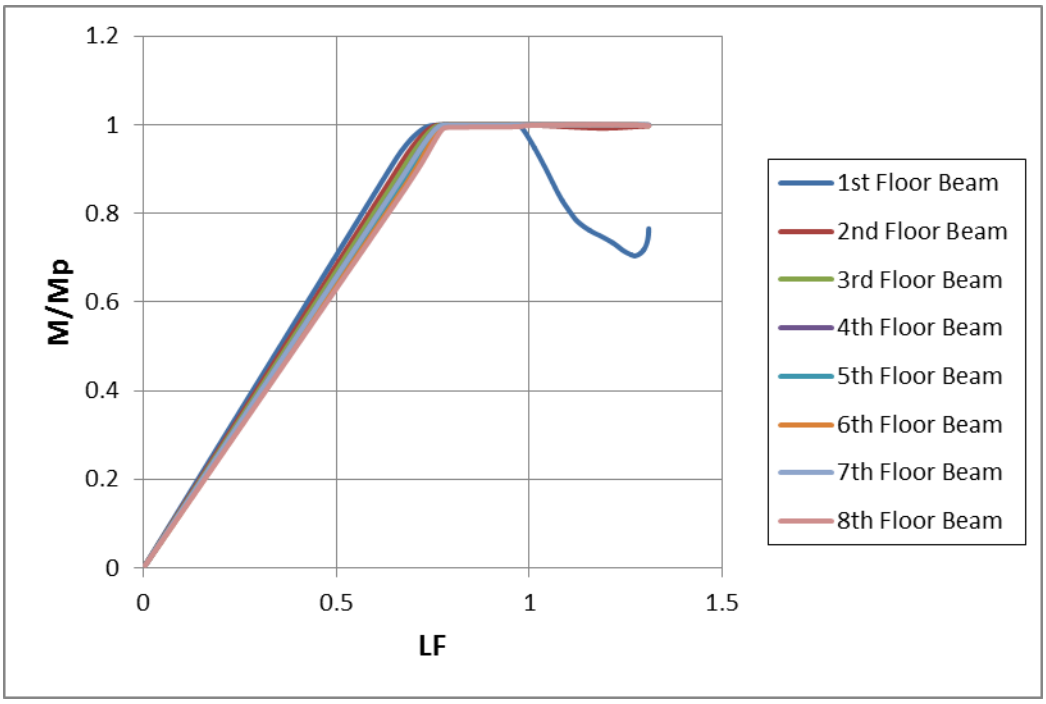

Figure A-8 M/Mp vs. LF (System P1-2)

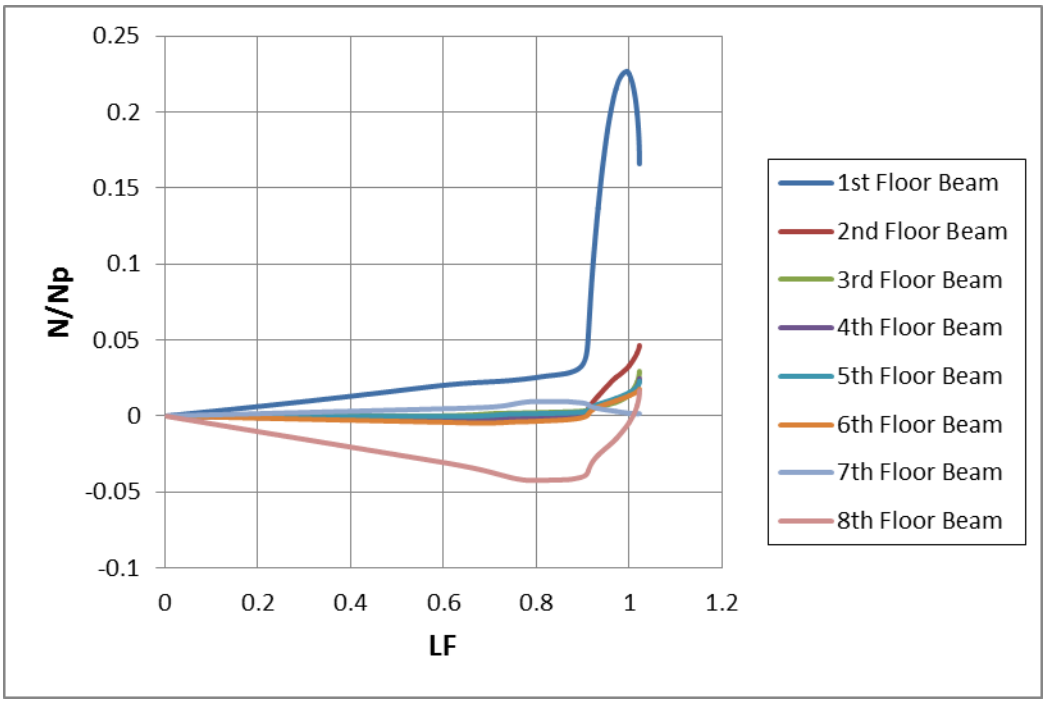

Figure A-9 N/Np vs. LF (System P1-1)

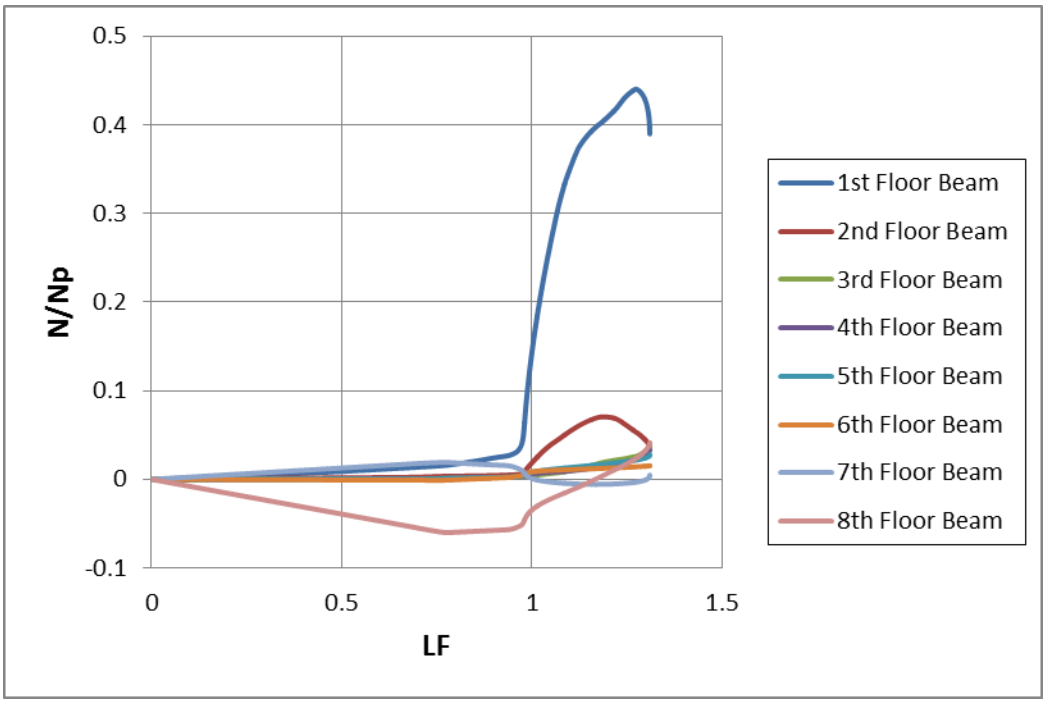

Figure A-10 N/Np vs. LF (System P1-2)

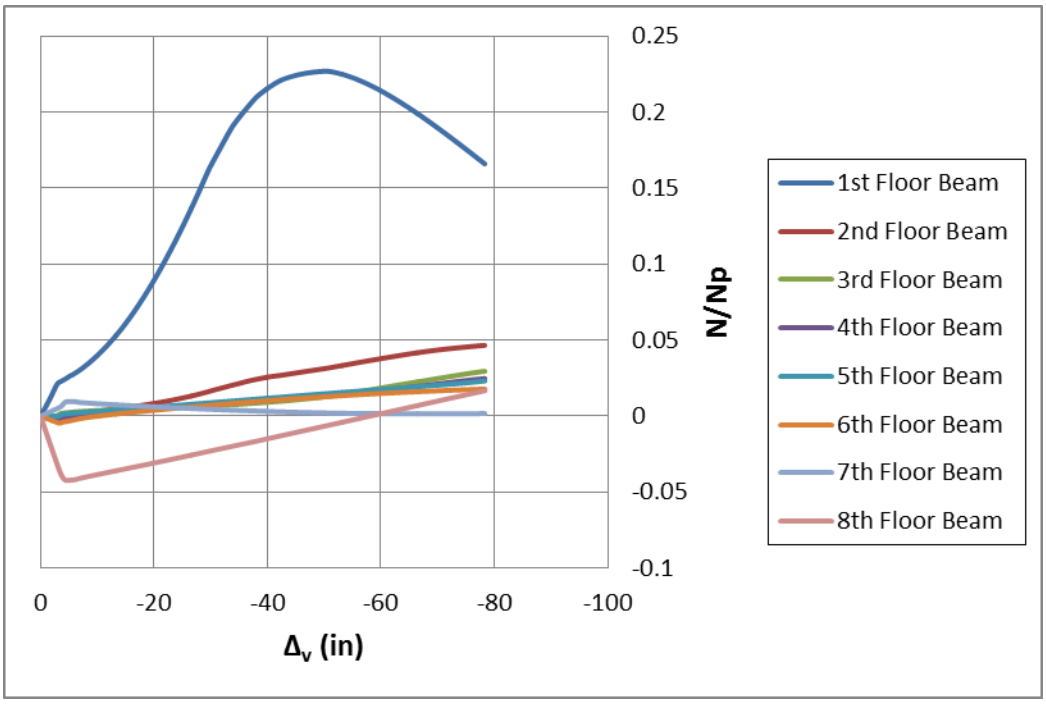

Figure A-11 N/Np vs. Vertical Deflection (System P1-1)

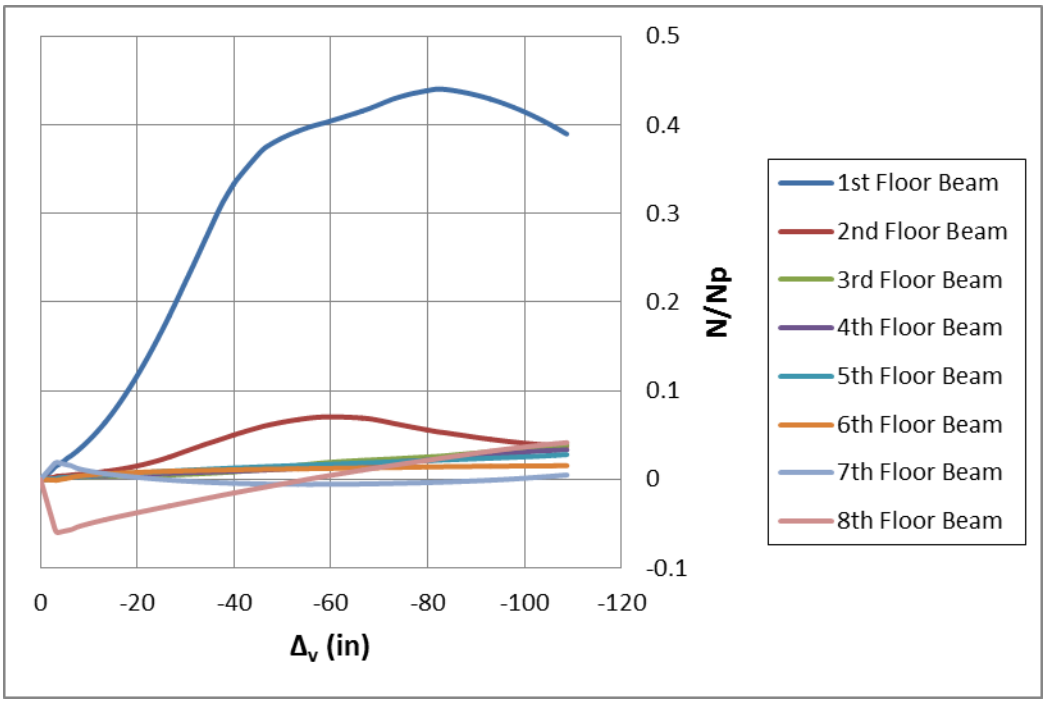

Figure A-12 N/Np vs. Vertical Deflection (System P1-2)

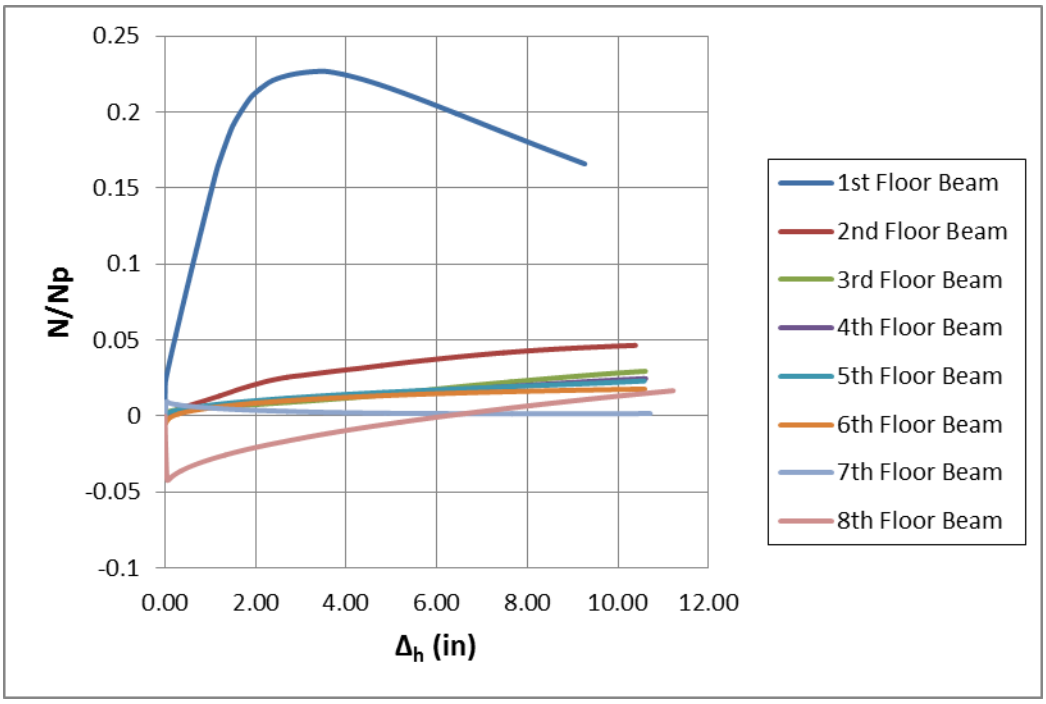

Figure A-13 N/Np vs. Horizontal Displacement (System P1-1)

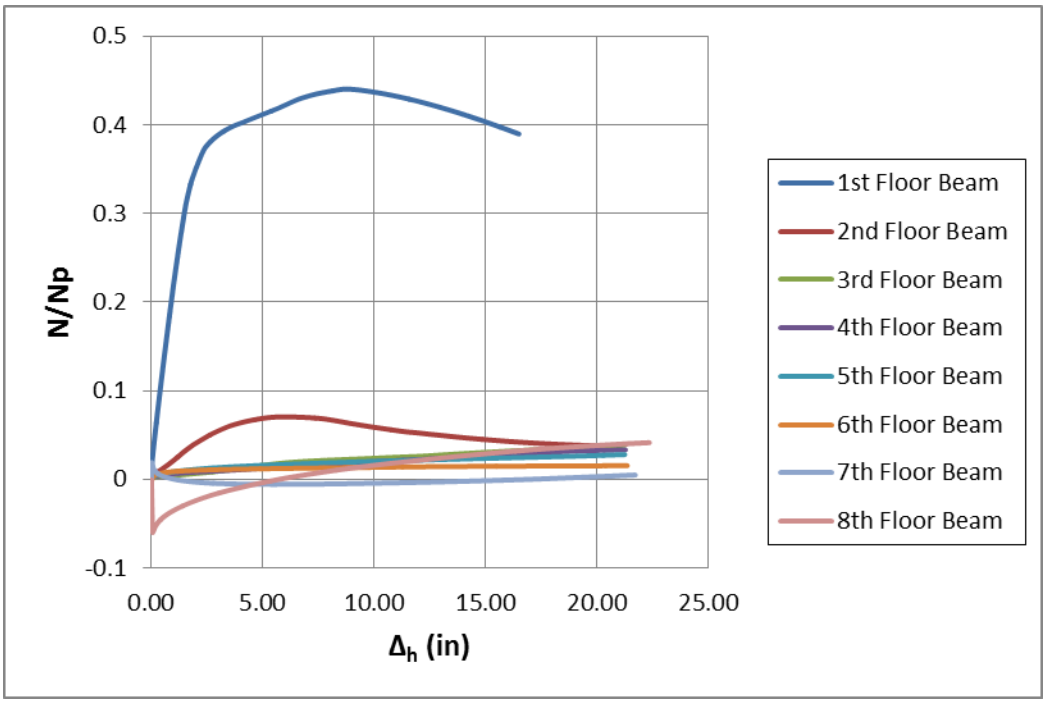

Figure A-14 N/Np vs. Horizontal Displacement (System P1-2)

Appendix B – Supplementary Plots for Systems P2-1 and P2-2

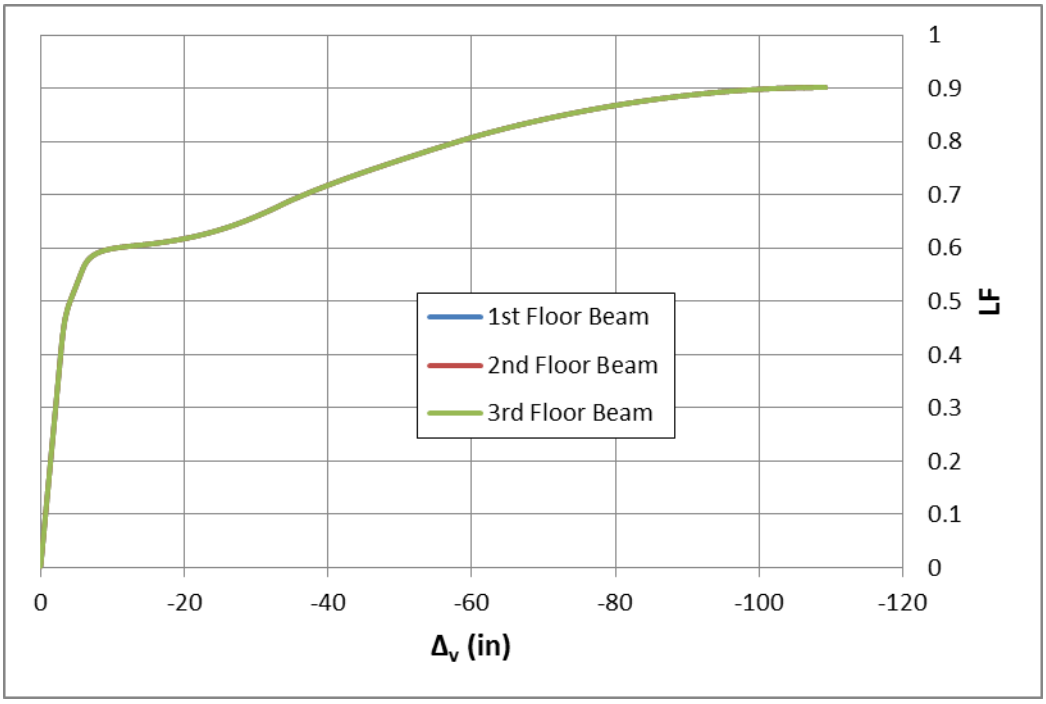

Figure B-1 LF vs. Vertical Deflection (System P2-1)

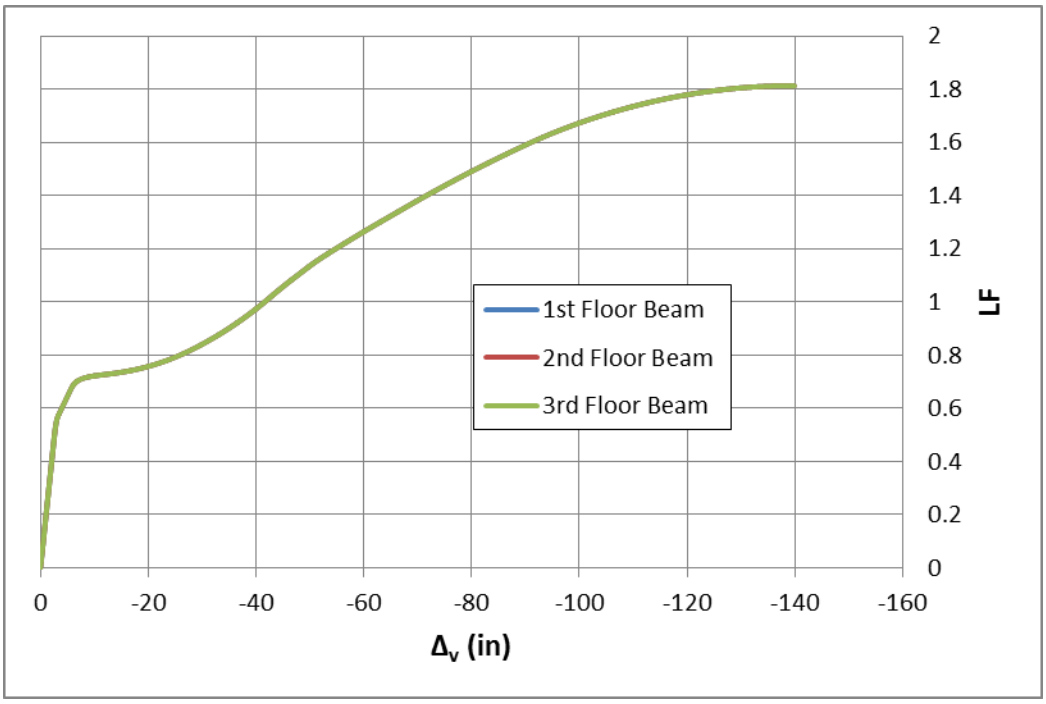

Figure B-2 LF vs. Vertical Deflection (System P2-2)

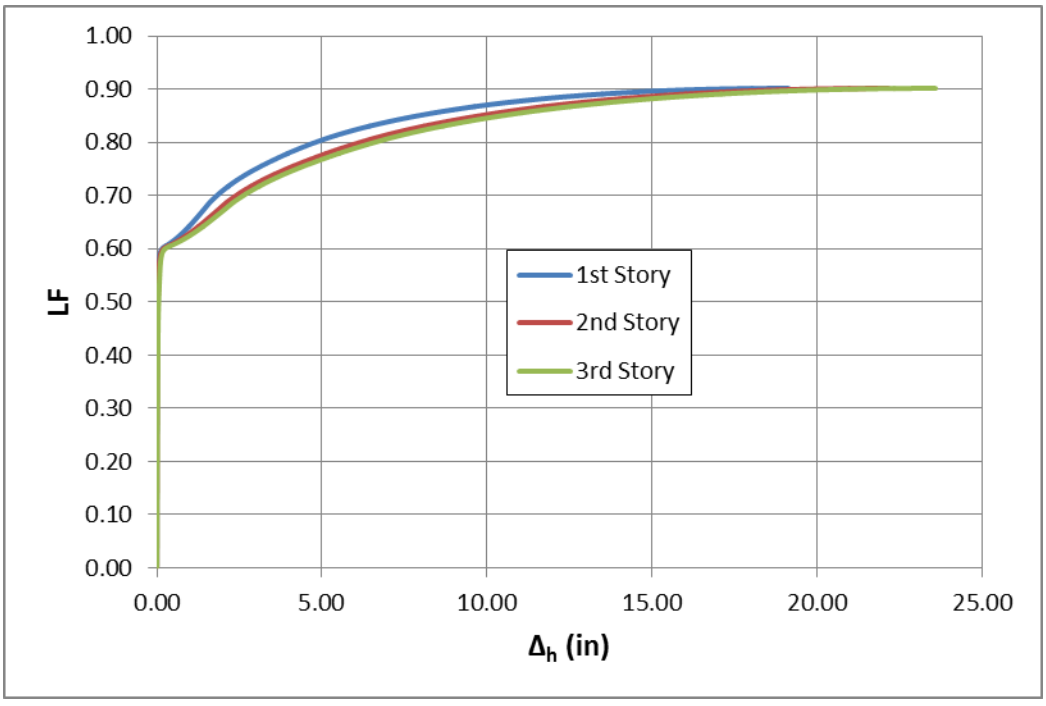

Figure B-3 LF vs. Horizontal Displacement (System P2-1)

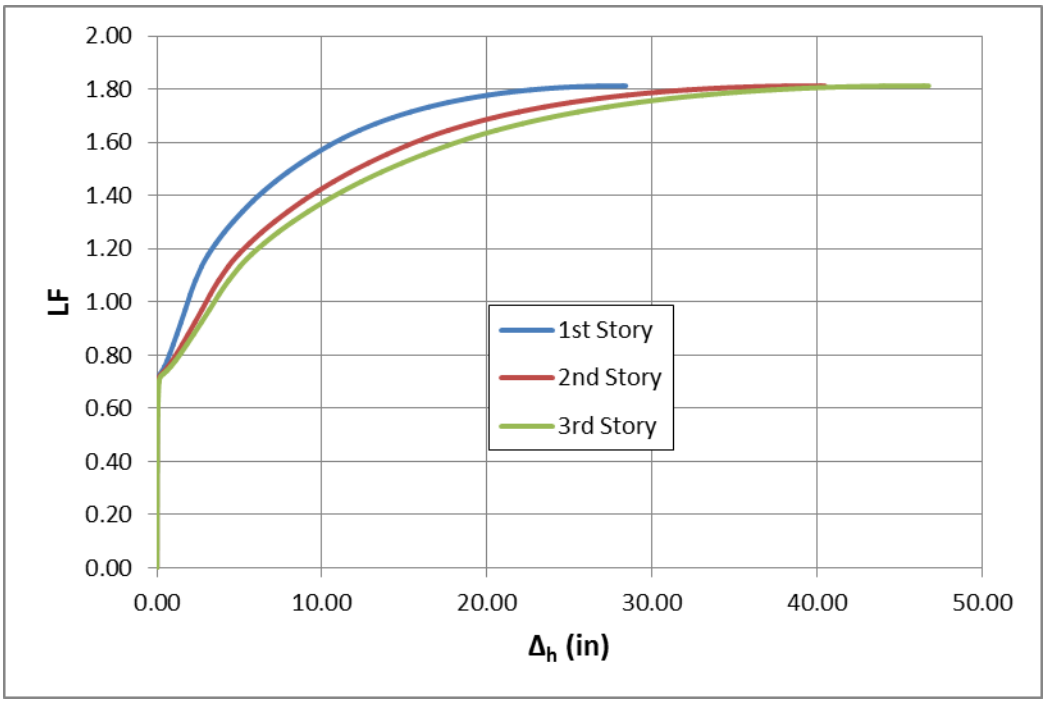

Figure B-4 LF vs. Horizontal Displacement (System P2-2)

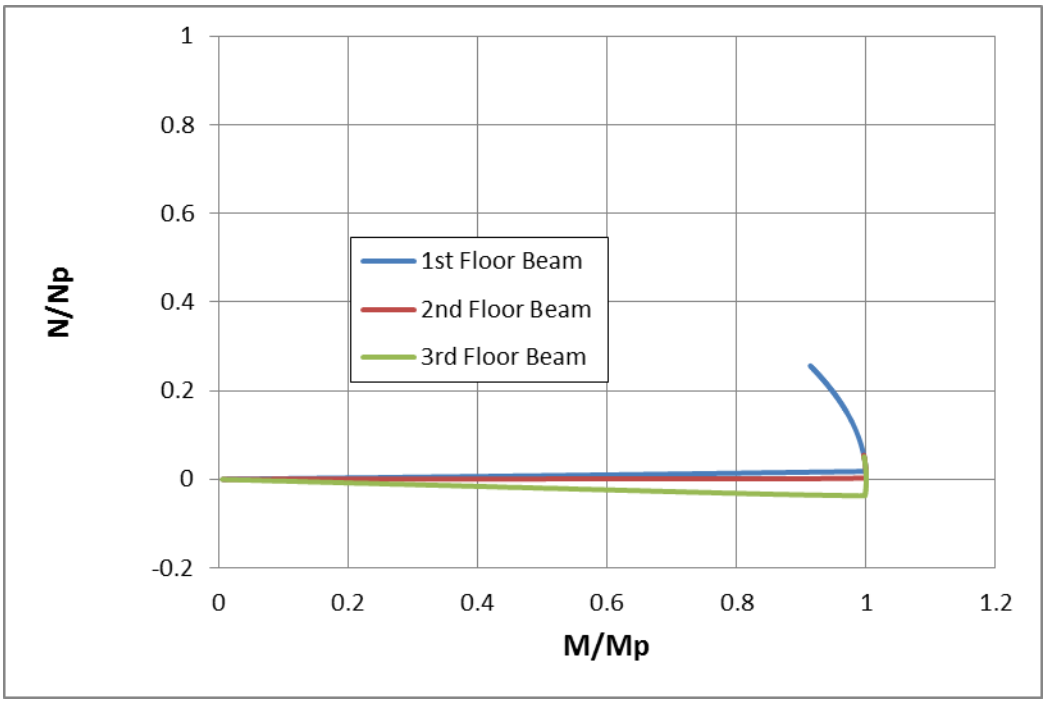

Figure B-5 N/Np vs. M/Mp (System P2-1)

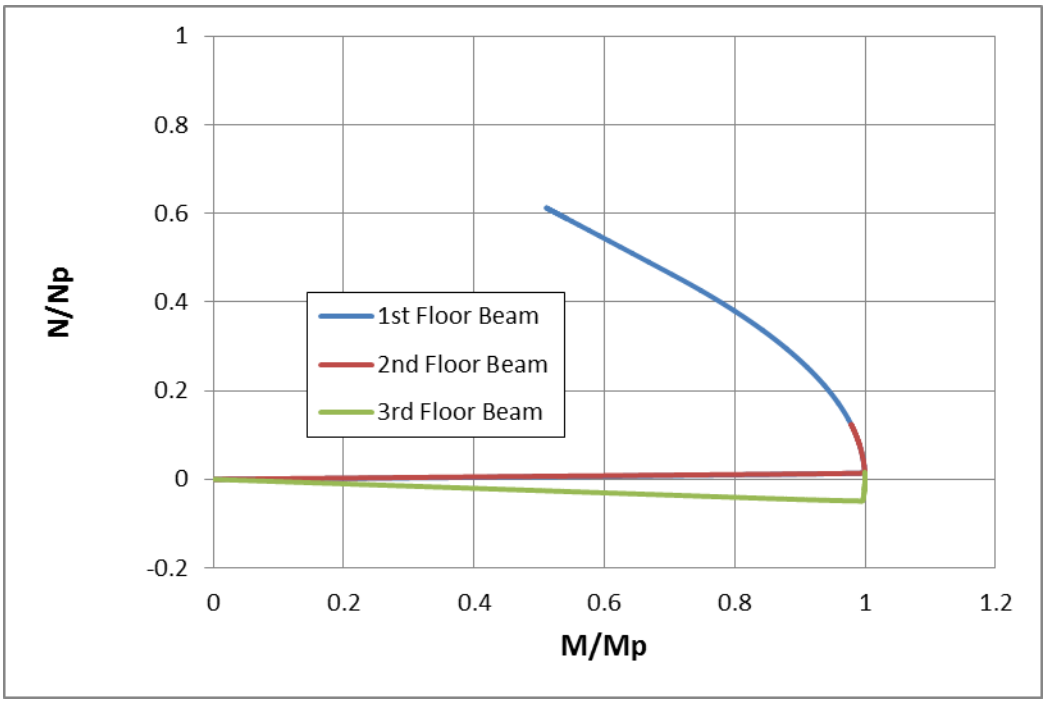

Figure B-6 N/Np vs. M/Mp (System P2-2)

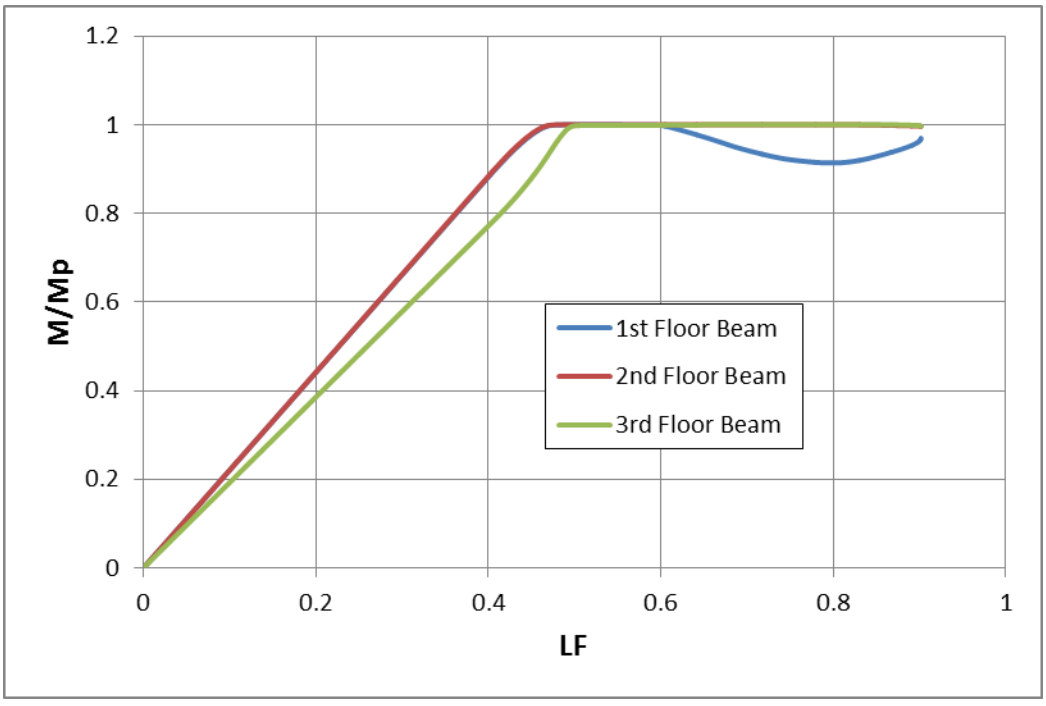

Figure B-7 M/Mp vs. LF (System P2-1)

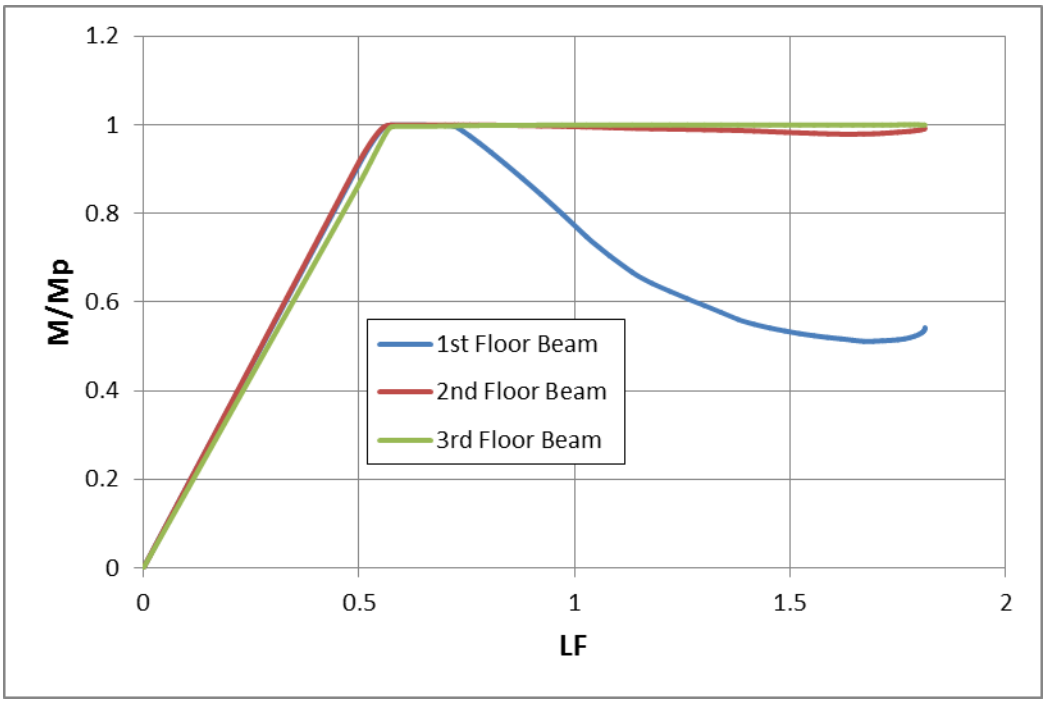

Figure B-8 M/Mp vs. LF (System P2-2)

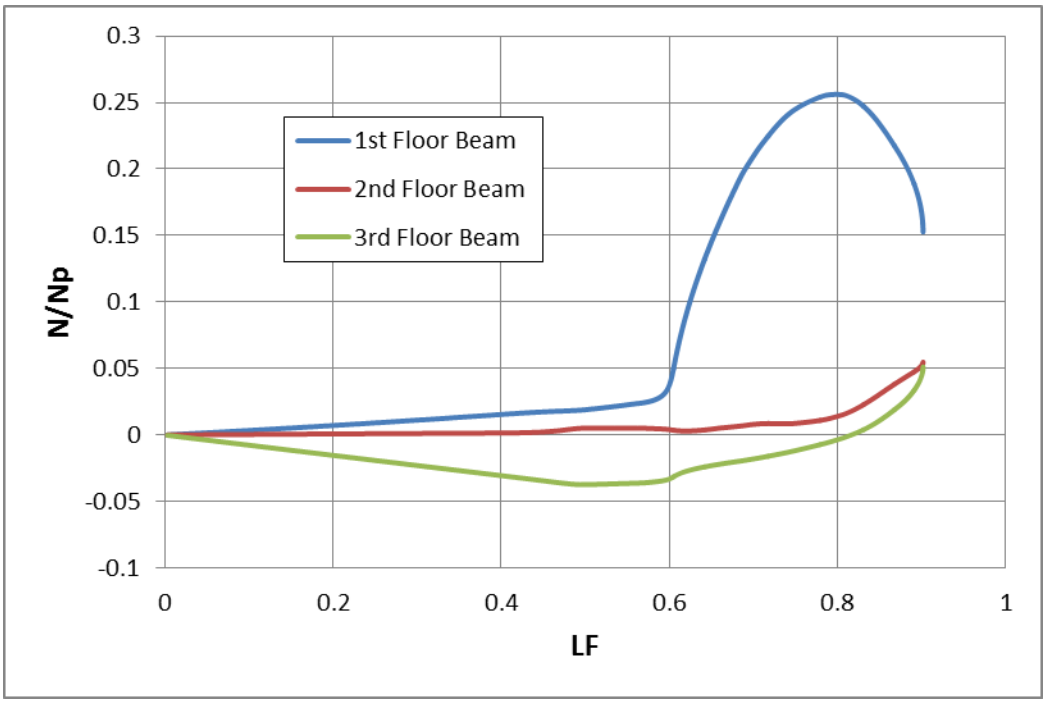

Figure B-9 N/Np vs. LF (System P2-1)

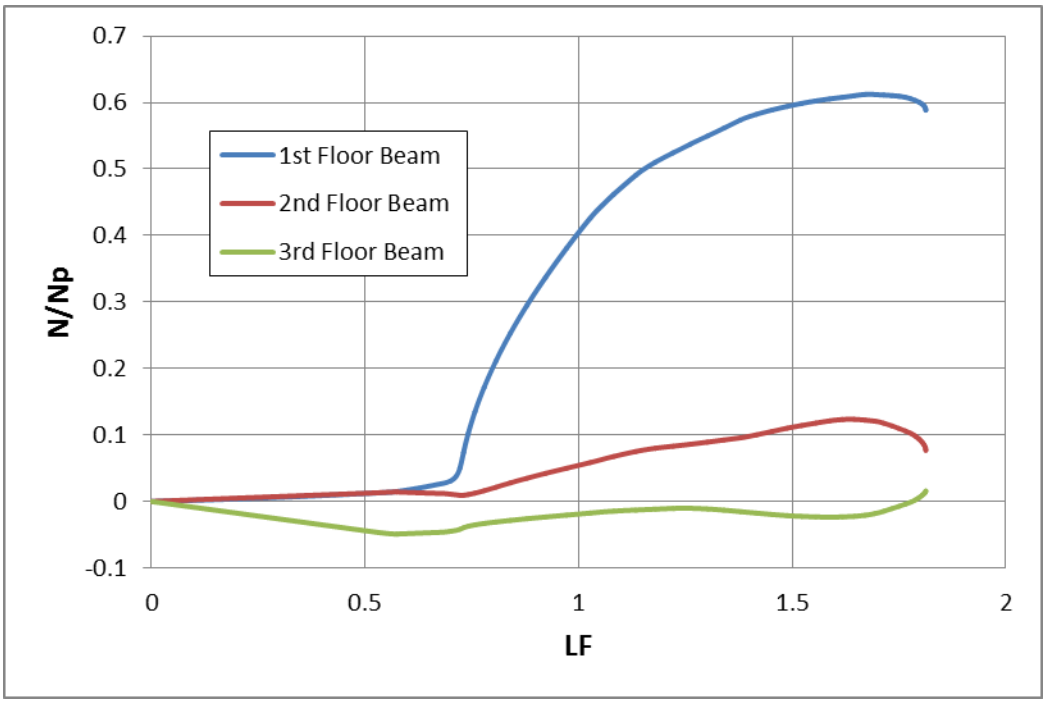

Figure B-10 N/Np vs. LF (System P2-2)

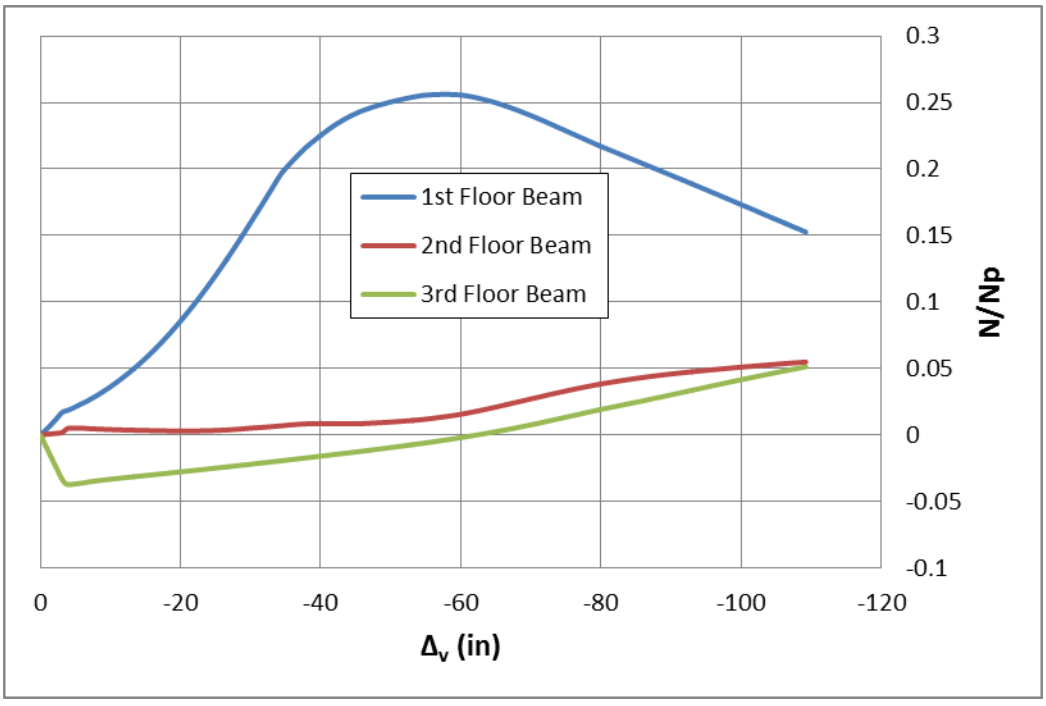

Figure B-11 N/Np vs. Vertical Deflection (System P2-1)

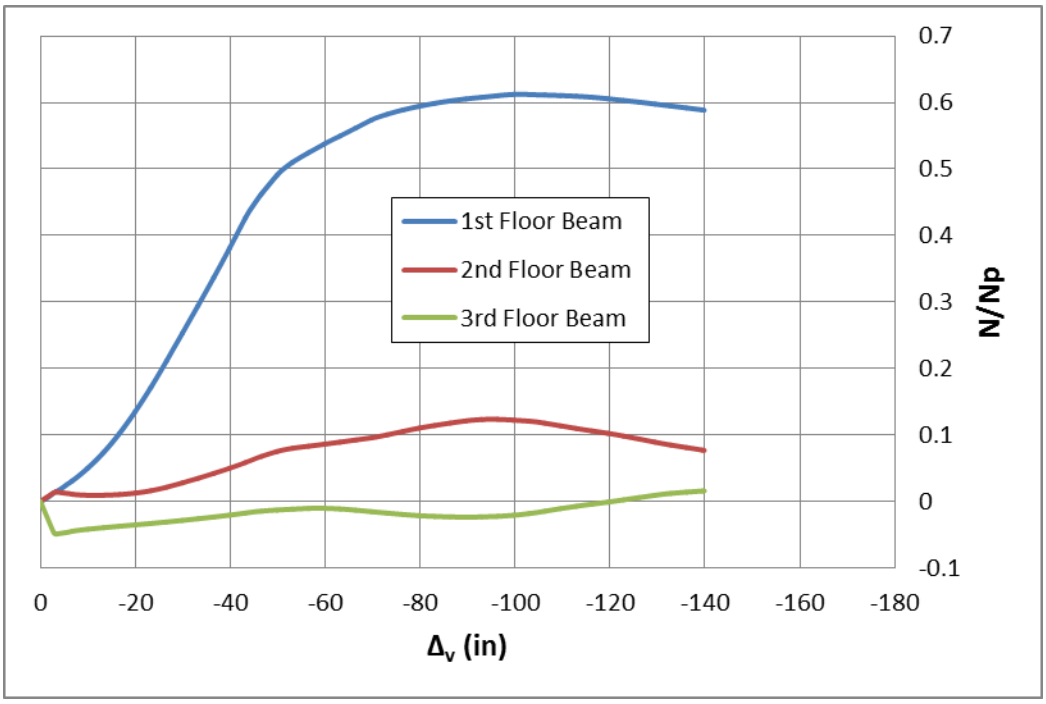

Figure B-12 N/Np vs. Vertical Deflection (System P2-2)

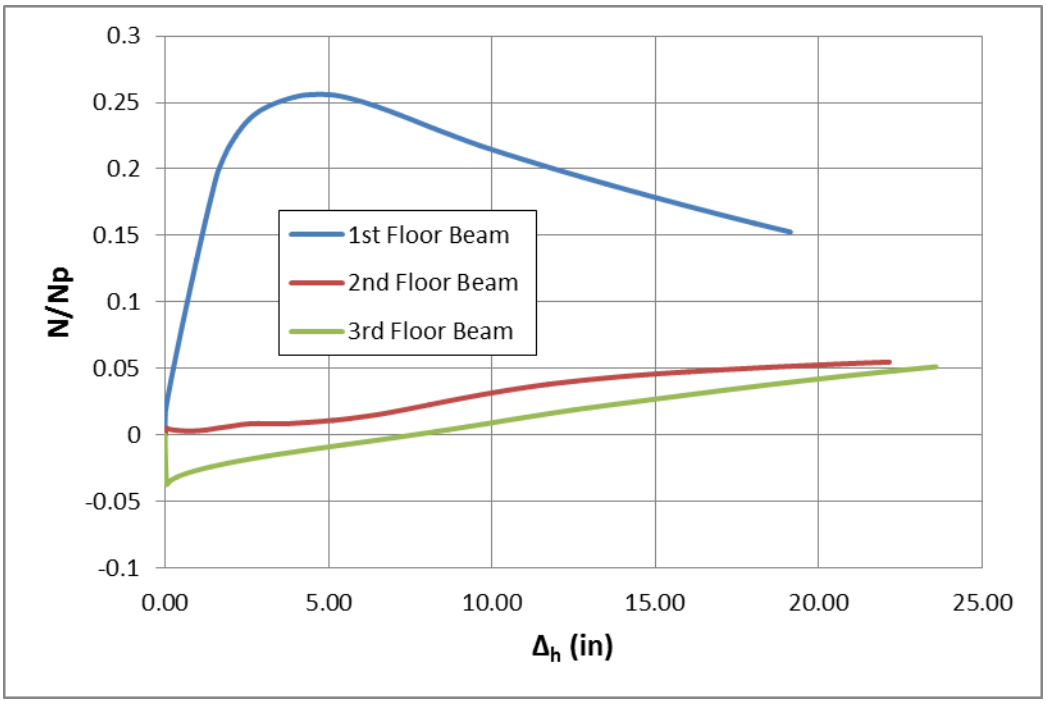

Figure B-13 N/Np vs. Horizontal Displacement (System P2-1)

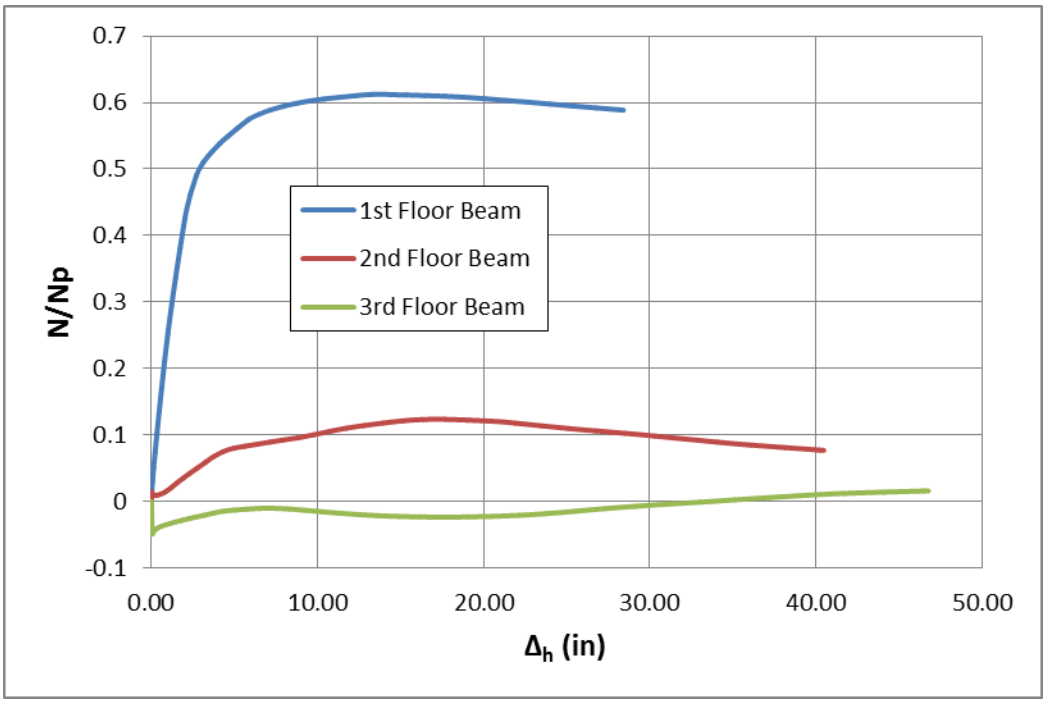

Figure B-14 N/Np vs. Horizontal Displacement (System P2-2)

Appendix C – Supplementary Plots for Systems P3-1 and P3-2

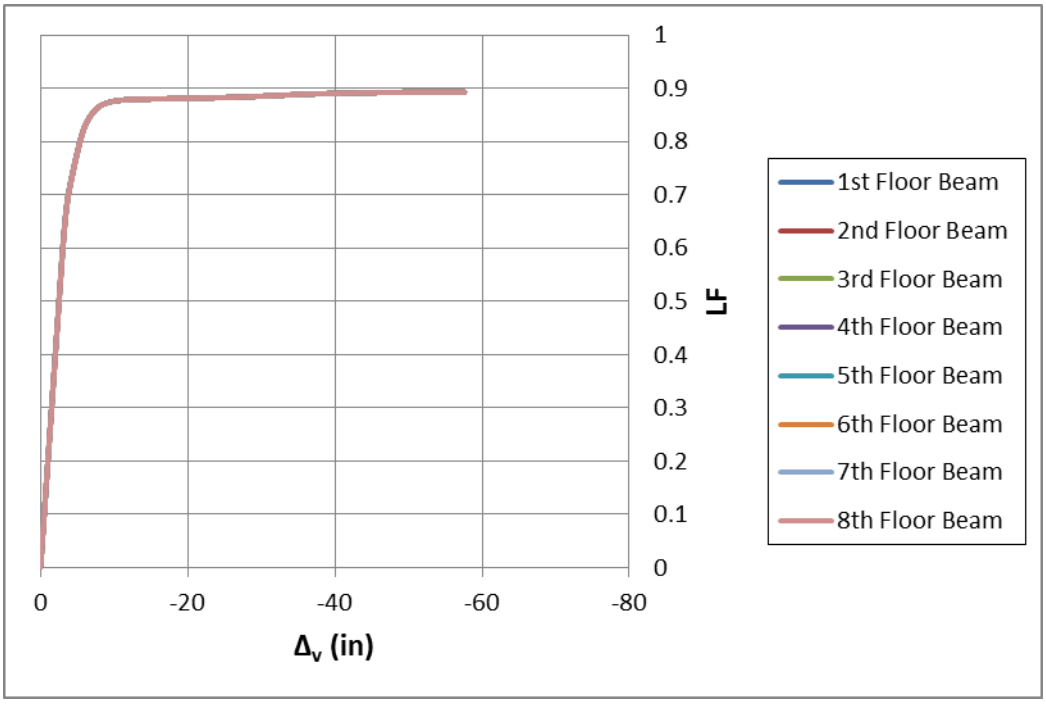

Figure C-1 LF vs. Vertical Deflection (System P3-1)

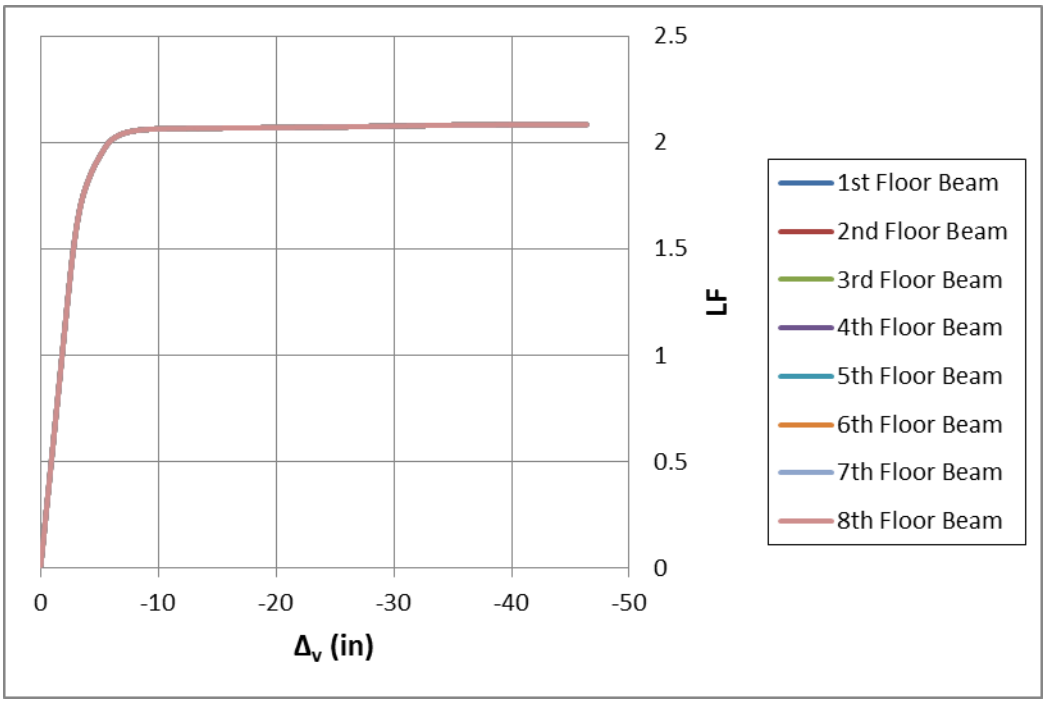

Figure C-2 LF vs. Vertical Deflection (System P3-2)

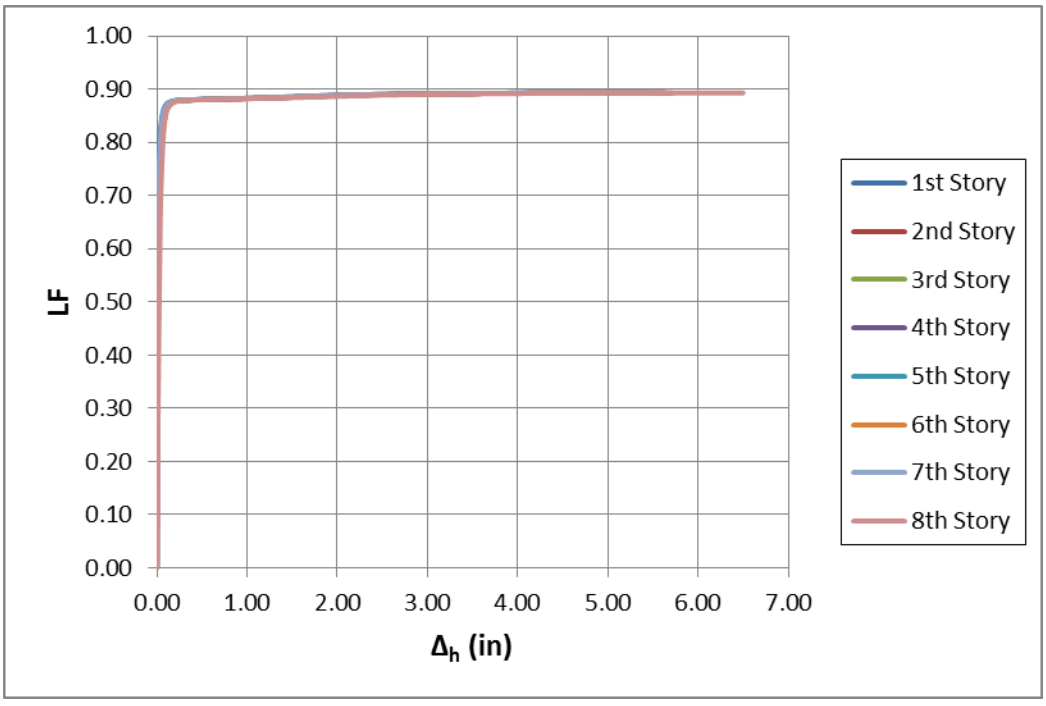

Figure C-3 LF vs. Horizontal Displacement (System P3-1)

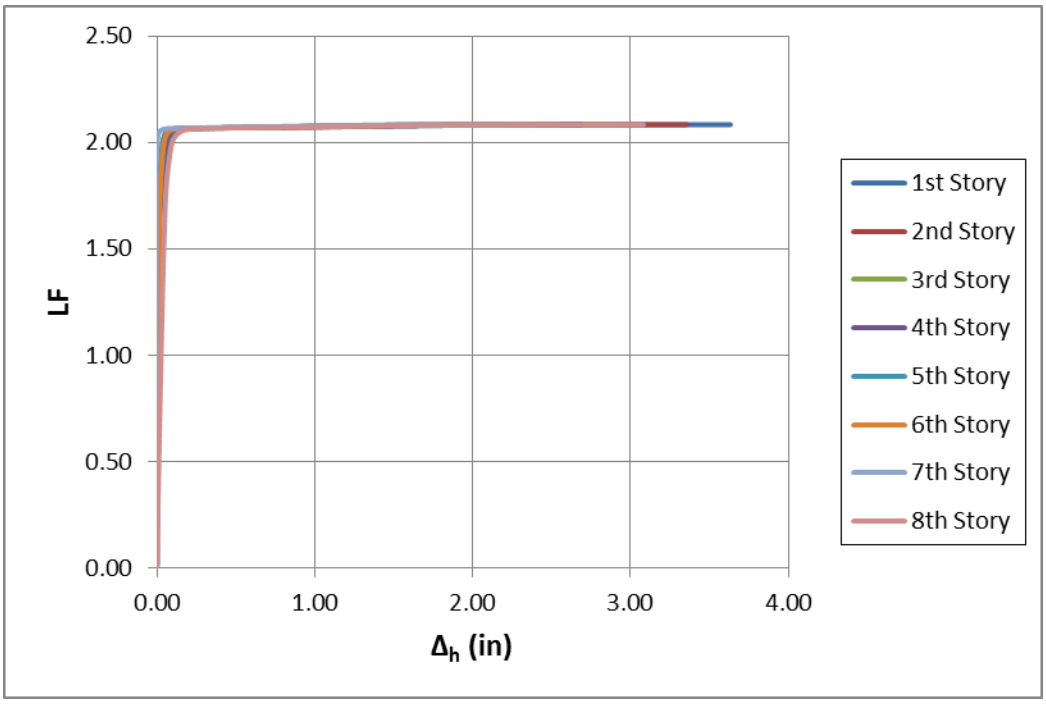

Figure C-4 LF vs. Horizontal Displacement (System P3-2)

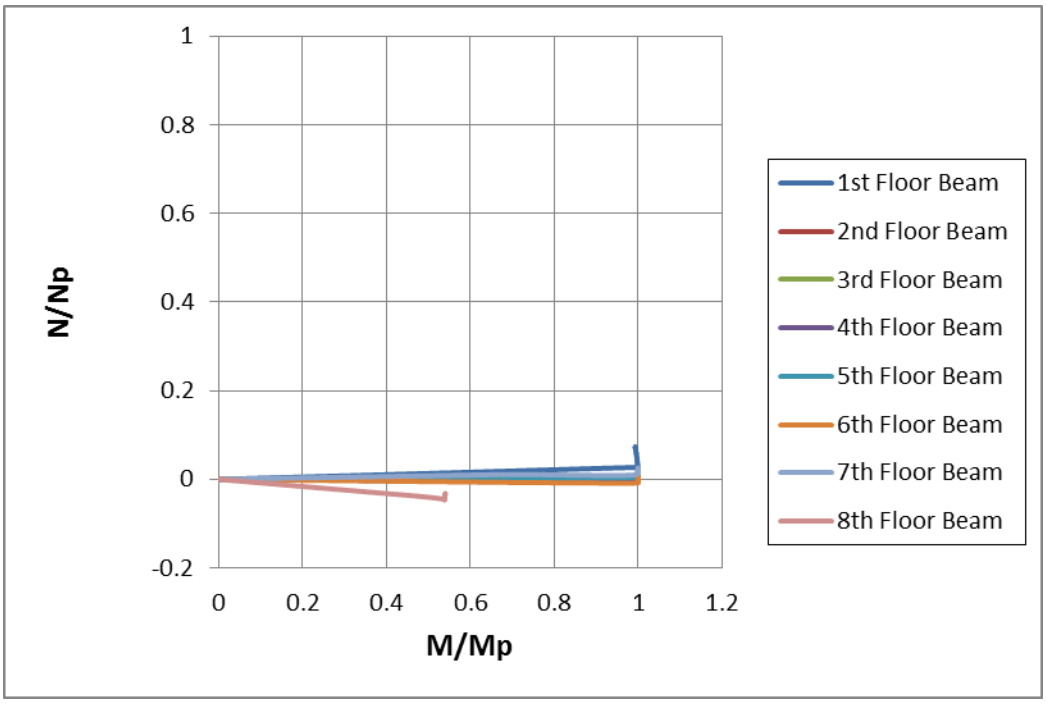

Figure C-5 N/Np vs. M/Mp (System P3-1)

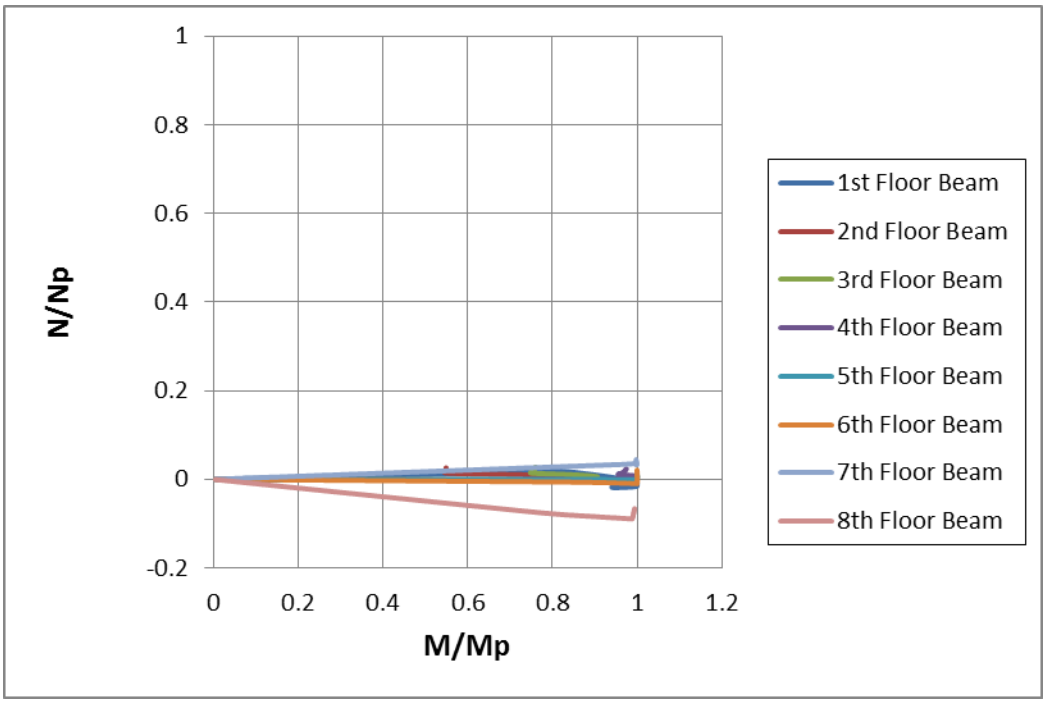

Figure C-6 N/Np vs. M/Mp (System P3-2)

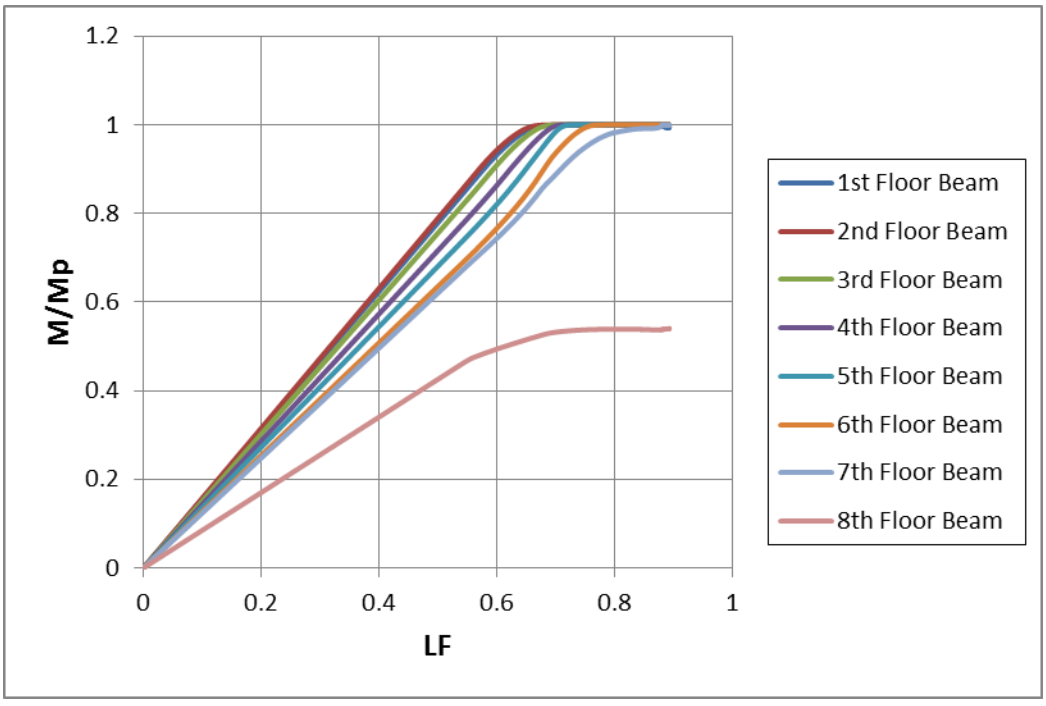

Figure C-7 M/Mp vs. LF (System P3-1)

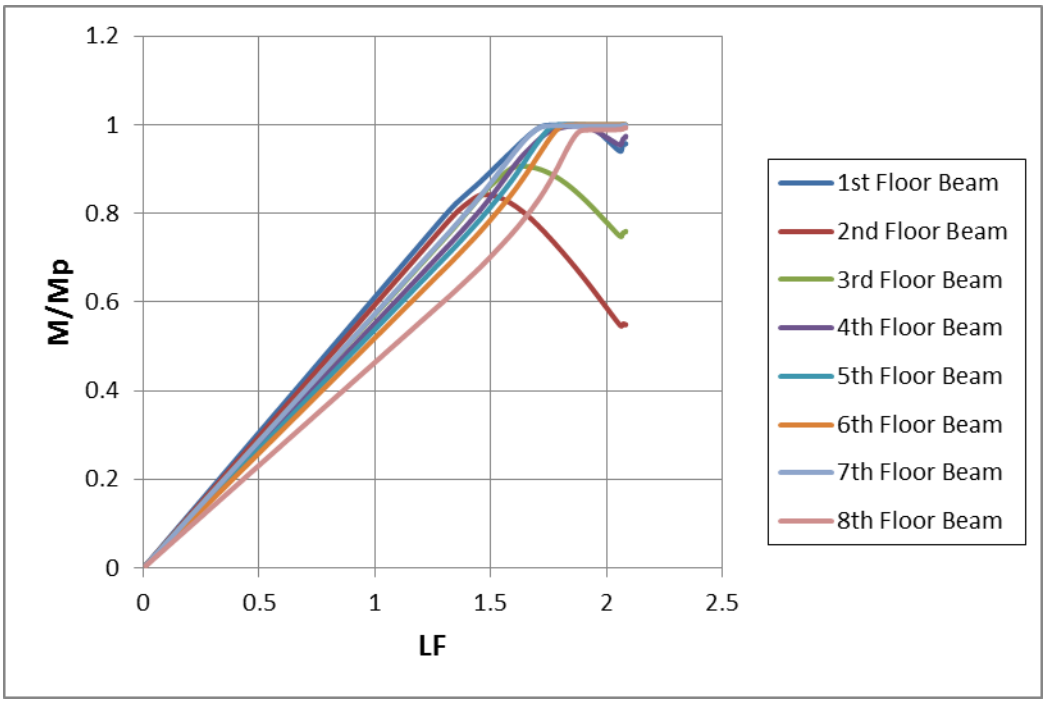

Figure C-8 M/Mp vs. LF (System P3-2)

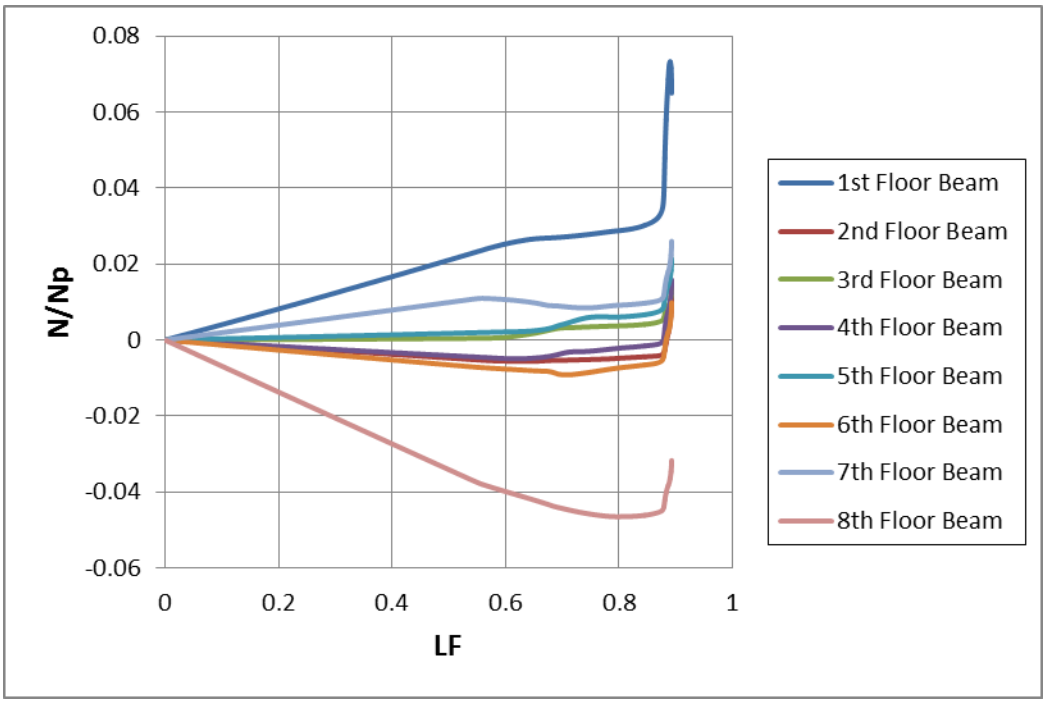

Figure C-9 N/Np vs. LF (System P3-1)

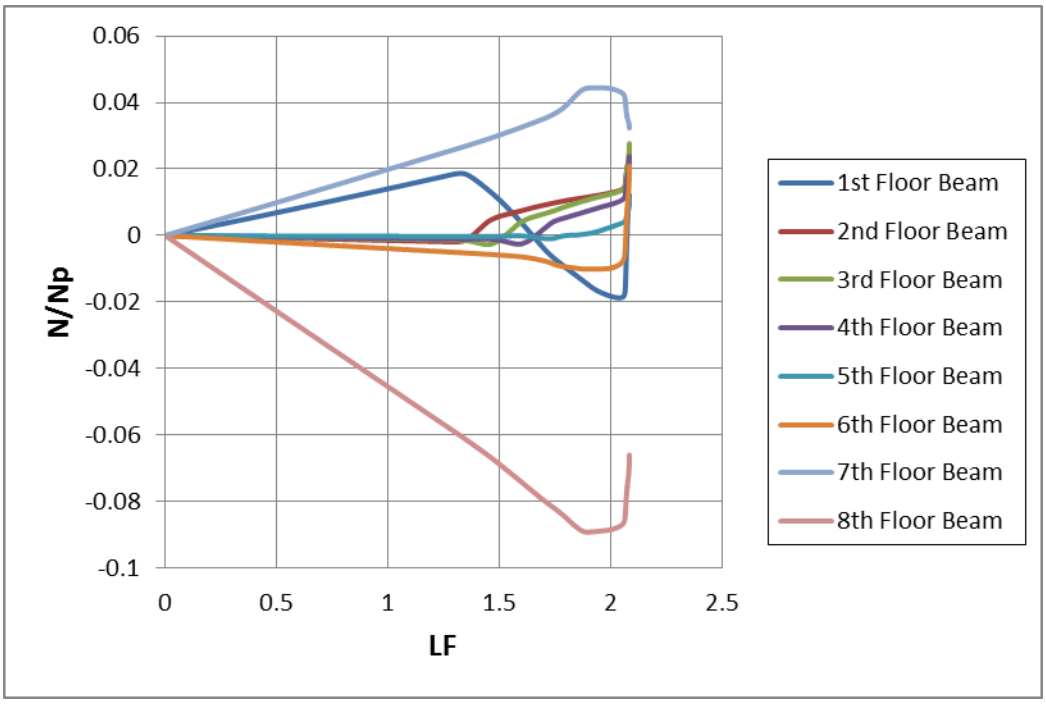

Figure C-10 N/Np vs. LF (System P3-2)

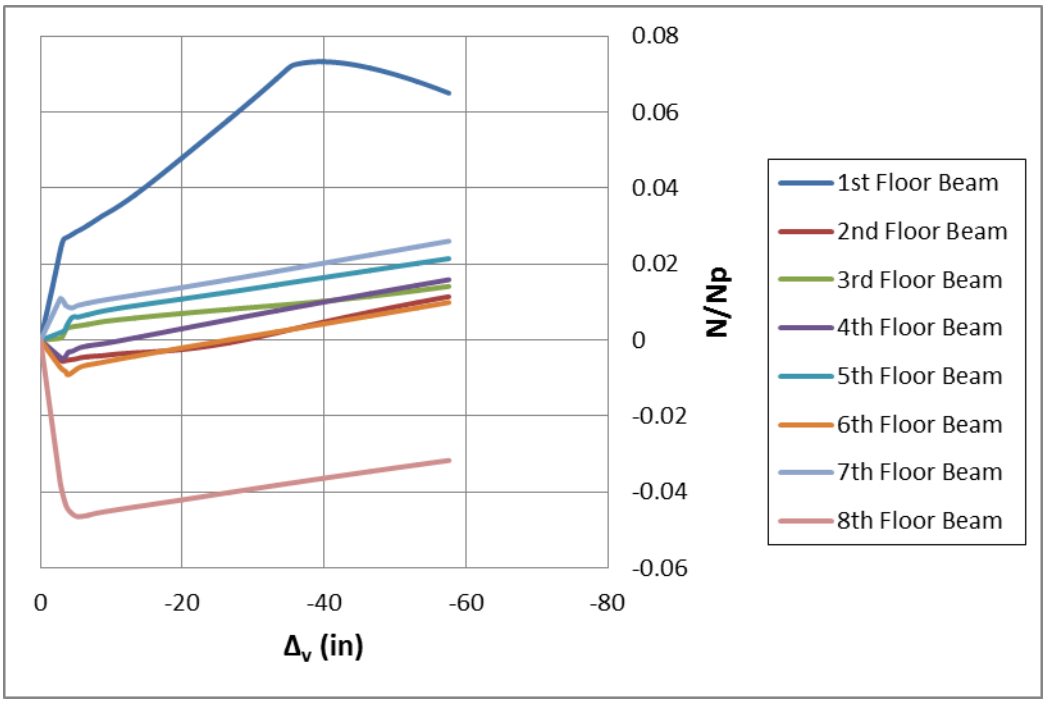

Figure C-11 N/Np vs. Vertical Deflection (System P3-1)

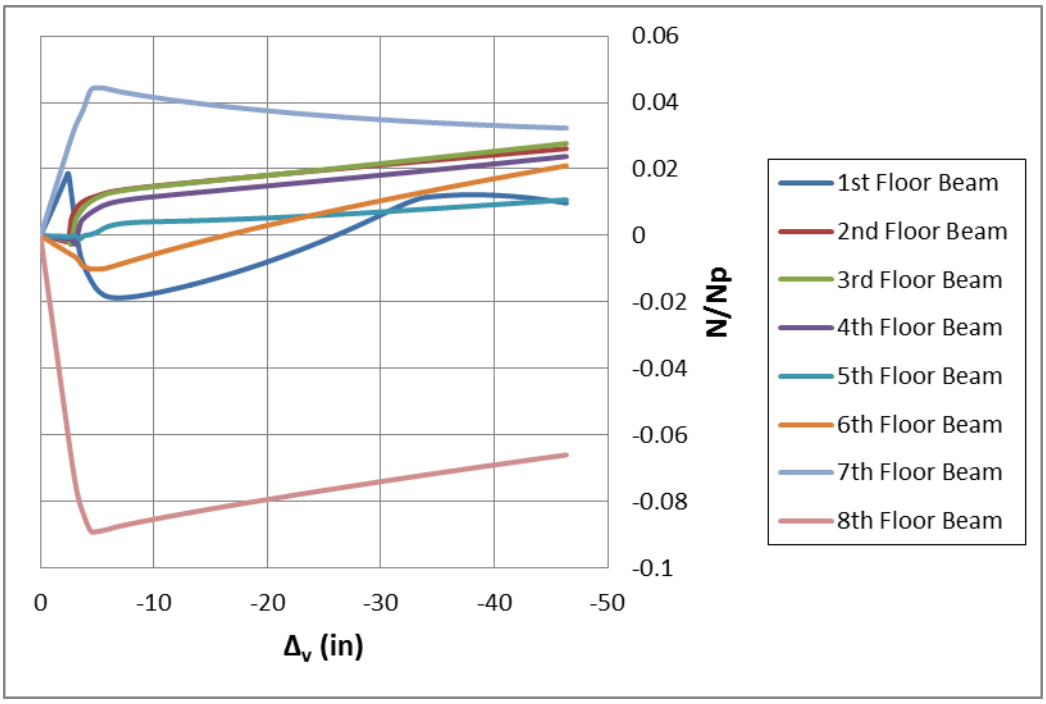

Figure C-12 N/Np vs. Vertical Deflection (System P3-2)

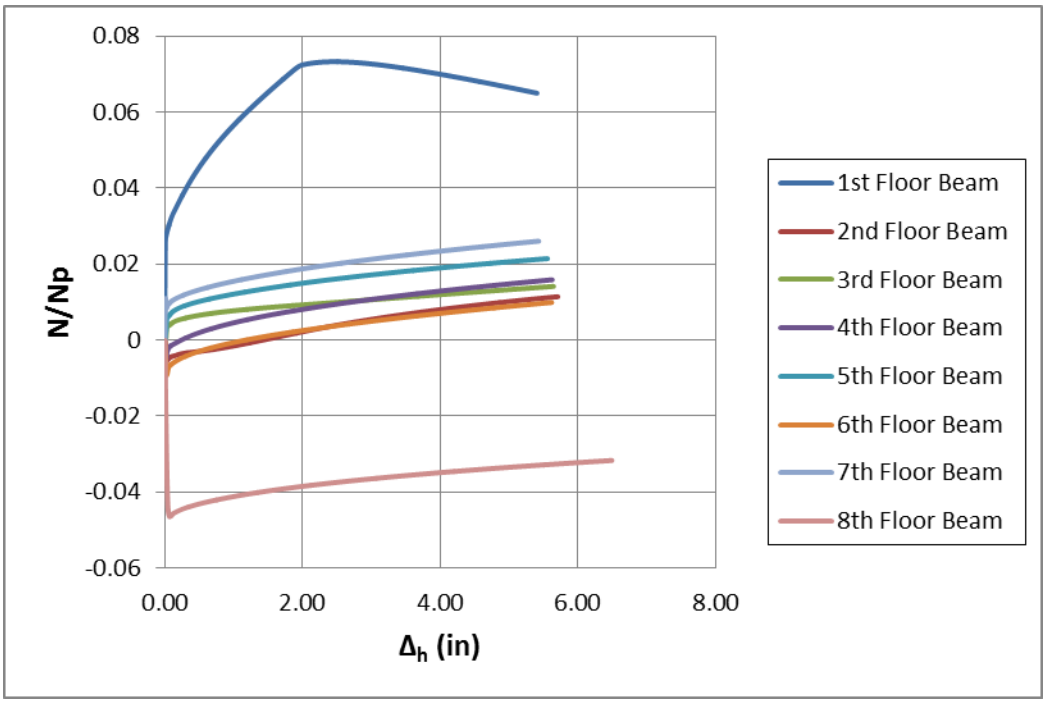

Figure C-13 N/Np vs. Horizontal Displacement (System P3-1)

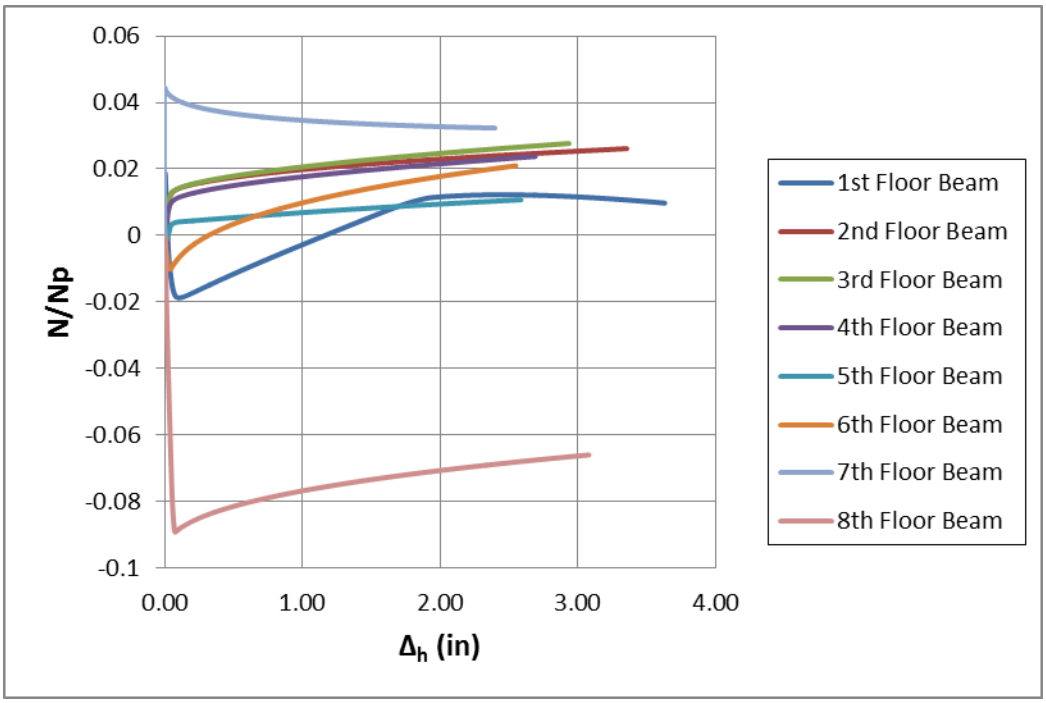

Figure C-15 N/Np vs. Horizontal Displacement (System P3-2)

Appendix D – Supplementary Plots for System P4-1

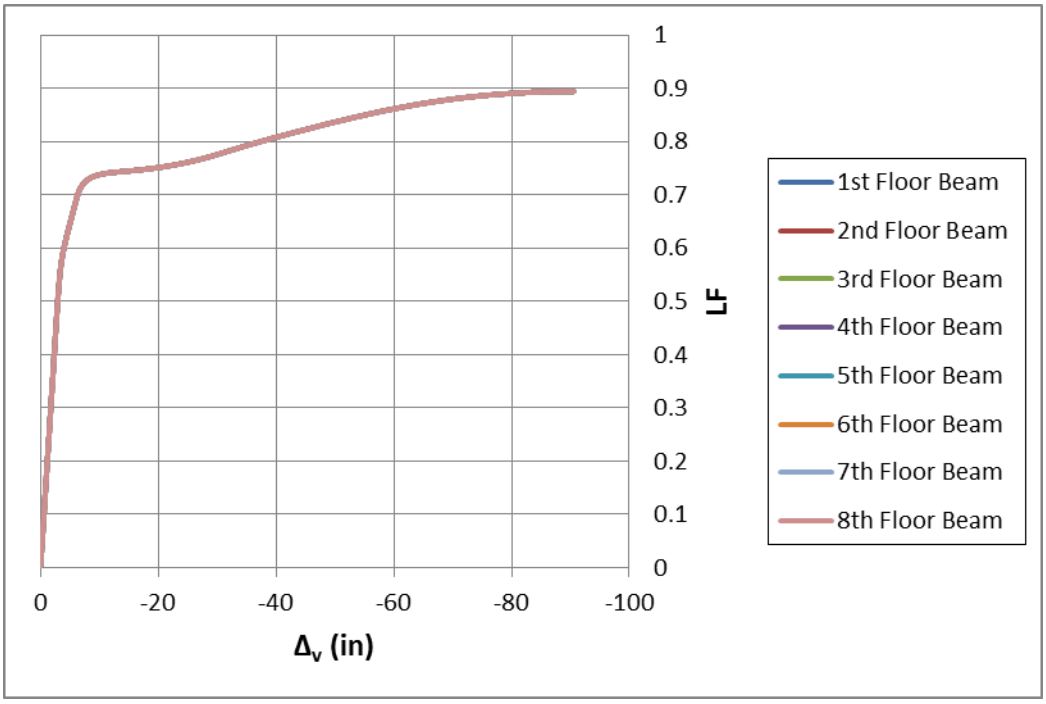

Figure D-1 LF vs. Vertical Deflection (System P4-1)

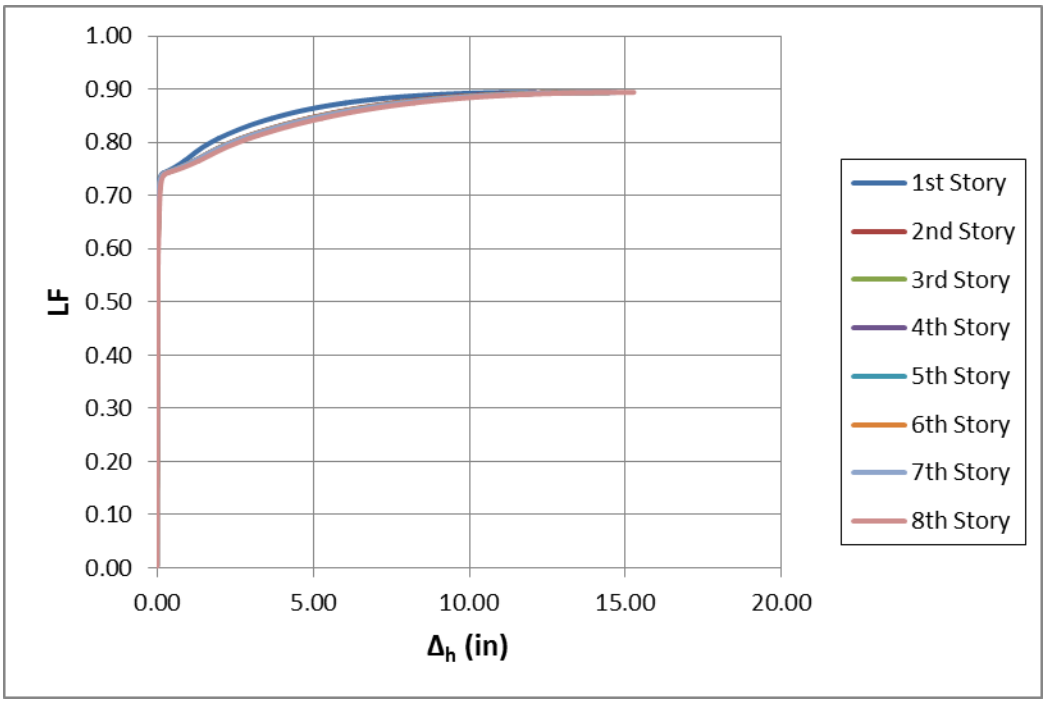

Figure D-2 LF vs. Horizontal Displacement (System P4-1)

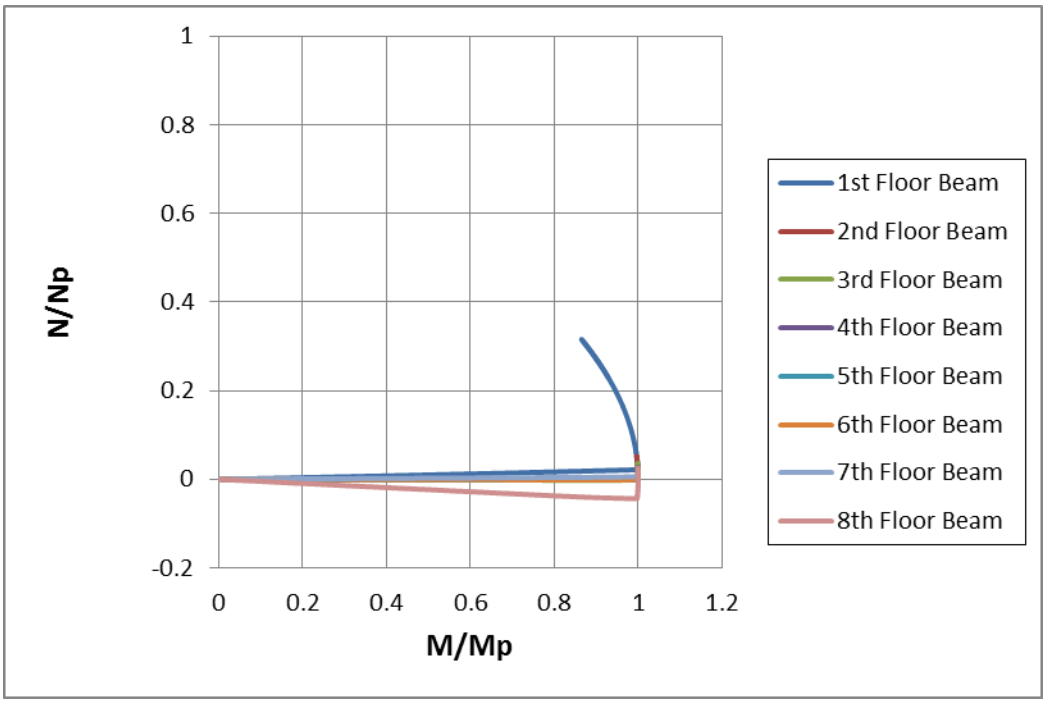

Figure D-3 N/Np vs. M/Mp (System P4-1)

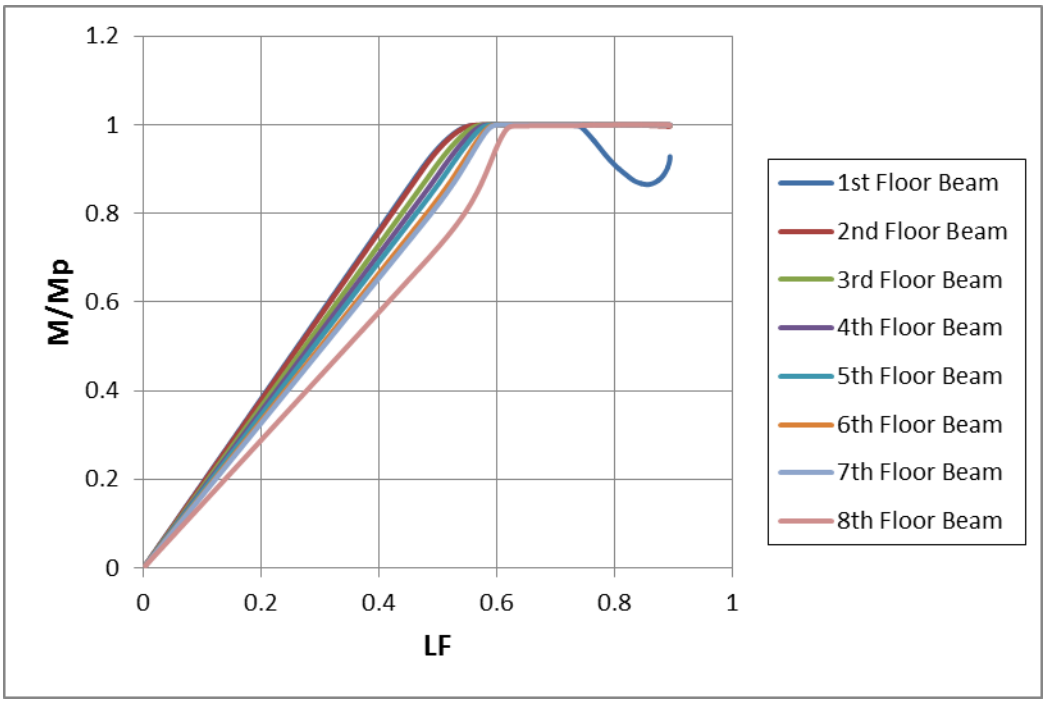

Figure D-4 M/Mp vs. LF (System P4-1)

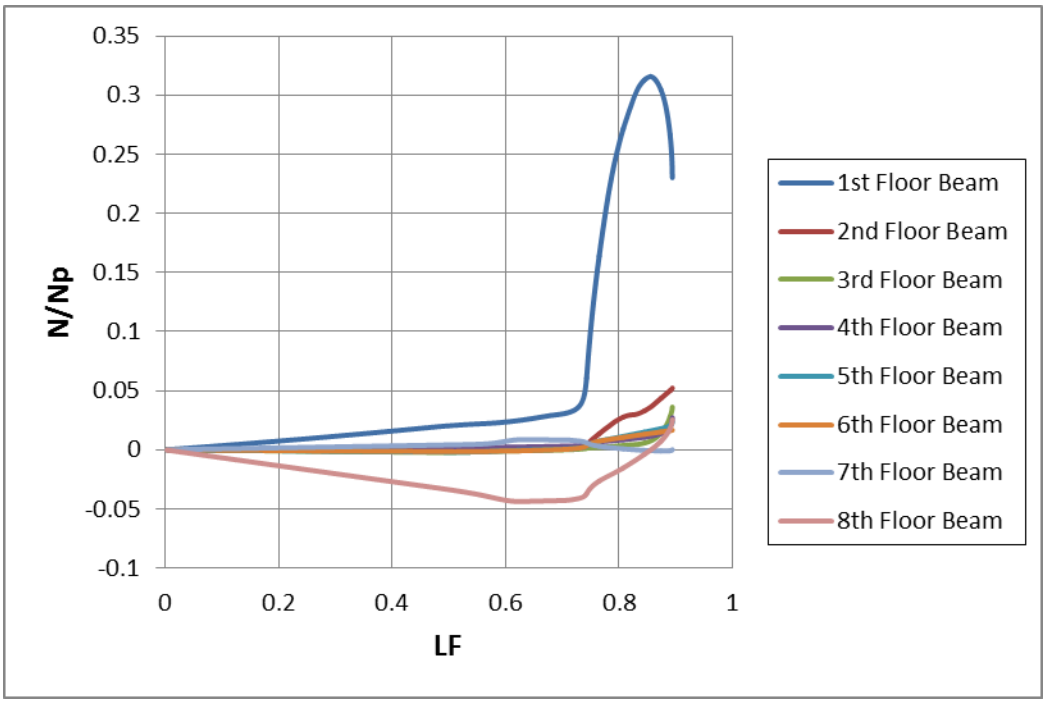

Figure D-5 N/Np vs. LF (System P4-1)

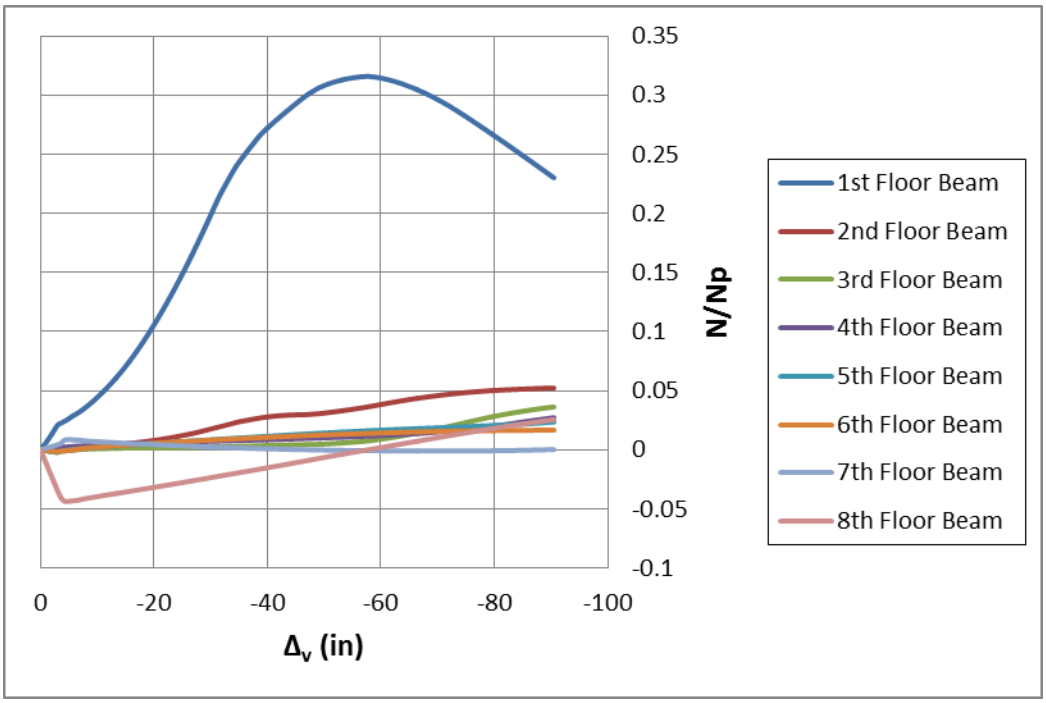

Figure D-6 N/Np vs. Vertical Deflection (System P4-1)

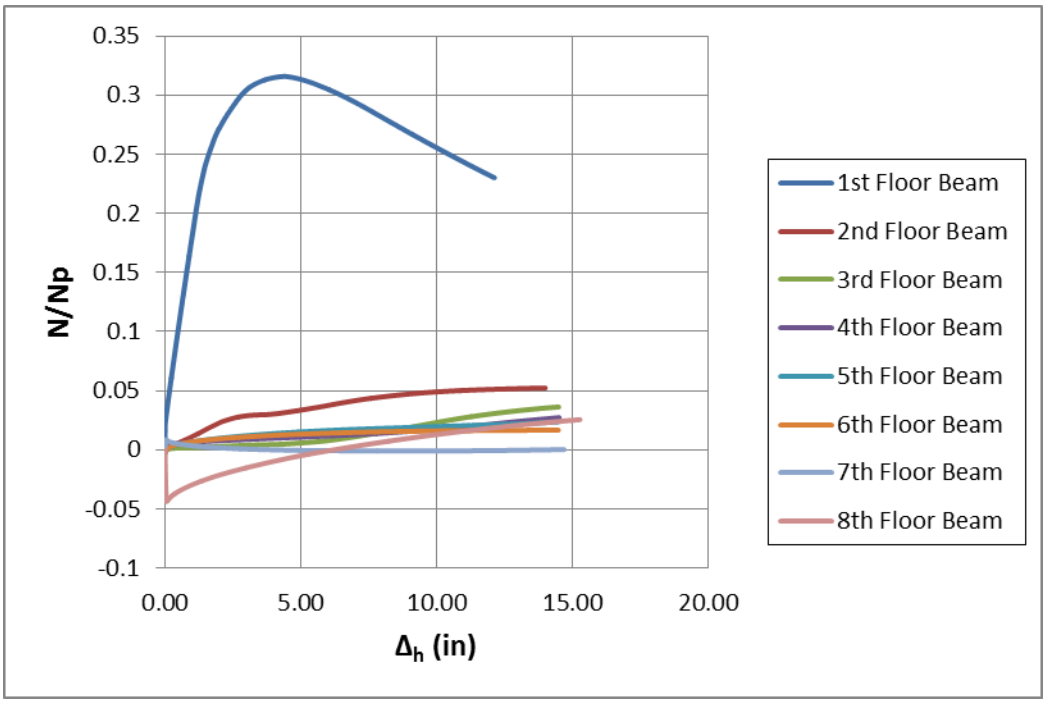

Figure D-7 N/Np vs. Horizontal Displacement (System P4-1)

Appendix E – Typical OpenSees Input File

```
wipe;
model basic -ndm 2 -ndf 3;
file mkdir 3x6_Frame_Atlanta;
node 1 0 0
node 2 0 180
node 3 0 324
node 4 0 468
node 5 288 0
node 6 288 180
node 7 288 324
node 8 288 468
node 9 576 0
for {set i 0} {$i<101} {incr i} {
set nodeTag [expr $i+100]
set xdim [expr $i*2.88+576]
node $nodeTag $xdim 180
}
for {set i 0} {$i<101} {incr i} {
set nodeTag [expr $i+201]
set xdim [expr $i*2.88+576]
node $nodeTag $xdim 324
```

```
}
for {set i 0} {$i<101} {incr i} {
set nodeTag [expr $i+302]
set xdim [expr $i*2.88+576]
node $nodeTag $xdim 468
}
puts "Nodes Defined"
fix 1 1 1 1;
fix 5 1 1 1;
fix 9 1 1 1;
fix 200 1 0 1;
fix 301 1 0 1;
fix 402 1 0 1;
puts "BC's Defined”
#--------Defining Geometric Transformations-------#
geomTransf Corotational 1;
geomTransf PDelta 2;
puts "Transformations Defined"
#--------Defining Material for Fiber Sections-------#
uniaxialMaterial ElasticPP 1 29000 .001724;
uniaxialMaterial Elastic 2 29000;
puts "Materials Defined"
#--------Defining Plastic Beam-------#
```

```
#Section--W16X26#
set d 15.7;
set tw .250;
set bf 5.50;
set tf .345;
set nfdw 3002;
set nftw 1;
set nfbf 1;
set nftf 69;
set dw [expr $d-2*$tf]
set y1 [expr -$d/2]
set y2 [expr -$dw/2]
set y3 [expr  $dw/2]
set y4 [expr  $d/2]
set z1 [expr -$bf/2]
set z2 [expr -$tw/2]
set z3 [expr  $tw/2]
set z4 [expr  $bf/2]
#
section fiberSec 1 {
    #             nfIJ  nfJK    yI  zI    yJ  zJ    yK  zK    yL  zL
    patch quadr  1 $nfbf $nftf   $y1 $z4   $y1 $z1   $y2 $z1   $y2 $z4
```

```
    patch quadr  1 $nftw $nfdw   $y2 $z3   $y2 $z2   $y3 $z2   $y3 $z3
    patch quadr  1 $nfbf $nftf   $y3 $z4   $y3 $z1   $y4 $z1   $y4 $z4
  }
puts "Plastic Beam Section Defined"
#--------Defining Columns-------#
#Section--W14x30#
set d 13.8;
set tw .270;
set bf 6.73;
set tf .385;
set nfdw 2606;
set nftw 1;
set nfbf 1;
set nftf 77;
set dw [expr $d-2*$tf]
set y1 [expr -$d/2]
set y2 [expr -$dw/2]
set y3 [expr  $dw/2]
set y4 [expr  $d/2]
set z1 [expr -$bf/2]
set z2 [expr -$tw/2]
set z3 [expr  $tw/2]
set z4 [expr  $bf/2]
```

```
#
section fiberSec 2 {
    #            nfIJ  nfJK    yI  zI    yJ  zJ    yK  zK    yL  zL
    patch quadr  1 $nfbf $nftf   $y1 $z4   $y1 $z1   $y2 $z1   $y2 $z4
    patch quadr  1 $nftw $nfdw   $y2 $z3   $y2 $z2   $y3 $z2   $y3 $z3
    patch quadr  1 $nfbf $nftf   $y3 $z4   $y3 $z1   $y4 $z1   $y4 $z4
  }
#Section--W14x43#
set d 13.7;
set tw .305;
set bf 8.0;
set tf .530;
set nfdw 2528;
set nftw 1;
set nfbf 1;
set nftf 106;
set dw [expr $d-2*$tf]
set y1 [expr -$d/2]
set y2 [expr -$dw/2]
set y3 [expr  $dw/2]
set y4 [expr  $d/2]
set z1 [expr -$bf/2]
set z2 [expr -$tw/2]
```

```
set z3 [expr  $tw/2]
set z4 [expr  $bf/2]
#
section fiberSec 3 {
    #            nfIJ  nfJK    yI  zI    yJ  zJ    yK  zK    yL  zL
    patch quadr  1 $nfbf $nftf   $y1 $z4   $y1 $z1   $y2 $z1   $y2 $z4
    patch quadr  1 $nftw $nfdw   $y2 $z3   $y2 $z2   $y3 $z2   $y3 $z3
    patch quadr  1 $nfbf $nftf   $y3 $z4   $y3 $z1   $y4 $z1   $y4 $z4
  }
#Section--W14x26#
set d 13.9;
set tw .230;
set bf 5.0;
set tf .335;
set nfdw 2646;
set nftw 1;
set nfbf 1;
set nftf 67;
set dw [expr $d-2*$tf]
set y1 [expr -$d/2]
set y2 [expr -$dw/2]
set y3 [expr  $dw/2]
set y4 [expr  $d/2]
```

```
set z1 [expr -$bf/2]
set z2 [expr -$tw/2]
set z3 [expr  $tw/2]
set z4 [expr  $bf/2]
#
section fiberSec 4 {
    #             nfIJ  nfJK    yI  zI    yJ  zJ    yK  zK    yL  zL
    patch quadr  1 $nfbf $nftf   $y1 $z4   $y1 $z1   $y2 $z1   $y2 $z4
    patch quadr  1 $nftw $nfdw   $y2 $z3   $y2 $z2   $y3 $z2   $y3 $z3
    patch quadr  1 $nfbf $nftf   $y3 $z4   $y3 $z1   $y4 $z1   $y4 $z4
  }
puts "Column Sections Defined"
#-------Defining Element Tags---------------#
for {set k 0} {$k<100} {incr k} {
set eltag [expr $k+100]
set inode [expr $k+100]
set jnode [expr $k+101]
element nonlinearBeamColumn $eltag $inode $jnode 3 1 1
}
for {set k 0} {$k<100} {incr k} {
set eltag [expr $k+200]
set inode [expr $k+201]
set jnode [expr $k+202]
```

```
element nonlinearBeamColumn $eltag $inode $jnode 3 1 1
}
for {set k 0} {$k<100} {incr k} {
set eltag [expr $k+300]
set inode [expr $k+302]
set jnode [expr $k+303]
element nonlinearBeamColumn $eltag $inode $jnode 3 1 1
}
puts "Catenary Beam Elements Created"
element nonlinearBeamColumn 1 1 2 3 2 1;
element nonlinearBeamColumn 2 5 6 3 3 1;
element nonlinearBeamColumn 3 9 100 3 3 1;
element nonlinearBeamColumn 4 2 3 3 4 1;
element nonlinearBeamColumn 5 6 7 3 2 1;
element nonlinearBeamColumn 6 100 201 3 2 1;
element nonlinearBeamColumn 7 200 301 3 2 1;
element nonlinearBeamColumn 8 3 4 3 4 1;
element nonlinearBeamColumn 9 7 8 3 4 1;
element nonlinearBeamColumn 10 201 302 3 4 1;
element nonlinearBeamColumn 11 301 402 3 4 1;
puts "Column Elements Created"
element nonlinearBeamColumn 12 2 6 3 1 2;
element nonlinearBeamColumn 13 6 100 3 1 2;
```

```
element nonlinearBeamColumn 14 3 7 3 1 2;
element nonlinearBeamColumn 15 7 201 3 1 2;
element nonlinearBeamColumn 16 4 8 3 1 2;
element nonlinearBeamColumn 17 8 302 3 1 2;
puts "Side Beam Elements Created"
recorder Node -file 3x6_Frame_Atlanta/NodeVDisp200.out -time -node 200 -dof 2 disp;
recorder Node -file 3x6_Frame_Atlanta/NodeVDisp301.out -time -node 301 -dof 2 disp;
recorder Node -file 3x6_Frame_Atlanta/NodeVDisp402.out -time -node 402 -dof 2 disp;
recorder Node -file 3x6_Frame_Atlanta/NodeHVRDisp100.out -time -node 100 -dof 1 2
3 disp;
recorder Node -file 3x6_Frame_Atlanta/NodeHVRDisp201.out -time -node 201 -dof 1 2
3 disp;
recorder Node -file 3x6_Frame_Atlanta/NodeHVRDisp302.out -time -node 302 -dof 1 2
3 disp;
recorder Element -file 3x6_Frame_Atlanta/ForceE100.out -time -ele 100 globalForce;
recorder Element -file 3x6_Frame_Atlanta/ForceE200.out -time -ele 200 globalForce;
recorder Element -file 3x6_Frame_Atlanta/ForceE300.out -time -ele 300 globalForce;
recorder Element -file 3x6_Frame_Atlanta/SForceE100.out -time -ele 100 section 1
force;
recorder Element -file 3x6_Frame_Atlanta/SForceE200.out -time -ele 200 section 1
force;
recorder Element -file 3x6_Frame_Atlanta/SForceE300.out -time -ele 300 section 1
force;
```

```
recorder Element -file 3x6_Frame_Atlanta/ForceE1.out -time -ele 1 globalForce;
recorder Element -file 3x6_Frame_Atlanta/ForceE2.out -time -ele 2 globalForce;
recorder Element -file 3x6_Frame_Atlanta/ForceE3.out -time -ele 3 globalForce;
recorder Element -file 3x6_Frame_Atlanta/S1ForceE1.out -time -ele 1 section 1 force;
recorder Element -file 3x6_Frame_Atlanta/S1ForceE2.out -time -ele 2 section 1 force;
recorder Element -file 3x6_Frame_Atlanta/S1ForceE3.out -time -ele 3 section 1 force;
recorder Element -file 3x6_Frame_Atlanta/S3ForceE1.out -time -ele 1 section 3 force;
recorder Element -file 3x6_Frame_Atlanta/S3ForceE2.out -time -ele 2 section 3 force;
recorder Element -file 3x6_Frame_Atlanta/S3ForceE3.out -time -ele 3 section 3 force;
recorder Element -file 3x6_Frame_Atlanta/ForceE12.out -time -ele 12 globalForce;
recorder Element -file 3x6_Frame_Atlanta/ForceE13.out -time -ele 13 globalForce;
recorder Element -file 3x6_Frame_Atlanta/S1ForceE12.out -time -ele 12 section 1 force;
recorder Element -file 3x6_Frame_Atlanta/S1ForceE13.out -time -ele 13 section 1 force;
recorder Element -file 3x6_Frame_Atlanta/S3ForceE12.out -time -ele 12 section 3 force;
recorder Element -file 3x6_Frame_Atlanta/S3ForceE13.out -time -ele 13 section 3 force;
pattern Plain 1 Linear {
        for {set k 101} {$k<200} {incr k} {
        load $k 0 -.4805 0;
}
        for {set k 202} {$k<301} {incr k} {
        load $k 0 -.4805 0;
}
        for {set k 303} {$k<402} {incr k} {
```

```
        load $k 0 -.5195 0;
}
        load 100 0 -.843 0;
        load 200 0 -.456 0;
        load 201 0 -.4032 0;
        load 301 0 -.4032 0;
        load 302 0 -.447 0;
        load 402 0 -.447 0;
        for {set k 12} {$k<16} {incr k} {
        eleLoad -ele $k -type -beamUniform -.14764;
}
        eleLoad -ele 16 -type -beamUniform -.15964;
        eleLoad -ele 17 -type -beamUniform -.15964;
        load 1 0 -.27 0;
        load 2 0 -.4572 0;
        load 3 0 -.3744 0;
        load 4 0 -.1872 0;
        load 5 0 -.387 0;
        load 6 0 -.603 0;
        load 7 0 -.4032 0;
        load 8 0 -.1872 0;
        load 9 0 -.387 0;
```

```
}
constraints Lagrange;
numberer RCM;
system BandGeneral;
test EnergyIncr 1.0e-9 10;
algorithm Newton;
integrator DisplacementControl 200 2 -0.02;
analysis Static
analyze 9000;
loadConst -time 0.0;

puts "Done!"
```